Probes of Strong-field Gravity

by

Leo Chaim Stein

B.S., California Institute of Technology (2006)

Submitted to the Department of Physics
in partial fulfillment of the requirements for the degree of

Doctor of Philosophy in Physics

at the

MASSACHUSETTS INSTITUTE OF TECHNOLOGY

June 2012

Author .....
Department of Physics
May 4, 2012

Certified by .....
Scott A. Hughes
Associate Professor
Thesis Supervisor

Accepted by .....
Krishna Rajagopal
Professor of Physics
Associate Department Head for Education

Probes of Strong-field Gravity

by

Leo Chaim Stein

Submitted to the Department of Physics
on May 4, 2012, in partial fulfillment of the
requirements for the degree of
Doctor of Philosophy in Physics

Abstract

In this thesis, I investigate several ways to probe gravity in the strong-field regime. These investigations focus on observables from the gravitational dynamics, i.e. when time derivatives are large: thus I focus on sources of gravitational waves.

Extreme mass-ratio inspirals (EMRIs) can be very sensitive probes of strong-field physics. Predicting observables from EMRIs must be done numerically, so accurate numerical methods are required to ensure that any comparison with measurement is not spoiled by numerical artefacts. The first investigation of this thesis is a spectral (in the angular sector), pseudospectral (in the radial sector) time-domain PDE solver for perturbations of a Kerr black hole (i.e. solving the Teukolsky equation). The method exhibits good convergence and prompts much future investigation.

A second approach to probing strong gravity is to consider theories which are general relativity (GR) with a few small corrections and investigate the effect of these corrections on observables. Since gravitational waves are the prime observable and they control the long-term evolution of dynamical systems, I investigate their properties in almost-GR theories. The second investigation of this thesis is a study of the propagation and energy content of gravitational waves in these theories. I find that in a large class of theories, approaching the asymptotically flat part of spacetime, gravitational waves propagate in the same fashion as in GR and have the same effective stress-energy tensor as in GR. Next, I study the strong-field correction to the structure of a Schwarzschild black hole in a class of theories. Finally, with these ingredients, I investigate the leading corrections to the dynamics and observables of a comparable mass-ratio inspiral using post-Newtonian techniques. The main result is the appearance of dipolar scalar radiation in this class of theories. The dipolar radiation has a frequency dependence which does not arise in GR and is a distinct signature of corrections. Such signatures should be testable using gravitational wave detection and pulsar timing.

Thesis Supervisor: Scott A. Hughes
Title: Associate Professor

Acknowledgments

Writing this thesis was made possible by the considerable support I've received from colleagues, family, friends, and the astrophysics community at MIT. It would have been quite boring to have spent these past years doing research in a vacuum, but the people with whom I've worked (and with whom I've avoided work) have made the past few years not just bearable but in fact enjoyable.

I thank Scott Hughes, my advisor, for giving me interesting problems, letting me pursue my own ideas, giving me help when I needed it and letting me work at my own pace. I acknowledge my other committee members, Nergis Mavalvala and Max Tegmark, and thank them for their interest in my work and their investment of time.

I also thank Nico Yunes, who acted as part collaborator, part advisor, part dinner party companion and friend, and attempted to accelerate my rate of work (though I tried very hard to continue at my more natural and much slower pace). I thank my collaborators, without whom some of the work in this thesis (and other work not in this thesis) would not exist: Takahiro Tanaka, Sarah Vigeland, Kent Yagi, and Nico Yunes. There are many other colleagues in the field who have answered my questions and from whom I have learned more than from textbooks, but there are too many to name individually. The `xAct` community similarly deserves thanks but who I can not name individually.

In addition, I thank my fellow graduate students, collectively the `astrograd` and `statmechsocial` mailing lists, especially those with whom I've shared offices and eaten lunch together in the Solarium. Over the past few years, I have also interacted with a number of postdocs, mostly over morning coffee, and I thank them for the guidance they have given me.

Finally, I would like to thank my family and especially my girlfriend, Jenny Meyer, for all their support, love, and keeping me sane over the past few years.

Contents

List of Figures

List of Tables

Chapter 1

Introduction

Gravity is the first force that humans recognized—and yet it is more mysterious than the other three which modern physics recognizes. Today we know of four fundamental 'forces': gravity, which has been known since time immemorial; electromagnetism (EM), which was first recognized through lodestones thousands of years ago; the weak nuclear force, recognized through radioactive decay at the turn of the 20^{th} century; and finally the strong nuclear force, first described in the 1930s.

What makes gravity so mysterious? The other three forces (EM, weak, and strong) are all now described by a *quantum* theory, known as the standard model (SM) of particle physics. Gravity, on the other hand, is described by general relativity (GR), which is *classical*. What this means is the following: in GR, at each point in spacetime, the "gravitational field" has one particular value. This is not so for the other three forces. The electromagnetic field is not described by a set of values at each point in spacetime; instead, the electromagnetic field is a *state*, which, when measured over any given region of spacetime with an *operator*, yields a measurement described by a probability distribution. The same holds for the weak and strong fields.

Why this distinction? Does nature act in two distinct fashions, classically for gravity, by quantum mechanically for the SM? There is good reason to think not. The simplest argument to suggest that gravity, too, should be quantum mechanical

comes from the Einstein field equation:

$$\underbrace{G_{ab}}_{\substack{\text{Geometry}\\(\text{classical})}} = 8\pi \underbrace{T_{ab}}_{\substack{\text{Matter}\\(\text{quantum})}} . \tag{1.1}$$

The left hand side is the Einstein tensor, a tensor field which describes (part of) how spacetime is curved. On the right hand side is the stress-energy tensor (SET) field, which describes how much energy density, momentum density, and momentum flux there is everywhere in spacetime. The problem with this equation is that GR is only prepared to handle a *classical* stress-energy tensor. In the standard model, the stress-energy tensor is not a classical field but a quantum operator. The above equation is meaningless: it tries to equate two objects of different varieties.

One approach to making sense of Eq. (1.1) is to take an expectation value of the right hand side, resulting in a classical tensor field $\langle T_{ab} \rangle$. This approach is useful so long as we are only interested in macroscopic physics above the quantum scale. But ultimately, the only resolution is to promote[1] gravity to be quantum mechanical—a quantum theory of gravity, which is fundamentally needed in order to make sense of gravitational phenomena. How do we physicists approach this lofty, possibly unattainable goal? We must probe strong gravitational fields.

1.1 Theory and experiment

The goal of physics is to build mathematical models (theories) that describes how nature acts. Theories are verified or discarded if experiments bear out their results or disfavor them. At times theory leads experiment to certain describe natural phenomena; at other times experiments measure a phenomenon before any theory predicts it. Most physical theories have been built in the latter scenario, to explain some measured phenomenon.

[1] This need not mean a direct quantization of gravity—see e.g. [81] for arguments suggesting that the Einstein field equations may arise from a thermodynamic coarse graining procedure.

The (possibly apocryphal) parable of Galileo's experiment of dropping balls from the leaning tower of Pisa comes to mind. At this time there were no quantitative theories of gravity, only qualitative ones: whether heavier objects fall at a different rate than light ones or not. Purportedly, Galileo observed that objects of the same composition but different masses accelerate at the same rate, thus rejecting the Aristotelian theory that heavier objects fall faster. This observation was an example of experiment leading theory. The experimental result was a *requirement* for Newton's theory of gravity—which it indeed includes. Newton's theory also agreed with Kepler's earlier phenomenological result, that planets move on eccentric ellipses about the Sun (one of the first examples of unification in physics).

In the late 1700s and the 1800s, the phenomena of electromagnetism were systematically quantified by Coulomb, Ørsted, Faraday, and others. This was again an example of experiment leading theory. These observations (especially the dynamical ones, e.g. where a time varying magnetic field induces a changing electric current) led to Maxwell constructing the theory of electromagnetism, which correctly incorporated all prior electrical and magnetic results (the second example of unification). At this point theory began to lead experiment, for example with the prediction of propagating EM waves, later confirmed by Hertz.

In the late 1800s and early 1900s, experiment was again leading theory in the realm of atomic and nuclear physics, leading to the development of quantum mechanics. The observations of the discreteness of atomic spectra, the photoelectric effect, Rutherford's scattering experiments, and many others led to rapid and radical developments in the theory of quantum mechanics. One of the most striking was the discovery of spin-1/2 particles by the Stern-Gerlach experiment. Only integer valued angular momentum can arise from orbital angular momentum. The discovery of half-integer angular momentum should not have been expected from any classical intuition of how angular momentum works. To agree with these experimental results, Paul Dirac had to overhaul the quantum theory of the day.

A very similar story played out in the 1950s and 1960s as nuclear energies were being probed at particle accelerators. Particle experiments revealed a large number

of hadrons. Gell-Mann and his contemporaries organized the newly-found particles into multiplets by their quantum numbers. This organization revealed that all of the particles could be explained by a simpler model where hadrons had substructure: they were composed of quarks, which needed an additional quantum number (color charge) not observed in hadrons. This is one of the most celebrated examples of experiment leading theory.

The history of general relativity contrasts with the development of particle physics in this fashion. Almost unilaterally, the story of GR is that of theory leading experiment. There was no experiment or observation which led to the development of GR.[2] Rather, after Einstein's development of the theory, there was a long checklist of predictions which were validated by observation: the perihelion precession of Mercury (technically a postdiction); the deflection of starlight by the Sun during a total Solar eclipse; the time delay of atomic clocks flown about the Earth; the gravitational redshift of light as it climbs out of the potential of the Earth (measured by the Pound-Rebka experiment); the Shapiro delay of light traversing a gravitational field; the geodetic and frame-dragging precession effects; and most relevant to this thesis, the orbital decay of the Hulse-Taylor pulsar binary.

There are two good reasons for theory leading experiment in the realm of gravitation. The first is that Einstein was very smart. The second, a more physical reason, is that gravity is extremely weak. Whereas we can probe large EM fields in the laboratory and generate high energy particles in accelerators to probe sub-nucleon length scales, we are incapable of generating strong gravitational fields in the laboratory. We have to rely on the kindness of nature to generate regions of large curvature and give us observational handles with which to probe these regions. Regions of strong gravity[3] are exotic and rare in the universe.

[2]The only possibility of a phenomenon unexplained by Newtonian gravity at the time was the perihelion precession of Mercury, which by itself could have led to any number of post-Newtonian theories besides GR.

[3]What comprises strong gravity is a matter of nomenclature. In this thesis, there are two senses: in Part I, systems with large "potentials" are studied, whereas in Part II, systems with large curvatures are studied.

1.2 To probe strong gravity

We find gravity theory in an uncomfortable situation. We can not treat general relativity as a fundamental theory (therefore it is an *effective field theory*), since it can not mesh with quantum mechanical matter. Therefore we wish to learn how nature behaves when the approximation regime of GR breaks down—these must be regions of large curvature, since we have put GR on trial in the regime of weak curvature, and it passes with flying colors. However, the weakness of gravity makes it much more difficult to find regimes where curvature is large.

How does one seek a more fundamental description of gravity? One approach is to build fundamental theories, calculate their observational signatures, and attempt to observe these signatures. There is a rich history of building fundamental quantum gravitational theories (for a good review, see [130]). Two modern approaches to quantum gravity are string theory (ST) and loop quantum gravity (LQG). Both approaches leapfrog an enormous energy range to arrive at quantum gravitational results. Experiments to date have probed up to the TeV energy scale. In both string theory and loop quantum gravity, the energy scale of interest is the Planck energy,

$$E_p \equiv \sqrt{\frac{\hbar c^5}{G}} \approx 10^{28} \text{ eV}\,! \tag{1.2}$$

as this is the natural energy scale involving quantum mechanics, through $\hbar$, and gravity, through G. There is a chasm of *16 orders of magnitude* between where we stand today and where ST and LQG try to make predictions.

It seems to this humble author an act of hubris to expect there to be no new gravitational physics in this chasm. Another approach is necessary: an approach guided by experiment and observation, and since we can not generate the large curvatures we want to probe, we have to rely on observations. But which observations? How do we know where to look, and what we're looking for?

A candidate system for observation obviously must exhibit strong gravity, which points to three possibilities: black holes (BHs), neutron stars (NSs), and the very early universe (I will not discuss the very early universe in this thesis). A candidate

system must also be a "clean" system, which is difficult to define. All of the physical phenomena in a clean system must be well understood and can be characterized independently of each other (or at least simultaneously over-constrained). This excludes systems such as accretion disks in active galactic nuclei (AGN) or interacting binary star systems such as low mass X-ray binaries (LMXBs). Both of the aforementioned systems involve dissipation in gas, viscosity, turbulence, magnetic fields, winds .... There are many unknowns in such systems, so it would be very challenging to use them as tests of gravity.

A candidate system should also exhibit gravitational *dynamics*. This expression means different things to different people. Typically, the motion of planets about the sun is considered gravitational dynamics. However, when looking at the metric of spacetime describing this system, time derivatives are far smaller than spatial derivatives. As far as spacetime is concerned, the situation is quasi-static. One must go to very extreme systems to find time derivatives (of the metric) as large as spatial derivatives. As soon as time derivatives approach the size of spatial derivatives, the metric begins to exhibit wave motion. The excitation of the metric propagates outward through spacetime—gravitational dynamics is synonymous with the generation, propagation, and back-reaction of these gravitational waves.

Our requirements so far are for strong gravity, a clean system, and true gravitational dynamics (i.e. generating gravitational waves). We will discuss two systems which fit the bill: the inspiral of two comparable mass compact objects (either a BH-BH, BH-NS, or NS-NS inspiral), and the inspiral of a stellar-mass body into a super-massive black hole (SMBH), called an extreme mass-ratio inspiral (EMRI).

For any given system, there are two approaches one might take to probing strong gravity. The first of these is the "discovery," "serendipity," or "null test" mode; the second is "targeted" mode. Serendipity mode means to find the GR observable that can be calculated to the highest precision possible and then try to find deviations away from it. Targeted mode, on the other hand, tries to calculate observables in theories other than GR in order to discover which systems are most likely to reveal the signatures of deviations away from GR. This thesis uses both approaches.

1.3 Organization and overview of this thesis

The two approaches (discovery mode and targeted mode) are reflected in the two parts of this thesis. Part I, General relativity, is in discovery mode—focusing on improving the precision of GR observables (here the gravitational waveforms of extreme mass-ratio inspirals). Part II, Beyond general relativity (BGR), is in targeted mode—focusing on calculating observables in theories which are "deformations" away from GR.

Within GR, the comparable mass-ratio inspiral has seen considerable success in analytical calculations of observables. These calculations go up to a very high order (in an expansion in powers of v/c, the relative velocity of the objects). Therefore these systems can already be used as null tests within general relativity. However, the EMRI problem is rather incomplete. Numerically addressing the EMRI problem is the focus of Part I, consisting solely of Chap. 2: A (pseudo-)spectral time-domain Teukolsky equation solver.

Chapter 2 focuses on numerical methods to integrate gravitational waves around a spinning black hole. While numerical methods already exist, they rely on the finite-difference method that may be too imprecise for the high accuracy required in the EMRI problem. This work instead implements a numerical integrator which uses the pseudo-spectral method, promising to be much more accurate than currently existing techniques. EMRI waveforms can be simulated in both the frequency domain and the time domain, but some physics is unavoidably in the time domain, so Chap. 2 focuses on simulating EMRIs in the time domain. The Teukolsky equation is decomposed in the basis of spin-weighted spherical harmonics (for the angular sector), and the radial sector is handled with either Chebyshev, Fourier, or discrete cosine series (the latter being more desirable because of boundary conditions). Time evolution is performed with the method of lines which allows the use of ODE steppers. I discuss how to implement these methods on a computer and present results from an implementation. The results show the expected exponential convergence in terms of basis functions,

suggest convergence of the dispersion relation, and display quasinormal ringing of the black hole spacetime.

Given the incomplete state of the EMRI problem, it can not be considered for targeted mode probes—there are too many effects which have not yet been calculated. However, the comparable mass-ratio inspiral can be used for targeted mode probes. This is the focus of Part II, which consists of three chapters.

Chapter 3, Effective Gravitational Wave Stress-energy Tensor in Alternative Theories of Gravity, goes about calculating the modeshapes, energetics, and propagation properties of gravitational waves in BGR theories. This is a prerequisite for studying gravitational wave systems in BGR theories. This work was the result of a collaboration with Nicolás Yunes and was published as Stein, L. C., Yunes, N. (2011), *Effective gravitational wave stress-energy tensor in alternative theories of gravity*, Phys. Rev. D **83** 064038 [138]. We present the perturbed Lagrangian approach and short-wavelength averaging, which are tools used to separate the gravitational wave perturbation from the smooth background spacetime. We then reproduce the classic result of how much stress-energy gravitational waves carry in GR. As a model theory, we also explicitly calculate the effective stress-energy tensor of Chern-Simons (CS) gravity, which is identical to that in GR when the CS scalar is dynamical and regular at spatial infinity. We then generalize to any higher-order gravity theory with similar properties and show when the effective stress-energy tensor coincides with that of GR.

Chapter 4, Non-Spinning Black Holes in Alternative Theories of Gravity, calculates the strong-field correction to the Schwarzschild (non-spinning black hole) solution in a class of BGR theories. In order to calculate gravitational wave signatures from black hole systems in BGR theories, the strong-field structure of a black hole must be determined. This work was another result of the collaboration with Nicolás Yunes and was published as Yunes, N., Stein, L. C. (2011), *Nonspinning black holes in alternative theories of gravity*, Phys. Rev. D **83** 104002 [171]. We consider all gravity theories with a dynamical scalar directly coupled to all possible quadratic curvature invariants in the action. This class of theories includes both dynamical Chern-Simons

and Einstein-Dilaton-Gauss-Bonnet gravity. In these theories of gravity, we compute the scalar hair for a non-spinning (Schwarzschild) black hole, which acts as a "charge" in the scalar field. This scalar hair also gravitates and acts to deform the spacetime, and we compute this deformation. From the deformation, we also calculate the modified Kepler relation for circular orbits (of particles traveling along geodesics), which allows to find the leading modification to the gravitational wave signature in such theories (though this signature is for "freely-falling" particles, which do not actually exist in this type of theory).

Finally, in Chapter 5, Post-Newtonian, Quasi-Circular Binary Inspirals in Quadratic Modified Gravity, we calculate the leading order corrections to observables from a comparable mass-ratio inspiral in a class of BGR theories. This work was the result of the collaboration with Kent Yagi, Nicolás Yunes, and Takahiro Tanaka, and was published as Yagi, K., Stein, L. C., Yunes, N., Tanaka, T. (2012), *Post-Newtonian, Quasi-Circular Binary Inspirals in Quadratic Modified Gravity*, Phys. Rev. D **85** 064022 [165]. We consider the same class of theories as in the previous chapter and compute the scalar field and gravitational wave (metric) solutions for a comparable mass-ratio binary inspiral, using post-Newtonian (PN) techniques. That is, the equations of motion of the scalar field and the metric are expanded about Minkowski space, in a multivariate expansion. The dominant solution is the leading order GR, PN solution for the metric (and a vanishing scalar). At next order we calculate the solution to the scalar field, which is sourced by black holes acting as scalar "charges" as found in the previous chapter. We find the solution in the near zone and far zone by performing an asymptotic matching. At this same order, we also calculate the deformation to the metric in the near zone and far zone, again employing asymptotic matching. Finally, the far zone solutions of the scalar and the metric deformation allow the calculation of the correction to the energy flux out of the binary. This correction modifies the rate at which the binary inspirals and leads directly to observables in the gravitational wave phase.

Part I

General relativity

Chapter 2

A (pseudo-)spectral time-domain Teukolsky equation solver

It all looks fine, except for the results.

Scott A. Hughes

Abstract

Extreme mass-ratio inspirals (EMRIs) promise to be a sensitive probe of gravity in the strong-field regime through their gravitational wave signatures. To use EMRIs as tests of gravity will require numerical simulations that are sufficiently precise: when comparing measurements to predictions, imprecision may be falsely misattributed to new or unaccounted-for physics. Since gravitational wave detection is so sensitive to the phase of the wave, one especially dangerous numerical artefact would be a numerical dispersion relationship which is not faithful to the continuum one. This Chapter implements a time-domain Teukolsky equation solver which is completely spectral in the angular sector and pseudo-spectral in the radial sector. This solver exhibits pseudo-spectral (exponential) convergence and excellent convergence in the numerical dispersion relationship.

2.1 Motivation

2.1.1 Why extreme mass-ratio inspirals?

In our quest to probe strong-field gravity, we are immediately drawn to black hole systems. But why, then, focus on extreme mass-ratio systems?

The amplitude of gravitational waves emitted from an EMRI is proportional to the mass ratio, $\eta \equiv m/M$. The inspiraling can be thought of as the back-action of these emitted waves on the small body itself, but this is a second order effect: the energy flux scales as

$$\dot{E} \sim -\frac{32}{5}\eta^2 v^{10}\,. \tag{2.1}$$

The result is that the small compact object (SCO) moves nearly on a geodesic, and spends an extremely long time in the strong-field region of the SMBH. Since the SCO moves nearly on a geodesic, it can be used as a tracer of the geometry of the spacetime (see e.g. [43, 151]).

But besides just being a tracer of the spacetime geometry, the gravitational waves from an EMRI should be extremely sensitive to strong-field effects. It is not the size of the gravitational waves, or their frequency content, which makes them such sensitive probes. Rather, it is the amount of time that the SCO spends in the strong-field region. The gravitational binding energy goes as $E \sim -Mm/r \sim -M^2\eta/r \sim -v^2\eta M$. This scaling, combined with the scaling of the energy flux in Eq. 2.1 means that the decay time scales as $t_{\rm insp} \sim M\eta^{-1}$. This extremely long decay time means that even small effects, such as resonances and spin-curvature coupling, can imprint on the gravitational wave signal through secular or integral effects.

This long decay time leads to a gravitational waveform with $\mathcal{O}(\eta^{-1})$ cycles—likely 10^5 cycles in the band of a LISA-like mission. A phase shift of just one cycle in such a long waveform is immediately evident in signal analysis. Thus EMRIs can serve as null tests, informing us as to whether or not our models contain all of the physics relevant to describe motion in the strong-field.

A better understanding of the EMR limit can also inform our understanding of the comparable mass ratio limit. As it currently stands, the computational complexity of EMRI calculations is much lower than that of full numerical relativity (which is required for the comparable mass ratio limit). Recent work in the "effective one-body" (EOB) formalism [32, 110] aims to bridge the gap between the comparable mass ratio problem and the speed and simplicity of analytics (in post-Newtonian theory) and of EMRI simulations. The EOB formalism, however, has various coefficients which need to be "calibrated" from both full numerical relativity and EMRI simulations in order to be valid for all mass ratios. Since full NR simulations are so computationally expensive, EMRI calculations are much cheaper to use for EOB calibration.

2.1.2 Why black hole perturbation theory?

In the past decade, fully non-linear GR simulations have gone from being a dream to commonplace for several research groups around the world. Why, then, would one want to numerically simulate perturbative equations instead of directly solving the full equation of GR? It turns out that calculating waveforms from EMRIs presents a unique computational challenge to numerical relativity. This can be seen from the simple scaling arguments which follow.

A numerical simulation needs to resolve all of the length and time scales of interest in a problem, and these scales set the fundamental computational requirements for any scheme to simulate them. Let us enumerate these length and time scales. The smallest length scale which must be resolved for a black hole of mass m is the size of its horizon, which is proportional to the mass, $\ell_{\rm horiz} \sim m$. Let us suppose that we wish to simulate an EMRI with a mass ratio of η in the range of 10^{-5} to 10^{-9}. The SCO starts at a large distance away from the central BH; let us suppose we wish to simulate an orbit starting from 10s of M away from the central black hole (of mass M). The total grid must have a linear dimension much larger, say a few $100M$. Already this represents an enormous computational complexity, in trying to resolve lengths on the order of ηM in a grid which spans $\sim 100M$; this represent a dynamic range in length of $\sim 10^2\eta^{-1}$.

More damning still are the dynamics of such a system. The shortest timescale of interest is related to the shortest length scale of interest, m. The longest timescale of interest is of course the inspiral time. As suggested above, the number of orbits goes as η^{-1}, or $t_{\rm insp} \sim \eta^{-1} t_{\rm orb}$. The net result is that for extreme mass ratios, the simulation needs i) finer spatial resolution, ii) smaller time steps, and iii) needs to be run for longer; the combined complexity of such a calculation goes as the tragically steep $\mathcal{O}(\eta^{-3})$.

How, then, does one simulate EMRIs? The smallness of η which curses attempts at full numerical relativity is also a blessing. With a small parameter in the problem, EMRIs are amenable to perturbation theory. One can treat the SCO and the gravitational waves as a perturbation on the background of a stationary (Kerr) black hole, and attempt to solve for both the motion of the SCO and the GWs which are emitted. To date, there are no simulations where both the motion of the SCO and GWs are solved for simultaneously in a self-consistent fashion[1]; this is still an active area of research.

2.1.3 Why the Teukolsky equation?

Typically, general relativity is treated as a theory for the metric of spacetime. Perturbation theory therefore typically takes the form of splitting the metric into a "background" piece and a small tensor perturbation h, and solving for h. The Teukolsky formalism, on the other hand, seeks a perturbation to the curvature tensor rather than the metric. There are a number of attractive reasons to consider curvature perturbations rather than metric perturbations.

First, let us touch on a fact relevant to simulating any "gauge" theory. A gauge theory is one which has a local symmetry transformation under which the theory is invariant. Both the standard model and GR are gauge theories, but GR is unique since the symmetry is actually diffeomorphisms of the manifold, rather than an "internal" symmetry of a fibre bundle of the manifold. The common trait that these theories

[1]Diener, Vega, Wardell, and Detweiler have performed self-consistent simulations of a particle coupled to a scalar field (forthcoming), but not gravitational waves.

share is that the fields in these theories have more components than the number of physical degrees of freedom, precisely because of the gauge freedom. What this means in numerical simulations is that the fields must be gauge fixed (i.e. choose a specific gauge, to restrict the space of possible fields) so that spurious and unphysical gauge degrees of freedom will not spoil the simulation for any number of reasons.

Performing metric perturbation theory would entail solving a system of 10 partial differential equations [4 elliptic (constraint-type) and 6 hyperbolic (wave-type)] for 10 metric components (6 physical degrees of freedom and 4 gauge degrees of freedom), all components being coupled to each other. In contrast, the Teukolsky equation(s) are for perturbations to the complex Weyl scalars [108],

$$\Psi_0 = -C_{abcd} l^a m^b l^c m^d \tag{2.2}$$

$$\Psi_4 = -C_{abcd} n^a \bar{m}^b n^c \bar{m}^d \,, \tag{2.3}$$

(and $\Psi_{1,2,3}$ which have been omitted) where C_{abcd} is the Weyl tensor, and l^a, n^a, m^a and $\bar{m}^a$ are two real null vectors and one complex null vector (and its conjugate) which form a Newman-Penrose tetrad [108].

We can now state why the Teukolsky formalism is attractive. First, because of the somewhat miraculous symmetries of the Kerr geometry,[2] the Weyl scalars ψ_0 and ψ_4 are gauge invariant quantities. These same symmetries also lead to the resulting equations being *decoupled*: the equation for the evolution of ψ_4 is not coupled to any other perturbative quantity. These properties mean that one does not have to be concerned with gauge fixing or concerned with non-physical gauge degrees of freedom spoiling the numerical simulation.

The final point of interest about the Teukolsky equation is that it is *separable*: it admits solution by separation of variables (although the eigenfunctions and separation constants must be found numerically). This is firstly important since before computation was cheap, these problems could only be attacked analytically. As we will mention in Sec. 2.1.4, our goal is to solve the Teukolsky equation in the time

[2]Specifically that Kerr is a Petrov type D spacetime [139]

domain, where the equation can no longer be separated and hence must be numerically integrated. However, the separability is still relevant to us; the second reason is that a body of literature with analytic results exists, which allows one to validate a numerical scheme.

As an aside, it is important to point out the difficulty of being self-consistent. The perturbation to the spacetime is caused by a small body (modeled as a point particle), but the trajectory of this small body is also affected by the perturbations to the spacetime. To be self-consistent, one would need to simultaneously solve for the trajectory of the perturber and the field. In order to calculate the trajectory of the small body, the metric perturbation is required. This does not completely preclude the curvature approach, since the metric perturbation may be reconstructed from the curvature perturbations via the Chrzanowski procedure [157]. However, this procedure involves more than just one curvature scalar at a time, so one would need to simultaneously integrate the PDEs for ψ_0 and ψ_4, which would then be coupled through their combined effect on the matter source term. Because this involves metric reconstruction, such a scheme does not seem any more attractive than direct integration of the metric, rather than curvature perturbations. For the time being, though, no self-consistent scheme is available; we resign ourselves to the simpler task of integrating the separated curvature equations, rather than trying to be self-consistent. In fact, in this work, we do not even address including the source term; that is left for future work.

2.1.4 Why the time domain?

To analytically separate the Teukolsky equation, one must use an ansatz for the temporal piece of the solution going as $T(t) \sim e^{i\omega t}$. Essentially, this is performing a temporal Fourier transform. This is very convenient for performing calculations on *geodesics* in Kerr spacetime, which are multi-periodic with three frequencies (the azimuthal, radial, and polar frequencies) and an infinite but discrete spectrum of their higher harmonics [133, 56].

The usual approach is to treat an inspiralling trajectory as an adiabatically-evolving family of geodesics. To compute the instantaneous flux of energy and angular momentum on an inspiralling trajectory, one instead calculated the flux of energy and angular momentum at infinity of the geodesic which goes through the same point with the same velocity—assuming that the particle has always been and always will be on that geodesic. One then applies the geodesic result to construct the family of geodesics.

While this assumption is warranted at early times, when the radiation-reaction time is very long compared to the orbital time, it breaks down at late times. This is very obvious when the inspiral is terminated by a final near-geodesic plunge into the event horizon—the plunge is not even a periodic orbit.

This approach also neglects other effects which may be comparable in magnitude to radiation-reaction, such as the conservative part of the self-force and the spin-coupling force. The computation must also be modified when two or more of the frequencies become commensurate with each other (and rational orbits are dense in all orbits, but likely only small integer ratios are important) [62, 64].

One must therefore abandon the original ansatz of quasi-periodicity in the temporal dimension. In doing so, one also abandons separability, and therefore the problem returns from being a set of coupled ODEs to being a PDE. Hence we will be solving the Teukolsky equation in the time domain, rather than the frequency domain.

2.1.5 Why (pseudo-)spectral methods?

We must address representing an infinite-dimensional function space on a computer, with a finite dimensionality (and finite precision). There are several popular approaches for numerically integrating partial differential equations; some of these are the finite difference, finite element, finite volume (flux conservative), spectral, Galerkin, and pseudo-spectral (collocation) methods (see [28] for a good pedagogical guide to spectral methods).

In the EMRI literature, the primary method has been that of finite differences [87, 140]. The pseudo-spectral method has seen some attention [40], but so far only in

Schwarzschild. One very compelling reason to use the pseudo-spectral method is the fidelity of the dispersion relationship the method provides, as compared to the errors introduced by finite differences [28].

Discretizing a differential operator (turning it into a difference operator) unavoidably introduces errors. A very useful way of quantifying these errors is to let the discrete operator act on plane wave solutions and decompose the error into amplitude and phase errors, corresponding to numerical *dissipation* and *dispersion*. For the purposes of gravitational wave detection, phase errors are much more important than amplitude errors, because of the phase sensitivity of matched-filtering. It is easy to see how numerical dispersion could corrupt the extracted gravitational wave signal from such a simulation: if high frequencies and low frequencies propagate out from the strong-field region at incorrect speeds, the extracted signal can be stretched or squeezed when it arrives at spatial infinity, where the signal is extracted. Thus it is very important to strive for a good numerical dispersion relationship.

A finite difference operator has a fixed polynomial order corresponding to the number of grid points used in the computation of a derivative. By contrast, calculating a derivative in a collocation method uses *all* of the grid points in the domain, effectively giving a derivative of the highest possible numerical order. The result is a dispersion relationship which is more faithful to the continuum limit than finite difference [28]. Since phase accuracy is the name of the game in gravitational wave detection and inference, pseudospectral methods are very compelling.

2.2 Mathematical formulation

The goal is to rewrite the Teukolsky equation in a (pseudo-)spectral fashion amenable to numerical evolution. In this Section we cover the necessary mathematical formulation. To decompose the angular sector, a generalization of the spherical harmonics is employed which is adapted to the problem. These are the spin-weighted spherical harmonics, discussed in Sec. 2.2.1. We then show how the angular sector of the Teukolsky equation decomposes in this basis in Sec. 2.2.2. In Sec. 2.2.3, we present

the standard coordinate transformations and ansatz for integrating the Teukolsky equation, which control the near-horizon and spatial infinity limits of the solution. In Sec. 2.2.4, we go over calculating spatial derivatives using the pseudospectral method. In Sec. 2.2.5, we discuss how to represent the field on a computer and the algorithmic complexity of the scheme described here. In Sec. 2.2.6, we discuss time-stepping via the so-called method of lines. Finally, in Sec. 2.2.7, we discuss how to implement purely-absorbing boundary conditions.

2.2.1 $\eth$ and spin-weighted spherical harmonics

We start with ordinary spherical harmonics. In terms of Wigner's D matrices, the spherical harmonics are

$$Y_{\ell,m}(\theta,\phi) = \sqrt{\frac{2\ell+1}{4\pi}}\, D^{\ell}_{0,m}(\phi,\theta,0)\,. \tag{2.4}$$

Here ℓ is a label to denote the dimension $(2\ell+1)$ of the matrix, and the two lower indices are matrix indices. Viewed as matrices with arguments (θ,ϕ,ψ) labeling a group element, the D matrices are irreducible representations of the rotation group, $SO(3)$.

Recall that we can define [132] raising and lowering operators to change the eigenvalue m,

$$L_{\pm} = e^{\pm i\phi}\left(\pm\frac{\partial}{\partial\theta} + i\cot\theta\frac{\partial}{\partial\phi}\right) \tag{2.5}$$

$$L_{\pm}Y_{\ell,m} = \sqrt{(\ell\mp m)(\ell\pm m+1)}Y_{\ell,m\pm1}\,. \tag{2.6}$$

We can view this as an operator acting on the second lower index of the D matrix. By analogy, we can introduce a set of operators to act on the first lower index. These operators are traditionally known as $\eth$ and $\bar{\eth}$, and the related eigennumber is known as the spin weight s. They are defined [69] as operating on some spin-weight s quantity

$\eth$ as

$$\eth\eta = -(\sin\theta)^s \left(\frac{\partial}{\partial\theta} + i\csc\theta\frac{\partial}{\partial\phi}\right)(\sin\theta)^{-s}\eta \tag{2.7}$$

$$\bar{\eth}\eta = -(\sin\theta)^{-s} \left(\frac{\partial}{\partial\theta} - i\csc\theta\frac{\partial}{\partial\phi}\right)(\sin\theta)^{s}\eta\,. \tag{2.8}$$

Then $\eth\eta$ has spin weight $s+1$, and quantity $\bar{\eth}\eta$ has spin weight $s-1$. The transformation properties of some spin-weight s quantity is $\eta \to e^{is\psi}\eta$ under a rotation by angle ψ, the third Euler angle.

Now, operating on the D matrices, one can associate

$${}_sY_{\ell,m}(\theta,\phi)e^{-is\psi} = \sqrt{\frac{2\ell+1}{4\pi}}\; D^{\ell}_{-s,m}(\phi,\theta,\psi)\,, \tag{2.9}$$

where ${}_sY_{\ell,m}$ is called the spin-s spherical harmonic. From the above we can see that the spin-0 spherical harmonics are also the ordinary spherical harmonics. We can see that the spin-s harmonics are defined only for $\ell \geq |s|$.

Just like the ordinary spherical harmonics, the spin-s harmonics are also eigenfunctions of $\frac{\partial}{\partial\phi}$ with eigenvalue

$$\frac{\partial}{\partial\phi}\,{}_sY_{\ell,m} = im\,{}_sY_{\ell,m}\,. \tag{2.10}$$

The action of $\eth, \bar{\eth}$ on the spin-weight s spherical harmonics is [69]

$$\eth\,{}_sY_{\ell,m} = +\sqrt{(l-s)(l+s+1)}\;\;{}_{s+1}Y_{\ell,m} \tag{2.11}$$

$$\bar{\eth}\,{}_sY_{\ell,m} = -\sqrt{(l+s)(l-s+1)}\;\;{}_{s+1}Y_{\ell,m} \tag{2.12}$$

$$\bar{\eth}\eth\,{}_sY_{\ell,m} = -\quad(l-s)(l+s+1)\qquad {}_sY_{\ell,m}\,. \tag{2.13}$$

The spherical harmonics of spin-weight s are eigenfunctions of $\bar{\eth}\eth$, and are therefore suited to act as basis functions to expand spin-s functions on the sphere. They in

fact form a basis, with orthogonality and completeness relations,

$$\iint d\Omega \, {}_sY^*_{\ell,m} \, {}_sY_{\ell',m'} = \delta_{\ell\ell'}\delta_{mm'} \tag{2.14}$$

$$\sum_{\ell m} {}_sY^*_{\ell,m} \, {}_sY_{\ell,m} = \delta(\phi - \phi')\delta(\cos\theta - \cos\theta'), \tag{2.15}$$

where an asterisk denotes complex conjugation. Note that there is no orthogonality relation amongst elements with different values of s; each set of spin-weight s harmonics forms a basis for functions on the sphere.

Angular functions and derivatives can be thought of as operators acting on the linear vector space $\mathcal{A}$ of square-integrable functions on the 2-sphere. At this point, it is convenient to use the bra-ket notation to represent elements $|v\rangle \in \mathcal{A}$ and $\langle v| \in \mathcal{A}^*$, the dual vector space. The inner product is defined in terms of integration over the 2-sphere as usual. We also write the spin-s harmonic basis elements in this notation, with $|s, \ell, m\rangle$ representing ${}_sY_{\ell,m}$. The value at some point on the sphere can be evaluated by taking

$${}_sY_{\ell,m}(\theta, \phi) = \langle \theta, \phi | s, \ell, m \rangle \, , \tag{2.16}$$

and the dual bra gives the value of the complex conjugate,

$${}_sY^*_{\ell,m}(\theta, \phi) = \langle s, \ell, m | \theta, \phi \rangle \, . \tag{2.17}$$

In this notation, the orthogonality (2.14) and completeness (2.15) relations can be written as

$$\langle s, \ell, m | s, \ell', m' \rangle = \delta_{\ell\ell'}\delta_{mm'} \tag{2.18}$$

$$\sum_{\ell m} |s, \ell, m\rangle\langle s, \ell, m| = \mathbf{1} \, , \tag{2.19}$$

where $\mathbf{1}$ is the identity operator.

We will need to be able to evaluate how certain operators "connect" different elements of the spin-s harmonics. These matrix elements may be calculated by decomposing some arbitrary function on the sphere into spin-0 (the usual) spherical harmonics, and then using the Clebsch-Gordan coefficients [39],

$$\iiint d\Omega d\psi \; D^{l_3 *}_{s_3 m_3} D^{l_2}_{s_2 m_2} D^{l_1}_{s_1 m_1} = \frac{8\pi^2}{2l_3+1} \langle l_3, m_3 | l_1, m_1; l_2, m_2 \rangle \langle l_3, s_3 | l_1, s_1; l_2, s_2 \rangle \,, \tag{2.20}$$

where $\langle l_3, m_3 | l_1, m_1; l_2, m_2 \rangle$ is the Clebsch-Gordan coefficient for $SO(3)$: the coefficients for decomposition of the product $|l_1, m_1\rangle \otimes |l_2, m_2\rangle$ into the basis $|l_3, m_3\rangle$. With no s label, a state $|l, m\rangle$ is taken to be an ordinary spherical harmonic with $s = 0$.

When $s_2 = s_3$ and $s_1 = 0$, one can multiply the first and second D matrices by $e^{\pm is\psi}$ and replace each D matrix by a spin-weighted spherical harmonic (the third one an ordinary spherical harmonic). Then there is no more ψ dependence, and the integral may be used to evaluate

$$\begin{aligned} \langle s, l_3, m_3 | Y_{l_1,m_1} | s, l_2, m_2 \rangle &\equiv \iint d\Omega \;\; {}_sY^*_{l_3,m_3} \, {}_sY_{l_2,m_2} \, {}_0Y_{l_1,m_1} \\ &= \sqrt{\tfrac{(2l_1+1)(2l_2+1)}{4\pi(2l_3+1)}} \langle l_3, m_3 | l_1, m_1; l_2, m_2 \rangle \langle l_3, -s | l_1, 0; l_2, -s \rangle \,. \end{aligned} \tag{2.21}$$

In particular, we will encounter

$$\cos\theta = \sqrt{\frac{4\pi}{3}} Y_{1,0} \tag{2.22}$$

$$\sin^2\theta = \frac{4\sqrt{\pi}}{3} \left(Y_{0,0} - \frac{1}{\sqrt{5}} Y_{2,0} \right) \,, \tag{2.23}$$

which we have decomposed into ordinary spherical harmonics. There is no dependence on ϕ, so only $m = 0$ harmonics are involved in the decomposition. From the Clebsch-Gordan selection rules, these only couple together states of equal m. The non-vanishing matrix elements are

$$\langle s, \ell, m | \cos\theta | s, j, m \rangle = \sqrt{\frac{2j+1}{2\ell+1}} \langle \ell, m | j, m; 1, 0 \rangle \langle \ell, -s | j, -s; 1, 0 \rangle \tag{2.24}$$

and

$$\langle s,\ell,m|\sin^2\theta|s,j,m\rangle = \frac{2}{3}\delta_{\ell,j} - \frac{2}{3}\sqrt{\frac{2j+1}{2\ell+1}}\langle \ell,m|j,m;2,0\rangle\langle \ell,-s|j,-s;2,0\rangle\,. \quad (2.25)$$

We see that the operator $\cos\theta$ is tridiagonal in ℓ's, i.e. it connects states ℓ to states $(\ell,\ell\pm1)$; whereas the operator $\sin^2\theta$ is pentadiagonal, connecting states ℓ to states $(\ell,\ell\pm1,\ell\pm2)$.

We can rewrite operators $\mathcal{O}\in\mathrm{End}(\mathcal{A})$ (i.e. $\mathcal{O}:\mathcal{A}\to\mathcal{A}$) in the algebra of $\mathcal{A}\times\mathcal{A}^*$. For example, we can write the ∂_ϕ and $\bar{\eth}\eth$ operators as

$$\frac{\partial}{\partial\phi} = \sum_{\ell,m}|s,\ell,m\rangle im\langle s,\ell,m| \quad (2.26)$$

$$\bar{\eth}\eth = \sum_{\ell,m}|s,\ell,m\rangle(s-\ell)(\ell+s+1)\langle s,\ell,m|\,. \quad (2.27)$$

We can now write the Teukolsky equation with the angular sector decomposed into the basis of spin-weighted spherical harmonics.

2.2.2 Teukolsky equation with spectral angular sector

We now apply the math of Sec. 2.2.1 to linear perturbations of a rotating black hole (Kerr) spacetime. The equations of motion of a spin s field on a Kerr background are described by the Teukolsky equation [145, 146, 127]. We can write this as

$$\Delta\mathcal{T}_s\Psi_s = 4\pi\Delta\Sigma T_s\,, \quad (2.28)$$

where the field Ψ_s can be different Newman-Penrose scalars and the associated source term T_s is different for each field (these can be found in [145]); and the Teukolsky differential operator (times Δ), in Boyer-Lindquist coordinates and in units where

$G = c = 1$, is

$$\begin{aligned}\Delta\mathcal{T}_s = &\left[\left(a^2+r^2\right)^2 - a^2\Delta\sin^2\theta\right]\frac{\partial^2}{\partial t^2} - \Delta^{-s+1}\frac{\partial}{\partial r}\Delta^{s+1}\frac{\partial}{\partial r} \\ &+ 4Mar\frac{\partial^2}{\partial t\partial\phi} - 2s\left[M(r^2-a^2) - \Delta(r+ia\cos\theta)\right]\frac{\partial}{\partial t} \\ &+ \left(a^2 - \frac{\Delta}{\sin^2\theta}\right)\frac{\partial^2}{\partial\phi^2} - \frac{\Delta}{\sin\theta}\frac{\partial}{\partial\theta}\sin\theta\frac{\partial}{\partial\theta} \\ &- 2s\left[a(r-M) + \frac{i\Delta\cos\theta}{\sin^2\theta}\right]\frac{\partial}{\partial\phi} + \Delta(s^2\cot^2\theta - s)\,, \end{aligned} \tag{2.29}$$

or, slightly more compactly,

$$\begin{aligned}\Delta\mathcal{T}_s = &\left[\left(a^2+r^2\right)^2 - a^2\Delta\sin^2\theta\right]\frac{\partial^2}{\partial t^2} - \Delta^{-s+1}\frac{\partial}{\partial r}\Delta^{s+1}\frac{\partial}{\partial r} \\ &+ 4Mar\frac{\partial^2}{\partial t\partial\phi} - 2s\left[M(r^2-a^2) - \Delta(r+ia\cos\theta)\right]\frac{\partial}{\partial t} \\ &+ a^2\frac{\partial^2}{\partial\phi^2} - 2sa(r-M)\frac{\partial}{\partial\phi} - \Delta\bar{\eth}\eth\,, \end{aligned} \tag{2.30}$$

where the usual Boyer-Lindquist quantities Δ, Σ are given by $\Delta = r^2 - 2Mr + a^2$, $\Sigma = r^2 + a^2\cos^2\theta$. In going from Eq. (2.29) to Eq. (2.30), we have identified the operator

$$\bar{\eth}\eth = \frac{1}{\sin^2\theta}\frac{\partial^2}{\partial\phi^2} + \frac{1}{\sin\theta}\frac{\partial}{\partial\theta}\sin\theta\frac{\partial}{\partial\theta} + 2s\frac{i\cos\theta}{\sin^2\theta}\frac{\partial}{\partial\phi} + (s - s^2\cot^2\theta) \tag{2.31}$$

in the Teukolsky operator. The Teukolsky operator is almost, but not quite, diagonal in the $|s,\ell,m\rangle$ basis. It does not connect states with differing m numbers, but it is pentadiagonal in the ℓ's, because of the appearance of $\cos\theta$ and $\sin^2\theta$ in the operator.

The field Ψ_s and source term $\Delta\Sigma T_s$ can be decomposed into the basis $|s,\ell,m\rangle$. We simply write

$$\Psi_s(t,r,\theta,\phi) = \langle\theta,\phi|\Psi_s(t,r)\rangle \tag{2.32}$$

$$|\Psi_s(t,r)\rangle = \sum_{\ell,m}\Psi_{s,\ell,m}(t,r)\ |s,\ell,m\rangle\,, \tag{2.33}$$

where the coefficients $\Psi_{s,\ell,m}(t,r)$ are found as

$$\Psi_{s,\ell,m}(t,r) = \langle s,\ell,m|\Psi_s(t,r)\rangle \tag{2.34}$$

$$= \iint d\Omega \;\; {}_sY^*_{\ell,m}(\theta,\phi)\;\Psi_s(t,r,\theta,\phi)\,, \tag{2.35}$$

and similarly for the source term,

$$\Delta\Sigma T_s(t,r,\theta,\phi) = \langle\theta,\phi|\tau_s(t,r)\rangle \tag{2.36}$$

$$|\tau_s(t,r)\rangle = \sum_{\ell,m} \tau_{s,\ell,m}(t,r)\;|s,\ell,m\rangle\,, \tag{2.37}$$

where the coefficients $\tau_{s,\ell,m}(t,r)$ are found as

$$\tau_{s,\ell,m}(t,r) = \langle s,\ell,m|\tau_s(t,r)\rangle \tag{2.38}$$

$$= \iint d\Omega \;\; {}_sY^*_{\ell,m}(\theta,\phi)\;\Delta\Sigma T_s(t,r,\theta,\phi)\,. \tag{2.39}$$

We can now view the Teukolsky operator (2.30) as a 1+1 dimensional linear, time-independent partial differential operator. The coefficients of this differential operator are built from the algebra of functions of r times matrix operators in $\mathcal{A}\times\mathcal{A}^*$ acting on functions on the 2-sphere. We can write a standard form for such PDEs as

$$\Delta\mathcal{T}_s|\Psi_s\rangle = \left(A^{tt}\partial_{tt} + A^{tr}\partial_{tr} + A^{rr}\partial_{rr} + B^t\partial_t + B^r\partial_r + C\right)|\Psi_s\rangle = |S\rangle\,, \tag{2.40}$$

and identifying the operator coefficients in Eq. (2.30),

$$A^{tt} = \left(a^2 + r^2\right)^2 - a^2 \Delta \sin^2\theta \tag{2.41a}$$

$$A^{tr} = 0 \tag{2.41b}$$

$$A^{rr} = -\Delta^2 \tag{2.41c}$$

$$B^t = 4Mar\frac{\partial}{\partial\phi} - 2s\left[M(r^2 - a^2) - \Delta(r + ia\cos\theta)\right] \tag{2.41d}$$

$$B^r = -(s+1)\Delta 2(r - M) \tag{2.41e}$$

$$C = a^2\frac{\partial^2}{\partial\phi^2} - 2sa(r - M)\frac{\partial}{\partial\phi} - \Delta\bar{\eth}\eth \tag{2.41f}$$

$$|S\rangle = 4\pi|\tau_s\rangle \tag{2.41g}$$

where $\cos\theta, \sin^2\theta, \partial_\phi$, and $\bar{\eth}\eth$ are all treated as angular operators with expansions given by Eqs. (2.24), (2.25), (2.26), and Eq. (2.27), respectively; and any radial function not multiplied by one of these angular operators is implicitly multiplied by the identity operator.

2.2.3 Coordinate transformations and radial falloff

Borrowing from the experience of successfully-implemented numerical integrations of the Teukolsky equation, we make standard transformations to the differential equation. These transformations follow the work of [87, 140, 188] and are motivated by the asymptotic behaviour of the solution to the Teukolsky equation in the near-horizon and spatial infinity limits.

First, the frame dragging of the ergosphere is "unwound" with the transformed azimuthal coordinate $\tilde{\phi}$ defined by

$$\mathrm{d}\tilde{\phi} = \mathrm{d}\phi + \frac{a}{\Delta}\mathrm{d}r\,, \tag{2.42}$$

which can be integrated to give

$$\tilde{\phi} = \phi + \frac{a}{r_+ - r_-}\ln\frac{r - r_+}{r - r_-}\,, \tag{2.43}$$

where as usual, $r_\pm$ are the larger and smaller roots of $\Delta = (r - r_+)(r - r_-) = 0$ and are given by

$$r_\pm = M \pm \sqrt{M^2 - a^2} \tag{2.44}$$

(the event horizon is located at r_+).

It is of great importance that the transformation of partial derivatives induced by this change of variables,

$$\frac{\partial}{\partial \phi} \to \frac{\partial}{\partial \tilde{\phi}} \tag{2.45}$$

$$\frac{\partial}{\partial r} \to \frac{\partial}{\partial r} + \frac{a}{\Delta}\frac{\partial}{\partial \tilde{\phi}}\,, \tag{2.46}$$

does not dramatically affect the angular sector. Specifically, the operator $\bar{\eth}\eth$ in the "tilde" coordinates has the same structure, which can be written as $\widetilde{\bar{\eth}\eth}$, by simply putting a tilde onto each ϕ. An identical decomposition into spin-weighted spherical harmonics can be performed in tilde coordinates, which we assume from here forward. The induced change on the coefficients of the Teukolsky operator in the tilde coordinates are

$$\tilde{A}^{tt} = A^{tt} \tag{2.47a}$$

$$\tilde{A}^{tr} = A^{tr} \tag{2.47b}$$

$$\tilde{A}^{rr} = A^{rr} \tag{2.47c}$$

$$\tilde{B}^{t} = B^{t} + A^{tr} J_{\tilde{\phi}} \frac{\partial}{\partial \tilde{\phi}} \tag{2.47d}$$

$$\tilde{B}^{r} = B^{r} + 2A^{rr} J_{\tilde{\phi}} \frac{\partial}{\partial \tilde{\phi}} \tag{2.47e}$$

$$\tilde{C} = C + A^{rr}\left[J_{\tilde{\phi}}^2 \frac{\partial^2}{\partial \tilde{\phi}^2} + \left(\frac{\partial}{\partial r} J_{\tilde{\phi}}\right)\frac{\partial}{\partial \tilde{\phi}}\right] + B^r J_{\tilde{\phi}} \frac{\partial}{\partial \tilde{\phi}}\,, \tag{2.47f}$$

where $J_{\tilde{\phi}} = a/\Delta$, all ∂_ϕ in the coefficients are replaced with $\partial_{\tilde{\phi}}$, and where $\bar{\eth}\eth$ is replaced with $\widetilde{\bar{\eth}\eth}$.

Still for the near-horizon limit, the "tortoise coordinate" r^* is introduced, defined by

$$\mathrm{d}r^* = \frac{a^2 + r^2}{\Delta}\mathrm{d}r\,. \tag{2.48}$$

This Jacobian may also be integrated to explicitly find

$$r^*(r) = r + \frac{2Mr_+}{r_+ - r_-}\ln\frac{r - r_+}{2M} - \frac{2Mr_-}{r_+ - r_-}\ln\frac{r - r_-}{2M}\,. \tag{2.49}$$

The significance of this coordinate transformation is that solutions to the Teukolsky equation are asymptotically periodic in r^* [146] in both the $r \to \infty$ ($r^* \to \infty$) limit and the $r \to r_+$ ($r^* \to -\infty$) limit; i.e. respectively the spatial infinity and horizon limits. This coordinate transformation induces the coefficient transformation

$$\tilde{A}^{*tt} = \tilde{A}^{tt} \tag{2.50a}$$

$$\tilde{A}^{tr*} = J_r\tilde{A}^{tr} \tag{2.50b}$$

$$\tilde{A}^{r*r*} = J_r^2\tilde{A}^{rr} \tag{2.50c}$$

$$\tilde{B}^{*t} = \tilde{B}^{t} \tag{2.50d}$$

$$\tilde{B}^{r*} = J_r\tilde{B}^{r} + \left(\frac{\partial}{\partial r}J_r\right)\tilde{A}^{rr} \tag{2.50e}$$

$$\tilde{C}^{*} = \tilde{C}\,, \tag{2.50f}$$

where $J_r = (a^2 + r^2)/\Delta$.

We now move to the spatial infinity limit. In this limit, the asymptotic behaviour of outgoing waves of ψ_4 behave as $\psi_4 \sim \exp(i\omega r*)/r$ [146]. The argument of the Teukolsky operator, Ψ_s for $s = -2$, is related to ψ_4 through $\Psi_{-2} = \rho^{-4}\psi_4$, where $\rho = -1/(r - ia\cos\theta)$. We are interested in the oscillatory behaviour in the spatial infinity limit, so to scale out radial power-law behaviour, we will rewrite the equation for the auxiliary field $\psi' \equiv r^{-3}\Psi_{-2}$. To keep things general, this can be accomplished by 'conjugating' the differential operator by some purely radial function f^n as follows:

$$\Delta\mathcal{T}_s|\Psi_s\rangle = 4\pi|\tau_s\rangle \tag{2.51a}$$

$$\Delta\mathcal{T}_s f^n f^{-n}|\Psi_s\rangle = 4\pi|\tau_s\rangle \tag{2.51b}$$

$$\left(f^{-n}\circ\Delta\mathcal{T}_s\circ f^n\right)|f^{-n}\Psi_s\rangle = 4\pi|f^{-n}\tau_s\rangle\,. \tag{2.51c}$$

The coefficients of the differential operator $(\Delta\mathcal{T}_s)_{f^n} \equiv (f^{-n}\circ\Delta\mathcal{T}_s\circ f^n)$ (the *inner automorphism* of $\Delta\mathcal{T}_s$ by f^n) will be written with subscript f^n, and are related to the pre-conjugated coefficients of $\Delta\mathcal{T}_s$ by

$$\tilde{A}^{*tt}_{f^n} = \tilde{A}^{*tt} \tag{2.52a}$$

$$\tilde{A}^{tr*}_{f^n} = \tilde{A}^{tr*} \tag{2.52b}$$

$$\tilde{A}^{r*r*}_{f^n} = \tilde{A}^{r*r*} \tag{2.52c}$$

$$\tilde{B}^{*t}_{f^n} = \tilde{B}^{*t} + n\frac{f'}{f}\tilde{A}^{tr*} \tag{2.52d}$$

$$\tilde{B}^{r*}_{f^n} = \tilde{B}^{r*} + 2n\frac{f'}{f}\tilde{A}^{r*r*} \tag{2.52e}$$

$$\tilde{C}^{*}_{f^n} = \tilde{C}^{*} + n\frac{f'}{f}\tilde{B}^{r*} + \left(n\frac{f''}{f} + n(n-1)\frac{f'^2}{f^2}\right)\tilde{A}^{r*r*} \tag{2.52f}$$

$$|\tilde{S}^{*}_{f^n}\rangle = |f^{-n}\tilde{S}^{*}\rangle\,, \tag{2.52g}$$

where the prime is a derivative with respect to the radial coordinate in the operator, here r^*. For our purposes, we have $f = r(r^*)$ and $n = +3$, and we need the derivatives $f' = \mathrm{d}r/\mathrm{d}r* = \Delta/(a^2+r^2)$ and

$$f'' = \frac{\partial}{\partial r^*}\frac{\Delta}{a^2+r^2} = \frac{\Delta}{a^2+r^2}\frac{2M\left(r^2-a^2\right)}{\left(a^2+r^2\right)^2}\,. \tag{2.53}$$

2.2.4 Radial sector: pseudo-spectral method

All of the angular operators (multiplying by a function, e.g. $\cos\theta$, and taking derivatives, e.g. $\partial_{\tilde{\phi}}$ and $\widetilde{\bar{\eth}\eth}$) have been transformed into sparse operators in spectral space. This is amenable to numerical simulation simply by choosing some sufficiently high

maximum $\ell_{\max}$ and truncating the angular harmonics higher than that value. As motivated in Sec. 2.1.5, we will address the radial sector with the pseudo-spectral or collocation method.

Under the umbrella of pseudo-spectral methods there is still the choice of collocation points, or equivalently, the choice of basis functions used to represent the data. Corresponding to each choice of basis functions is a different representation of the derivative operator, which in general is a dense $N_r \times N_r$ matrix, with N_r the number of radial collocation points (or spectral coefficients). However, two choices of basis functions avoid dense derivative operators: the Fourier and Chebyshev bases. That the Chebyshev basis has this property follows from the Chebyshev polynomials being re-mapped Fourier basis functions,

$$T_n(\cos\theta) = \cos(n\theta)\,, \tag{2.54}$$

so the sparsity of the derivative operator in the Chebyshev basis follows from the sparsity of the derivative operator in the Fourier basis. The other ingredient which makes the derivative operator sparse in the Fourier and Chebyshev bases is the ability to perform a fast Fourier transform (FFT). Calculating a derivative then corresponds to going into the spectral domain with an FFT (which costs $\mathcal{O}(N_r \log N_r)$), calculating a derivative (which costs $\mathcal{O}(N_r)$), and then transforming back to the collocation (grid points) domain. The derivative calculation in a Fourier or Chebyshev basis is thus only $\mathcal{O}(N_r \log N_r)$, compared with the typically $\mathcal{O}(N_r^2)$ cost in a generic basis. The basis transformations and derivative operations are laid out below.

Fourier basis

The discrete Fourier transform (DFT) is defined on N complex data points labeled $\{f_j\}_{j=0}^{N-1}$, at standard grid points $\{x_j = j\}_{j=0}^{N-1}$. The basis functions, in the convention of FFTW [60, 66], are

$$e_k(x) = e^{+2\pi i k x/N}\,, \quad k = 0 \ldots N-1\,. \tag{2.55}$$

These basis functions are orthogonal (but not normalized) under the discrete integral, i.e. the sum over grid points. Then the DFT is defined as

$$\tilde{f}_k = \sum_{j=0}^{N-1} f_j e_k^*(x_j) = \sum_{j=0}^{N-1} f_j e^{-2\pi i jk/N} , \tag{2.56a}$$

and the "inverse" as

$$f_j = \sum_{k=0}^{N-1} \tilde{f}_k e^{+2\pi i jk/N} . \tag{2.56b}$$

Applying successively Eq. (2.56a) and Eq. (2.56b) results in an overall multiplication by N which must be divided out. The DFT may be computed in $\mathcal{O}(N \log N)$ time with the fast Fourier transform (FFT), making use of the factorization of the transform into two transforms of smaller size.[3]

The coefficients $\tilde{f}_k$ are arranged so that the first $\lceil N/2 \rceil$ coefficients are positive frequencies and the remaining ones negative. To take a derivative of a function in the Fourier representation, the function's Fourier coefficients are multiplied by a factor proportional to k. This factor is clear from the derivatives of the basis functions,

$$\frac{d}{dx} e_k(x) = \begin{cases} 2\pi i \frac{k}{N} e_k(x) & k \leq \lfloor N/2 \rfloor \\ 2\pi i \frac{N-k}{N} e_k(x) & k > \lfloor N/2 \rfloor \end{cases} . \tag{2.57}$$

Therefore the derivative is calculated as

$$\left(\widetilde{\frac{df}{dx}} \right)_k = \begin{cases} 2\pi i \frac{k}{N} \tilde{f}_k & k \leq \lfloor N/2 \rfloor \\ 2\pi i \frac{N-k}{N} \tilde{f}_k & k > \lfloor N/2 \rfloor \end{cases} . \tag{2.58}$$

The above derivative calculation is appropriate on the standard domain of $\{x_j = j\}_{j=0}^{N-1}$. One may apply an affine transformation to change the domain to $\{x_j = x_{\min} + j\Delta x\}_{j=0}^{N-1}$, with $\Delta x = (x_{\max} - x_{\min})/(N-1)$ (such that the smallest grid point has value $x_0 = x_{\min}$

[3]This is true even for sizes N which are not multiples of 2. For a size with a factorization $N = pq$, the DFT may be decomposed into p DFTs of size q and q DFTs of size p.

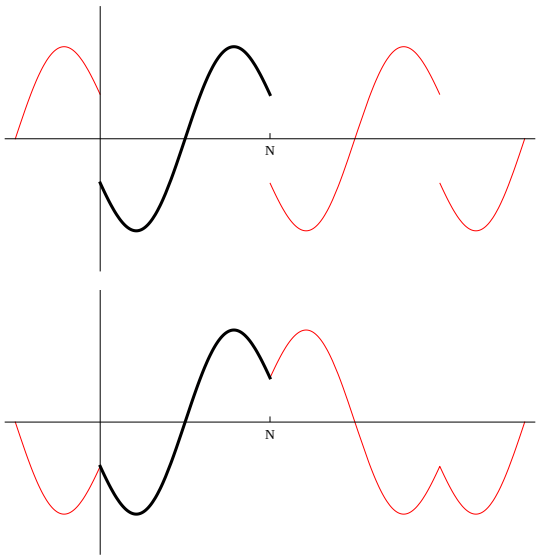

Figure 2-1: A function (in black) on the domain $[0, N]$ and its extension (in red) to the whole real line. In the top panel, the extension uses the Fourier basis, resulting in a jump discontinuity at the boundary. In the bottom panel, the extension uses the discrete cosine basis, leading to continuity at the boundary (but a discontinuity in the first derivative).

and the largest grid point value is $x_{N-1} = x_{\max}$). Then the derivative is found as

$$\left(\widetilde{\frac{df}{dx}}\right)_k = \begin{cases} 2\pi i \frac{k}{N} \frac{N-1}{x_{\max}-x_{\min}} \tilde{f}_k & k \leq \lfloor N/2 \rfloor \\ 2\pi i \frac{N-k}{N} \frac{N-1}{x_{\max}-x_{\min}} \tilde{f}_k & k > \lfloor N/2 \rfloor \end{cases} . \tag{2.59}$$

Though simple and generally useful, the Fourier basis is actually adapted to periodic boundary conditions, i.e. $f_{i+N} = f_i$; that is, the Fourier series representation of a function on a compact domain defines an extension of the function to the whole real line (see Fig. 2-1). However, for the problem at hand, there is no reason that the value of ψ at the left and right boundaries should be equal. This results in a jump discontinuity for the Fourier extension of the function. The Fourier representation of a step function only has *algebraic* convergence in Fourier coefficients: the power in the k coefficient goes as $\tilde{f}_k \propto 1/k$. In general, for a function with a jump discontinuity in the p^{th} derivative, the convergence of the spectral representation is algebraic with slope $\tilde{f}_k \propto k^{p-1}$. An infinitely differentiable function, on the other hand, has

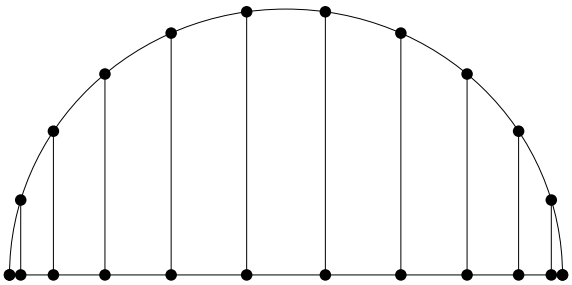

Figure 2-2: The Chebyshev-Gauss-Lobatto collocation points. Points are equally spaced in angle on the semicircle over the domain $[-1, 1]$. The collocation points come from projecting down the co-ordinates. Figure inspired by Fig. 4.4 of [28].

geometric convergence, $\tilde{f}_k \propto e^{-\mu k}$ for some number μ [28]. To recover this potentially geometric convergence, other bases should be considered.

Chebyshev basis

The basis of Chebyshev polynomials $T_n(x)$ is complete and orthonormal on $x \in [-1, +1]$ with integration kernel $w(x) = (1 - x^2)^{-1/2}$. This corresponds to Gaussian quadrature with the *collocation* points given by [126]

$$x_j = \cos\left(\frac{j\pi}{N-1}\right), \quad j = 0 \ldots N-1\,, \tag{2.60}$$

which is the Chebyshev-Gauss-Lobatto grid (the grid includes the endpoints of the domain). The collocation points can be visualized as in Fig. 2-2. Note that here x_0 corresponds to the rightmost grid point and x_{N-1} is the leftmost grid point. A function with values f_j on this grid can be written as a linear combination of basis polynomials as

$$f_j = \sum_{k=0}^{N-1} \tilde{f}_k T_k(x_j) = \sum_{k=0}^{N-1} \tilde{f}_k \cos\left(k\frac{j\pi}{N-1}\right)\,, \tag{2.61a}$$

from the identity $T_n(\cos\theta) = \cos(n\theta)$, and where the spectral coefficients can be found from the Gaussian quadrature

$$\tilde{f}_k = \frac{1}{N-1}\sum_{j=0}^{N-1}{}'' f_j T_k(x_j) = \frac{1}{N-1}\sum_{j=0}^{N-1}{}'' f_j \cos\left(k\frac{j\pi}{N-1}\right), \tag{2.61b}$$

where the prime on the summation means that the first and last terms of the sum are multiplied by $\frac{1}{2}$ in accordance with the trapezoidal rule for Gaussian quadrature.

Notice that Eqs. (2.61a) and (2.61b) are identical up to an overall scaling of $\frac{1}{N-1}$ and the factors of $\frac{1}{2}$ on the first and last terms of the sum in Eq. (2.61b). One can therefore use a convention where instead the first and last Chebyshev coefficients are replaced with twice their values and the sum in Eq. (2.61a) replaced with a "primed" sum $\sum''$ as in Eq. (2.61b) to compensate,

$$f_j = \sum_{k=0}^{N-1}{}'' \tilde{f}'_k T_k(x_j), \tag{2.62}$$

and where $\tilde{f}'_k = \tilde{f}_k$ for $k = 1 \ldots N-2$ and $\tilde{f}'_k = 2\tilde{f}_k$ for $k = 0, k = N-1$. Then, besides the scaling by $\frac{1}{N-1}$, both operations are achieved by the first type of discrete cosine transform (the so-called DCT-I [60]). The DCT, like the Fourier transform, can also be computed in $\mathcal{O}(N \log N)$ time by breaking it up into subproblems of smaller size and combining their results.

The derivative $\frac{d}{dx}T_n(x)$ of a Chebyshev polynomial, when expanded in the Chebyshev basis, has contribution from all lower polynomials of opposite parity; that is, the derivative has a dense expansion in this basis rather than a sparse one. However, the use of a recurrence relationship can reduce the time for calculating the derivative to $\mathcal{O}(N)$. This recurrence is

$$2T_n(x) = \frac{1}{n+1}\frac{d}{dx}T_{n+1}(x) - \frac{1}{n-1}\frac{d}{dx}T_{n-1}(x). \tag{2.63}$$

For a fixed expansion order N (i.e. having N coefficients), the expansion $\tilde{f}'_k$ clearly has no contribution from T_N, T_{N+1}, or higher. Therefore the derivative of the expansion,

$\left(\widetilde{\frac{df}{dx}}\right)'_k$ has no coefficient in front of T_{N-1}, T_N, or higher. This is enough to start the recurrence calculation for the expansion of the derivative [31],

$$\left(\widetilde{\frac{df}{dx}}\right)'_{N-1} \leftarrow 0\,, \tag{2.64a}$$

$$\left(\widetilde{\frac{df}{dx}}\right)'_{N-2} \leftarrow (N-1)\tilde{f}'_{N-1}\,, \qquad \text{(because coefficients are "primed")} \tag{2.64b}$$

$$\left(\widetilde{\frac{df}{dx}}\right)'_{k-1} \leftarrow \left(\widetilde{\frac{df}{dx}}\right)'_{k+1} + 2k\tilde{f}'_k\,, \qquad k = (N-2)\ldots 1\,, \tag{2.64c}$$

[but note that Eq. (2.64b) differs from Eq. (6) of Broucke [31] since his largest coefficient is not "primed"]. The above derivative calculation takes place on the standard grid given in Eq. (2.60) which goes from $[-1, +1]$. The Chebyshev series expansion can be applied on any compact domain $[x_{\min}, x_{\max}]$ through an affine transformation; then the derivative calculation must be multiplied overall by the Jacobian of this affine tranformation, which is simply a factor of $\frac{2}{x_{\max}-x_{\min}}$.

The advantage of the Chebyshev basis is that it does not impose a periodic boundary condition as the Fourier basis does. This means that each endpoint can have an arbitrary value (and arbitrary first derivative) without affecting spectral convergence. The Chebyshev basis also greatly increases the resolution near the boundary—the grid spacing towards either boundary goes as N^{-2}, as compared to the N^{-1} spacing of the Fourier basis. While this can be beneficial, it is also potentially problematic for a hyperbolic (time-evolution) problem. Typically, the stability of a hyperbolic problem is controlled by the size of the time step δt. The size of the stability region is controlled by the largest eigenvalue of the time-evolution operator, which in turn comes from the largest eigenvalue of the spatial derivative operator. This in turn comes from the finest spatial scale which is resolved—i.e. from the grid spacing. The net result is that a Chebyshev code unfortunately requires a much smaller time step than a Fourier code, and therefore more wall clock time per simulation time. One potential approach to alleviate this unfortunate situation is to use *domain decomposition*, where the domain of the simulation is subdivided into several intervals, each of which is covered with a Chebyshev grid, and the domains passing information be-

tween each other. Domain decomposition is beyond the scope of this work and is left as a potential future improvement to this technique.

Discrete cosine/sine basis

One returns then to evenly spaced grids, but with different boundary conditions than the Fourier basis. One approach is to use the discrete cosine basis, which extends compactly-supported functions to the real line in a way different than Fourier series. The boundary conditions of the discrete cosine basis are such that the extension of a function to the real line is even about both of the endpoints of its domain, i.e. for a function f defined on $x \in [x_{\min}, x_{\max}]$, the function is even about both $x = x_{\min}$ and $x = x_{\max}$. If f is continuous on $[x_{\min}, x_{\max}]$, then the extension is automatically continuous on the real line. The derivative of this extension has the opposite parity at each endpoint, and is therefore a sine series rather than a cosine series (see Fig. 2-1).

For discretely sampled functions, there are actually several basis choices. These are described by i) parity at each endpoint (4 choices total) and ii) whether the point of parity (or reflection) is on a sampled grid point or midway *between* sampled grid points (another factor of 2), leading to a total of 8 basis choices altogether. These are the DCT and DST of types I, II, III, and IV, each with their own conventions. As mentioned in Sec. 2.2.4, the Chebyshev transform is accomplished with a DCT-I, which is its own inverse (up to a factor of $N-1$). The DCT-II and DCT-III are each others' inverses (up to a factor of N), as are the DST-II and DST-III. The remaining transforms are all self-inverting (up to a factor of N).

To implement a DST/DCT basis, one needs a cosine and sine transform (and their inverses) which have the same points of parity. In practice we use the conventions of FFTW [60, 66], presented below. All of the transforms are on the standard grid of $\{x_j = j\}_{j=0}^{N-1}$. The DCT-II (named REDFT10 in FFTW) has even parity about the points $x = -1/2$ and $x = N - 1/2$, and is defined as

$$\tilde{f}_k^+ = 2 \sum_{j=0}^{N-1} f_j \cos[\pi(j + 1/2)k/N] \,. \tag{2.65a}$$

The DCT-III (REDFT01) has even parity about $k = 0$ and odd parity about $k = N$, and is defined as

$$f_j = \tilde{f}_0^+ + 2\sum_{k=1}^{N-1} \tilde{f}_k^+ \cos[\pi k(j+1/2)/N]\,. \tag{2.65b}$$

The DST-II (RODFT10) has odd parity about $x = -1/2$ and $x = N - 1/2$, and is defined as

$$\tilde{f}_k^- = 2\sum_{j=0}^{N-1} f_j \sin[\pi(j+1/2)(k+1)/N]\,. \tag{2.65c}$$

Finally, the DST-III (RODFT01) has odd parity about $k = -1$ and even parity about $k = N - 1$, and is defined as

$$f_j = (-1)^j \tilde{f}_{N-1}^- + 2\sum_{k=0}^{N-2} \tilde{f}_k^- \sin[\pi(k+1)(j+1/2)/N]. \tag{2.65d}$$

The transforms have been written in such a way that the DCT-II and DST-II are used to go into the spectral domain (labeled by k), and the DCT-III and DST-III return to the values at grid points (labeled by j), dividing by $2N$ to normalize the transforms. The derivative of a cosine series is performed in the spectral domain, resulting in a sine series, and vice versa. The basis functions for the DCT-II are

$$e_k^+(x) = \cos\left(\pi k(x+1/2)/N\right) \qquad\qquad k = 0 \ldots N-1\,, \tag{2.66a}$$

and the basis functions for the DST-II are

$$e_k^-(x) = \sin\left(\pi(k+1)(x+1/2)/N\right) \qquad\qquad k = 0 \ldots N-1\,. \tag{2.66b}$$

Taking derivatives of the basis functions yields

$$\frac{d}{dx} e_k^+(x) = \left(-\frac{\pi k}{N}\right) e_{k-1}^-(x) \tag{2.67a}$$

$$\frac{d}{dx} e_k^-(x) = \left(+\frac{\pi(k+1)}{N}\right) e_{k+1}^+(x)\,. \tag{2.67b}$$

The derivative calculation is as follows. Start with samples of the function f_j at the grid point x_j. Construct the cosine series $\tilde{f}_k^+$ by applying the DCT-II. Take the derivative, resulting in the *sine* series $\left(\widetilde{\frac{df}{dx}}\right)_k^-$, given by

$$\left(\widetilde{\frac{df}{dx}}\right)_k^- = \left(-\frac{\pi(k+1)}{N}\right)\tilde{f}_{k+1}^+ \,, \tag{2.68}$$

and where $\left(\widetilde{\frac{df}{dx}}\right)_{N-1}^- = 0$. Then the sine series may be transformed back to grid points via the DST-III.

Similarly, one may start with a sine series $\tilde{f}_k^-$. Taking a derivative results in the *cosine* series $\left(\widetilde{\frac{df}{dx}}\right)_k^+$, given by

$$\left(\widetilde{\frac{df}{dx}}\right)_k^+ = \left(\frac{\pi k}{N}\right)\tilde{f}_{k-1}^- \,, \tag{2.69}$$

and where $\left(\widetilde{\frac{df}{dx}}\right)_0^+ = 0$. As mentioned earlier, these derivatives are all calculated on the standard grid $\{x_j = j\}_{j=0}^{N-1}$. Again one can make an affine transformation to a grid with $x_0 = x_{\min}$, $x_{N-1} = x_{\max}$; and on this grid all of the derivative calculations must be multiplied by an overall factor of the Jacobian, $\frac{N-1}{x_{\max}-x_{\min}}$.

2.2.5 Numerical representation, computational complexity

In Section 2.2.2, we showed how to treat the Teukolsky equation's angular sector spectrally, discretizing it; this discretization may be truncated at some sufficiently high $\ell_{\max}$ for simulation on a computer. In Section 2.2.4, we showed how to treat the radial sector with the pseudospectral/collocation approach: derivatives calculated in the spectral domain, and multiplying by radial functions performed on collocated grid points (where the residual of the truncated spectral series vanishes). The numerical

state of the field ψ can now be represented as an $N_r \times N_\ell$ array of coefficients

$$\psi(t) = \begin{bmatrix} \langle\psi(t, r_0^*)|\ell_{\min}\rangle & \langle\psi(t, r_0^*)|\ell_{\min}+1\rangle & \dots & \langle\psi(t, r_0^*)|\ell_{\max}\rangle \\ \langle\psi(t, r_1^*)|\ell_{\min}\rangle & \langle\psi(t, r_1^*)|\ell_{\min}+1\rangle & \dots & \langle\psi(t, r_1^*)|\ell_{\max}\rangle \\ \vdots & \vdots & \ddots & \vdots \\ \langle\psi(t, r_{N_r-1}^*)|\ell_{\min}\rangle & \langle\psi(t, r_{N_r-1}^*)|\ell_{\min}+1\rangle & \dots & \langle\psi(t, r_{N_r-1}^*)|\ell_{\max}\rangle \end{bmatrix} \tag{2.70}$$

where the s, m indices have been suppressed in the basis kets as they are the same for all elements. This is an element of the vector space $\mathcal{F} \equiv \mathcal{R}_{N_r} \times \mathcal{A}_{N_\ell}$ where $\mathcal{R}_{N_r}$ is the vector space of (complex) radial functions discretized at N_r points, and $\mathcal{A}_{N_\ell}$ is the space spanned by the first N_ℓ angular harmonics of spin-weight s and azimuthal number m of complex functions on the 2-sphere with m-fold azimutal symmetry.

Now we can discuss how the different operators act in this representation. An angular operator such as $\cos\theta$, ∂_ϕ or $\bar{\eth}\eth$ is represented by a square $N_\ell \times N_\ell$ matrix (with matrix elements given in Sec. 2.2.1). Acting with an angular operator in this representation amounts to multiplication from the right by the transpose of the matrix (though all the matrices we deal with are symmetric, so the transpose has no effect). For example,

$$\begin{aligned} \bar{\eth}\eth\psi = &\begin{bmatrix} \ddots & \vdots & \\ \dots & \langle\psi(t, r_j^*)|\ell_I\rangle & \dots \\ & \vdots & \ddots \end{bmatrix} \times \\ &\times \begin{bmatrix} (s-\ell_{\min})(\ell_{\min}+s+1) & 0 & \dots \\ 0 & (s-\ell_{\min}-1)(\ell_{\min}+s+2) & 0 \\ \vdots & 0 & \ddots \end{bmatrix}. \end{aligned} \tag{2.71}$$

In general, this would scale as $\mathcal{O}(N_r N_\ell^2)$. However, all of the angular operators involved are sparse in the basis of spin-weighted spherical harmonics. Therefore such operations only cost $\mathcal{O}(N_r N_\ell)$.

Multiplying by a radial function $f(r^*)$ is accomplished by multiplying each *row* r_j^* by the value $f_j = f(r_j^*)$. This, too, can be represented by a matrix operator: this

time a square $N_r \times N_r$ diagonal matrix which acts from the left,

$$f(r^*)\psi = \begin{bmatrix} f_0 & 0 & \dots \\ 0 & f_1 & 0 \\ \vdots & 0 & \ddots \end{bmatrix} \times \begin{bmatrix} \ddots & \vdots & \\ \dots & \langle \psi(t, r_j^*) | \ell_I \rangle & \dots \\ & \vdots & \ddots \end{bmatrix} . \tag{2.72}$$

This operation clearly scales as $\mathcal{O}(N_r N_\ell)$.

Transforming into the spectral domain may too be represented by a square matrix acting from the left, but this matrix would not be sparse. Instead, each column (a fixed-ℓ subspace over $\mathcal{R}$) is individually transformed with a fast Chebyshev transform, FFT, or DCT/DST;[4] this is $\mathcal{O}(N_\ell N_r \log N_r)$. As shown in Sec. 2.2.4, for each of the bases considered, taking a derivative when in the spectral representation is an $\mathcal{O}(N_r)$ operation for each column, and therefore also $\mathcal{O}(N_r N_\ell)$. For the FFT basis, taking a derivative corresponds to multiplying each row by a factor given in Eq. (2.59). This can be treated as matrix multiplication from the left by a diagonal matrix where the k^{th} element on the diagonal is proportional to the wavenumber of the k^{th} radial basis element. For the Chebyshev basis, the derivative must be computed by starting at the bottom row of the array and applying the recursion relation in Eq. (2.64), working upward through the array. For the DCT/DST bases, the derivative corresponds to shifting the whole array up or down by one row (and filling the top/bottom row with zeros), and then multiplying each row by the appropriate factor given in Eq. (2.67) (which can also be represented by multiplying from the left by a diagonal matrix); always keeping track of whether the array represents a cosine or sine series.

There are three ingredients necessary for good scaling: sparsity of angular operators, fast pseudospectral transformations, and fast derivative calculations. As long as all three of these requirements are met, then the asymptotic scaling is dominated by the pseudospectral transformation: $\mathcal{O}(N_\ell N_r \log N_r)$ per timestep.

[4]Here a practical matter is important for implementation on a real computer. An FFT (or DCT or fast Chebyshev transform) will be fastest if the data being transformed are contiguous in memory, thus avoiding cache misses and allowing vectorization. Therefore, radial grid points should be adjacent in memory; this is called "column-major" storage order for the array presented in Eq. (2.70).

2.2.6 Time evolution: Method of lines

Thus far we have discussed the angular and radial sectors, but not the temporal sector. Starting with the infinite dimensional function space of complex functions with m-fold symmetry on S_2 over $r^* \in (-\infty, +\infty)$, we have truncated the angular space to be only N_ℓ dimensional over each r^*, truncated the radial domain to $r^* \in [r^*_{\rm min}, r^*_{\rm max}]$, and further discretized the radial domain to be N_r dimensional, represented either by the N_r values at the collocation points or equivalently by the N_r spectral coefficients which have no residual at those collocation points.

We now have an $N_r N_\ell$ dimensional function space $\mathcal{F}$ with a well-posed initial-value problem. That there exists a well-posed IVP comes from the hyperbolicity of the Teukolsky equation [and can simply be read off of the principal part of the differential operator in e.g. Eqs. (2.41), (2.47), (2.50), and Eq. (2.52)].

A point in the function space labeled by time t corresponds to a field configuration $\psi(t)$. The solution to the PDE is a curve $\psi : t \to \mathcal{F}$ in the function space, which is a sequence of field configurations evolving over time. In a sense, the PDE has become an "ODE" on the function space (this viewpoint can only be taken for PDEs with a well-posed IVP).

Leaving the temporal direction continuous while discretizing the spatial directions is sometimes referred to as the "method of lines," with each "line" coupled to the others, since the resulting solution has support on a set of timelike lines in the $t - r$ space. Evolving this "ODE" can be approached with any standard ODE technique such as the Runge-Kutta method or Adams-Bashforth-Moulton predictor-corrector method. These methods can be either explicit or implicit, and with a fixed time step or adaptive time step.

Regardless of whether the method is explicit or implicit, there is no guarantee of stability, though implicit methods ought to be more stable. This author is unaware of any analytical results on the stability of numerical methods for simulating perturbations to a Kerr spacetime. Even the stability of the continuum limit (no discretization) is an open question—the available results are for per-mode stability [156]

or for $|a| \ll M$ [49]. Regardless of the lack of analytic results, the experience of earlier numerical simulations suggests that the problem is stable [140] with certain steppers.

In practice we use the ODE drivers available in the GNU Scientific Library (GSL) [75]. The only "Jacobian"-free implicit method available in the GSL is the multi-step Adams-Bashforth-Moulton predictor-corrector method. To use any of these drivers, the system must be put into first-order (in time) form. Order reduction is always possible by introducing auxiliary variables which are derivatives of the field variables.

Starting with our generic second order equation with field u, introduce the auxiliary variable which is the field "velocity" $v \equiv \partial_t u$. Then the original system

$$\left[A^{tt}\partial_t^2 + A^{tr}\partial_t\partial_r + A^{rr}\partial_r^2 + B^t\partial_t + B^r\partial_r + C\right] u = 0 \tag{2.73}$$

can be rewritten as the system of two first-order (in time) equations in two fields, u and v,

$$\partial_t u = v \tag{2.74a}$$

$$\partial_t v = -\left(A^{tt}\right)^{-1}\left[A^{tr}\partial_r v + A^{rr}\partial_r^2 u + B^t v + B^r\partial_r u + Cu\right] . \tag{2.74b}$$

Note that for our purposes, A^{tt} is a symmetric, positive-definite, pentadiagonal matrix. It can therefore be decomposed as $A^{tt} = LDL^T$ where L is a lower triangular matrix with all elements on the main diagonal equal to 1, D is a diagonal matrix of definite signature (positive in this case), and L^T is the transpose of L. Furthermore, L has only one subdiagonal, since A^{tt} has two. The system can be efficiently solved by forward- and back-substitution in $\mathcal{O}(N_\ell)$ per radial grid point (if A^{tt} was dense, this would instead be quadratic in N_ℓ). These sparse matrix routines are available in most linear algebra systems; we use the Eigen template matrix library [59]. The LDL^T decomposition is slightly better than the classical Cholesky decomposition (i.e. LL^T) since it avoids square roots of diagonal elements and is defined for both positive- and negative-definite matrices (but not indefinite matrices).

The system is now in a standard first order form,

$$\frac{d}{dt} f_j = F_j \left(t, \vec{f} \right) \tag{2.75}$$

which is expected by generic ODE integation routines such as those in the GSL. The index j is actually a super-index running over both u and v, the radial index, and the angular mode numbers.

2.2.7 Boundary conditions

The spatial boundary of our domain is non-empty, and therefore our hyperbolic PDE also requires boundary conditions (BCs). Physically, we do not want waves entering our spatial domain from infinity ($r^* \to +\infty$) or from the event horizon ($r^* \to -\infty$). The conditions to impose are called outgoing BCs or absorbing BCs.

Mathematically, we want to ensure that only rightgoing (respectively leftgoing) waves are supported at the right (respectively left) boundary. This is straightforward for the simplest of wave equations: consider the non-dispersive, non-dissipative scalar wave equation

$$\left[\partial_t^2 - c^2 \partial_x^2 \right] \psi = 0 \,, \tag{2.76}$$

for some real number c. The differential operator may be directly factored into first order differential operators which have leftgoing and rightgoing waves in their kernels,

$$\left(\partial_t + c\partial_x \right) \left(\partial_t - c\partial_x \right) \psi = 0 \,. \tag{2.77}$$

A wave in the kernel of either operator is a solution of Eq. (2.76). Then at the rightmost boundary of the domain x_R, one can impose the boundary condition

$$\partial_t \psi_R = -c\partial_x \psi_R \tag{2.78}$$

which is solved only by rightgoing waves $\psi = \exp\left(i\omega t - ikx\right)$ (and with the opposite sign for the leftmost boundary).

For a general wave equation with dispersion and dissipation, one can not impose a first order boundary condition which absorbs *all* wavenumbers without reflection. What made it possible to impose Eq. (2.78) for all wavenumbers is the linearity of the associated dispersion relation $\omega(k)$, or equivalently that the phase velocity $c(k) = \omega(k)/k$ is constant in k. Ideally, one would allow $\omega(k)$ to act not only on real numbers k but also on operators, constructing the general boundary condition

$$\frac{1}{i}\frac{\partial}{\partial t}\psi = \omega_+\left(\frac{1}{-i}\frac{\partial}{\partial x}\right)\psi\,, \tag{2.79}$$

where ω_+ gives the rightgoing dispersion relationship. However, such an operator would have spatial derivatives of arbitrarily high order.

In general, though, the phase velocity $c(k)$ asymptotes to a constant in the limit as $k \to \infty$. This constant is the instantaneous slope of *characteristics* of the wave equation in the $t-x$ plane. Equivalently, the dispersion relationship $\omega_+(k)$ asymptotes to a linear function $\omega_+(k) \approx c_\infty k$, where $c_\infty \equiv \lim_{k\to\infty} \frac{\omega_+(k)}{k}$.

An equivalent way to identify the speed of characteristics is to look only at the principal part of a differential operator, i.e. the highest order derivative operators. The principal part of the Teukolsky operator in the form presented in Eq. (2.52) is

$$\mathrm{Pr}\left[(\Delta\mathcal{T}_s)_{fn}\right] = \tilde{A}^{*tt}_{fn}\partial_t^2 + \tilde{A}^{tr*}_{fn}\partial_{tr} + \tilde{A}^{r*r*}_{fn}\partial^2_{r*} \tag{2.80}$$

$$\mathrm{Pr}\left[(\Delta\mathcal{T}_s)_{fn}\right] = \left[\left(a^2+r^2\right)^2 - a^2\Delta\sin^2\theta\right]\partial_t^2 - \left(a^2+r^2\right)^2\partial^2_{r*}\,. \tag{2.81}$$

In some sufficiently small region about a boundary of the domain, the solution should consist of some linear combination of N_ℓ purely outgoing plane wave modes with speeds c_j and mode shapes $|v_j\rangle$, where each mode individually satisfies

$$\mathrm{Pr}\left[(\Delta\mathcal{T}_s)_{fn}\right]\exp\left[i\omega\left(t - c_j^{-1}r*\right)\right]|v_j\rangle = 0\,, \tag{2.82}$$

and where the mode shapes are normalized $\langle v_j|v_j\rangle = 1$. These speeds and mode shapes are found by operating with the differential operator,

$$\left\{\left[\left(a^2+r^2\right)^2 - a^2\Delta\sin^2\theta\right] - \left(a^2+r^2\right)^2 c_j^{-2}\right\}\omega^2|v_j\rangle = 0\,. \tag{2.83}$$

This is an eigenvalue problem,

$$\left[I - \frac{a^2\Delta}{\left(a^2+r^2\right)^2}\sin^2\theta\right]|v_j\rangle = c_j^{-2}|v_j\rangle\,. \tag{2.84}$$

The operator $S \equiv I - a^2\Delta\sin^2\theta/\left(a^2+r^2\right)^2$ is symmetric and positive definite at all values of r. It is non-degenerate except when spin vanishes and at the horizon and $r=\infty$. The splitting in the spectrum is somewhat small, though. It can be estimated from the splitting in the spectrum of $\sin^2\theta$, which has a typical splitting on the order of $\delta\sin^2\theta \approx 1/N_\ell$; thus the splitting in the spectrum of S is given approximately by $\delta S \approx a^2\Delta/\left[N_\ell\left(a^2+r^2\right)^2\right]$, where Δ and r are evaluated at the boundary (either the left or right boundary).

Given that the operator S is non-degenerate (except for $a=0$ and at the horizon and spatial infinity), the eigenvalues c_j^{-2} are all unique, and S may be diagonalized; there are no degenerate subspaces, so the eigenvectors may be orthonormalized, $\langle v_j|v_k\rangle = \delta_{jk}$. Since the eigenvalues are all positive, the eigenvectors are all real and the transformation matrix O to go into the diagonal basis is an orthogonal matrix, $S = O^T D O$, with D a diagonal matrix with the j^{th} diagonal component c_j^{-2}. Then in the standard basis of $|s,\ell,m\rangle$ vectors, the transformation matrix O is given by

$$O = \sum_{j=0}^{N-1} |s,\ell_{\min}+j,m\rangle\langle v_j|\,, \tag{2.85}$$

i.e. the j^{th} column is given by the j^{th} eigenvector.

The j^{th} modeshape satisfies the rightgoing-only first order "scalar" (for only this component) equation

$$\left[\frac{\partial}{\partial t} + c_j\frac{\partial}{\partial r^*}\right]\psi = 0\,. \tag{2.86}$$

Then if one were in the diagonal basis, the vector wave equation

$$\left[\frac{\partial}{\partial t} + \begin{pmatrix} c_0 & & \\ & c_1 & \\ & & \ddots \end{pmatrix} \frac{\partial}{\partial r^*}\right] \psi = \left(\frac{\partial}{\partial t} + D^{-1/2}\frac{\partial}{\partial r^*}\right)\psi = 0 \tag{2.87}$$

would appropriately allow only rightgoing modes. This equation can be rotated back into the standard basis of $|s, \ell, m\rangle$ through the transformation matrix O,

$$\left(\frac{\partial}{\partial t} + OD^{-1/2}O^T\frac{\partial}{\partial r^*}\right)\psi = 0\,. \tag{2.88}$$

This condition, with O, D calculated at the location of the rightmost boundary, is the appropriate outgoing boundary condition at the right boundary. The same condition but with an opposite sign (and again with O, D calculated at the location of the leftmost boundary) is the outgoing boundary condition at the leftmost boundary.

2.3 Numerical experiments

We performed a number of numerical experiments to characterize the performance of the method. There are several questions one should ask about this numerical method which we address in this Section.

Figure 2-3 shows an example of the output from one numerical experiment. The output data are snapshots of the angular harmonics of the field across the radial grid, at various times. The simulation parameters for Fig. 2-3 were a radial grid $r^* \in [-70, 630]$ with 3072 evenly spaced grid points (and using the DCT/DST basis for derivative calculations); 16 angular harmonics were simulated in the range of $\ell \in [2, 17]$; the black hole spin was taken to be $a = 0$; the simulation was for the $m = 2$ mode of the field $r^3\Psi_{-2}$; the integration took place over the time span $t \in [0, 499]$ with $\Delta t = 0.002$, using the first order Adams-Bashforth-Moulton method. The initial conditions were a real gaussian in r^* centered at $r^* = 100$ with $\sigma = 25$, and amplitude in the ℓ^{th} harmonic $A_\ell = 1/(\ell(\ell+1))$. The initial time derivative of

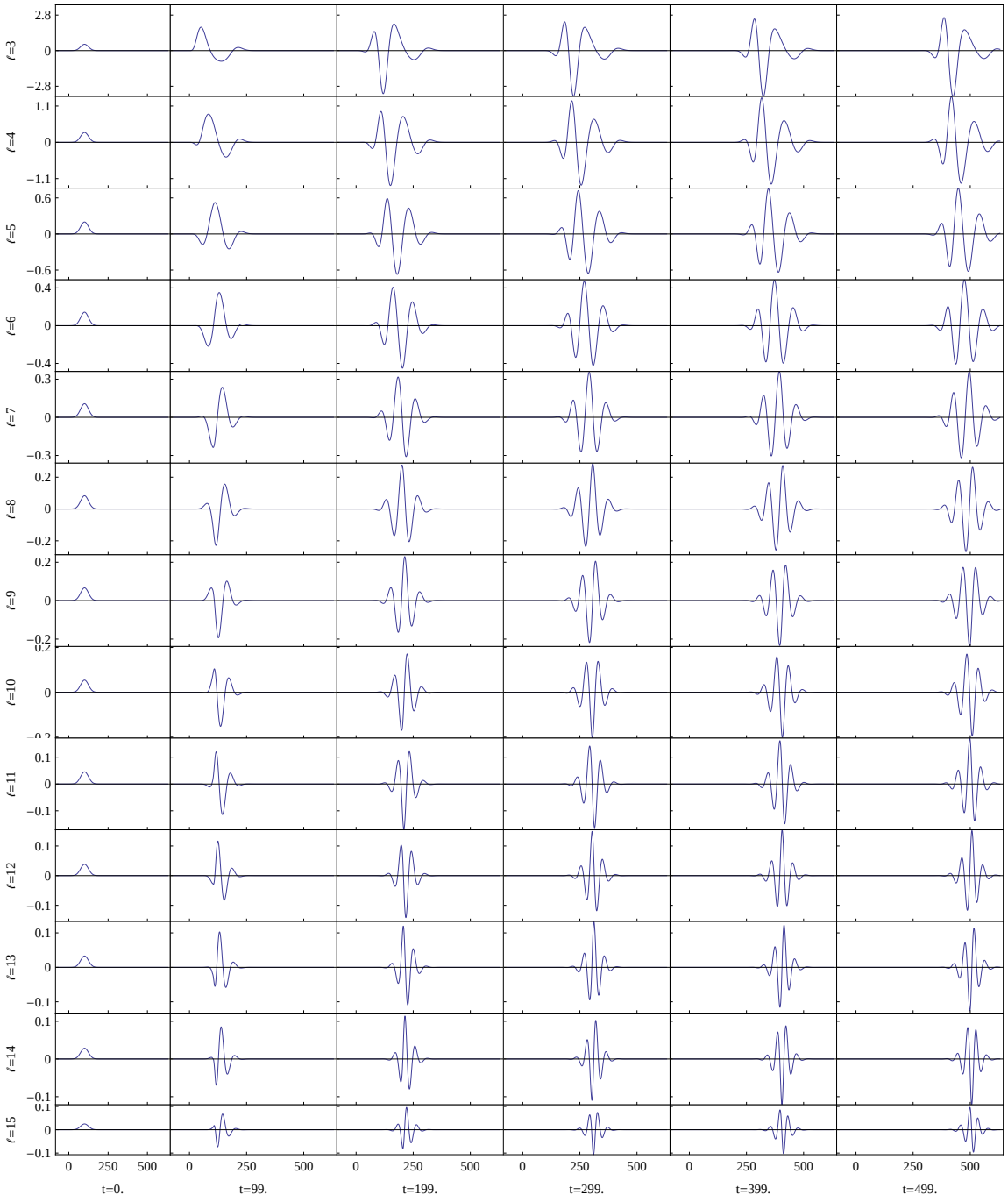

Figure 2-3: The evolution of an outgoing pulse of radiation. Each column is a different time slice ($t = 0, 99, 199, 299, 399, 499$) and each row is a different ℓ mode ($\ell \in [3, 15]$). The horizontal axis of each individual tile is $r^* \in [-70, 630]$ and the vertical axis is the real part of $r^{-3}\Psi_{-2}$ for the $m = 2$ mode for a black hole with $a = 0$. The simulation was performed with 3072 grid points spaced evenly in r^*, using the DCT/DST bases for derivatives, using the first order Adams-Bashforth-Moulton time stepping routine with $\Delta t = 0.002$. The initial conditions were a Gaussian in r^* centered at $r^* = 100$, with $\sigma = 25$, with amplitude in the ℓ^{th} mode $A_\ell = 1/(\ell(\ell + 1))$. The initial field velocity was chosen as if the wave was a right-going solution to the flat wave equation $\partial_t^2 - \partial_{r^*}^2 = 0$ with velocity 1.

the field corresponds to a right-going solution to the flat wave equation $\partial_t^2 - \partial_{r^*}^2 = 0$ with unit spatial velocity.[5]

There are several wave phenomena visible in Fig. 2-3. The most apparent is dispersion: the gaussian contains multiple frequencies which each have differing phase velocities. Therefore the wave packet does not maintain its shape, leading to the multiple oscillations within the wave. Looking across the panels (going forward in time), you can observe the phase fronts moving within the wave packet (unfortunately, the time dimension on the plot is too coarsely sampled to make this motion obvious). Also visible are the differing group velocities amongst the various ℓ modes.

In Sec. 2.3.1, we suggest that the method converges in the pseudospectral sense. In Sec. 2.3.2, we study the power-law convergence of the method of lines. In Sec. 2.3.3, we observe the convergence of the numerical dispersion relationship. Finally, in Sec. 2.3.4, we observe the quasinormal ringing of the spacetime in order to compare with analytic results.

2.3.1 Pseudospectral convergence

The first question to ask is whether or not the method actually displays convergence in the pseudospectral sense, i.e. that the spectral coefficients have a geometric (exponential) decay at high k-number, as compared to algebraic (power-law).

Evidence to support pseudospectral convergence is presented in Figure 2-4. This figure presents the radial spectral components of the field after evolution for a time of $t = 100$, with initial data as described above. The salient feature is a straight line in the log-linear plot—which is exponential decay, i.e. pseudospectral convergence.

2.3.2 Temporal convergence

The time evolution in this scheme, the method of lines, is implemented in terms of an ODE integrator—in our case, the first order Adams-Bashforth-Moulton predictor-

[5]This is the asymptotic form, at large r^*, of the Teukolsky equation (in the conjugated form used in this work). Of course, because there is a well-posed IVP for the Teukolsky equation, any initial data will do. The goal of this type of initial data is to try to have a mostly right-going solution for simplicity.

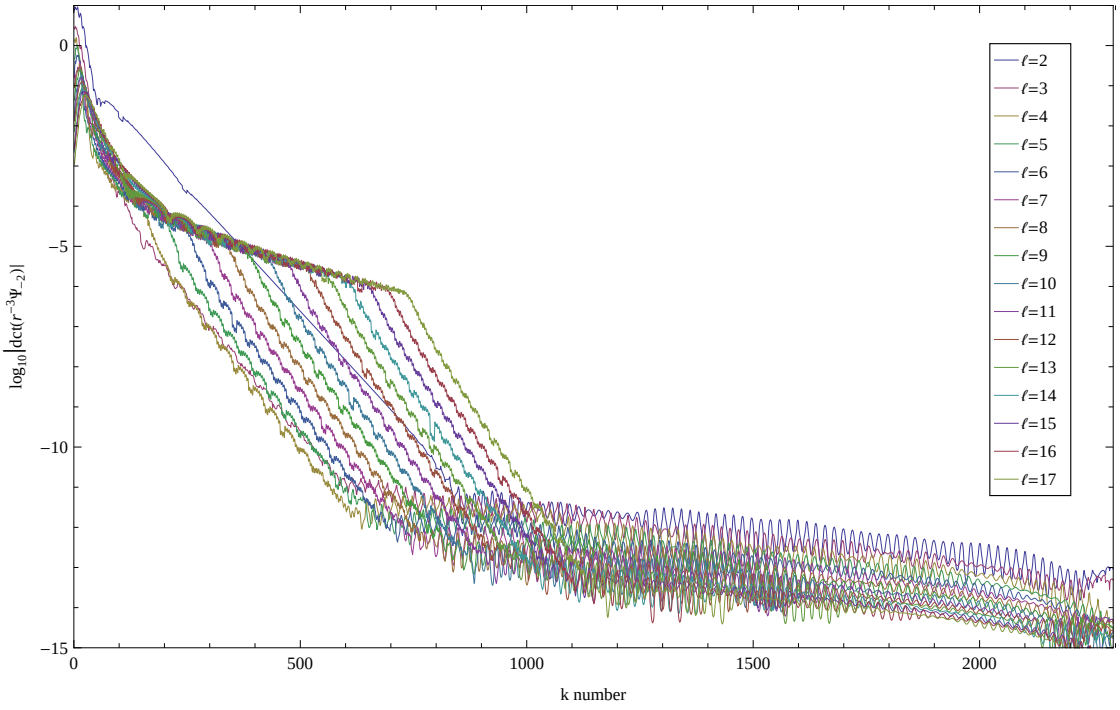

Figure 2-4: Pseudo-spectral convergence: Snapshot of the DCT-II of the field $r^{-3}\Psi_{-2}$ shows an exponential decay at sufficiently high k-number, where the solution becomes resolved. The snapshot was taken at $t = 100$. The initial conditions are the same as those described in Fig. 2-3. The simulation had parameters $a = 0$, $m = 2$, with 2304 radial points (or basis functions), using the DCT/DST basis. For legibility, the logs of the spectral data have been smoothed with a 10-point moving window average.

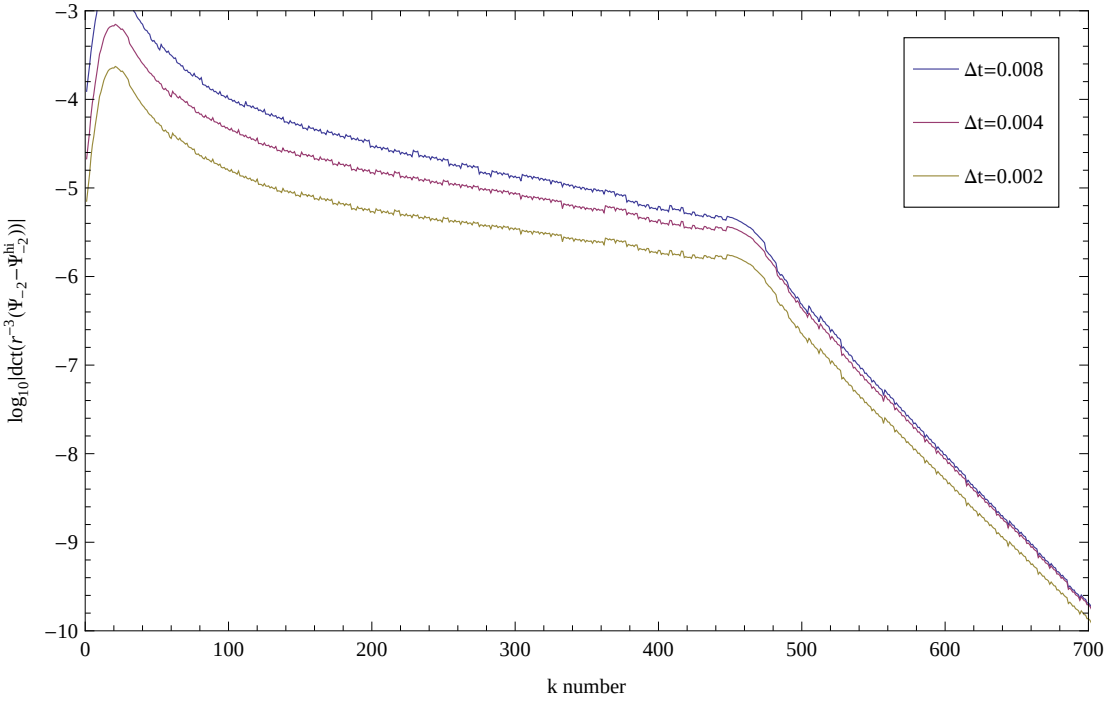

Figure 2-5: Temporal convergence: The $\ell = 11$ mode after $t = 198.$, compared against $\Delta t = 0.001$. The vertical axis is the error between the highest temporal resolution run ($\Delta t = 0.001$) and the stated temporal resolution (from top to bottom, $\Delta t = 0.008, 0.004, 0.002$). A more careful analysis suggests linear convergence with Δt at low k numbers. For legibility, the logs of the spectral data have been smoothed with a 30-point moving window average.

corrector method. The convergence with respect to choice of timestep Δt is tied to this scheme. Since it is first order in time (meaning errors are of order $\mathcal{O}(\Delta t^2)$), one should expect to see exactly this polynomial dependence as one varies the timestep.

To test the temporal convergence, several integrations were performed with all parameters and initial conditions fixed but varying the timestep Δt. The initial conditions are the same as those described above; the grid had 3072 points and 16 angular harmonics ($\ell = [2, 17]$). Data from the $\ell = 11$ mode (arbitrarily chosen) are plotted in Fig. 2-5 from runs with different Δt, after evolving for $t = 198$. Plotted are the differences between the highest temporal resolution run (at $\Delta t = 0.001$) and three lower resolution runs (from top to bottom, $\Delta t = 0.008, 0.004, 0.002$).

Numerical experiments suggestion linear convergence with Δt at low k numbers where the spectral representation has significant power. Each mode in k space seems to have a different convergence coefficient in front of Δt.

2.3.3 Phase errors/dispersion relation

One of the main motivations for this work was to improve the phase accuracy of the extracted gravitational waveforms, since gravitational wave detection relies so heavily on phase sensitivity. One way of judging the convergence of the numerical dispersion relationship is to run several simulations with only the spatial resolution varying and compare their outputs. Such a comparison is presented in Figure 2-6.

Several simulations with identical initial conditions (as described before) but different spatial resolution were integrated for $t = 498$ to try to accrue as much phase difference as possible.

This numerical experiment suggests that the convergence of the numerical phase relationship is extremely good. At the scale of the waveform itself (top panel in Fig. 2-6), it is impossible to make out any difference between the results of simulations at different resolutions. To suss out any difference, the waveforms were interpolated with 5-point interpolating polynomials in order to compare across the differing grids. The differences between the interpolating polynomials are presented in the bottom

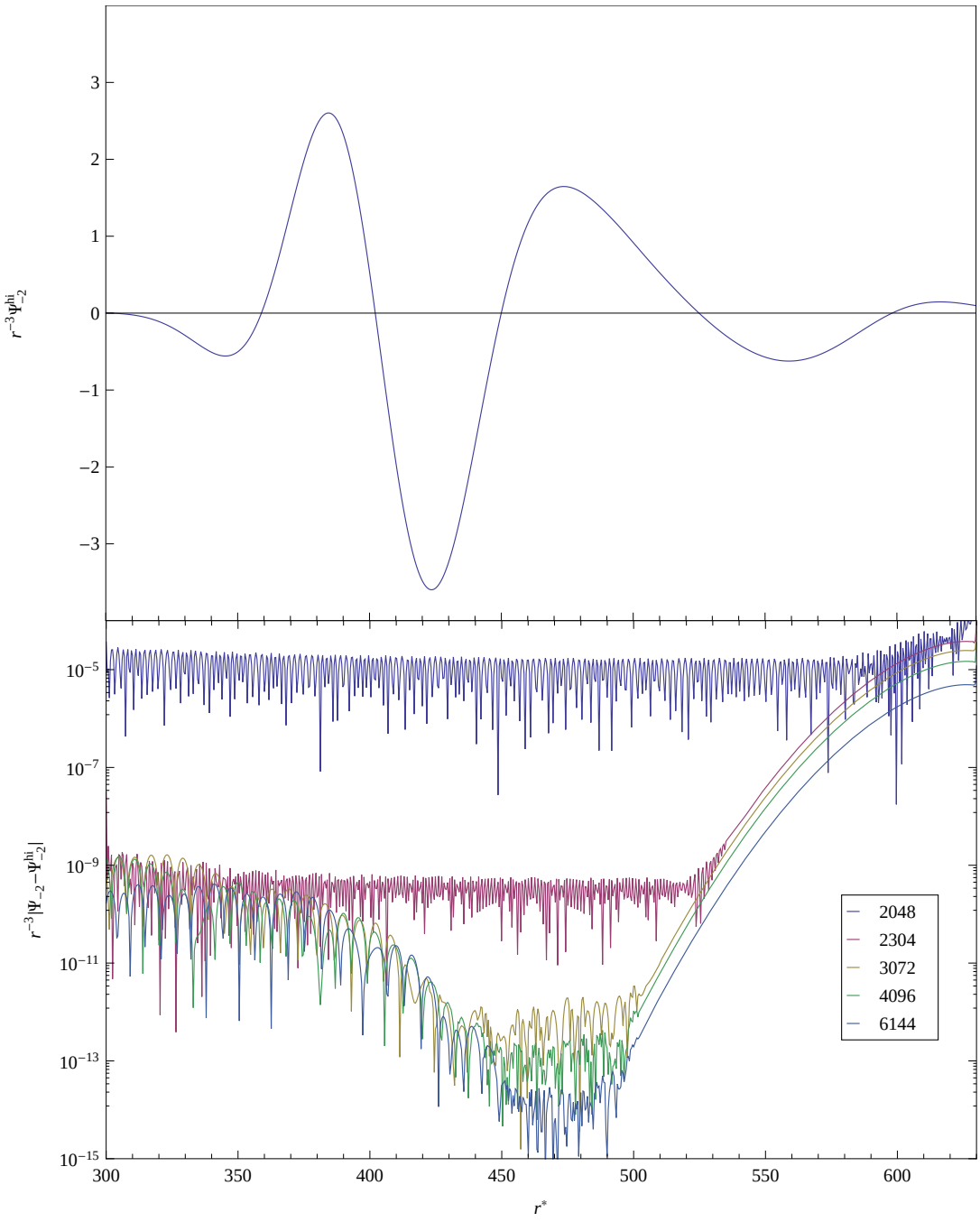

Figure 2-6: Convergence in dispersion relation. Top panel: The field $r^{-3}\Psi_{-2}$ in the $m = 2, \ell = 3$ mode after evolving for $t = 498$ with initial data as before and $a = 0$. All resolutions look identical at this scale. Bottom panel: The differences between various resolutions and the highest resolution (8192 grid points). From top to bottom, the resolutions are 2048, 2304, 3072, 4096, and 6144. Since all runs have different grids, the field is interpolated between grid points with 5-point interpolating polynomials. The artefact at right is likely a spurious reflection off of the domain boundary.

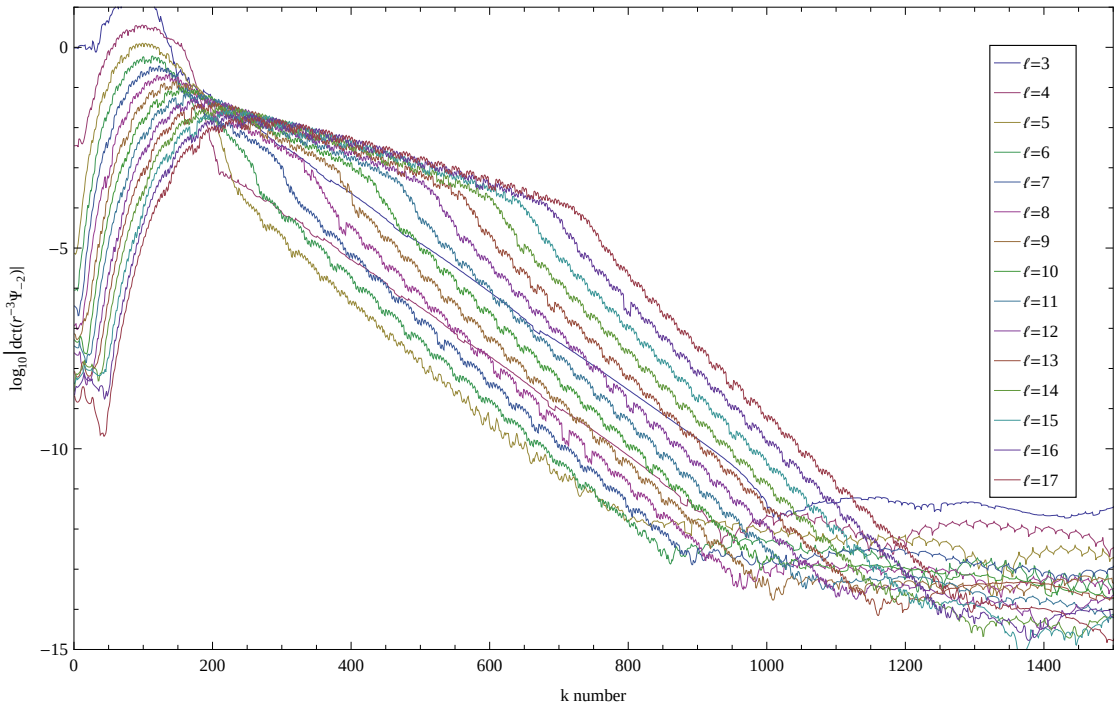

Figure 2-7: Spectral convergence with quasinormal ringing: Same as Fig. 2-4 but with an initially ingoing pulse as described in Sec. 2.3.4. The field snapshot is taken at $t = 100$.

panel of Fig. 2-6. That the differences are so small is a sign of the convergence of the numerical dispersion relation.

2.3.4 Quasinormal ringing

Quasinormal (QN) frequencies can be calculated from the Teukolsky equation without resorting to time-domain integration; they are found in the process of separating the equation in the frequency domain. There is already a large body of literature (see e.g. [17]) which has calculated the real and imaginary quasinormal mode (QNM) frequencies which can be used for validation of our numerical method.

To excite QNMs, a different set of initial conditions were used. Rather than an outgoing pulse of radiation, an *ingoing* pulse was used, since most of the ringing is generated near the light ring (near $r^* = 0$). The initial conditions were again a gaussian in r^*, but this time centered at $r^*_c = 15$ with a width of $\sigma = 5$, and again amplitude in the ℓ^{th} harmonic $A_\ell = 1/(\ell(\ell+1))$. The time derivative of the field

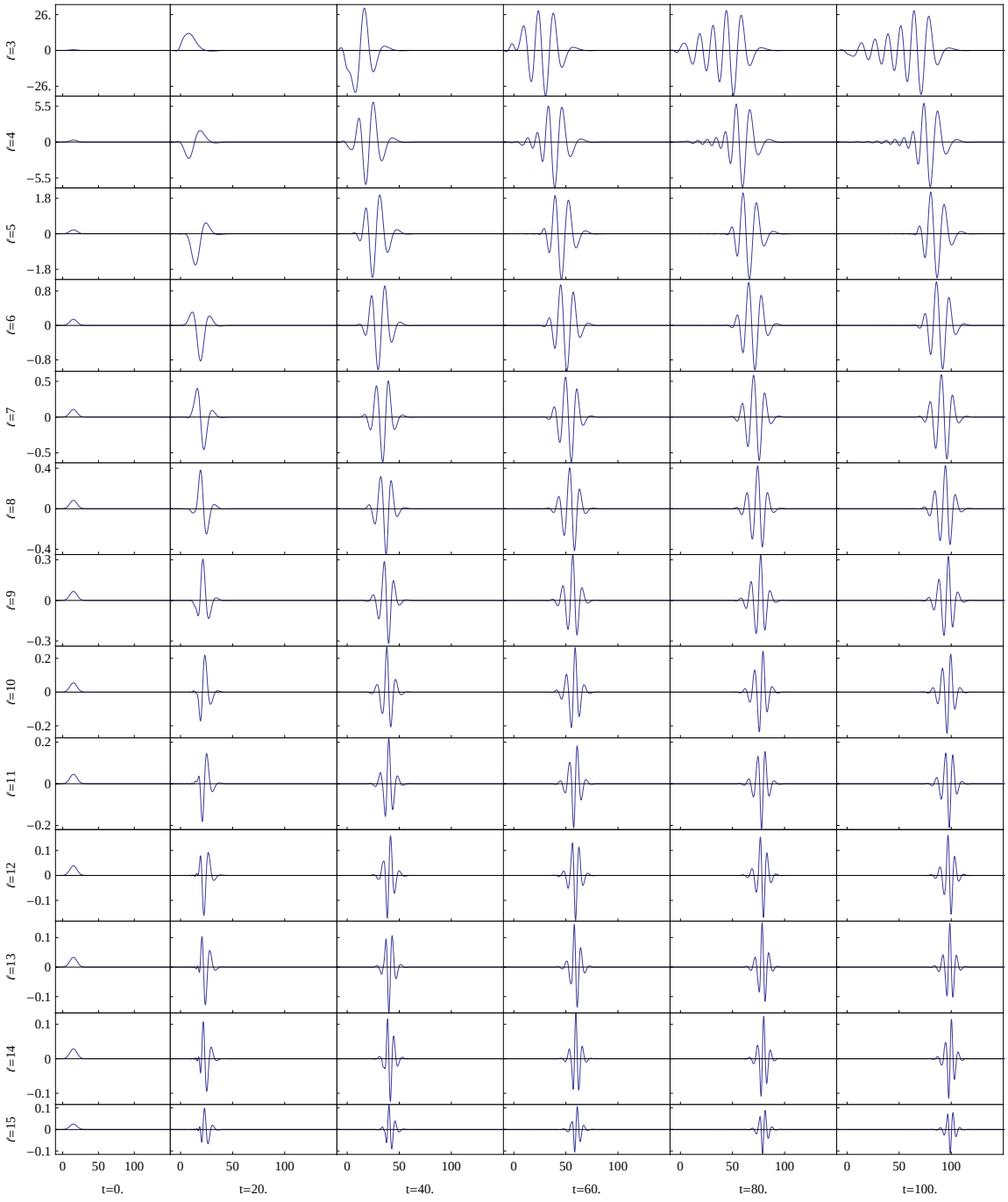

Figure 2-8: A reflected pulse with quasinormal ringing tails: Same as Fig. 2-3 but for an initially ingoing pulse, as described in Sec. 2.3.4.

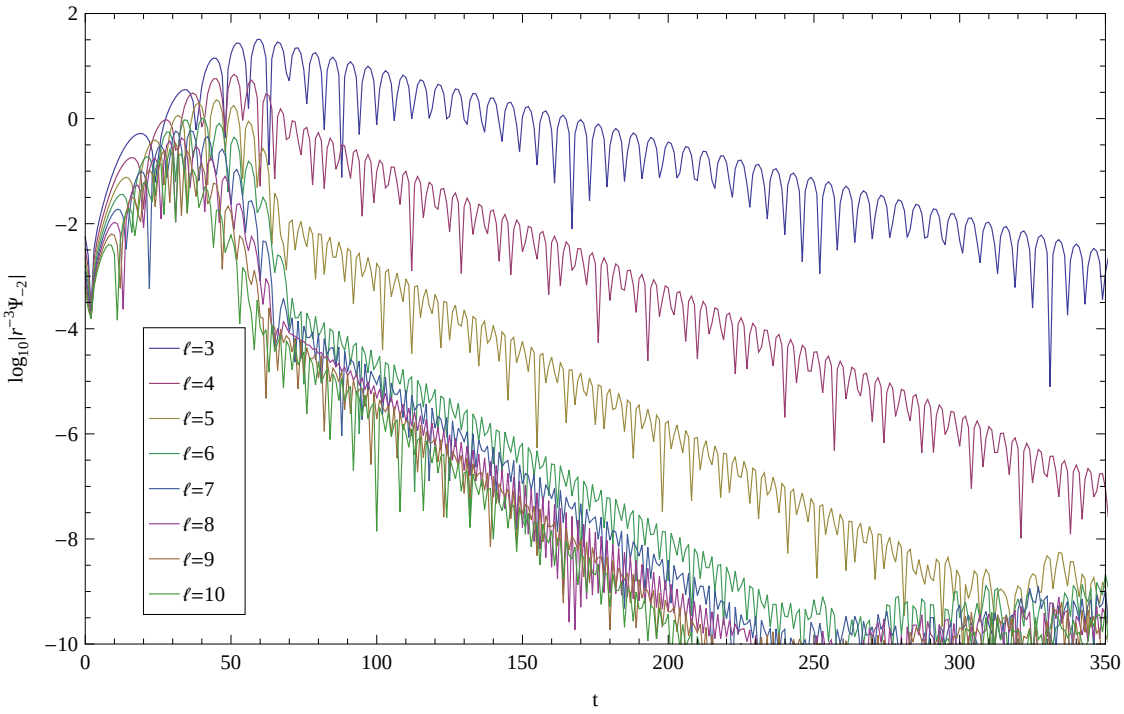

Figure 2-9: Quasinormal ringing: The reflected pulse of radiation has exponentially decaying tails, which are a proxy for the QN mode frequencies. Extracting the field at a fixed radius of $r^* = 30$ and letting time pass allows one to see the exponential decay. Higher ℓ modes damp more quickly, so reading downward is monotonically increasing in $\ell \in [3, 10]$.

was chosen as if this was a purely leftgoing solution of $\partial_t^2 - \partial_{r^*}^2 = 0$, so there are both leftgoing and rightgoing parts in the Teukolsky equation. This is not a problem, though, since the QN ringing is seen in the reflection of the ingoing pulse, and this reflection is not contaminated by the originally outgoing pulse. The run parameters were as before, $a = 0$, $\ell \in [2, 17]$, $r^* \in [-70, 630]$, with 4096 points in r^*, and $t \in [0, 499]$ with $\Delta t = 0.002$. The integrator exhibits exponential convergence wih ingoing data as well, as illustrated in Fig. 2-7. A snippet of the timeseries can be seen in Fig. 2-8.

One can clearly see an exponentially damped tail following the reflected wave packets in the top two rows. This exponential decay can be examined more closely by "extracting" the waveform at a fixed r^* as time passes. This is clearly visible in Fig. 2-9, which was extracted at a radius of $r^* = 30$. You can clearly see the pulse arriving at around $t = 50$ (time enough for the pulse to go from the initial position

of $r_c^* = 15$ to the light ring near $r^* = 0$ and back to the extraction radius at $r^* = 30$), followed by the exponentially damping tail. Higher ℓ modes have slower decay times, so reading downward in Fig. 2-9 is monotonically increasing in ℓ. The decay time seems to asymptotes to a constant at large ℓ.

From the numerical simulation, decay times could be extracted and compared against QN frequencies in the literature. Unfortunately, our decay times seem to be quite a bit off from those in [17]. This is likely a symptom of an error in the integrator. Note also that the $\ell = 2$ mode has anti-damping, rather than damping; another sign that there is a bug in the code.

2.4 Future work

Several avenues of improvement and extensions to the work are open. Four possibilities are expounded upon below: in Sec. 2.4.1, including a higher order implicit method; in Sec. 2.4.2, using hyperbolic slicing to include future null infinity in the domain and obviate the need for boundary conditions; in Sec. 2.4.3, using domain decomposition to allow using the Chebyshev basis with a reasonable Courant condition; and finally, in Sec. 2.4.4, introducing the source term, which is essential for generating EMRI waveforms. This list is by no means exhaustive, but is simply meant to highlight some of the research which we intend to pursue in the future.

2.4.1 Higher order implicit method

Due to reliance upon the GSL for ODE steppers, the only implicit, Jacobian-free method available is the Adams-Bashforth-Moulton predictor-corrector method. The implementation in the GSL can adaptively vary in order, though this order-varying only takes place when the method is driven with an adaptive step size and automatic error control. For the studies at hand, using a fixed time step is preferable (for ease of control). Furthermore, the Adams method seems to have a bug wherein it attempts to change the order by more than one at a time, resulting in an internal inconsistency

and terminating the integration. Therefore for technical reasons, this code is limited to a first order implicit method.

A higher order implicit method would be a straightforward improvement. This would require switching to another ODE driver package, such as the odeint [109] package; or alternatively, reinventing the wheel and writing a stepper by hand. Either way, this is not a fundamental limitation of the technique presented here and would be straightforward to implement.

2.4.2 Hyperbolic slicing

Any numerical integration on a computer must take place on a finite number of grid points (or basis functions), and both the grid point coordinates and values of the fields must be finite numbers (representable with floating point numbers). This automatically limits the simulation to take place on a compact domain. However, the observables in the EMRI problem (waveforms) are extracted at asymptotic future null infinity.

One might ask, "why not compactify the radial coordinate, bringing infinity in to a finite radial coordinate?" There is a fundamental flaw in this approach, though. On a slice of constant t, an outgoing plane wave solution has an infinite number of zero crossings between any finite radial coordinate and spatial infinity. Trying to compactify the radial coordinate would introduce an essential singularity in the domain of calculation, which can never be expressed with any finite number of basis functions or grid points. An example of this type of essential singularity is displayed in Fig. 2-10.

A promising recent proposal goes by the name of hyperbolic slicing or hyperboloidal compactification [187, 188]. For a hyperbolic wave equation, an initial value problem exists only for a *Cauchy surface*, which has a timelike normal everywhere. Typically this Cauchy surface is taken to be surfaces of constant coordinate time t for some convenient coordinate—in the case of Kerr, often the Boyer-Lindquist coordinate time t.

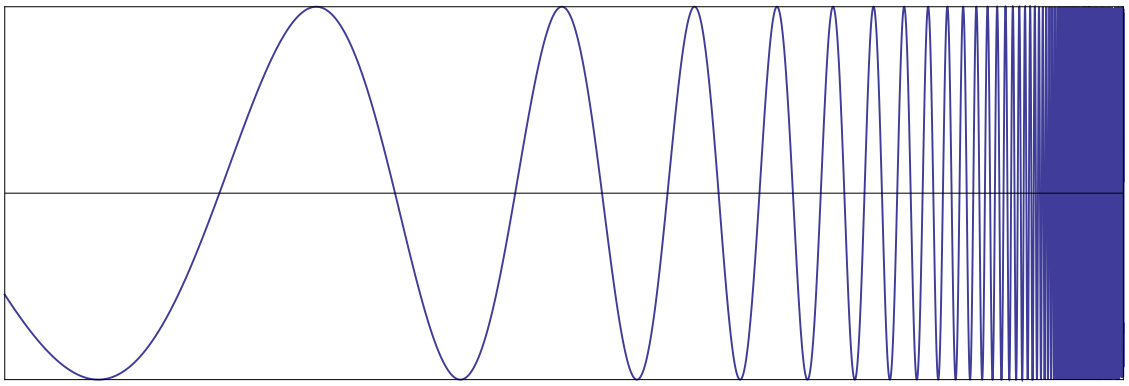

Figure 2-10: An example of the type of essential singularity resulting from radial compactification for a hyperbolic wave equation. This problem is alleviated by using hyperbolic slicing.

However, a perfectly good Cauchy surface is one which asymptotes to being tangent to a characteristic (null ray) as one approaches spatial infinity. Asymptotically approaching infinity, the characteristics also become lines of constant *phase* for outgoing waves. When sliced with an asymptotically null Cauchy surface, outgoing waves no longer experience an infinite number of oscillations approaching infinity. Instead, they asymptote to a constant. There is then no problem with compactifying the radial domain when using an asymptotically null slicing.

To change coordinates to such a slicing can again be considered a transformation along the lines of Eqs. (2.47), (2.50), or Eq. (2.52). Following [188], define a radial compactification with a conformal factor Ω through

$$r = \frac{\rho}{\Omega(\rho)}\,, \quad \Omega(S) = 0\,, \quad \Omega'(S) \neq 0\,, \tag{2.89}$$

where $\Omega'(\rho) \equiv d\Omega/d\rho$ and $\rho = S$ corresponds to the $r = \infty$ limit. Then define a time transformation via a "height function" $h(r)$,

$$\tau \equiv t - h(r) \quad \text{and} \quad \tau - \rho = t - r \tag{2.90}$$

$$\Longrightarrow h = r - \rho = \frac{\rho}{\Omega} - \rho \tag{2.91}$$

$$H \equiv \frac{dh}{dr} = 1 - \frac{\Omega^2}{\Omega - \rho\Omega'}\,. \tag{2.92}$$

Then transforming derivatives, $\partial_t = \partial_\tau$, $\partial_r = -H\partial_\tau + (1-H)\partial_\rho$. Turning this into a coefficient transformation, if one started with coefficients A^{tt}, A^{tr}, A^{rr}, B^t, B^r, and C, one would find

$$A^{\tau\tau} = A^{tt} - HA^{tr} + H^2 A^{rr} \tag{2.93a}$$

$$A^{\tau\rho} = (1-H)\left(A^{tr} - 2HA^{rr}\right) \tag{2.93b}$$

$$A^{\rho\rho} = (1-H)^2 A^{rr} \tag{2.93c}$$

$$B^\tau = B^t - HB^r - (1-H)H'A^{rr} \tag{2.93d}$$

$$B^\rho = (1-H)\left(B^r - H'A^{rr}\right) \tag{2.93e}$$

$$C = C\,. \tag{2.93f}$$

Note that this transformation preserves the sparsity of angular operators, so this slicing has the same computational complexity as claimed in Sec. 2.2.5. Zenginoglu and Khanna used

$$\Omega = 1 - \left(\frac{\rho - \rho_{\text{Tr.}}}{S - \rho_{\text{Tr.}}}\right)^4 \Theta(\rho - \rho_{\text{Tr.}})\,, \tag{2.94}$$

so that to the left of the transition point $\rho_{\text{Tr.}} < S$, one would have $\Omega = 1$ and the slicing would coincide with constant t slicing. The fourth power in Ω is to ensure a sufficiently high number of vanishing derivatives in Ω at the transition point.

In this scheme, one would then not need to do any extraction to future null infinity: it is included in the computation domain at $\rho = S$. Zenginoglu and Khanna [188] have studied the differential equation approaching the endpoint and found it to be regular, and needing no boundary condition, which is somewhat remarkable. This can be understood by looking at the speeds of leftgoing and rightgoing characteristics in the $\tau - \rho$ coordinates. Approaching the boundary, the incoming wave speed approaches 0, taking on that value exactly at the boundary. Exactly at the boundary, the partial differential equation should become an ODE, obviating the need for a boundary condition.

2.4.3 Domain decomposition

Both the Fourier and DCT/DST bases make unphysical assumptions about boundary conditions of the field. The only basis considered which both admits an $\mathcal{O}(N \log N)$ spectral transformation and an $\mathcal{O}(N)$ derivative which does not make unphysical assumptions on the BCs is the Chebyshev basis (thus ensuring geometric, rather than algebraic, convergence). Unfortunately, the Chebyshev basis results on $\mathcal{O}(N^{-2})$ grid point spacing approaching the boundary, leading to a Courant condition which similarly scales as $\mathcal{O}(N^{-2})$.

One possible solution to this problem is domain decomposition. Rather than one global domain, the computational domain is split into M smaller domains Ω_j which each have N/M grid points and correspondingly N/M harmonic coefficients, typically at least $N/M = 8$ (the boundary between finite element methods and pseudospectral domain decomposition is somewhat blurry). The minimal grid spacing then becomes $\mathcal{O}(M^2 N^{-2})$, as does the Courant condition. The computational complexity of the pseudospectral transformation is $\mathcal{O}(N/M \log(N/M))$ in each subdomain, or $\mathcal{O}(N \log(N/M))$ overall. One then needs to ensure continuity between the subdomains Ω_j and Ω_{j+1} at the boundary, for both the field and some number of derivatives. Care needs to be taken to properly transmit information between adjacent domains. Such a technique has been implemented e.g. in [40].

2.4.4 Source term

This work has discussed only a source-free (homogeneous) integrator. Of course to generate EMRI waveforms, one needs to introduce a small body to perturb the spacetime of a SMBH, thus we need an inhomogenous integrator.

In the Teukolsky equation for Ψ_{-2}, where $\Delta \mathcal{T}_{-2} \Psi_{-2} = 4\pi \Delta \Sigma T_{-2}$ (where here $\Delta = r^2 - 2Mr + a^2$ and π is the real number), the source term is given in the

Newman-Penrose formalism as [146]

$$T_{-2} = (\widetilde{\Delta} + 3\gamma - \bar{\gamma} + 4\mu + \bar{\mu}) \left[(\bar{\delta} - 2\bar{\tau} + 2\alpha) T_{n\bar{m}} - (\widetilde{\Delta} + 2\gamma - 2\bar{\gamma} + \bar{\mu}) T_{\bar{m}\bar{m}} \right] + (\bar{\delta} - \bar{\tau} + \bar{\beta} + 3\alpha + 4\pi) \left[(\widetilde{\Delta} + 2\gamma + 2\bar{\mu}) T_{n\bar{m}} - (\bar{\delta} - \bar{\tau} + 2\bar{\beta} + 2\alpha) T_{nn} \right] , \quad (2.95)$$

where the null tetrad employed is the Kinnersley one, which in Boyer-Lindquist coordinates has components

$$l^{\mu} = \left[(r^2 + a^2)/\Delta, 1, 0, a/\Delta \right] \quad (2.96a)$$

$$n^{\mu} = \left[r^2 + a^2, -\Delta, 0, a \right] / (2\Sigma) \quad (2.96b)$$

$$m^{\mu} = \left[ia \sin\theta, 0, 1, i/\sin\theta \right] / \left[2^{1/2} (r + ia\cos\theta) \right] , \quad (2.96c)$$

which has the non-vanishing spin coefficients

$$\rho = -1/(r - ia\cos\theta) \quad (2.97a)$$

$$\beta = -\bar{\rho}\cot\theta/(2\sqrt{2}) \quad (2.97b)$$

$$\pi = ia\rho^2 \sin\theta/\sqrt{2} \quad (2.97c)$$

$$\tau = -ia\rho\bar{\rho}\sin\theta/\sqrt{2} \quad (2.97d)$$

$$\mu = \rho^2\bar{\rho}\Delta/2 \quad (2.97e)$$

$$\gamma = \mu + \rho\bar{\rho}(r - M)/2 \quad (2.97f)$$

$$\alpha = \pi - \bar{\beta} \quad (2.97g)$$

and where the scalar differential operators are $D = l^{\mu}\partial/\partial x^{\mu}$, $\widetilde{\Delta} = n^{\mu}\partial/\partial x^{\mu}$, and $\delta = m^{\mu}\partial/\partial x^{\mu}$ (note that in Eq. (2.95), $\widetilde{\Delta}$ is a differential operator and π is a spin coefficient).

The stress-energy tensor $T^{\alpha\beta}$ appearing in Eq. (2.95) is given by that of a point particle of mass m with world-line coordinates $\gamma : z^{\mu}(\lambda)$ and tangent vector $\dot{z}^{\mu}(\lambda)$,

namely [118],

$$T^{\alpha\beta}(x) = m \int_\gamma \frac{g^\alpha{}_\mu(x,z) g^\beta{}_\nu(x,z) \dot{z}^\mu \dot{z}^\nu}{\sqrt{-g_{\mu\nu}\dot{z}^\mu \dot{z}^\nu}} \delta^{(4)}(x,z) d\lambda \,, \tag{2.98}$$

with $g^\alpha{}_\mu(x,z)$ the bitensor of parallel transport and $\delta^{(4)}(x,z)$ a properly normalized 4-dimensional Dirac delta function.

Earlier approaches modeled the source term with a representation spread out over several grid points, satisfying some integration conditions for delta functions [140]. However, the source term is fundamentally divergent at the location of the particle. This should spoil the convergence of a spectral method.

First note that T_{-2} will need to be decomposed into $\tau_{s,\ell,m}(t,r)$ as in Eq. (2.38) by integrating against basis bras $\langle s,\ell,m|$. We can estimate the power in the ℓ^{th} component. First, note that a delta function on the sphere has equal power in all ℓ components. Next note that an angular derivative of a delta function can be rewritten as $\eth\delta$ plus lower order (in number of derivatives) parts. Thus evaluating the ℓ coefficient of p derivatives of a delta function can be evaluated by using integration by parts p times, moving all $\eth$'s onto the basis function ${}_sY_{\ell,m}$. Using the properties in Eqs. (2.11) and (2.12), we can see that the ℓ coefficient of $\partial^p\delta$ goes as

$$\langle s,\ell,m|\partial^p\delta\rangle \propto \ell^p \,. \tag{2.99}$$

For the source term T_{-2}, we have $p=2$—there is overall increasing power in higher ℓ components of $\tau_{s,\ell,m} \propto \ell^2$. This is likely offset by the faster exponential decay rate of higher ℓ modes of the field, so it is potentially not an issue.

The radial scaling has the same problem. A radial delta function has equal power in all k modes; the p^{th} derivative of a radial delta function will have power growing as $\propto k^p$ in the k^{th} pseudospectral coefficient of the function. How many derivatives of a delta function end up in the field Ψ_{-2}? The source term has $\partial^2\delta$ as the highest number of derivatives of a radial delta function (coming from the $\widetilde{\Delta}\widetilde{\Delta}T_{\bar{m}\bar{m}}$ term). This is to be equated to the Teukolsky operator acting on Ψ_{-2}, and the Teukolsky operator is

second order; therefore Ψ_{-2} needs only contain a delta function and Heaviside theta functions, not any derivatives of a delta function. The spectral convergence of Ψ_{-2} would be k^0.

There is, however, a technique to avoid this spectral catastrophe. This technique is called the "particle-without-particle" technique [40] or more formally the method of extended homogeneous solutions [77, 15]. The idea is rather straightforward: perform domain decomposition with a domain boundary at exactly the location of the particle. The solution has three parts,

$$\Psi_{-2} = \Psi_L \Theta(r_p(t) - r) + \Psi_P \delta(r - r_p(t)) + \Psi_R \Theta(r - r_p(t)) \,. \tag{2.100}$$

That is, the solution can be decomposed into a regular piece on the left, Ψ_L, a regular piece on the right, Ψ_R, and a delta function contribution at the location of the particle, Ψ_P. In a weak formulation, integrate

$$\int f \cdot (\Delta \mathcal{T}_{-2} \Psi_{-2} - 4\pi \Sigma \Delta T_{-2}) \, dr = 0 \,, \tag{2.101}$$

where f is a sufficiently smooth test function. This gives jump conditions (or Rankine-Hugoniot conditions) at the location of the particle: the magnitude of Ψ_P, the size of the jump $[\Psi]_{r_p} \equiv \Psi_R(r_p) - \Psi_L(r_p)$, the size of the jump in the first derivative, $[\Psi']_{r_p}$, etc.

Though this approach is probably workable, it may be prohibitively slow. At each time-step, the domains to the left and right of the particle need to be changed, the coefficients of the differential operator at the locations of the grid points recalculated, and so on. Still, this method warrants investigation.

2.5 Outlook

This Chapter has demonstrated a new numerical method for numerically integrating the source-free Teukolsky equation. The three main ingredients to the method are i)

a fully spectral decomposition of the angular sector, ii) a pseudo-spectral approach to calculating radial derivatives, and iii) evolution with the method of lines.

The method presented here shows exponential convergence in pseudospectral number, and polynomial convergence in timestep, as determined by the order of the ODE method employed in the method of lines. The convergence of the numerical phase relationship is excellent. Quasinormal ringing is observed, but deviates from published damping times; this deviation needs to be investigated further.

There is a plethora of future work. A higher order implicit method would improve the temporal convergence. Hyperbolic slicing will obviate the need for boundary conditions at $r^* = +\infty$ and allow direct waveform extraction at infinity. Domain decomposition will allow using the (preferable) Chebyshev basis without sacrificing with a tiny timestep. Finally, the source term needs to be included to actually integrate up EMRI waveforms, which should be possible by using the technique of extended homogenous solution with moving domain decompositions.

The gravity community has only just scratched the surface of the rich dynamics present in EMRIs. In order to use EMRIs as probes of strong gravity, we need to know that all of the effects are understood and under numerical control. But even if we understand all the physics that goes on in the strong field regime, simulations are meaningless unless the numerical methods employed do not contaminate the results and are well understood. This chapter is one small but crucial step in building high precision EMRI simulations.

Part II

Beyond general relativity

Chapter 3

Effective Gravitational Wave Stress-energy Tensor in Alternative Theories of Gravity[†]

Abstract

The inspiral of binary systems in vacuum is controlled by the stress-energy of gravitational radiation and any other propagating degrees of freedom. For gravitational waves, the dominant contribution is characterized by an effective stress-energy tensor at future null infinity. We employ perturbation theory and the short-wavelength approximation to compute this stress-energy tensor in a wide class of alternative theories. We find that this tensor is generally a modification of that first computed by Isaacson, where the corrections can dominate over the general relativistic term. In a wide class of theories, however, these corrections identically vanish at asymptotically flat, future, null infinity, reducing the stress-energy tensor to Isaacson's. We exemplify this phenomenon by first considering dynamical Chern-Simons modified gravity, which corrects the action via a scalar field and the contraction of the Riemann tensor and its dual. We then consider a wide class of theories with dynamical scalar fields coupled to higher-order curvature invariants, and show that the gravitational wave stress-energy tensor still reduces to Isaacson's. The calculations presented in this paper are crucial to perform systematic tests of such modified gravity theories through the orbital decay of binary pulsars or through gravitational wave observations.

[†]This chapter originally appeared as Stein, L. C., Yunes, N. (2011), *Effective gravitational wave stress-energy tensor in alternative theories of gravity*, Phys. Rev. D **83** 064038 [138].

3.1 Introduction

Feynman has argued that no matter how beautiful or elegant a certain theory is, or how authoritative its proponents, if it does not agree with experiments, then it must be wrong. For the past 40 years, this philosophy has been applied to gravitational theories with great success. Many modified gravity theories that were prominent in the 1970's, have now been essentially discarded, as they were found to disagree with Solar System experiments or binary pulsar observations [159]. Similarly, this decade is beginning to bring a wealth of astrophysical information that will be used to constrain new modified gravity theories. In fact, precision double binary pulsar observations [33, 91, 86] have already allowed us to constrain modified theories to exciting new levels [181, 167]. Future gravitational wave (GW) observations on Earth, with the Advanced Laser Interferometer Gravitational Observatory (aLIGO) [89, 1, 42], aVIRGO [154] and its collaborators, and in space, through the Laser Interferometer Space Antenna (LISA) [90, 128, 52, 51], will allow new precision tests of strong field gravity [134].

Such tests of alternative theories of gravity will be very sensitive to the motion of compact bodies in a regime of spacetime where gravitational fields and velocities are large, i.e. the so-called strong-field. Gralla [70] has shown that motion in classical field theories that satisfy certain conditions (the existence of a Bianchi-like identity and field equations no higher than second-order) is "universally" geodesic to leading-order in the binary system's mass-ratio, with possible deviations from geodesicity due to the bodies' internal structure. He also argues that one might be able to relax the second condition, as it does not seem necessary. In fact, motion in certain higher-order theories, such as Chern-Simons modified gravity [6], is already known to be purely geodesic to leading-order in the mass-ratio, without influence of internal structure due to additional symmetries in the theory.

Tests of modified gravity theories in the strong-field, however, not only require a prescription for the conservative sector of motion, but also of the dissipative sector, that which describes how the objects inspiral. Geodesic motion must thus be naturally

corrected by a radiation-reaction force that drives non-geodesic motion toward an ultimate plunge and merger [14]. Similarly, one can think of such motion as geodesic, but with *varying* orbital elements [125, 71, 123, 124, 122] (energy, angular momentum and Carter constant). The rate of change of such orbital elements is governed by the rate at which all degrees of freedom (gravitational and non-gravitational) radiate.

In the gravitational sector and to leading order in the metric perturbation, such a rate of change is controlled by an effective stress-energy tensor for GWs, first computed by Isaacson in General Relativity (GR) [78, 79]. In his approach, Isaacson expanded the Einstein equations to second order in the metric perturbation about an arbitrary background. The first-order equations describe the evolution of gravitational radiation. The second-order equation serves as a source to the zeroth-order field equations, just like a stress-energy tensor, and it depends on the square of the first-order perturbation. This tensor can then be averaged over several gravitational wavelengths, assuming the background length scale is much longer than the GW wavelength (the short-wavelength approximation). In this approximation, Isaacson found that the effective GW energy-momentum tensor is proportional to the square of first partial derivatives of the metric perturbation, i.e. proportional to the square of the gravitational frequency. Components of this stress-energy then provide the rate of change of orbital elements, leading to the well-known quadrupole formula.

Alternative theories of gravity generically lead to a modified effective GW stress-energy tensor. It is sometimes assumed that this stress-energy tensor will take the same form as in GR [107, 106], but this need not be the case. In GR, the scaling of this tensor with the GW frequency squared can be traced to the Einstein-Hilbert action's dependence on second-derivatives of the metric perturbation through the Ricci scalar. If the action is modified through the introduction of higher-powers of the curvature tensor, then the stress-energy tensor will be proportional to higher powers of the frequency. Therefore, the consistent calculation of the modified Isaacson tensor needs to be carried out until terms similar to the GR contribution (proportional to frequency squared) are obtained. This in turn implies that calculations of effective energy-momentum tensors in modified gravity theories to *leading-order in the GW*

frequency can sometimes be insufficient for determining the rate of change of orbital elements.

In this paper, we present a formalism to compute the energy-momentum tensor consistently in generic classical field theories. We employ a scheme where the action itself is first expanded in the metric perturbation to second order, and the background metric and metric perturbation are treated as independent fields. Varying with respect to the background metric leads to an effective GW stress-energy tensor that can then be averaged over several wavelengths. This produces results equivalent to Isaacson's calculation.

We exemplify this formulation by first considering CS gravity [6]. This theory modifies the Einstein-Hilbert action through the addition of the product of a scalar field with the contraction of the Riemann tensor and its dual. This scalar field is also given dynamics through a kinetic term in the action. The leading-order contribution to the CS-modified GW stress-energy tensor should appear at order frequency to the fourth-power, but Sopuerta and Yunes [137] have shown that this contribution vanishes at future null infinity.

We here continue this calculation through order frequency cubed and frequency squared and find that such CS modifications still vanish at future null infinity. This is because the background scalar field must decay at a certain rate for it to have a finite amount of energy in an asymptotically-flat spacetime. If one insists on ignoring such a requirement, such as in the case of the non-dynamical theory, then frequency-cubed CS modifications to the energy-momentum do not vanish.

We explicitly calculate such modifications for a canonical embedding, where the scalar field is a linear function of time in inertial coordinates. This is similar to previous work [76] that calculated another effective stress-energy tensor for the non-dynamical version of Chern-Simons. In this case, the dominant modification to the radiation-reaction force is in the rate of change of radiated momentum, which leads to so-called recoil velocities after binary coalescence. In GR, such recoil is proportional to the product of the (mass) quadrupole and octopole when multipolarly decomposing the radiation field. In non-dynamical CS gravity with a canonical embedding, the

recoil is proportional to the square of the mass quadrupole, which dominates over the GR term.

We then construct a wide class of alternative theories that differ from GR through higher order curvature terms in the action coupled to a scalar field. We compute the GW stress-energy-momentum tensor in such theories and find that corrections to the Isaacson tensor vanish at future null infinity provided the following conditions are satisfied: (i) the curvature invariants in the modification are quadratic or higher order; (ii) the non-minimally coupled scalar field is dynamical; (iii) the modification may be modeled as a weak deformation away from GR; (iv) the spacetime is asymptotically flat at future null infinity. These results prove that the effective stress-energy tensor assumed in [107, 106] is indeed correct[1].

Even if the effective GW energy-momentum tensor is identical to that in GR, in terms of contractions of first derivatives of the metric perturbation, this does not imply that GWs will not be modified. First, background solutions could be modified. For example, in dynamical CS gravity, the Kerr metric is not a solution to the modified field equations for a rotating black hole (BH) [74], but it is instead modified in the shift sector [169]. Second, the solution to the GW evolution equation could also be modified. For example, in non-dynamical CS gravity, GWs become amplitude birefringent as they propagate [80, 2, 176]. Third, additional degrees of freedom may also be present and radiate, thus changing the orbital evolution. All of these facts imply that even if the Isaacson tensor correctly describes the effective GW energy-momentum tensor, GWs themselves can and generically will be modified in such alternative theories.

In the remainder of this paper we use the following conventions. Background quantities are always denoted with an overhead bar, while perturbed quantities of first-order with an overhead tilde. We employ decompositions of the type $\mathrm{g}_{\mu\nu} = \bar{\mathrm{g}}_{\mu\nu} + \epsilon\, \tilde{h}_{\mu\nu} + \mathcal{O}(\epsilon^2)$, where $\mathrm{g}_{\mu\nu}$ is the full metric, $\bar{\mathrm{g}}_{\mu\nu}$ is the background metric and $\tilde{h}_{\mu\nu}$ is a small perturbation ($\epsilon \ll 1$ is a book-keeping parameter). Covariant differen-

[1]The authors of [107, 106] presented an energy loss formula which was not evaluated at $\mathscr{I}^+$. In the limit of $r \to \infty$, their energy loss formula reduces to the Isaacson formula.

tiation with respect to the background metric is denoted via $\bar{\nabla}_\mu B_\nu$, while covariant differentiation with respect to the full metric is denoted via $\nabla_\mu B_\nu$. Symmetrization and antisymmetrization are denoted with parentheses and square brackets around the indices respectively, such as $A_{(\mu\nu)} \equiv [A_{\mu\nu} + A_{\nu\mu}]/2$ and $A_{[\mu\nu]} \equiv [A_{\mu\nu} - A_{\nu\mu}]/2$. We use the metric signature $(-,+,+,+)$ and geometric units, such that $G = c = 1$.

This paper is organized as follows: Section 3.2 describes the perturbed Lagrangian approach used in this paper to compute the effective GW stress-energy tensor. Section 3.3 applies this framework to GR. Section 3.4 discusses dynamical CS gravity. Section 3.5 computes the full effective stress-energy tensor in this theory. Section 3.6 generalizes the calculation to a wider class of alternative theories. Section 3.7 concludes and points to future research.

3.2 Perturbed Lagrangian approach

Isaacson [78, 79] introduced what is now the standard technique to obtain an effective stress-energy tensor for gravitational radiation, via second-order perturbation theory on the equations of motion. This technique requires an averaging procedure to construct an *effective* stress-energy tensor. This is because of the inability to localize the energy of the gravitational field to less than several wavelengths of the radiation, and because of the ambiguities of the metric perturbation on distances of order the wavelength due to gauge freedom.[2] Isaacson employed the Brill-Hartle [29] averaging scheme, although one can arrive at an identical quantity by using different schemes [185, 186, 184], e.g. Whitham or macroscopic gravity.

An alternative approach to derive field equations and an effective stress-energy tensor for GWs is to work at the level of the action. One possibility is to use the Palatini framework [101, 41], where the connection is promoted to an independent field that is varied in the action, together with the metric tensor. Such a framework,

[2]Gauge freedom in perturbation theory stands for the freedom to identify points between the physical and "background" manifolds [104, 105].

however is problematic in alternative theories of gravity, as it need not lead to the same field equations as variation of the action with respect to the metric tensor only.

A similar but more appropriate approach is that of *second-variation* [92]. In this approach, the action is first expanded to second order in the metric perturbation, assuming the connection is the Christoffel one $\Gamma^{\sigma}_{\mu\nu}$. Then, the action is promoted to an effective one, by treating the background metric tensor and the metric perturbation as *independent fields*. Variation of this effective action with respect to the metric perturbation and the background metric yields the equations of motion. The former variation leads to the first-order field equations, when the background field equations are imposed. The latter variation leads to the background field equations to zeroth order in the metric perturbation and to an effective GW stress-energy tensor to second order.

Let us begin by expanding all quantities in a power series about a background solution

$$\varphi = \bar{\varphi} + \epsilon\tilde{\varphi} + \epsilon^2\tilde{\tilde{\varphi}} + \mathcal{O}(\epsilon^3) \ , \tag{3.1}$$

where $\epsilon \ll 1$ is an order counting parameter and φ represents all tensor fields of the theory with indices suppressed: $\bar{\varphi}$ is the background field, $\tilde{\varphi}$ is the first-order perturbation to φ, and $\tilde{\tilde{\varphi}}$ is the second-order perturbation. The action can then be expanded, as

$$S[\varphi] = S^{(0)}[\bar{\varphi}] + S^{(1)}[\bar{\varphi}, \tilde{\varphi}] + S^{(2)}[\bar{\varphi}, \tilde{\varphi}, \tilde{\tilde{\varphi}}] + \mathcal{O}(\epsilon^3) \, , \tag{3.2}$$

where $S^{(1)}$ is linear in $\tilde{\varphi}$ and $S^{(2)}$ is quadratic in $\tilde{\varphi}$ but linear in $\tilde{\tilde{\varphi}}$. We now define the effective action as Eq. (3.2) but promoting $\bar{\varphi}$ and $\tilde{\varphi}$ to independent fields.

One might wonder why the field $\tilde{\tilde{\varphi}}$ is not also treated as independent. First, variation of the action with respect to $\tilde{\tilde{\varphi}}$ would lead to second-order equations of motion, which we are not interested in here. Second, the variation of the action with respect to $\tilde{\varphi}$ cannot introduce terms that depend on $\tilde{\tilde{\varphi}}$, because the product of $\tilde{\varphi}$ and $\tilde{\tilde{\varphi}}$ never appears in Eq. (3.2), as this would be of $\mathcal{O}(\epsilon^3)$. Third, the variation of the action with respect to $\bar{\varphi}$ can only introduce terms linear in $\tilde{\tilde{\varphi}}$, which vanish upon

averaging, as we describe in Sec. 3.2.1. This is because averages of any odd number of short-wavelength quantities generically vanish. Therefore, we can safely neglect all terms that depend on $\tilde{\tilde{\varphi}}$ in the effective action, which renders Eq. (3.2) a functional of only $\bar{\varphi}$ and $\tilde{\varphi}$.

As in the standard approach, the second-order variation method still requires that one performs a short-wavelength average of the effective stress-energy tensor. Upon averaging, the variation of the first-order piece of the action $S^{(1)}$ with respect to $\bar{\varphi}$ vanishes because it generates terms linear in $\tilde{\varphi}$. Since $S^{(1)}$ does not contribute to the effective stress-energy tensor, we can safely drop it from the effective action for now.

The effective action reduces to

$$S^{\text{eff}}[\bar{\varphi}, \tilde{\varphi}] = S^{\text{eff}(0)}[\bar{\varphi}] + S^{\text{eff}(2)}[\bar{\varphi}, \tilde{\varphi}] \ . \tag{3.3}$$

Naturally, the variation of $S^{\text{eff}(0)}$ with respect to the background metric $\bar{\text{g}}^{\mu\nu}$ yields the background equations of motion. The effective stress-energy tensor comes from averaging the variation of $S^{\text{eff}(2)}$ with respect to $\bar{\text{g}}^{\mu\nu}$,

$$\delta S^{\text{eff}(2)} = \epsilon^2 \int \mathrm{d}^4x \sqrt{-\bar{\text{g}}} \ \delta\bar{\text{g}}^{\mu\nu} t_{\mu\nu} \ , \tag{3.4a}$$

$$T^{\text{eff}}_{\mu\nu} \equiv -2\epsilon^2 \langle\langle t_{\mu\nu} \rangle\rangle \ , \tag{3.4b}$$

where the factor of 2 is conventional for agreement with the canonical stress-energy tensor, and $\langle\langle \ \rangle\rangle$ is the averaging operator, which we discuss below. One of the immediate benefits of working from an action principle comes from the diffeomorphism invariance of the action. The diffeomorphism invariance immediately implies that the variation of the total action with respect to the metric is divergence free [41]. When the matter stress-energy tensor is itself divergence free, then the gravity sector – the sum of the stress-energy of non-minimally coupled degrees of freedom and the effective stress-energy tensor of gravitational waves – will also be divergence free.

3.2.1 Short-wavelength averaging

The goal of the averaging scheme is to distinguish radiative quantities, those which are rapidly-varying functions of spacetime, from Coulomb-like quantities, those which are slowly-varying functions. This is accomplished by defining the operator $\langle\langle\ \rangle\rangle$ as a linear integral operator. This operator may either be an average over the phase of the rapidly varying quantities or over spacetime. If the integral is over spacetime, there is an averaging kernel with characteristic length scale $L_{\rm ave}$ that separates the foreground short-wavelength $\lambda_{\rm GW}$ from the background length scale $L_{\rm bg}$, that is, $\lambda_{\rm GW} \ll L_{\rm ave} \ll L_{\rm bg}$.

The details of the averaging scheme are not as important as their properties [185, 186, 184], since one arrives at equivalent results using different schemes. The most useful properties of $\langle\langle\ \rangle\rangle$ are:

1. The average of a product of an odd number of short-wavelength quantities vanishes.

2. The average of a derivative of a tensor vanishes, e.g. for some tensor expression $T^{\mu}{}_{\alpha\beta}$, $\langle\langle \overline{\nabla}_{\mu} T^{\mu}{}_{\alpha\beta}\rangle\rangle = 0$.

3. As a corollary to the above, integration by parts can be performed, e.g. for tensor expressions $R^{\mu}{}_{\alpha}, S_{\beta}$, $\langle\langle R^{\mu}{}_{\alpha}\overline{\nabla}_{\mu} S_{\beta}\rangle\rangle = -\langle\langle S_{\beta}\overline{\nabla}_{\mu} R^{\mu}{}_{\alpha}\rangle\rangle$.

Let us briefly mention where some of these properties come from and some caveats. When considering monochromatic functions, an odd oscillatory integral has an average value about zero, while an even oscillatory integral has a non-zero average. This is enough to find that that averages of expressions linear in a short-wavelength quantity will vanish. Expressions at third (and higher odd) order would vanish for monochromatic radiation, but not in general. However, these are at sufficiently high order that we neglect them.

The vanishing of averages of derivatives is a subtle point. In the spacetime average approach, this is found by integrating by parts, leaving a term with a derivative on the averaging kernel. This term is smaller than nonvanishing averages by a factor of

$\mathcal{O}(\lambda_{\rm GW}/L_{\rm ave})$ and depends on the averaging kernel. From physical grounds, the choice of averaging kernel should not affect any physical quantities, so the average should in fact vanish identically. From the action standpoint, the average of a derivative can be seen to arise from an action term which is a total divergence. Since total divergences in the action do not affect the equations of motion, the average of a derivative vanishes.

A similar argument holds for integration by parts. In the Brill-Hartle average scheme, integration by parts incurs an error of order $\mathcal{O}(\lambda_{\rm GW}/L_{\rm ave})$ from a derivative of the averaging kernel. From the action standpoint, though, integration by parts at the level of the action incurs no error, since there is no averaging kernel in the action.

The fact that the variation of $S^{(1)}$ with respect to $\bar{\varphi}$ does not contribute to the effective stress-energy tensor is a direct consequence of property (1) above. The vanishing of all terms linear in $\tilde{\tilde{\varphi}}$ upon averaging is also a consequence of (1). As one can see, these properties greatly simplify all further calculations.

3.2.2 Varying Christoffel and curvature tensors

Let us now consider what types of terms arise from the variation of the effective action with respect to $\bar{\rm g}^{\mu\nu}$. In order to perform this variation properly, any implicit dependence of the action on $\bar{\rm g}^{\mu\nu}$ must be explicitly revealed; for example, terms which contain the trace $\tilde{h}$ must be rewritten as $\bar{\rm g}_{\mu\nu}\tilde{h}^{\mu\nu}$. Indices should appear in their "natural" positions (see Sec. 3.2.4), for indices raised and lowered with the metric have implicit dependence on it. Furthermore, since we are approaching gravity from the metric formulation, rather than the Palatini formulation, there will be contributions from the variation of $\overline{\nabla}_\mu$ and curvature tensors.

Consider a term in the effective action such as

$$S^{\rm ex.1} = \int {\rm d}^4x \sqrt{-\bar{\rm g}}\; T^{\gamma\cdots}{}_{\delta\cdots}\; \overline{\nabla}_\mu\; S^{\alpha\cdots}{}_{\beta\cdots}\;, \tag{3.5}$$

where g is the determinant of the metric and $T^{\gamma\cdots}{}_{\delta\cdots}, S^{\alpha\cdots}{}_{\beta\cdots}$ are some tensor expressions, with all indices contracted in some fashion, as the action must be a scalar.

When such a term is varied with $\bar{\mathrm{g}}^{\mu\nu} \to \bar{\mathrm{g}}^{\mu\nu} + \delta\bar{\mathrm{g}}^{\mu\nu}$, besides the obvious contributions from $\delta\sqrt{-\bar{\mathrm{g}}}$, and explicit dependence of $T^{\gamma\cdots}{}_{\delta\cdots}, S^{\alpha\cdots}{}_{\beta\cdots}$ on $\bar{\mathrm{g}}^{\mu\nu}$, there are also contributions from varying the Christoffel connection $\Gamma^{\lambda}_{\mu\beta}$ in $\overline{\nabla}_{\mu}$. The general expression is

$$\delta(\overline{\nabla}_{\mu} S^{\alpha_1\cdots\alpha_n}{}_{\beta_1\cdots\beta_m}) = \overline{\nabla}_{\mu}(\delta S^{\alpha_1\cdots\alpha_n}{}_{\beta_1\cdots\beta_m}) + \\ + \sum_{i=1}^{n} \delta\bar{\Gamma}^{\alpha_i}_{\mu\lambda} S^{\cdots\lambda\cdots}{}_{\beta_1\cdots\beta_m} - \sum_{j=1}^{m} \delta\bar{\Gamma}^{\lambda}_{\mu\beta_j} S^{\alpha_1\cdots\alpha_n}{}_{\cdots\lambda\cdots} , \quad (3.6)$$

where $\cdots\lambda\cdots$ in the i^{th} term of a sum means replacing α_i or β_i in the index list with λ; and where

$$\delta\bar{\Gamma}^{\sigma}_{\mu\nu} = -\frac{1}{2}\left[\bar{\mathrm{g}}_{\lambda\mu}\overline{\nabla}_{\nu}\delta\bar{\mathrm{g}}^{\lambda\sigma} + \bar{\mathrm{g}}_{\lambda\nu}\overline{\nabla}_{\mu}\delta\bar{\mathrm{g}}^{\lambda\sigma} - \bar{\mathrm{g}}_{\mu\alpha}\bar{\mathrm{g}}_{\nu\beta}\overline{\nabla}^{\sigma}\delta\bar{\mathrm{g}}^{\alpha\beta}\right] . \quad (3.7)$$

Curvature tensors also depend on derivatives of the connection, so one naturally expects terms of the form $\overline{\nabla}_{\rho}\overline{\nabla}_{\sigma}\delta\bar{\mathrm{g}}^{\mu\nu}$ from the variation of curvature quantities, i.e. the Riemann tensor $R^{\mu}{}_{\nu\alpha\beta}$, Ricci tensor $R_{\mu\nu}$, or Ricci scalar R. For example, one can show that

$$\delta\bar{R}^{\mu}{}_{\nu\alpha\beta} = 2\overline{\nabla}_{[\alpha}\delta\bar{\Gamma}^{\mu}_{\beta]\nu} , \quad (3.8)$$

where the contribution from $\Gamma \wedge \Gamma$ cancels [41]. Upon integration by parts any scalar in the action that contains curvature tensors, one can convert a term containing $\overline{\nabla}_{\rho}\overline{\nabla}_{\sigma}\delta\bar{\mathrm{g}}^{\mu\nu}$ into

$$\delta S^{\text{ex.2}} = \int \mathrm{d}^4x \, \sqrt{-\bar{\mathrm{g}}} \; P^{\sigma}{}_{\mu\nu}\overline{\nabla}_{\sigma}\delta\bar{\mathrm{g}}^{\mu\nu} . \quad (3.9)$$

In fact, many terms in the variation of the action can be written in the form of Eq. (3.9).

The contribution of Eq. (3.9) to the effective stress-energy tensor is found by integrating by parts and then averaging, according to Eq. (3.4). Upon averaging, however, one finds that such terms do not contribute to the effective stress-energy tensor because

$$T^{\text{eff,ex.2}}_{\mu\nu} = 2\langle\langle\overline{\nabla}_{\sigma}P^{\sigma}{}_{\mu\nu}\rangle\rangle , \quad (3.10)$$

vanishes according to property (2) in Sec. 3.2.1.

The above arguments and results imply that the variations of curvature tensors and connection coefficients with respect to $\bar{g}_{\mu\nu}$ do not contribute to the effective stress-energy tensor. Only metric tensors which are raising, lowering, and contracting indices in the action contribute to this tensor. We can thus concentrate on these, when computing $T^{\rm eff}_{\mu\nu}$.

3.2.3 Contributions at asymptotic infinity

When calculating the radiation-reaction force to leading order in the metric perturbation, it is crucial to account for all the energy-momentum loss in the system. The first contribution is straightforward: energy-momentum is radiated outward, toward future, null infinity, $\mathscr{I}^+$. Since the stress-energy tensor is covariantly conserved, the energy-momentum radiated to $\mathscr{I}^+$ can be calculated by performing a surface integral over a two-sphere at future, null infinity[3].

However, not all energy-momentum loss escapes to infinity, as energy can also be lost due to the presence of trapped surfaces in the interior of the spacetime. Trapped surfaces can effectively absorb GW energy-momentum, which must also be accounted for, e.g. in the calculation of EMRI orbits around supermassive BHs [174, 175]. Calculations of such energy-momentum loss at the BH horizon are dramatically more complicated than those at $\mathscr{I}^+$ and we do not consider them here.

What is the relative importance of energy-momentum lost to $\mathscr{I}^+$ and that lost into trapped surfaces? To answer this question, we can concentrate on the magnitude of the leading-order energy flux, as the argument trivially extends to momentum. The post-Newtonian (PN) approximation [21], which assumes weak-gravitational fields and slow velocities, predicts that the energy flux carried out to $\mathscr{I}^+$ is proportional to v^{10} to leading-order in v, where v is the orbital velocity of a binary system in a quasi-circular orbit (see e.g. [21]). On the other hand, a combination of the PN approximation and BH perturbation theory predicts that, to leading-order in v, the

[3]We will not consider spacetimes which are not asymptotically flat, e.g. de Sitter space; the calculations are more involved in such spacetimes.

energy flux carried into trapped surfaces is proportional to v^{15} for spinning BHs and v^{18} for non-spinning BHs [99]. BH GW flux absorption is then clearly smaller than the GW flux carried out to $\mathscr{I}^+$ if $v < 1$, which is true for EMRIs for which the PN approximation holds.

Intuitively, this hierarchy in the magnitude of energy-momentum flux lost by BH binaries can be understood by considering the BH as a geometric absorber in the radiation field. Radiation which is longer in wavelength than the size of the BH is very weakly absorbed. Only at the end of an inspiral will the orbital frequency be high enough that GWs will be significantly absorbed by the horizon. Notice that this argument is independent of the particular theory considered, only relying on the existence of trapped surfaces. This result does not imply that BH absorption should be neglected in EMRI modeling, but just that it is a smaller effect than the flux carried out to infinity [174, 175].

In the remainder of the paper, we will only address energy-momentum radiated to $\mathscr{I}^+$ and relegate any analysis of radiation lost into trapped surface to future work. The only terms which can contribute to an energy-momentum flux integral on a 2-sphere at $\mathscr{I}^+$ are those which decay as r^{-2}, since the area element of the sphere grows as r^2. No terms may decay more slowly than r^{-2}, as the flux must be finite, i.e. the effective stress-energy cannot scale as r^{-1}, as a constant or with positive powers of radius. Similarly, any terms decaying faster than r^{-2} do not contribute, as they would vanish at $\mathscr{I}^+$. Of course, to determine which terms contribute and which do not, one must know the leading asymptotic forms of all quantities in the effective stress-energy tensor.

In GR, as we shall see in Sec. 3.3, the only fields appearing in the effective stress-energy tensor are the background metric $\bar{\mathrm{g}}_{\mu\nu}$ and derivatives of the metric perturbation $\tilde{h}_{\mu\nu}$. As one approaches $\mathscr{I}^+$, $\bar{\mathrm{g}}_{\mu\nu} \sim \eta_{\mu\nu}$ in Cartesian coordinates, while $|\tilde{h}_{\mu\nu}| \sim r^{-1} \sim |\overline{\nabla}_\rho \tilde{h}_{\mu\nu}|$. Curvature tensors scale as $|\overline{R}_{\mu\nu\delta\sigma}| \sim r^{-3}$, since they quantify tidal forces. For a theory that is a deformation away from GR, and far away from regions of strong curvature, these asymptotic forms cannot change.

Consider now terms in the general effective action at order $\mathcal{O}(\epsilon^2)$ that contain background curvature tensors. Due to their ordering, they would contribute to the effective stress-energy. One such term is

$$S^{\text{ex.3}} = \epsilon^2 \int \mathrm{d}^4x \sqrt{-\bar{\mathrm{g}}}\; \overline{\nabla}_\rho \tilde{\varphi}_1^\sigma \; \overline{\nabla}_\alpha \tilde{\varphi}_2^\beta \; \overline{R}^\rho{}_{\beta\sigma\kappa} \; \bar{\mathrm{g}}^{\alpha\kappa} \; , \tag{3.11}$$

where $\tilde{\varphi}_1, \tilde{\varphi}_2$ are the first-order perturbations to two fields in the theory (e.g. the metric perturbation $\tilde{h}_{\mu\nu}$ and the CS scalar perturbation $\tilde{\vartheta}$ that we introduce in Sec. 3.5). Since there is no contribution to the effective stress-energy tensor from the variation of curvature quantities (see Sec. 3.2.2), the only contributions to the effective stress-energy comes from

$$T^{\text{eff,ex.3}}_{\mu\nu} = -2\epsilon^2 \left\langle\!\!\left\langle \left(-\frac{1}{2}\bar{\mathrm{g}}_{\mu\nu}\bar{\mathrm{g}}^{\alpha\kappa} + \delta^\alpha{}_{(\mu}\delta^\kappa{}_{\nu)} \right) \underbrace{\overline{\nabla}_\rho \tilde{\varphi}_1^\sigma}_{r^{-1}} \; \underbrace{\overline{\nabla}_\alpha \tilde{\varphi}_2^\beta}_{r^{-1}} \; \underbrace{\overline{R}^\rho{}_{\beta\sigma\kappa}}_{r^{-3}} \right\rangle\!\!\right\rangle \; , \tag{3.12}$$

which has the same functional form as the integral. Note that the curvature tensor always remains when varying with respect to $\bar{\mathrm{g}}^{\mu\nu}$.

Combining this result with the asymptotic arguments above, such terms can be ignored as one approaches $\mathscr{I}^+$. Each of the first-order fields possess a radiative part that scales as r^{-1}. The square of the first-order fields would then satisfy the r^{-2} scaling requirement for the flux integral. The curvature tensor, however, scales as r^{-3}, which implies that the term in Eq. (3.12) vanishes at $\mathscr{I}^+$.

We then conclude that terms in the action that contain background curvature quantities at $\mathcal{O}(\epsilon^2)$ may be ignored in calculating the effective stress-energy tensor at $\mathscr{I}^+$. As an immediate corollary to this simplification, we may also freely commute background covariant derivatives if we are interested in the stress-energy tensor at infinity only, since the commutator is proportional to background curvature tensors.

3.2.4 Imposing gauge in the effective action

We will choose as our dynamical field not $\tilde{h}_{\mu\nu}$ but rather $\underline{\tilde{h}}^{\mu\nu}$, where the underline stands for the trace-reverse operation, and we take the "natural" position of the

indices to be contravariant. The resulting stress-energy tensor is equal to the one calculated using $\tilde{h}_{\mu\nu}$ *after* evaluating both of them on-shell, i.e. imposing the equations of motion.

We also impose a gauge condition to simplify future expressions: the Lorenz gauge condition,

$$\overline{\nabla}_\mu \underline{\tilde{h}}^{\mu\nu} = 0\,. \tag{3.13}$$

Typically one may not impose a gauge condition at the level of the action. However, in our case, the gauge condition in Eq. (3.13) has the important property of having all of the indices in their natural positions: the contraction of the indices does not involve the metric.

Consider a term in the effective action that contains this divergence,

$$S^{\text{ex.4}} = \epsilon^2 \int \mathrm{d}^4x \sqrt{-\bar{\mathrm{g}}}\; T_\beta\; \overline{\nabla}_\alpha \underline{\tilde{h}}^{\alpha\beta}\,, \tag{3.14}$$

with T_β some tensor expression at first order in ϵ. The α index that is contracted above does not require the metric for such contraction. Therefore, $\overline{\nabla}_\alpha \underline{\tilde{h}}^{\alpha\beta}$ always remains upon variation,

$$T^{\text{eff,ex.4}}_{\mu\nu} = -2\epsilon^2 \left\langle \left\langle \left(-\frac{1}{2} \bar{\mathrm{g}}_{\mu\nu} T_\beta + \frac{\delta T_\beta}{\delta \bar{\mathrm{g}}^{\mu\nu}} \right) \overline{\nabla}_\alpha \underline{\tilde{h}}^{\alpha\beta} \right\rangle \right\rangle\,. \tag{3.15}$$

If we delayed imposing the Lorenz gauge condition until after the calculation of the effective stress-energy tensor, we would find the same effective tensor as if we had imposed the gauge condition at the level of the action. Having said that, one should not impose the gauge condition when varying with respect to $\underline{\tilde{h}}^{\mu\nu}$ as clearly $\overline{\nabla}_\alpha \underline{\tilde{h}}^{\alpha\beta}$ must also be varied.

3.3 Effective Stress-Energy in GR

Let us now demonstrate the principles described in the previous section by deriving the standard Isaacson stress-energy tensor in GR. Consider the Einstein-Hilbert

action,

$$S_{\rm GR} = \kappa \int \mathrm{d}^4x\sqrt{-\mathrm{g}}\, R, \tag{3.16}$$

where $\kappa = (16\pi G)^{-1}$. Now perturb to second order to form the effective action,

$$S^{\rm eff}_{\rm GR} = S^{\rm eff(0)}_{\rm GR} + S^{\rm eff(2)}_{\rm GR}, \tag{3.17a}$$

$$S^{\rm eff(0)}_{\rm GR} = \kappa \int \mathrm{d}^4x\sqrt{-\bar{\mathrm{g}}}\, \bar{R}, \tag{3.17b}$$

$$S^{\rm eff(2)}_{\rm GR} = \epsilon^2\kappa \int \mathrm{d}^4x\, \mathcal{L}^{\rm eff,1}_{\rm GR} + \mathcal{L}^{\rm eff,2}_{\rm GR}\ , \tag{3.17c}$$

where

$$\mathcal{L}^{\rm eff,1}_{\rm GR} = \frac{1}{8}\sqrt{-\bar{\mathrm{g}}}\left[4\bar{R}_{\alpha\beta}\left(2\tilde{\underline{h}}^{\alpha}{}_{\mu}\tilde{\underline{h}}^{\beta\mu} - \tilde{\underline{h}}^{\alpha\beta}\tilde{\underline{h}}\right) + \bar{R}\left(\tilde{\underline{h}}^{2} - 2\tilde{\underline{h}}_{\alpha\beta}\tilde{\underline{h}}^{\alpha\beta}\right)\right]\ , \tag{3.17d}$$

and

$$\begin{aligned}\mathcal{L}^{\rm eff,2}_{\rm GR} = \sqrt{-\bar{\mathrm{g}}}\Bigg[&-\tilde{\underline{h}}^{\alpha\beta}\overline{\nabla}_{\alpha}\overline{\nabla}_{\mu}\tilde{\underline{h}}^{\mu}{}_{\beta} - \frac{1}{8}(\overline{\nabla}_{\mu}\tilde{\underline{h}})(\overline{\nabla}^{\mu}\tilde{\underline{h}}) - \\ &(\overline{\nabla}_{\mu}\tilde{\underline{h}}^{\mu}{}_{\alpha})(\overline{\nabla}_{\nu}\tilde{\underline{h}}^{\nu\alpha}) + \frac{1}{2}(\overline{\nabla}_{\nu}\tilde{\underline{h}})(\overline{\nabla}_{\mu}\tilde{\underline{h}}^{\mu\nu}) - \tilde{\underline{h}}^{\alpha\beta}\overline{\nabla}_{\mu}\overline{\nabla}_{\alpha}\tilde{\underline{h}}^{\mu}{}_{\beta} \\ &+ \frac{1}{2}\tilde{\underline{h}}\overline{\nabla}_{\mu}\overline{\nabla}_{\nu}\tilde{\underline{h}}^{\mu\nu} + \tilde{\underline{h}}^{\alpha\beta}\bar{\Box}\tilde{\underline{h}}_{\alpha\beta} - \frac{1}{4}\tilde{\underline{h}}\bar{\Box}\tilde{\underline{h}} \\ &-\frac{1}{2}(\overline{\nabla}_{\mu}\tilde{\underline{h}}_{\nu\alpha})(\overline{\nabla}^{\nu}\tilde{\underline{h}}^{\mu\alpha}) + \frac{3}{4}(\overline{\nabla}_{\mu}\tilde{\underline{h}}_{\alpha\beta})(\overline{\nabla}^{\mu}\tilde{\underline{h}}^{\alpha\beta})\Bigg]\ ,\end{aligned} \tag{3.17e}$$

and $(\bar{R}_{\mu\nu}, \bar{R})$ refer to the background Ricci tensor and scalar respectively. The integrands have been written in terms of the trace-reversed metric perturbation, $\tilde{\underline{h}}^{\mu\nu}$. From Sec. 3.2.3, $\mathcal{L}^{\rm eff,1}_{\rm GR}$ does not contribute at $\mathscr{I}^+$ because it depends explicitly on curvature quantities, so we ignore it. The variation and averaging of $\mathcal{L}^{\rm eff,2}_{\rm GR}$ produces the Isaacson stress-energy tensor.

By integrating by parts, all terms in Eq. (3.17e) can be written as $(\overline{\nabla}_{\alpha}\tilde{\underline{h}}^{\rho\sigma})(\overline{\nabla}_{\beta}\tilde{\underline{h}}^{\kappa\lambda})$ (with indices contracted to form a scalar) rather than $\tilde{\underline{h}}^{\rho\sigma}\overline{\nabla}_{\alpha}\overline{\nabla}_{\beta}\tilde{\underline{h}}^{\kappa\lambda}$ (again, with

indices contracted). $\mathcal{L}_{\rm GR}^{\rm eff,2}$ is thus rewritten in the more compact form

$$\mathcal{L}_{\rm MT} = \sqrt{-\bar{\rm g}}\left[\frac{1}{2}(\overline{\nabla}_\mu \tilde{\underline{h}}^{\nu\alpha})(\overline{\nabla}_\nu \tilde{\underline{h}}^{\mu}{}_{\alpha}) - \frac{1}{4}(\overline{\nabla}_\mu \tilde{\underline{h}}_{\alpha\beta})(\overline{\nabla}^\mu \tilde{\underline{h}}^{\alpha\beta}) + \frac{1}{8}(\overline{\nabla}_\mu \tilde{\underline{h}})(\overline{\nabla}^\mu \tilde{\underline{h}})\right] \ , \quad (3.18)$$

which is the expression that appears in MacCallum and Taub [92]. With this simplified expression at hand, we can promote $\tilde{\underline{h}}^{\mu\nu}$ to an independent dynamical field in Eq. (3.17) and vary it with respect to both $\bar{\rm g}^{\mu\nu}$ and $\tilde{\underline{h}}^{\mu\nu}$ to obtain the effective stress-energy tensor and the first-order equations of motion respectively.

Let us first derive the first-order equations of motion. Varying Eq. (3.17) with respect to $\tilde{\underline{h}}^{\mu\nu}$, we find

$$\bar{\Box}\tilde{\underline{h}}_{\mu\nu} - 2\overline{\nabla}^\alpha \overline{\nabla}_{(\mu}\tilde{\underline{h}}_{\nu)\alpha} - \frac{1}{2}\bar{\rm g}_{\mu\nu}\bar{\Box}\tilde{\underline{h}} = 0 \ , \quad (3.19a)$$

whose trace is

$$2\overline{\nabla}_\alpha \overline{\nabla}_\beta \tilde{\underline{h}}^{\alpha\beta} + \bar{\Box}\tilde{\underline{h}} = 0 \ . \quad (3.19b)$$

We can now impose the Lorenz gauge on Eq. (3.19b), which then leads to $\bar{\Box}\tilde{\underline{h}} = 0$. If $\tilde{\underline{h}} = 0$ is further imposed on an initial hypersurface while maintaining Lorenz gauge, then the evolution equation preserves the trace-free gauge [101]. The combination of these two gauge choices (Lorenz gauge plus trace-free) is the transverse-tracefree gauge, or TT gauge.

After commuting derivatives in Eq. (3.19a) and imposing TT gauge, the tensor equation of motion reads

$$\bar{\Box}\tilde{\underline{h}}_{\mu\nu} + 2\bar{R}_{\mu\alpha\nu\beta}\tilde{\underline{h}}^{\alpha\beta} = 0 \, , \quad (3.19c)$$

where $\bar{R}_{\mu\alpha\nu\beta}$ is the background Riemann tensor. At $\mathscr{I}^+$, this equation reduces to $\bar{\Box}\tilde{\underline{h}}_{\mu\nu} = 0$, which leads to the standard dispersion relation for GWs, traveling at the speed of light.

Let us now calculate the effective stress-energy tensor. Note that the first term in $\mathcal{L}_{\rm MT}$ may be integrated by parts and covariant derivatives commuted to form the Lorenz gauge condition, so the first term may be ignored. Varying the action with

respect to $\bar{\mathrm{g}}^{\mu\nu}$, we find

$$\kappa G_{\mu\nu} = -\epsilon^2\kappa \left\langle\left\langle \frac{1}{\sqrt{-\bar{\mathrm{g}}}}\frac{\delta}{\delta\bar{\mathrm{g}}^{\mu\nu}}\mathcal{L}_{\mathrm{MT}}\right\rangle\right\rangle \equiv \frac{1}{2}T^{\mathrm{eff}}_{\mathrm{MT}\mu\nu}\ , \tag{3.20a}$$

where

$$\begin{aligned} T^{\mathrm{eff}}_{\mathrm{MT}\mu\nu} &= 2\epsilon^2\kappa\left\langle\left\langle \frac{1}{4}\overline{\nabla}_\mu\tilde{\underline{h}}^{\alpha\beta}\overline{\nabla}_\nu\tilde{\underline{h}}_{\alpha\beta} - \frac{1}{2}\overline{\nabla}_\alpha\tilde{\underline{h}}_{\beta\mu}\overline{\nabla}^\alpha\tilde{\underline{h}}_\nu{}^\beta \right.\right. \\ &\quad - \frac{1}{8}\overline{\nabla}_\mu\tilde{\underline{h}}\overline{\nabla}_\nu\tilde{\underline{h}} + \frac{1}{4}\overline{\nabla}_\alpha\tilde{\underline{h}}_{\mu\nu}\overline{\nabla}^\alpha\tilde{\underline{h}} \\ &\quad \left.\left. + \frac{1}{2}\bar{\mathrm{g}}_{\mu\nu}(-\bar{\mathrm{g}})^{-1/2}\mathcal{L}_{\mathrm{MT}}\right\rangle\right\rangle\ , \end{aligned} \tag{3.20b}$$

which we refer to as the MacCallum-Taub tensor. Terms that depend on the trace $\tilde{\underline{h}}^\mu{}_\mu$ in this tensor can be eliminated in TT gauge.

Let us now evaluate the MacCallum-Taub tensor on shell, by imposing the equations of motion [Eq. (3.19)]. When short-wavelength averaging, derivatives that are contracted together can be converted into the d'Alembertian via integration by parts; such terms vanish at $\mathscr{I}^+$. What results is the usual Isaacson stress-energy tensor,

$$T^{\mathrm{eff}}_{\mathrm{GR}\mu\nu} = \epsilon^2\frac{\kappa}{2}\left\langle\left\langle\left(\overline{\nabla}_\mu\tilde{\underline{h}}^{\alpha\beta}\right)\left(\overline{\nabla}_\nu\tilde{\underline{h}}_{\alpha\beta}\right)\right\rangle\right\rangle\ . \tag{3.20c}$$

Notice that this expression is only valid at $\mathscr{I}^+$ and in TT gauge. As mentioned earlier, this tensor cannot be used to model energy-momentum loss through trapped surfaces, since then curvature quantities cannot be ignored.

3.4 Chern-Simons Gravity

CS gravity is a modified theory introduced first by Jackiw and Pi [80] (for a recent review see [6]). The dynamical version of this theory modifies the Einstein-Hilbert action through the addition of the following terms:

$$S = S_{\mathrm{EH}} + S_{\mathrm{CS}} + S_\vartheta + S_{\mathrm{mat}}, \tag{3.21}$$

where

$$
\begin{aligned}
S_{\rm EH} &= \kappa \int d^4x \, \sqrt{-\mathrm{g}} \, R \,, \\
S_{\rm CS} &= \frac{\alpha}{4} \int d^4x \, \sqrt{-\mathrm{g}} \quad \vartheta \; {}^*R \, R \,, \\
S_{\vartheta} &= -\frac{\beta}{2} \int d^4x \, \sqrt{-\mathrm{g}} \, \mathrm{g}^{\mu\nu} \left(\nabla_\mu \vartheta\right) \left(\nabla_\nu \vartheta\right) \,, \\
S_{\rm mat} &= \int d^4x \, \sqrt{-\mathrm{g}} \, \mathcal{L}_{\rm mat} \,.
\end{aligned}
\tag{3.22}
$$

The quantity $\kappa = (16\pi G)^{-1}$ is the gravitational constant, while α and β are coupling constants that control the strength of the CS coupling to the gravitational sector and its kinetic energy respectively. In the non-dynamical version of the theory, $\beta = 0$ and there are no dynamics for the scalar field, which is promoted to a prior-geometric quantity.

The quantity ϑ is the CS field, which couples to the gravitational sector via the parity-violating Pontryagin density, ${}^*R\,R$, which is given by

$$
{}^*R\,R := R_{\alpha\beta\gamma\delta} \, {}^*R^{\alpha\beta\gamma\delta} = \frac{1}{2} \varepsilon^{\alpha\beta\mu\nu} R_{\alpha\beta\gamma\delta} R^{\gamma\delta}{}_{\mu\nu} \,,
\tag{3.23}
$$

where the asterisk denotes the dual tensor, which we construct using the antisymmetric Levi-Civita tensor $\varepsilon^{\alpha\beta\mu\nu}$. This scalar is a topological invariant, as it can be written as the divergence of a current

$$
{}^*R\,R = 4\nabla_\mu \left[\varepsilon^{\mu\alpha\beta\gamma} \Gamma^\sigma_{\alpha\tau} \left(\frac{1}{2} \partial_\beta \Gamma^\tau_{\gamma\sigma} + \frac{1}{3} \Gamma^\tau_{\beta\eta} \Gamma^\eta_{\gamma\sigma} \right) \right] \,.
\tag{3.24}
$$

Equation (3.21) contains several terms that we describe below: the first one is the Einstein-Hilbert action; the second one is the CS coupling to the gravitational sector; the third one is the CS kinetic term; and the fourth one stands for additional matter degrees of freedom. The CS kinetic term is precisely the one that distinguishes the non-dynamical and the dynamical theory. In the former, the scalar field is *a priori* prescribed, while in the dynamical theory, the scalar field satisfies an evolution equation.

The field equations of this theory are obtained by varying the action with respect to all degrees of freedom:

$$G_{\mu\nu} + \frac{\alpha}{\kappa} C_{\mu\nu} = \frac{1}{2\kappa}\left(T^{\rm mat}_{\mu\nu} + T^{(\vartheta)}_{\mu\nu}\right), \tag{3.25a}$$

$$\beta\Box\vartheta = -\frac{\alpha}{4}\,{}^{*}R\,R, \tag{3.25b}$$

where $T^{\rm mat}_{\mu\nu}$ is the matter stress-energy tensor and $T^{(\vartheta)}_{\mu\nu}$ is the CS scalar stress-energy:

$$T^{(\vartheta)}_{\mu\nu} = \beta\left[(\nabla_\mu\vartheta)(\nabla_\nu\vartheta) - \frac{1}{2}{\rm g}_{\mu\nu}(\nabla^\sigma\vartheta)(\nabla_\sigma\vartheta)\right]. \tag{3.26}$$

The C-tensor $C^{\mu\nu}$ is given by

$$C^{\alpha\beta} = (\nabla_\sigma\vartheta)\,\varepsilon^{\sigma\delta\nu(\alpha}\nabla_\nu R^{\beta)}{}_\delta + (\nabla_\sigma\nabla_\delta\vartheta)\;{}^{*}R^{\delta(\alpha\beta)\sigma}. \tag{3.27}$$

Many solutions to these field equations have been found. In their pioneering work, Jackiw and Pi showed that the Scwharzschild metric is also a solution in CS gravity [80]. Later on, a detailed analysis showed that all spherically symmetric spaces, such as the Friedman-Robertson-Walker metric, are also solutions [74]. Axially-symmetric spaces, however, are not necessarily solutions, because the Pontryagin density does not vanish in this case, sourcing a non-trivial scalar field. Specifically, this implies the Kerr metric is not a solution.

A slowly-rotating solution, however, does exist in dynamical CS gravity. Yunes and Pretorius [169] found that when the field equations are expanded in the Kerr parameter $a/M \ll 1$ and in the small-coupling parameter $\zeta \equiv \xi/M^4 = \alpha^2/(\beta\kappa M^4) \ll 1$, then the CS field equations have the solution

$$\begin{aligned} d\bar{s}^2 &= ds^2_{\rm Kerr} + \frac{5}{8}\zeta\frac{Ma}{r^4}\left(1 + \frac{12}{7}\frac{M}{r} + \frac{27}{10}\frac{M^2}{r^2}\right)\sin^2\theta dt d\phi\,, \\ \bar{\vartheta} &= \frac{5}{8}\frac{\alpha}{\beta}\frac{a}{M}\frac{\cos\theta}{r^2}\left(1 + \frac{2M}{r} + \frac{18M^2}{5r^2}\right), \end{aligned} \tag{3.28}$$

to second order in a/M and to first order in ζ, assuming no matter sources. These equations employ Boyer-Lindquist coordinates (t, r, θ, ϕ) and $ds^2_{\rm Kerr}$ is the Kerr line

element. The solution for ϑ may also include an arbitrary additive constant, but this constant is unimportant, since only derivatives of ϑ enter the CS field equations. Recently, the same solution has been found to linear order in a/M in the Einstein-Cartan formulation of the non-dynamical theory [35].

The divergence of the field equations reduce to $\nabla^\mu T^{\rm mat}_{\mu\nu} = 0$. This is because the divergence of the Einstein tensor vanishes by the Bianchi identities. Meanwhile, the divergence of the C-tensor exactly cancels the divergence of the CS scalar field stress-energy tensor, upon imposition of the equations of motion [Eq. (3.25b)]. Therefore, test-particle motion in dynamical CS gravity is exactly geodesic[4]. This result automatically implies the weak-equivalence principle is satisfied.

The gravitational perturbation only possesses two independent, propagating degrees of freedom or polarizations. Jackiw and Pi showed that this was the case in the non-dynamical theory [80], while Sopuerta and Yunes did the same in the dynamical version [137]. One can also show easily that a transverse and approximately traceless gauge exists in dynamical CS gravity. The trace of the field equations take the interesting form

$$-R = \frac{1}{2\kappa}\left(T^{\rm mat} + T^{(\vartheta)}\right) , \tag{3.29}$$

where R is the Ricci scalar and T is the trace of the stress-energy tensor. Notice that the trace of the C-tensor vanishes identically.

In vacuum ($T^{\rm mat}_{\mu\nu} = 0$) and when expanding to linear order about a Minkowski background, Eq. (3.29) reduces to

$$\bar{\Box}\tilde{h} = \frac{\beta}{2\kappa}(\overline{\nabla}^\sigma\bar{\vartheta})(\overline{\nabla}_\sigma\bar{\vartheta}) . \tag{3.30}$$

where $\tilde{h} \equiv \eta^{\mu\nu}h_{\mu\nu}$ is the trace of the metric perturbation, $\bar{\Box}$ is the d'Alembertian operator with respect to the background metric and $\bar{\vartheta}$ is the background scalar field. Since the latter must satisfy the evolution equation [Eq. (3.25b)], we immediately see that $\vartheta \propto \alpha/\beta$. This means that the right-hand side of Eq. (3.30) is proportional to

[4]This statement is true only in the absence of spins, since otherwise the CS effective worldline action would contain new self-interaction terms.

ζ. To zeroth order in the small-coupling approximation, $\tilde{h}$ then satisfies a free wave equation and can thus be treated as vanishing. Deviations from the trace-free condition can only arise at $\mathcal{O}(\zeta)$ and they are suppressed by factors of the curvature tensor, as $\bar{\vartheta}$ must satisfy Eq. (3.25b). Approaching $\mathscr{I}^+$, the right hand side of Eq. (3.30) vanishes. This allows one to impose TT gauge at future null infinity.

3.5 Effective Stress-Energy in CS Gravity

The perturbed Lagrangian for the Einstein-Hilbert action has already been calculated, so here we need only consider the contribution from $S_{\rm CS}$. At $\mathcal{O}(\epsilon^2)$, there are a large number of terms generated (we used the package *xPert* [94, 96, 95, 30, 164] to calculate the perturbations). Many of these terms are irrelevant when considering their contribution at $\mathscr{I}^+$.

Let us classify the types of terms that arise in $S_{\rm CS}$. At $\mathcal{O}(\epsilon^2)$, these are of two types:

1. the second-order part of one field, or

2. the product of first-order parts of two fields.

As mentioned in Sec. 3.2.1, terms containing the second-order part of one field are linear in a short-wavelength quantity, which vanishes under averaging. Thus we only need to consider the latter case. There are five fields in $S_{\rm CS}$ ($\sqrt{-\mathrm{g}}$, ε, ϑ, R, and ${}^*R$), so one would at first think that there are $\binom{5}{2} = 10$ types of terms arising; however, from the definition of the Levi-Civita tensor, we have

$$\sqrt{-\mathrm{g}}\,\varepsilon^{\alpha\beta\mu\nu} = \mathrm{sign}(\mathrm{g})\,[\alpha\beta\mu\nu]\,, \tag{3.31}$$

where $[\alpha\beta\mu\nu]$ is the Levi-Civita *symbol*, which is not a spacetime field. The combination $\sqrt{-\mathrm{g}}\,\varepsilon^{\alpha\beta\mu\nu}$ therefore has no perturbation, and there are only three spacetime fields which contribute. We are left with only $\binom{3}{2} = 3$ possibilities for the types of terms that could appear, corresponding to two perturbed fields and one unperturbed

one among the set $(\vartheta, R_{\alpha\beta\sigma\delta}, R_{\alpha\beta\sigma\delta})$. Two of these possibilities are actually the same by exchanging the two copies of $R_{\alpha\beta\sigma\delta}$.

Therefore, we are left with only the following two types of terms in the CS Lagrangian density:

$$\mathcal{L}_{\tilde{\vartheta}\tilde{R}} \sim \sqrt{-\bar{\mathrm{g}}}\,\bar{\varepsilon}^{\alpha\beta\mu\nu}\,\tilde{\vartheta}\,\tilde{R}^{\gamma}{}_{\delta\alpha\beta}\bar{R}^{\delta}{}_{\gamma\mu\nu} \tag{3.32a}$$

$$\mathcal{L}_{\tilde{R}\tilde{R}} \sim \sqrt{-\bar{\mathrm{g}}}\,\bar{\varepsilon}^{\alpha\beta\mu\nu}\,\bar{\vartheta}\,\tilde{R}^{\gamma}{}_{\delta\alpha\beta}\tilde{R}^{\delta}{}_{\gamma\mu\nu} \tag{3.32b}$$

where $\tilde{R}^{\gamma}{}_{\delta\alpha\beta}$ is the first-order perturbation to the Riemann tensor, in terms of $\underline{\tilde{h}}^{\mu\nu}$. Variation of these terms with respect to the background metric yields the CS contributions to the effective stress-energy tensor, while variation with respect to the metric perturbation yields CS corrections to the first order equations of motion.

3.5.1 Variation with respect to the Perturbation

Just as in GR, the final expression for the stress-energy tensor must be put on-shell by imposing the equations of motion. The first-order equations of motion of dynamical CS gravity, in vacuum and at $\mathscr{I}^{+}$, are

$$\bar{\Box}\underline{\tilde{h}}_{\mu\nu} = -\frac{1}{\kappa}\tilde{T}^{(\vartheta)}_{\mu\nu} + \frac{\alpha}{\kappa}\Big[\overline{\nabla}_{\alpha}\bar{\vartheta}\,\overline{\nabla}_{\beta}\bar{\Box}\underline{\tilde{h}}_{\gamma(\mu}\,\bar{\varepsilon}^{\alpha\beta\gamma}{}_{\nu)} + \overline{\nabla}_{\alpha}\overline{\nabla}_{\beta}\bar{\vartheta}\,\bar{\varepsilon}^{\alpha}{}_{\gamma\delta(\mu}\,\overline{\nabla}^{\delta}\left(\overline{\nabla}_{\nu)}\underline{\tilde{h}}^{\beta\gamma} - \overline{\nabla}^{\beta}\underline{\tilde{h}}_{\nu)}{}^{\gamma}\right)\Big]\,. \tag{3.33}$$

Imposing these equations of motion is easier when taking advantage of the weak-coupling limit, $\zeta_{\mathrm{GW}} \ll 1$, where $\zeta_{\mathrm{GW}} \equiv \alpha\overline{\nabla}\vartheta/(\kappa\lambda_{\mathrm{GW}})$ quantifies the size of the deformation away from GR. Let us then expand the metric perturbation in a Taylor series

$$\underline{\tilde{h}}_{\mu\nu} = \sum_{n=0}^{\infty}(\zeta_{\mathrm{GW}})^{n}\underline{\tilde{h}}^{(n)}_{\mu\nu}\,. \tag{3.34}$$

To zeroth-order, it is clear that Eq. (3.33) reduces to $\bar{\Box}\underline{\tilde{h}}^{(0)}_{\mu\nu} = 0$, which is the standard GR equation of motion. To next order, the the leading-order piece of the right-hand

side vanishes and one is then left with

$$\bar{\Box}\tilde{\underline{h}}^{(1)}_{\mu\nu} = \frac{\alpha}{\kappa}\,\overline{\nabla}_\alpha\overline{\nabla}_\beta\bar{\vartheta}\,\bar{\varepsilon}^\alpha{}_{\gamma\delta(\mu}\,\overline{\nabla}^\delta\left(\overline{\nabla}_{\nu)}\tilde{\underline{h}}^{\beta\gamma}_{(0)} - \overline{\nabla}^\beta\tilde{\underline{h}}_{\nu)}{}^{\gamma}_{(0)}\right) - \frac{1}{\kappa}\tilde{T}^{(\vartheta)}_{\mu\nu}\,. \tag{3.35}$$

In the remainder of this section, we drop the superscripts that indicate $\zeta_{\rm GW}$-ordering.

3.5.2 Variation with respect to the Background

Let us first discuss terms of type $\mathcal{L}_{\tilde{\vartheta}\tilde{R}}$ under variation with respect to $\bar{\mathrm{g}}^{\mu\nu}$. From Sec. 3.2.2, only total derivative terms arise from $\delta\bar{R}^\gamma{}_{\delta\alpha\beta}$, and these vanish upon averaging. The remaining terms contain $\bar{R}^\gamma{}_{\delta\alpha\beta}$, which must vanish at $\mathscr{I}^+$. Thus, as mentioned before, terms in the effective action which contain curvature tensors do not contribute to the effective stress-energy tensor at $\mathscr{I}^+$.

We are then only left with $\mathcal{L}_{\tilde{R}\tilde{R}}$. Writing these in terms of $\tilde{\underline{h}}^{\mu\nu}$, the effective action reads

$$S^{\rm eff(2)}_{\rm CS} = \epsilon^2\frac{\alpha}{4}\int \mathrm{d}^4x\;\mathcal{L}^{\rm eff,1}_{\rm CS} + \mathcal{L}^{\rm eff,2}_{\rm CS}\;, \tag{3.36}$$

where

$$\mathcal{L}^{\rm eff,1}_{\rm CS} = +\sqrt{-\bar{\mathrm{g}}}\;\bar{\varepsilon}^{\alpha\beta\gamma\delta}\;\bar{\vartheta}\;\overline{\nabla}^\rho\overline{\nabla}_\beta\tilde{\underline{h}}_\alpha{}^\sigma\;\overline{\nabla}_\delta\overline{\nabla}_\rho\tilde{\underline{h}}_{\sigma\gamma}\;, \tag{3.37a}$$

$$\mathcal{L}^{\rm eff,2}_{\rm CS} = -\sqrt{-\bar{\mathrm{g}}}\;\bar{\varepsilon}^{\alpha\beta\gamma\delta}\;\bar{\vartheta}\;\overline{\nabla}_\beta\overline{\nabla}_\rho\tilde{\underline{h}}_\alpha{}^\sigma\;\overline{\nabla}_\sigma\overline{\nabla}_\delta\tilde{\underline{h}}^\rho{}_\gamma\;. \tag{3.37b}$$

Naively, one might think that these expressions lead to an effective stress-energy tensor at $\mathcal{O}(\lambda^{-4}_{\rm GW})$. This is premature, however, as there can be a cancellation of $\lambda^{-4}_{\rm GW}$-terms that lead to a less steep wavelength dependence. One should try to move as many derivatives away from the perturbed quantities as possible before proceeding. In fact, we know that this must be possible from [80]: the Pontryagin density can be written as the divergence of a 4-current, so at least one derivative can be moved off of $\tilde{\underline{h}}^{\mu\nu}$. This automatically implies that there cannot be $\lambda^{-4}_{\rm GW}$ terms in the effective stress-energy tensor, as shown explicitly by Yunes and Sopuerta [137].

Let us transform $\mathcal{L}^{\rm eff,1}_{\rm CS}$ in the following way. The Levi-Civita tensor is contracted onto two derivative operators ($\overline{\nabla}_\beta$ and $\overline{\nabla}_\delta$). One may integrate by parts to move one

of these derivative operators onto the remaining terms in Eq. (3.37a). This generates two types of terms: one with three derivatives acting on the metric perturbation and one with one derivative on the CS scalar (the term acting on the Levi-Civita tensor or the determinant of the metric vanishes by metric compatibility). Let us focus on the former first. Because of the contraction onto the Levi-Civita tensor, only the antisymmetric part of the second derivative operator would contribute. Such a combination is nothing but the commutator of covariant derivatives, which can be written as the Riemann tensor, and thus vanishes at $\mathscr{I}^+$. The remaining term with a covariant derivative of the CS scalar does not generically vanish. Dropping terms proportional to the Riemann tensor, $\mathcal{L}_{\rm CS}^{\rm eff,1}$ becomes

$$\mathcal{L}_{\rm CS}^{\rm eff,1} = \sqrt{-\overline{\rm g}}\bar{\varepsilon}^{\alpha\beta\gamma\delta}\ \overline{\nabla}_\alpha\bar{\vartheta}\ \overline{\nabla}^\rho\tilde{\underline{h}}_\beta{}^\sigma\overline{\nabla}_\delta\overline{\nabla}_\rho\tilde{\underline{h}}_{\sigma\gamma}\ . \tag{3.38a}$$

Equation (3.37b) can be analyzed with the property discussed in Sec. 3.2.4: Lorenz gauge may be imposed at the level of the action for the purposes of calculating the effective stress-energy tensor. This means that if one integrates by parts, moving $\overline{\nabla}_\sigma$ and $\overline{\nabla}_\rho$ onto remaining terms, the only term that survives is proportional to $\bar{\vartheta}$, as the divergence of $\tilde{\underline{h}}^{\mu\nu}$ vanishes (after commuting derivatives, dropping Riemann terms and imposing Lorenz gauge). Thus $\mathcal{L}_{\rm CS}^{\rm eff,2}$ becomes

$$\mathcal{L}_{\rm CS}^{\rm eff,2} = \sqrt{-\overline{\rm g}}\bar{\varepsilon}^{\alpha\beta\gamma\delta}\ \overline{\nabla}_\rho\overline{\nabla}_\sigma\bar{\vartheta}\ \overline{\nabla}_\alpha\tilde{\underline{h}}_\beta{}^\sigma\overline{\nabla}_\gamma\tilde{\underline{h}}_\delta{}^\rho\ . \tag{3.38b}$$

With these simplified Lagrangian densities at hand, we can now compute the total effective stress-energy tensor for GWs in CS gravity:

$$T_{{\rm CS}\mu\nu}^{\rm eff} = T_{{\rm MT}\mu\nu}^{\rm eff} + T_{{\rm CS}\mu\nu}^{\rm eff,1} + T_{{\rm CS}\mu\nu}^{\rm eff,2}\ , \tag{3.39}$$

where $T^{\text{eff},1}_{\text{CS}\mu\nu}$ and $T^{\text{eff},2}_{\text{CS}\mu\nu}$ are due to the variation of $\mathcal{L}^{\text{eff},1}_{\text{CS}}$ and $\mathcal{L}^{\text{eff},2}_{\text{CS}}$ respectively. These expressions are

$$\begin{aligned} T^{\text{eff},1}_{\text{CS}\mu\nu} &= -\epsilon^2\frac{\alpha}{2}\left\langle\left\langle \overline{\nabla}_\alpha\bar{\vartheta}\left[\bar{\varepsilon}^{\alpha\beta\gamma\delta}\left(\overline{\nabla}_{(\mu}\underline{\tilde{h}}_{|\beta|}{}^{\sigma}\ \overline{\nabla}_{\nu)}\overline{\nabla}_\delta\underline{\tilde{h}}_{\sigma\gamma}\right.\right.\right.\right. \\ &\quad \left.\left. - \overline{\nabla}^\rho\underline{\tilde{h}}_{\beta(\mu}\overline{\nabla}_{|\delta|}\overline{\nabla}_{|\rho|}\underline{\tilde{h}}_{\nu)\gamma}\right) \right. \\ &\quad \left.\left. - 2\bar{\varepsilon}^{\alpha}{}_{(\mu}{}^{\gamma\delta}\overline{\nabla}^\rho\underline{\tilde{h}}_{\nu)\sigma}\overline{\nabla}_\delta\overline{\nabla}_\rho\underline{\tilde{h}}^{\sigma}{}_{\gamma}\right]\right\rangle\right\rangle \end{aligned} \tag{3.40a}$$

and

$$T^{\text{eff},2}_{\text{CS}\mu\nu} = -\epsilon^2\alpha\left\langle\left\langle \overline{\nabla}_\sigma\overline{\nabla}_\rho\bar{\vartheta}\ \bar{\varepsilon}^{\alpha}{}_{(\mu}{}^{\gamma\delta}\overline{\nabla}_{|\alpha|}\underline{\tilde{h}}_{\nu)}{}^{\sigma}\overline{\nabla}_\gamma\underline{\tilde{h}}^{\rho}{}_{\delta}\right\rangle\right\rangle\ . \tag{3.40b}$$

3.5.3 Imposing the On-Shell Condition

The equation of motion may be imposed anywhere $\bar{\Box}\underline{\tilde{h}}_{\alpha\beta}$ may be formed in $T^{\text{eff}}_{\text{CS}\mu\nu}$ via integration by parts. There is no contraction of derivative operators onto each other in $T^{\text{eff},2}_{\text{CS}\mu\nu}$, so it remains unchanged. In the final two terms of $T^{\text{eff},1}_{\text{CS}\mu\nu}$, the derivative operator $\overline{\nabla}_\rho$ may be moved onto $\overline{\nabla}_\alpha\bar{\vartheta}\ \overline{\nabla}^\rho\underline{\tilde{h}}_{\kappa\lambda}$. This would generally make two terms, but the term proportional to $\overline{\nabla}_\alpha\bar{\vartheta}\ \bar{\Box}\underline{\tilde{h}}_{\kappa\lambda}$ is $\mathcal{O}(\zeta^2_{\text{GW}})$ relative to the Isaacson piece, so we only keep one term. This gives

$$\begin{aligned} T^{\text{eff},1}_{\text{CS}\mu\nu} &= -\epsilon^2\frac{\alpha}{2}\left\langle\left\langle \bar{\varepsilon}^{\alpha\beta\gamma\delta}\left(\overline{\nabla}_\alpha\bar{\vartheta}\ \overline{\nabla}_{(\mu}\underline{\tilde{h}}_{|\beta|}{}^{\sigma}\ \overline{\nabla}_{\nu)}\overline{\nabla}_\delta\underline{\tilde{h}}_{\sigma\gamma}\right.\right.\right. \\ &\quad \left.\left. + \overline{\nabla}_\rho\overline{\nabla}_\alpha\bar{\vartheta}\ \overline{\nabla}^\rho\underline{\tilde{h}}_{\beta(\mu}\overline{\nabla}_{|\delta|}\underline{\tilde{h}}_{\nu)\gamma}\right) \right. \\ &\quad \left.\left. + 2\overline{\nabla}_\rho\overline{\nabla}_\alpha\bar{\vartheta}\ \bar{\varepsilon}^{\alpha}{}_{(\mu}{}^{\gamma\delta}\ \overline{\nabla}^\rho\underline{\tilde{h}}_{\nu)\sigma}\overline{\nabla}_\delta\underline{\tilde{h}}^{\sigma}{}_{\gamma}\right\rangle\right\rangle\ . \end{aligned} \tag{3.41}$$

Let us now evaluate $T^{\text{eff}}_{\text{MT}\mu\nu}$ on shell. Since $T^{\text{eff}}_{\text{MT}\mu\nu}$ is $\mathcal{O}((\zeta_{\text{GW}})^0)$, imposing the equation of motion Eq. (3.35) will introduce terms of $\mathcal{O}(\zeta_{\text{GW}})$, which are kept since they are the same order as $T^{\text{eff},1}_{\text{CS}\mu\nu}$ and $T^{\text{eff},2}_{\text{CS}\mu\nu}$. We can also impose a gauge condition. We have already imposed the Lorenz gauge throughout at the level of the action. We may further specialize this to the TT gauge. While the TT gauge may not be imposed globally, it may be imposed at $\mathscr{I}^+$, where the effective stress-energy tensor is being

evaluated. In TT gauge,

$$\begin{aligned} T^{\text{eff}}_{\text{MT}\mu\nu} &= \epsilon^2\kappa \left\langle\left\langle \frac{1}{2}\overline{\nabla}_\mu \tilde{\underline{h}}_{\alpha\beta}\overline{\nabla}_\nu \tilde{\underline{h}}^{\alpha\beta} - \overline{\nabla}_\rho \tilde{\underline{h}}_{\alpha\mu}\overline{\nabla}^\rho \tilde{\underline{h}}_\nu{}^\alpha \right.\right. \\ &\qquad \left.\left. - \frac{1}{4}\bar{\mathrm{g}}_{\mu\nu}\overline{\nabla}_\rho \tilde{\underline{h}}_{\alpha\beta}\overline{\nabla}^\rho \tilde{\underline{h}}^{\alpha\beta} \right\rangle\right\rangle \qquad (3.42a) \\ &= T^{\text{eff}}_{\text{GR}\mu\nu} + T^{\text{eff,1}}_{\text{MT}\mu\nu} + T^{\text{eff,2}}_{\text{MT}\mu\nu}\,, \end{aligned}$$

where

$$T^{\text{eff,1}}_{\text{MT}\mu\nu} = -\epsilon^2\kappa \left\langle\left\langle \overline{\nabla}_\rho \tilde{\underline{h}}_{\alpha\mu}\overline{\nabla}^\rho \tilde{\underline{h}}_\nu{}^\alpha \right\rangle\right\rangle \qquad (3.42b)$$

$$T^{\text{eff,2}}_{\text{MT}\mu\nu} = -\epsilon^2\frac{\kappa}{4} \left\langle\left\langle \bar{\mathrm{g}}_{\mu\nu}\overline{\nabla}_\rho \tilde{\underline{h}}_{\alpha\beta}\overline{\nabla}^\rho \tilde{\underline{h}}^{\alpha\beta} \right\rangle\right\rangle . \qquad (3.42c)$$

Integrating by parts, imposing the equations of motion Eq. (3.35), and integrating by parts again where appropriate, these contributions to the effective stress-energy tensor at $\mathscr{I}^+$ are

$$\begin{aligned} T^{\text{eff,1}}_{\text{MT}\mu\nu} &= -\epsilon^2 \left\langle\left\langle \tilde{\underline{h}}^\alpha{}_{(\mu}\tilde{T}^{(\vartheta)}_{\nu)\alpha} \right\rangle\right\rangle \\ &\quad - \epsilon^2\frac{\alpha}{2} \left\langle\left\langle \overline{\nabla}_\sigma\overline{\nabla}_\rho\bar{\vartheta}\ \overline{\nabla}^\delta \tilde{\underline{h}}^\alpha{}_\mu\ \bar{\varepsilon}^\sigma{}_{\gamma\delta(\alpha} \left(\overline{\nabla}_{\nu)}\tilde{\underline{h}}^{\rho\gamma} - \overline{\nabla}^\rho \tilde{\underline{h}}_{\nu)}{}^\gamma\right) \right.\right. \\ &\quad \left.\left. + (\mu \leftrightarrow \nu) \right\rangle\right\rangle \qquad (3.42d) \\ T^{\text{eff,2}}_{\text{MT}\mu\nu} &= \frac{1}{4}\bar{\mathrm{g}}_{\mu\nu}\bar{\mathrm{g}}^{\alpha\beta}T^{\text{eff,1}}_{\text{MT}\alpha\beta}\,. \qquad (3.42e) \end{aligned}$$

Finally, we may write an expression for $T^{\text{eff}}_{\text{CS}\mu\nu}$ at $\mathscr{I}^+$ after imposing the equations of motion,

$$\begin{aligned} T^{\text{eff}}_{\text{CS}\mu\nu} &= T^{\text{eff}}_{\text{GR}\mu\nu} + \delta T^{\text{eff}}_{\text{CS}\mu\nu} \qquad (3.43a) \\ \delta T^{\text{eff}}_{\text{CS}\mu\nu} &= T^{\text{eff,1}}_{\text{MT}\mu\nu} + T^{\text{eff,2}}_{\text{MT}\mu\nu} + T^{\text{eff,1}}_{\text{CS}\mu\nu} + T^{\text{eff,2}}_{\text{CS}\mu\nu}\,, \qquad (3.43b) \end{aligned}$$

where $\delta T^{\text{eff}}_{\text{CS}\mu\nu}$ contains the Chern-Simons correction at $\mathcal{O}(\zeta_{\text{GW}})$. The summands are taken from Eqs. (3.40b), (3.41), (3.42d), and (3.42e). Putting them together for

convenience, the final result is

$$\begin{aligned}
\delta T^{\rm eff}_{{\rm CS}\mu\nu} &= -\epsilon^2 \left\langle\left\langle \tilde{\underline{h}}^{\alpha}{}_{(\mu}\tilde{T}^{(\vartheta)}_{\nu)\alpha} + \frac{1}{4}\bar{\mathrm{g}}_{\mu\nu}\tilde{\underline{h}}^{\alpha\beta}\tilde{T}^{(\vartheta)}_{\alpha\beta}\right\rangle\right\rangle \\
&\quad - \epsilon^2\frac{\alpha}{2}\left\langle\left\langle \overline{\nabla}_\sigma\overline{\nabla}_\rho\bar{\vartheta}\ \left[\overline{\nabla}^\delta\tilde{\underline{h}}^{\alpha}{}_{\mu}\ \bar{\varepsilon}^{\sigma}{}_{\gamma\delta(\alpha}\left(\overline{\nabla}_{\nu)}\underline{\tilde{h}}^{\rho\gamma} - \overline{\nabla}^\rho\underline{\tilde{h}}_{\nu)}{}^{\gamma}\right) + \overline{\nabla}^\delta\tilde{\underline{h}}^{\alpha}{}_{\nu}\ \bar{\varepsilon}^{\sigma}{}_{\gamma\delta(\alpha}\left(\overline{\nabla}_{\mu)}\underline{\tilde{h}}^{\rho\gamma} - \overline{\nabla}^\rho\underline{\tilde{h}}_{\mu)}{}^{\gamma}\right)\right. \right. \\
&\qquad + \frac{1}{2}\bar{\mathrm{g}}_{\mu\nu}\overline{\nabla}^\delta\tilde{\underline{h}}^{\alpha\beta}\ \bar{\varepsilon}^{\sigma}{}_{\gamma\delta(\alpha}\left(\overline{\nabla}_{\beta)}\underline{\tilde{h}}^{\rho\gamma} - \overline{\nabla}^\rho\underline{\tilde{h}}_{\beta)}{}^{\gamma}\right) + 2\bar{\varepsilon}^{\alpha}{}_{(\mu}{}^{\gamma\delta}\overline{\nabla}_{|\alpha|}\underline{\tilde{h}}_{\nu)}{}^{\sigma}\overline{\nabla}_\gamma\tilde{\underline{h}}^{\rho}{}_{\delta} \\
&\qquad + \bar{\varepsilon}^{\sigma\beta\gamma\delta}\overline{\nabla}^\rho\tilde{\underline{h}}_{\beta(\mu}\overline{\nabla}_{|\delta|}\tilde{\underline{h}}_{\nu)\gamma} + 2\bar{\varepsilon}^{\sigma}{}_{(\mu}{}^{\gamma\delta}\ \overline{\nabla}^\rho\tilde{\underline{h}}_{\nu)\sigma}\overline{\nabla}_\delta\tilde{\underline{h}}^{\sigma}{}_{\gamma}\Big] \\
&\qquad \left. + \bar{\varepsilon}^{\alpha\beta\gamma\delta}\overline{\nabla}_\alpha\bar{\vartheta}\ \overline{\nabla}_{(\mu}\underline{\tilde{h}}_{|\beta|}{}^{\sigma}\ \overline{\nabla}_{\nu)}\overline{\nabla}_\delta\tilde{\underline{h}}_{\sigma\gamma}\right\rangle\right\rangle . \qquad (3.44)
\end{aligned}$$

In the above, we have organized the terms by their scaling with powers of wavelength. The first line contains terms which scale as $\lambda_{\rm GW}^0$ and $\lambda_{\rm GW}^{-1}$; the first of these corresponds to a "mass" term in the effective stress-energy tensor. Both of these scale more slowly with inverse wavelength than the GR contribution, so they are subdominant. The next three lines have the same scaling with inverse wavelength as GR, $\lambda_{\rm GW}^{-2}$. The final line scales more strongly with inverse wavelength, $\lambda_{\rm GW}^{-3}$. This term in principle could dominate over the GR term in the high frequency limit.

Notice that the effective stress-energy tensor presented here is applicable to both the dynamical and the non-dynamical version of CS gravity. Also note that if ϑ were a constant, rather than a function, the effective stress-energy tensor would be identical to that of GR (which is expected, since, in that case, the modification to the action is purely a boundary or topological term).

3.5.4 In dynamical CS gravity

From asymptotic arguments, we can argue that $\delta T^{\rm eff}_{{\rm CS}\mu\nu}$ does not contribute to dissipation laws at $\mathscr{I}^+$ in the dynamical version of CS gravity. As mentioned in Sec. 3.2.3, the dissipation of energy, linear and angular momentum of a system is computed by integrating components of the stress-energy tensor on a 2-sphere at $\mathscr{I}^+$. Since the area of the 2-sphere grows as r^2, for the dissipation integrals to be finite, the components of the stress-energy tensor must fall-off at least as r^{-2}. In fact, only the r^{-2} part of the stress-energy contributes as one takes the $r \to \infty$ limit. Therefore, any

part of the stress-energy tensor that decays faster than r^{-2} does not contribute to dissipation laws.

The CS correction to the effective stress-energy tensor, $\delta T^{\rm eff}_{{\rm CS}\mu\nu}$, always falls off faster than r^{-2} in the dynamical theory. To see this, we must analyze the behavior of ϑ, which is restricted. This restriction comes from demanding that the field ϑ sourced by an isolated system and in an asymptotically flat space contains a finite amount of energy. The energy in ϑ is computed by integrating the time-time component of $T^{(\vartheta)}_{\mu\nu}$ on a hypersurface of constant time and over all space. For the energy to be finite, the integral $\int^{\infty} (\nabla\vartheta)^2\, r^2 {\rm d}r$ (in an asymptotically flat, Cartesian spatial slice, appropriate to $\mathscr{I}^+$) must be finite. This restricts $\nabla\vartheta$ to fall off at least faster than $r^{-3/2}$. We then conclude that the CS correction to the energy-momentum tensor must vanish at $\mathscr{I}^+$, as $T^{\rm eff,1}_{{\rm MT}\mu\nu}$, $T^{\rm eff,2}_{{\rm MT}\mu\nu}$, $T^{\rm eff,1}_{{\rm CS}\mu\nu}$ and $T^{\rm eff,2}_{{\rm CS}\mu\nu}$ decay at least as $r^{-7/2}$ or faster.

The only contribution at $\mathscr{I}^+$ to the effective stress-energy of GWs in dynamical CS gravity which decays as r^{-2} is the GR part,

$$T^{\rm eff}_{{\rm CS}\mu\nu} = T^{\rm eff}_{{\rm GR}\mu\nu}\,. \tag{3.45}$$

Again, we stress that this only accounts for the outgoing GW radiation. However, the same argument as in Sec. 3.2.3 holds; the correction to the energy flux absorbed by trapped surfaces is only important at the end of an inspiral, both in GR and deformations away from GR. This is supported by the small velocity, small mass ratio expansion of [99] (see also [174, 175]).

3.5.5 In non-dynamical CS gravity

In the dynamical theory, since the scalar field ϑ must carry a finite energy, we were able to argue for the vanishing of $\delta T^{\rm eff}_{{\rm CS}\mu\nu}$ at $\mathscr{I}^+$. In the non-dynamical theory, there is no such demand and no further simplification can be made beyond the vanishing of $T^{(\vartheta)}_{\mu\nu}$. However, for a particular choice of $\bar{\vartheta}$ field, the effective stress-energy tensor may be evaluated. We demonstrate this below.

In the canonical embedding

The canonical embedding of non-dynamical CS gravity is given by [80]

$$v_\mu \equiv \overline{\nabla}_\mu \bar{\vartheta} \doteq (1/\mu, 0, 0, 0) \ , \tag{3.46}$$

in Cartesian coordinates in the asymptotically-flat part of the spacetime. Approaching infinity, this yields

$$\overline{\nabla}_\alpha \overline{\nabla}_\beta \bar{\vartheta} = 0 \tag{3.47}$$

so by extension $T^{\text{eff},2}_{\text{CS}\mu\nu} = 0$, the first-order equation of motion becomes $\bar{\Box}\underline{\tilde{h}}_{\mu\nu} = 0 + \mathcal{O}(\zeta^2_{\text{GW}})$, the final two terms of $T^{\text{eff},1}_{\text{CS}\mu\nu}$ vanish, and $T^{\text{eff},1}_{\text{MT}\mu\nu} = 0 = T^{\text{eff},2}_{\text{MT}\mu\nu}$. Notice that here there is no amplitude birefringence in flat spacetime as $\ddot{\vartheta} = 0$ [3, 2, 176, 168].

The first term of $T^{\text{eff},1}_{\text{CS}\mu\nu}$ is the only $\mathcal{O}(\zeta_{\text{GW}})$ correction which survives. The total stress-energy tensor in the canonical embedding of non-dynamical Chern-Simons gravity at $\mathscr{I}^+$, with this correction, is

$$\begin{aligned} T^{\text{eff}}_{\text{CS}\mu\nu} &= T^{\text{eff}}_{\text{GR}\mu\nu} + \delta T^{\text{eff}}_{\text{CS}\mu\nu} \, , \\ \delta T^{\text{eff}}_{\text{CS}\mu\nu} &= -\epsilon^2 \frac{\alpha}{2} \left\langle\!\!\left\langle \overline{\nabla}_\alpha \bar{\vartheta} \ \bar{\varepsilon}^{\alpha\beta\gamma\delta} \overline{\nabla}_{(\mu} \underline{\tilde{h}}_{|\beta|}{}^{\sigma} \overline{\nabla}_{\nu)} \overline{\nabla}_\delta \underline{\tilde{h}}_{\sigma\gamma} \right\rangle\!\!\right\rangle \\ &= +\epsilon^2 \frac{\alpha}{2\mu} \left\langle\!\!\left\langle \bar{\varepsilon}^{ijk} \overline{\nabla}_{(\mu} \underline{\tilde{h}}_{|i|}{}^{\sigma} \overline{\nabla}_{\nu)} \overline{\nabla}_k \underline{\tilde{h}}_{\sigma j} \right\rangle\!\!\right\rangle \ , \end{aligned} \tag{3.48}$$

where $\bar{\varepsilon}^{ijk}$ is the Levi-Civita tensor on the 3-space orthogonal to $(\partial/\partial t)^\mu$, and the sign change arises from the factor of sign(g) in Eq. (3.31).

From the form of the correction $\delta T^{\text{eff}}_{\text{CS}\mu\nu}$, we can briefly mention the leading modification to radiation reaction in a binary inspiral at Newtonian order. At this order, there is no modification to the trajectories of the two bodies from the $\bar{\vartheta}$ field. Since the first-order equation of motion is identical to that of GR at order $\mathcal{O}(\zeta_{\text{GW}})$, the leading solution to $\underline{\tilde{h}}_{\mu\nu}$ is the same as in GR, $\underline{\tilde{h}}_{\mu\nu} = \underline{\tilde{h}}^{\text{GR}}_{\mu\nu}$.

Inserting this solution in TT gauge into $\delta T^{\text{eff}}_{\text{CS}\mu\nu}$, the energy, linear momentum, and angular momentum radiated by the system can be computed. Adopting a Cartesian coordinate system at asymptotic infinity, the correction to the radiated quantities is

given by

$$\delta\dot{E}^{\rm CS} = -\int {\rm d}\Omega\ r^2\ \delta T^{\rm eff}_{{\rm CS}0j} n_j = +\int {\rm d}\Omega\ r^2\ \delta T^{\rm eff}_{{\rm CS}00} \tag{3.49a}$$

$$\delta\dot{P}^{\rm CS}_i = +\int {\rm d}\Omega\ r^2\ \delta T^{\rm eff}_{{\rm CS}ij} n_j = -\int {\rm d}\Omega\ r^2\ \delta T^{\rm eff}_{{\rm CS}i0} \tag{3.49b}$$

$$\delta\dot{J}^{\rm CS}_i = -\int {\rm d}\Omega\ r^2\ \varepsilon_{ijk} x_j \delta T^{(-3)}_{{\rm CS}kl} n_l\,, \tag{3.49c}$$

where $\delta T^{(-3)}_{{\rm CS}\mu\nu}$ is the part of $\delta T^{\rm eff}_{{\rm CS}\mu\nu}$ which decays as r^{-3} [147]. In evaluating these integrals, the only angular dependence is in factors of n_i or x_i. An angular integral of an odd number of such factors vanishes, while an integral of an even number of them reduces to a symmetrized product of Kronecker delta tensors. These factors arise explicitly in the definitions of Eqs. (3.49) and from spatial derivatives acting on $\underline{\tilde{h}}_{\mu\nu}$ in $T^{\rm eff}_{\mu\nu}$. The most important difference between $T^{\rm eff}_{{\rm GR}\mu\nu}$ and $\delta T^{\rm eff}_{{\rm CS}\mu\nu}$ is the parity of the number of derivatives, which leads to the following behaviour.

In GR, the leading contribution to $\dot{E}^{\rm GR}$ is from the (mass quadrupole)^2 combination. Compare this with the same integral for $\delta T^{\rm eff}_{{\rm CS}00}$, where the (mass quadrupole)^2 term has an odd number of factors of n_i, and thus vanishes. The leading contribution is then from the product of the mass quadrupole and mass octupole.

The same situation takes place in calculating $\dot{J}_i$. In GR, the leading contribution is from the product of mass quadrupole with itself. In the correction from CS gravity, the mass quadrupole squared term has an odd number of factors of n_i; the dominant contribution is again from the mass quadrupole times the mass octupole.

Finally, the situation is different in the calculation of $\dot{P}_i$. In GR, the quadrupole squared contribution to $\dot{P}_i$ has an odd number of n_i factors. The dominant contribution is from the mass quadrupole times the mass octupole. However, for the CS correction, the quadrupole squared term has an even number of factors of n_i. Using

$$\underline{\tilde{h}}^{\rm TT}_{ij} = \frac{1}{8\pi\kappa r}\ddot{\mathcal{I}}^{\rm TT}_{ij}(t-r)\,, \tag{3.50}$$

this evaluates to

$$\delta \dot{P}_i^{\rm CS} = -\frac{\alpha}{120\pi\kappa^2\mu}\varepsilon_{ijk}\mathcal{I}_{lj}^{(3)}\mathcal{I}_{lk}^{(4)}\,, \tag{3.51}$$

where $\mathcal{I}_{ij}$ is the reduced quadrupole moment of the matter, and $\mathcal{I}_{ij}^{(n)} \equiv (\mathrm{d}/\mathrm{d}t)^n\mathcal{I}_{ij}$.

For a binary in a circular orbit about the $\hat{z}$-axis with masses m_1, m_2, total mass $m = m_1 + m_2$, symmetric mass ratio $\eta = m_1 m_2/m^2$, separation d, and orbital frequency ω, we find the momentum flux correction to be

$$\delta \dot{P}_z^{\rm CS} = -\frac{8\alpha}{15\pi\kappa^2\mu}(\eta m d^2)^2\omega^7\,, \tag{3.52a}$$

or, in terms of the velocity $v = \omega d$, with Kepler's third law $v^2 = m/d$,

$$\delta \dot{P}_z^{\rm CS} = -\frac{128}{15}\left(\frac{\alpha}{\kappa\mu m}\right)\eta^2 v^{13}\,, \tag{3.52b}$$

where notice that the quantity in parentheses is dimensionless. This is to be compared with the leading momentum luminosity in GR, which is proportional to $\dot{P}_z^{\rm GR} \propto \eta^2 v^{11}\delta m/m$, where $\delta m = m_1 - m_2$ [26]. Although the GR effect is two powers of v stronger, it depends on the difference in masses, whereas the non-dynamical CS correction only depends on the total mass. This implies that in the limit of comparable masses $m_1 \approx m_2$, the recoil velocity would not asymptote to zero in CS gravity, as it does in GR for non-spinning binaries.

A physical interpretation of this effect is related to the parity-violating nature of the theory. When one chooses a canonical embedding, the action becomes parity-violating as the Pontryagin density is parity odd. The embedding coordinate chooses a (temporal) direction to which the modification to the Einstein equations can couple to, inducing a new term in the stress-energy that is proportional to the curl of the metric perturbation. Because kicks are predominantly generated during merger, the CS modification is indeed dominant over the GR result, leading to the first, non-linear, strong-field modification computed in CS gravity.

3.6 Effective Stress-Energy Tensor of Modified Gravity Theories

Let us now consider a broader class of modified gravity theories. There is an infinite variety of GR modifications one could construct. However, there are several properties that are desirable and that we require here:

1. Metric theories: the action depends on a symmetric metric tensor that controls the spacetime dynamics.

2. Deformations of GR: analytically controllable and small corrections to the Einstein-Hilbert action with a continuous GR limit.

3. High-Rank Curvature: corrections depend on quadratic or higher products of the Riemann tensor, Ricci tensor, or Ricci scalar.

4. Minkowski stable: the theory must admit Minkowski spacetime as a stable vacuum solution, and future null infinity should be asymptotically flat for isolated matter spacetimes.

Besides the metric, there may be new fields introduced which are considered part of the "gravity sector". This distinction means that said fields are not minimally coupled, i.e. they may be coupled to connection and curvature quantities. These additional fields may be of any spin: scalars, spinors, vectors, etc. For simplicity, we will only consider scalar fields here, but the results may also be extended to higher spin fields. Scalar fields are well-motivated from quantum completions of GR, e.g. moduli fields are common appearances in string theoretical models [120].

3.6.1 Action

In defining a modified gravity theory, let us consider what terms may arise in the action. These terms must include the Einstein-Hilbert and matter terms, along with

modifications built from additional scalar fields and curvature invariants. Additionally, it ought to contain a dynamical term for the scalars that couple to the curvature invariants, as we will motivate in Sec. 3.6.2.

In principle, there are an infinite number of curvature invariants to consider. The first few of these are simple to construct: Λ, R, R^2, $\nabla_\mu R \nabla^\mu R$, $R_{\mu\nu}R^{\mu\nu}$, $R_{\alpha\beta\mu\nu}R^{\alpha\beta\mu\nu}$, ..., where Λ is any scalar constant, e.g. the cosmological constant. These may be specified by their rank, r, which is the number of curvature tensors which are contracted together, and by further specifying a list of r non-negative integers $\{\lambda_1, \ldots, \lambda_r\}$, where λ_i specifies the number of derivatives acting on the i^{th} curvature tensor. For a rank r and case $\{\lambda_i\}_{i=1}^r$, there are a finite number of independent curvature invariants corresponding to the number of ways to contract indices. Thus all curvature invariants may be countably enumerated, assigning some number n to each independent invariant.

We here consider only combinations of *algebraic* curvature invariants, i.e. $\lambda_i = 0$ for all cases. This means we do not allow modifications that depend on derivatives of curvature tensors. Such a simplification is a good one, from the standpoint that it automatically guarantees the field equations to be no higher than fourth-order.

Consider then a modified gravity theory defined by the action

$$S = S_{\text{EH}} + S_{\text{mat}} + S_{\text{int}} + S_\vartheta \,, \tag{3.53a}$$

where S_ϑ is the canonical kinetic term for ϑ,

$$S_\vartheta = -\frac{\beta}{2}\int \mathrm{d}^4x\sqrt{-\mathrm{g}}\; \mathrm{g}^{\mu\nu}\left[(\nabla_\mu\vartheta)(\nabla_\nu\vartheta) + 2V(\vartheta)\right] \,, \tag{3.53b}$$

with V an arbitrary potential function; and where $S_{\rm int}$ is the interaction term between the scalar ϑ and some algebraic combination of curvature tensors, for example

$$S_{\rm int,0} = \alpha_0 \int \mathrm{d}^4x\sqrt{-\mathrm{g}}\; f_0(\vartheta)\Lambda \tag{3.53c}$$

$$S_{\rm int,1} = \alpha_1 \int \mathrm{d}^4x\sqrt{-\mathrm{g}}\; f_1(\vartheta)R \tag{3.53d}$$

$$S_{\rm int,2} = \alpha_2 \int \mathrm{d}^4x\sqrt{-\mathrm{g}}\; f_2(\vartheta)R^2\,, \tag{3.53e}$$

or generally

$$S_{\rm int} = \alpha \int \mathrm{d}^4x\sqrt{-\mathrm{g}}\; f(\vartheta)\mathcal{R}\,, \tag{3.53f}$$

with f an arbitrary "coupling function" and $\mathcal{R}$ an algebraic combination of curvature invariants. Alternatively, notice that we could have assigned each term proportional to α_i a separate ϑ_i coupling with its associated kinetic and potential terms. The arguments presented below would also hold for such constructions.

3.6.2 Dynamical scalar fields

The requirement for the scalar ϑ to be dynamical arises from demanding diffeomorphism invariance in the theory. Consider the infinitesimal transformation of the action under a diffeomorphism generated by the vector field v^μ. Specifically, look at the terms containing ϑ, i.e. the sum $S_{\rm mod} = S_{\rm int} + S_\vartheta$. The infinitesimal transformation under the diffeomorphism is

$$\begin{aligned}\delta S_{\rm mod} = \int \mathrm{d}^4x \left(\frac{\delta}{\delta \mathrm{g}_{\mu\nu}}\mathcal{L}_{\rm int}\right)\mathcal{L}_v \mathrm{g}_{\mu\nu} + \left(\frac{\delta}{\delta\vartheta}\mathcal{L}_{\rm int}\right)\mathcal{L}_v\vartheta \\ + \int \mathrm{d}^4x \left(\frac{\delta}{\delta \mathrm{g}_{\mu\nu}}\mathcal{L}_{\vartheta}\right)\mathcal{L}_v \mathrm{g}_{\mu\nu} + \left(\frac{\delta}{\delta\vartheta}\mathcal{L}_{\vartheta}\right)\mathcal{L}_v\vartheta\,,\end{aligned} \tag{3.54}$$

where $\mathcal{L}_{\rm int}$ is the interaction Lagrangian density, $\mathcal{L}_\vartheta$ is the kinetic Lagrangian density, and $\mathcal{L}_v$ stands for the Lie derivative along v^μ.

For a theory to be diffeomorphism invariant, the infinitesimal transformation in the total action must vanish, $\delta S = 0$. Since $\mathcal{L}_v\vartheta$ may be arbitrary for some ϑ and some v^μ, the functional multiplying $\mathcal{L}_v\vartheta$ must vanish for δS to vanish. This means

$$\frac{\delta}{\delta\vartheta}\left(\mathcal{L}_{\text{int}} + \mathcal{L}_\vartheta\right) = 0\,. \tag{3.55}$$

When the scalar field ϑ has dynamics, i.e. $\beta \neq 0$, then Eq. (3.55) is identical to the equations of motion of the field ϑ and is therefore automatically satisfied. However, if the field is *not* dynamical, $\beta = 0$, then Eq. (3.55) gives

$$f'(\vartheta)\mathcal{R} = 0\,. \tag{3.56}$$

Except in the case where $f'(\vartheta) = 0$, this is an additional constraint on the geometry of spacetime, namely that $\mathcal{R} = 0$. Given that the equations of motion already saturate the number of equations for the degrees of freedom present, this would be an overconstrained system. This is in fact the case in the non-dynamical version of CS gravity, as discussed in [74, 180]. We therefore only admit dynamical scalar fields, or terms with no scalar field dependence ($f(\vartheta) = const.$).

3.6.3 Special cases: zeroth and first rank

Before doing a calculation for a general curvature invariant $\mathcal{R}$, let us briefly discuss some special cases. As we will see, curvature invariants of zeroth and first rank will not be considered.

Zeroth rank

At zeroth rank, there is only one algebraic curvature invariant: a constant. The non-constant part of $f_0(\vartheta)$ may simply be reabsorbed into the potential $V(\vartheta)$. This gives a minimally coupled scalar field, which may be absorbed into S_{mat}. The constant part of f_0 leads to a "cosmological constant." Since we are only considering theories which are Minkowski stable and asymptotically flat, this cosmological part must vanish.

First rank

There is only one algebraic curvature invariant of rank 1, the Ricci scalar R. If we allow f to be a non-constant function, we would have a classical scalar-tensor theory, akin to Brans-Dicke theory (see e.g. [159]). The effective GW stress-energy tensor for scalar-tensor theory has been computed, for example in Brans-Dicke theory (see [158]), so we do not consider it here. Since we already include the Einstein-Hilbert term in Eq. (3.53a), there can be no additional term linear in R without affecting Newton's constant. Thus we only consider quadratic and higher rank curvature invariants.

3.6.4 Cubic and Higher Ranks

At cubic rank, one can easily show that there are five algebraic invariants that may not be factored as products of lower rank invariants ($R^{\mu}{}_{\nu}R^{\nu}{}_{\rho}R^{\rho}{}_{\mu}$, $R^{\mu\nu}R^{\alpha\beta}R_{\mu\alpha\nu\beta}$, $R^{\alpha\beta}{}_{\mu\nu}R^{\mu\nu}{}_{\rho\sigma}R^{\rho\sigma}{}_{\alpha\beta}$, ${}^{*}R^{\rho\sigma\mu\nu}R^{\kappa\lambda}{}_{\mu\nu}R_{\rho\sigma\kappa\lambda}$, and ${}^{*}R_{\rho\sigma}{}^{\alpha\beta}R^{\rho}{}_{\alpha}R^{\sigma}{}_{\beta}$) and four that may be factorized (R^3, $RR_{\mu\nu}R^{\mu\nu}$, $RR_{\mu\nu\alpha\beta}R^{\mu\nu\alpha\beta}$, and $R\,{}^{*}R^{\rho}{}_{\sigma}{}^{\mu\nu}R^{\sigma}{}_{\rho\mu\nu}$). The arguments that follow work for all of them, so for concreteness we choose just one: $R^{\mu}{}_{\nu}R^{\nu}{}_{\rho}R^{\rho}{}_{\mu}$. The modification to the action arising from this term is

$$S_{\text{ex.5}} = \alpha \int \mathrm{d}^4x\sqrt{-\mathrm{g}}\; f(\vartheta)R^{\mu}{}_{\nu}R^{\nu}{}_{\rho}R^{\rho}{}_{\mu}\,. \tag{3.57}$$

The contribution from this term to the effective action at second order is

$$S^{\text{eff}(2)}_{\text{ex.5}} = \epsilon^2\alpha \int \mathrm{d}^4x\sqrt{-\bar{\mathrm{g}}}\left[\frac{\tilde{h}}{2}\left(f'(\bar{\vartheta})\tilde{\vartheta}\;\bar{R}^{\mu}{}_{\nu}\bar{R}^{\nu}{}_{\rho}\bar{R}^{\rho}{}_{\mu} + 3f(\bar{\vartheta})\;\tilde{R}^{\mu}{}_{\nu}\bar{R}^{\nu}{}_{\rho}\bar{R}^{\rho}{}_{\mu}\right)\right.$$
$$\left. + 3f'(\bar{\vartheta})\tilde{\vartheta}\;\tilde{R}^{\mu}{}_{\nu}\bar{R}^{\nu}{}_{\rho}\bar{R}^{\rho}{}_{\mu} + 3f(\bar{\vartheta})\tilde{R}^{\mu}{}_{\nu}\tilde{R}^{\nu}{}_{\rho}\bar{R}^{\rho}{}_{\mu}\right]\,. \tag{3.58}$$

Immediately we see that all terms have at least one power of background curvature tensors. This means that each term can be written similarly to an earlier example in Sec. 3.2.3, in Eq. (3.11). When evaluating this effective stress- energy tensor at $\mathscr{I}^+$, all of the background curvature tensors vanish. This automatically implies that cubic

and higher rank terms in the action do not contribute to the effective stress energy tensor at asymptotically-flat, future null infinity.

The stress-energy tensor is then given by the MacCallum-Taub tensor, Eq. (3.20b), which need not be identical to the GR one yet, as one must first impose the first-order equations of motion at $\mathscr{I}^+$. These equations could be modified by the introduction of higher-order operators in the action. Let us analyze such equations again through the example of Eq. (3.57). As the calculation depends only on the rank of the curvature invariant appearing in the action and not on its specific form, the results shown below extend to all cubic and higher rank algebraic curvature invariants as well.

The equation of motion arising from Eq. (3.57) is

$$\begin{aligned}\kappa G_{\mu\nu} + 3\alpha f(\vartheta) R_{\mu\beta} R^{\beta}{}_{\gamma} R^{\gamma}{}_{\nu} - \frac{\alpha}{2} \mathrm{g}_{\mu\nu} f(\vartheta) R^{\alpha}{}_{\beta} R^{\beta}{}_{\gamma} R^{\gamma}{}_{\alpha} \\ + \frac{3\alpha}{2} \left[\mathrm{g}_{\mu\nu} \nabla_{\alpha} \nabla_{\beta} \left(f(\vartheta) R^{\alpha}{}_{\gamma} R^{\gamma\beta} \right) + \Box \left(f(\vartheta) R_{\mu\gamma} R^{\gamma}{}_{\nu} \right) \right. \\ \left. - 2 \nabla_{\beta} \nabla_{(\mu} \left(f(\vartheta) R^{\gamma}{}_{\nu)} R^{\beta}{}_{\gamma} \right) \right] = T^{\mathrm{mat}}_{\mu\nu} + T^{(\vartheta)}_{\mu\nu} \,. \end{aligned} \tag{3.59}$$

The important feature to note is that all terms containing α, that is, all terms deforming away from GR, are cubic or quadratic in curvature tensors. This is a general feature: from a term in the action of rank r, terms in the equations of motion will be of rank r and rank $r-1$.

Now consider evaluating the first-order equations of motion at asymptotically-flat, future null infinity, which we need in order to put the MacCallum-Taub stress-energy tensor on-shell. We will not write out the full first-order equations of motion; it suffices to say that the modification terms (those terms containing α) are of rank r, $r-1$, and $r-2$ in the first-order equations of motion. When going to $\mathscr{I}^+$, only the terms of rank 0 survive, e.g. $\bar{\Box} \underline{\tilde{h}}_{\mu\nu}$.

Immediately we see that the only modifications to the action that affect the first-order equations of motion at $\mathscr{I}^+$ are those of rank 2 and lower. Thus for modifications that are cubic and higher, the first-order equations of motion at $\mathscr{I}^+$ are simply those of GR, $\bar{\Box} \underline{\tilde{h}}_{\mu\nu} = 0$.

Inserting this asymptotically-flat, on-shell condition into the MacCallum-Taub stress-energy tensor yields the Isaacson stress-energy tensor. Cubic and higher rank modifications to the Lagrangian do not modify the effective stress-energy tensor due to GWs. We again emphasize that radiation reaction will still be different in a higher order theory because of different motion in the strong field, additional energy carried in the scalar field ϑ, and energy carried down horizons being different. But the energy of a GW at $\mathscr{I}^+$ is the same as in GR.

3.6.5 Quadratic terms

Let us now consider quadratic deformations to the action, as these are the only ones left to study, and let us classify the types of modifications possible. There are two important characteristics that we use for such a classification. The first depends on the nature of the curvature quantity $\mathcal{R}$. This quantity may either be topological or not. A curvature quantity that is topological may be expressed as the divergence of a current, $\mathcal{R} = \nabla_\mu \mathcal{K}^\mu$. As we mentioned in Sec. 3.4, Eq. (3.24), the Pontryagin density, ${}^*R\,R$, is a topological curvature invariant. In metric gravity, the only other non-vanishing, algebraic, second rank curvature invariant that is topological is the Gauss-Bonnet term,

$$\mathcal{G} = R_{\alpha\beta\mu\nu}R^{\alpha\beta\mu\nu} - 4R_{\mu\nu}R^{\mu\nu} + R^2\,, \tag{3.60}$$

as the Nieh-Yan invariant vanishes in torsion-free theories.

The second characteristic we can use to classify theories is the behaviour of the scalar field ϑ, which depends on the potential $V(\vartheta)$. The two possibilities are a potential that is flat, $V(\vartheta) = 0$, or one that is non-flat, V varying with ϑ. A flat potential does not choose out any preferred values of the scalar field, whereas a non-flat potential must be bounded from below for stability, and thus has a global minimum (or several minima). The presence or absence of a preferred field value is important in the limit going to $\mathscr{I}^+$.

For non-flat potentials, without loss of generality, the global minimum can be shifted to $\vartheta = 0$ by simultaneously shifting the potential function and the coupling

function f. Such a shift does not affect the derivative term in the kinetic term for ϑ, since it simply adds a global constant to the field. The only problematic situation is if the global minimum is in the limit $\vartheta \to \pm\infty$, which we do not allow here.

We begin by discussing the asymptotic behaviour of ϑ, which satisfies the sourced wave equation

$$\beta\left(\Box\vartheta - V'(\vartheta)\right) = -\alpha f'(\vartheta)\mathcal{R}\,. \tag{3.61a}$$

At $\mathscr{I}^+$, the right hand side vanishes. Furthermore, if we are interested in static or quasistatic background solutions for $\bar{\vartheta}$ around which we can expand, time derivatives in the d'Alembertian will vanish leaving only the Laplacian,

$$\overline{\nabla}^2\bar{\vartheta} - V'(\bar{\vartheta}) = 0\,. \tag{3.61b}$$

For a non-flat potential, $V'(\vartheta) \neq 0$, the zeroth order asymptotic solution will be $\bar{\vartheta}$ going to the minimum of the potential, which we have shifted to $\bar{\vartheta} = 0$.

For a flat potential, the background equation of motion for ϑ, Eq. (3.61b), at $\mathscr{I}^+$ becomes

$$\overline{\nabla}^2\bar{\vartheta} = 0\,. \tag{3.61c}$$

There are two asymptotic solutions: ϑ asymptotes to a constant or ϑ asymptotes to a function linear in Cartesian coordinates. The latter case would contribute a constant stress-energy tensor $T^{(\vartheta)}_{\mu\nu}$ at $\mathscr{I}^+$. This would lead to an asymptotically de Sitter spacetime, not an asymptotically flat spacetime. Therefore, we only consider the case where ϑ asymptotes to a constant.

The equation of motion Eq. (3.61c) does not determine to what value $\bar{\vartheta}$ asymptotes. A boundary condition is required in this case. Again, without loss of generality, for some given asymptotic value determined by some boundary condition, the field and coupling function $f(\vartheta)$ may be shifted so as to redefine the asymptotic value to be $\vartheta \to 0$ without changing the physics.

A boundary condition is *not* required if the theory is "shift symmetric." In a shift symmetric theory, the translation operation $\vartheta \to \vartheta + c$, where c is a constant, leaves

the equations of motion invariant. Such a theory, therefore, must have equations of motion that depend only on the derivative $\nabla_\mu \vartheta$. Such is the case, for example, if the action depends on a topological term multiplied by some scalar field, $f(\vartheta)\nabla_\mu \mathcal{K}^\mu$, as then the action can be rewritten as $(\nabla_\mu f(\vartheta))\mathcal{K}^\mu$ via integration by parts. Of course, in this case, the potential must also be flat and f must be linear for the theory to be shift-symmetric. Such types of corrections arise naturally in the low-energy limit of string theory [8, 7, 68, 6].

Let us rewrite the action and split the interaction term into a dynamical and non-dynamical part. Since we can always shift the field, potential, and coupling function so that the asymptotic value is $\vartheta \to 0$, let us define

$$\alpha' \equiv \alpha f(0) \tag{3.62a}$$

$$F(\vartheta) \equiv f(\vartheta) - f(0)\,. \tag{3.62b}$$

Then, the interaction term in Eq. (3.53f) may be rewritten as

$$\begin{aligned} S_{\text{int}} &= S_{\text{n-d}} + S_{\text{dyn}} \\ &= \alpha' \int \mathrm{d}^4x\sqrt{-\mathrm{g}}\,\mathcal{R} + \alpha \int \mathrm{d}^4x\sqrt{-\mathrm{g}}\,F(\vartheta)\mathcal{R}\,. \end{aligned} \tag{3.62c}$$

The first term is the non-dynamical part, i.e. the part that does not couple to the scalar field, while the second part is the dynamical part. If $\mathcal{R}$ is a topological curvature invariant, then the first term in Eq. (3.62c) does not contribute to the equations of motion, as it is the integral of a total derivative.

Dynamical contribution

Let us perturb S_{dyn} to second order to calculate the contribution to the effective action, keeping in mind that $\tilde{\tilde{\vartheta}}$ and $\tilde{\tilde{h}}$ do not contribute. This part of the effective

Field	Asymptotic form	Field	Asymptotic form
$\bar{\mathrm{g}}$	$\mathcal{O}(1+r^{-1})$	$\overline{\nabla}\bar{\vartheta}$	At least $r^{-3/2}$
$\bar{\Gamma}$	r^{-2}	$\bar{\vartheta}$	At least $r^{-1/2}$
$\bar{R}$	r^{-3}	$F(\bar{\vartheta})$	At least $r^{-1/2}$
$\bar{\mathcal{R}} \sim \bar{R}^2$	r^{-6}	$F^{(n)}(\bar{\vartheta})$	$\mathcal{O}(1)$
$\tilde{h},\ \overline{\nabla}^{(n)}\tilde{h}$	r^{-1}	$\tilde{\vartheta},\ \overline{\nabla}^{(n)}\tilde{\vartheta}$	r^{-1}
$\tilde{\mathcal{R}} \sim \bar{R}(\overline{\nabla}^2\tilde{h})$	r^{-4}	$\tilde{\tilde{\mathcal{R}}} \sim (\overline{\nabla}^2\tilde{h})^2$	r^{-2}

Table 3.1: The asymptotic forms of fields appearing in the effective action for a rank-2 modification to the action. All tensor indices have been suppressed.

action is

$$\begin{aligned} S_{\mathrm{dyn}}^{\mathrm{eff}(2)} &= \epsilon^2\alpha\int \mathrm{d}^4x\sqrt{-\bar{\mathrm{g}}}\,\Big[F(\bar{\vartheta})\,\tilde{\tilde{\mathcal{R}}} \\ &\quad + \left(\frac{\tilde{h}}{2}F(\bar{\vartheta}) + F'(\bar{\vartheta})\,\tilde{\vartheta}\right)\tilde{\mathcal{R}} \\ &\quad + \frac{1}{8}\left(\tilde{h}^2 - 2\tilde{h}^{\mu\nu}\tilde{h}_{\mu\nu}\right)F(\bar{\vartheta})\,\bar{\mathcal{R}} \\ &\quad + \frac{1}{2}\left(\tilde{h}\,F'(\bar{\vartheta})\tilde{\vartheta} + F''(\bar{\vartheta})\,\tilde{\vartheta}^2\right)\bar{\mathcal{R}}\Big]\,. \end{aligned} \tag{3.63}$$

To determine the contribution to the effective stress energy tensor at $\mathscr{I}^+$, again analyze the asymptotic form of all of the fields appearing in Eq. (3.63). The asymptotic forms are summarized in Table 3.1.

The simplest way to see that the dynamical part of the effective action does not contribute at $\mathscr{I}^+$ is to examine the asymptotics of $\bar{\mathcal{R}}$, $\tilde{\mathcal{R}}$, and $\tilde{\tilde{\mathcal{R}}}$. Since curvature tensors $\bar{R}_{\alpha\beta\mu\nu}$ are tidal tensors, they goes as r^{-3}; since $\bar{\mathcal{R}}$ contains two curvature tensors, it scales as r^{-6}. The slowest decaying (i.e. leading) part of $\tilde{\mathcal{R}}$ roughly comes from $\bar{R}\tilde{R}$ (with indices suppressed); the leading part of $\tilde{R}$ is $\overline{\nabla}^2\tilde{h}$, which, being radiative, goes as r^{-1}. This means that $\tilde{\mathcal{R}} \sim r^{-4}$. Similarly, the leading part of $\tilde{\tilde{\mathcal{R}}}$ goes as $(\overline{\nabla}^2\tilde{h})(\overline{\nabla}^2\tilde{h})$, so $\tilde{\tilde{\mathcal{R}}} \sim r^{-2}$.

Examining the effective action, Eq. (3.63), we see that there are no terms that decay as r^{-2}, which are the only ones that can contribute to the GW effective stress-energy tensor at $\mathscr{I}^+$. Any term with $\bar{\mathcal{R}}$ or $\tilde{\mathcal{R}}$ already decay too quickly; only terms

with $\tilde{\tilde{\mathcal{R}}}$ could remain, and only if they were multiplied by terms that asymptote as $\mathcal{O}(1)$.

Having performed the splitting into the dynamical and non-dynamical parts, $\tilde{\tilde{\mathcal{R}}}$ is multiplied by $\sqrt{-\bar{\mathrm{g}}}F(\bar{\vartheta})$ in the effective action. This splitting was specifically constructed so that $F(0) = 0$. Since F must be differentiable at $\vartheta = 0$, $F(\bar{\vartheta})$ must go to zero at least as fast as $\bar{\vartheta}$ goes to zero, which is at least $r^{-1/2}$.

We have thus shown that the dynamical part of the interaction term does not contributed to the effective stress-energy tensor at $\mathscr{I}^+$ directy. However, it could still contribute indirectly through the imposition of the first order field equations. We examine this in a later section.

Non-dynamical contribution

Let us now consider $S_{\text{n-d}}$ in Eq. (3.62c). This term generically contributes to the effective stress-energy tensor of GWs at $\mathscr{I}^+$. To show this contribution, consider the general rank 2 modification as the linear combination of the four independent rank 2 curvature invariants

$$\alpha\mathcal{R} \equiv \alpha_1 R^2 + \alpha_2 R_{\mu\nu}R^{\mu\nu} + \alpha_3 R_{\alpha\beta\mu\nu}R^{\alpha\beta\mu\nu} + \alpha_4\, {}^*R\, R\,, \tag{3.64a}$$

and absorb $f(0)$ into the coefficients α_i' in the non-dynamical part,

$$\alpha'\mathcal{R} \equiv \alpha_1' R^2 + \alpha_2' R_{\mu\nu}R^{\mu\nu} + \alpha_3' R_{\alpha\beta\mu\nu}R^{\alpha\beta\mu\nu} + \alpha_4'\, {}^*R\, R\,. \tag{3.64b}$$

Note that this form also includes the Weyl squared invariant, which is a dependent linear combination of the above terms, $C^{\alpha\beta\mu\nu}C_{\alpha\beta\mu\nu} = R^2/3 - 2R^{\alpha\beta}R_{\alpha\beta} + R^{\alpha\beta\mu\nu}R_{\alpha\beta\mu\nu}$, which is considered in [107, 106]. The Pontryagin density ${}^*R\,R$, being a topological invariant, does not contribute to the action in $S_{\text{n-d}}$, so we may drop the final term. Similarly, if the linear combination is proportional to the Gauss-Bonnet (or Euler) invariant, which has $\alpha_1 = 1 = \alpha_3$, $\alpha_2 = -4$, then $\mathcal{R}$ would be topological and there

would be no contribution to $S_{\text{n-d}}$ and hence no contribution to the effective stress-energy tensor of GWs.

The calculation of the effective action for the non-dynamical term is straightforward but long, so we do not show the steps here. An outline of the calculation is to perturb $\sqrt{-\mathrm{g}}\mathcal{R}$ to second order; the only parts that may contribute to an effective stress-energy tensor at $\mathscr{I}^+$ are of the form $\sqrt{-\bar{\mathrm{g}}}\tilde{R}\tilde{R}$, where again we have suppressed indices on the perturbed curvature tensor $\tilde{R}$. This is calculated in terms of the trace-reversed metric perturbation $\tilde{\underline{h}}^{\mu\nu}$. As before, Lorenz gauge may be imposed at the level of the action. All terms that remain will be of the form $\overline{\nabla}_\alpha\overline{\nabla}_\beta\tilde{\underline{h}}^{\mu\nu}\ \overline{\nabla}_\kappa\overline{\nabla}_\lambda\tilde{\underline{h}}^{\rho\sigma}$ with all indices contracted to form a scalar. If any derivative is contracted onto $\tilde{\underline{h}}^{\mu\nu}$, by integrating by parts and commuting covariant derivatives, one may form the Lorenz gauge condition $\overline{\nabla}_\mu\tilde{\underline{h}}^{\mu\nu}=0$ and ignore the term in the effective action. Thus the only surviving terms have derivatives contracted together, which can be put into one of two forms, $\bar{\Box}\tilde{\underline{h}}^{\mu\nu}\ \bar{\Box}\tilde{\underline{h}}_{\mu\nu}$ and $\bar{\Box}\tilde{\underline{h}}\ \bar{\Box}\tilde{\underline{h}}$. After the explicit calculation, the prefactors are found and

$$S^{\text{eff}(2)}_{\text{n-d}}=\frac{\epsilon^2}{4}\int \mathrm{d}^4x\sqrt{-\bar{\mathrm{g}}}\ \left[(\alpha_1'-\alpha_3')\,\bar{\Box}\tilde{\underline{h}}\ \bar{\Box}\tilde{\underline{h}}+(\alpha_2'+4\alpha_3')\,\bar{\Box}\tilde{\underline{h}}^{\mu\nu}\ \bar{\Box}\tilde{\underline{h}}_{\mu\nu}\right]\ . \tag{3.65}$$

Note again that α_4 does not appear, and if $\alpha_1,\ \alpha_2,\ \alpha_3$ are in the Gauss-Bonnet ratio, then the effective action of Eq. (3.65) vanishes.

Putting all indices in their natural positions, so as to expose implicit metric dependence, and varying the effective action of Eq. (3.65) with respect to $\bar{\mathrm{g}}^{\mu\nu}$, the contribution to the effective stress-energy tensor is

$$\begin{aligned}T^{\text{eff}}_{\text{n-d}\mu\nu}=\epsilon^2\Big\langle\Big\langle&(\alpha_1'-\alpha_3')\,\bar{\Box}\tilde{\underline{h}}\left(\bar{\Box}\tilde{\underline{h}}_{\mu\nu}-\overline{\nabla}_\mu\overline{\nabla}_\nu\tilde{\underline{h}}\right)\\&+(\alpha_2'+4\alpha_3')\left(\bar{\Box}\tilde{\underline{h}}_{\alpha\mu}\ \bar{\Box}\tilde{\underline{h}}_\nu{}^\alpha-\bar{\Box}\tilde{\underline{h}}_{\alpha\beta}\ \overline{\nabla}_{(\mu}\overline{\nabla}_{\nu)}\tilde{\underline{h}}^{\alpha\beta}\right)\Big\rangle\Big\rangle\ .\end{aligned} \tag{3.66}$$

We then find that the effective stress-energy tensor of GWs at $\mathscr{I}^+$ is given by the MacCallum-Taub stress-energy tensor (coming from the Einstein-Hilbert action) plus the direct contribution from the non-dynamical part of the rank 2 interaction term,

$T^{\text{eff}}_{\text{n-d}\mu\nu}$,

$$T^{\text{eff}}_{\mu\nu} = T^{\text{eff}}_{\text{MT}\mu\nu} + T^{\text{eff}}_{\text{n-d}\mu\nu}\,. \tag{3.67}$$

The only remaining part of the calculation is to put the stress-energy tensor on-shell, that is, to impose the first-order equations of motion at $\mathscr{I}^+$.

First-order equations of motion

We need the first-order equations of motion at $\mathscr{I}^+$ of the full theory, including both the dynamical and non-dynamical terms of the action. At $\mathscr{I}^+$, however, $\bar{\vartheta}$ and $\overline{\nabla}_\mu\bar{\vartheta}$ decay at least as $r^{-1/2}$ and $r^{-3/2}$. The only remaining dependence on $\bar{\vartheta}$ is through $f(\bar{\vartheta}) \to f(0)$.

The general zeroth and first-order equations of motion are quite long, so we do not reproduce them here, but they do simplify as $r \to \infty$. These equations are linear in $\underline{\tilde{h}}_{\mu\nu}$ and $\tilde{\vartheta}$, which are both radiative and decay as r^{-1}. This r^{-1} scaling is the asymptotic scaling of the first-order equations of motion, as there are terms of the form $\bar{\Box}\underline{\tilde{h}}_{\mu\nu}$ that appear with no curvature tensors or background scalar field $\bar{\vartheta}$ multiplying them. However, all terms containing $\tilde{\vartheta}$ have curvature tensors multiplying them, so they decay faster than the leading behaviour of r^{-1}.

Keeping only the terms that go as r^{-1}, the first-order equation of motion in Lorenz gauge at asymptotically-flat, future null infinity is

$$\begin{aligned}\kappa\bar{\Box}\underline{\tilde{h}}_{\mu\nu} &= -\left(2\alpha_1+\alpha_2+2\alpha_3\right) f(\bar{\vartheta})\left(\overline{\nabla}_\mu\overline{\nabla}_\nu\bar{\Box} - \bar{\mathrm{g}}_{\mu\nu}\bar{\Box}\bar{\Box}\right)\underline{\tilde{h}} \\ &\quad -\left(\alpha_2+4\alpha_3\right) f(\bar{\vartheta})\bar{\Box}\bar{\Box}\underline{\tilde{h}}_{\mu\nu}\,,\end{aligned} \tag{3.68a}$$

and the trace of this equation is

$$\kappa\bar{\Box}\underline{\tilde{h}} = 2\left(3\alpha_1+\alpha_2+\alpha_3\right) f(\bar{\vartheta})\bar{\Box}\bar{\Box}\underline{\tilde{h}}\,. \tag{3.68b}$$

Again we see that if the α coefficients are in the Gauss-Bonnet ratio, the GR equation of motion is recovered at $\mathscr{I}^+$.

This wave equation can be seen to be a massive wave equation for the auxiliary variable $\tilde{r}_{\mu\nu} \equiv \bar{\Box}\underline{\tilde{h}}_{\mu\nu}$, with mass $m \sim 1/\bar{\lambda}$, where $\bar{\lambda}^2 \sim |\alpha_i| f(0)/\kappa$. In the weak coupling limit, $\bar{\lambda}/\lambda_{\rm GW} \ll 1$, the equations simplify considerably. This simplification comes from treating the solution to the full theory as a *deformation* away from GR; this means expanding the fields as power series in a small parameter, namely $\bar{\zeta} = (\bar{\lambda}/\lambda_{\rm GW})^2$. As in Eq. (3.34), we impose

$$\underline{\tilde{h}}_{\mu\nu} = \sum_{n=0}^{\infty} \bar{\zeta}^n \underline{\tilde{h}}^{(n)}_{\mu\nu} \,, \tag{3.69}$$

and similarly for other fields, where the zeroth field $\underline{\tilde{h}}^{(0)}_{\mu\nu}$ is the GR solution. Inserting this expansion in the first-order equation of motion Eq. (3.68) and matching order by order gives

$$\begin{aligned} \kappa\bar{\Box}\underline{\tilde{h}}^{(n+1)}_{\mu\nu} \;=\; & -\left(2\alpha_1 + \alpha_2 + 2\alpha_3\right) f(\bar{\vartheta}) \\ & \times \left(\overline{\nabla}_\mu \overline{\nabla}_\nu \bar{\Box} - \mathrm{g}_{\mu\nu}\bar{\Box}\bar{\Box}\right) \underline{\tilde{h}}^{(n)} \\ & - \left(\alpha_2 + 4\alpha_3\right) f(\bar{\vartheta}) \bar{\Box}\bar{\Box}\underline{\tilde{h}}^{(n)}_{\mu\nu} \,, \end{aligned} \tag{3.70a}$$

for all orders $n \geq 0$, and

$$\bar{\Box}\underline{\tilde{h}}^{(0)}_{\mu\nu} = 0 \,, \tag{3.70b}$$

for the GR solution. Substituting Eq. (3.70b) into Eq. (3.70a) and iteratively solving the field equations one order at a time, we find at all orders that

$$\bar{\Box}\underline{\tilde{h}}^{(n)}_{\mu\nu} = 0 \,. \tag{3.70c}$$

This is the GR first-order equation of motion, and just as in GR, we may specialize the Lorenz gauge to the TT gauge at $\mathscr{I}^+$[5]. This expansion has discontinuously turned the massive wave equation into a massless one by killing the massive modes in the

[5]To prove that the TT gauge exists at $\mathscr{I}^+$ for this theory, the proof in Appendix A of Flanagan and Hughes (FH) [63] must be extended. Their Eq. (A.12) must be replaced by our (3.68a) and a small coupling expansion performed. The result will again be (3.70c), which is identical to FH's Eq. (A.12).

limit of $m \to \infty$. Such an order-reduction procedure, where certain solutions are eliminated through perturbative constraints, has been shown to select the physically correct ones in all studied cases [65, 162, 169].

We can now evaluate the complete effective stress-energy tensor of GWs at $\mathscr{I}^+$. As shown in Sec. 3.6.5, there is no direct contribution from the dynamical part of the interaction term. Section 3.6.5 showed that the non-dynamical part does contribute directly, but imposing Eq. (3.70c) forces this contribution to also vanish. Since the MacCallum-Taub tensor on-shell is equal to the Isaacson tensor, we then have

$$T^{\text{eff}}_{\mu\nu} = \left(T^{\text{eff}}_{\text{MT}\mu\nu} + T^{\text{eff}}_{\text{n-d}\mu\nu}\right)\Big|_{(\bar{\Box}\tilde{\underline{h}}_{\alpha\beta}=0)} = T^{\text{eff}}_{\text{GR}\mu\nu}\,. \tag{3.71}$$

That is, the effective GW stress-energy tensor is identical to the Isaacson one at $\mathscr{I}^+$ for this wide class of modified gravity theories.

3.7 Conclusions

We have here addressed the energy content of GWs in a wide class of modified gravity theories. We focused on theories that are weak deformations away from GR and calculated the effective stress-energy tensor where GWs are extracted: in the asymptotically-flat region of spacetime.

The main calculation tool we employed was the perturbed Lagrangian approach. We demonstrated the calculation explicitly for GR, recovering the Isaacson effective stress-energy tensor. We also explicitly calculated this effective tensor in dynamical modified CS gravity, where again the result at $\mathscr{I}^+$ reduces to the Isaacson tensor. The features of CS gravity that lead to the effective stress-energy tensor being identical to the one in GR are the dynamical nature of the scalar field and the topological nature of the curvature correction to the action.

We then generalized this finding to all action modifications of a similar nature: a dynamical scalar field coupled to a scalar curvature invariant of rank 2 or higher in a spacetime that is asymptotically flat. For scalar curvature invariants of rank

3 or higher, we showed that there is no modification to the stress-energy tensor or the equations of motion at $\mathscr{I}^+$. For rank 2, we calculated the contribution to the effective stress-energy tensor and to the first-order equation of motion. In the weak coupling limit, the only solutions to the first-order equations of motion satisfy the GR first-order equations of motion at $\mathscr{I}^+$, namely $\bar{\Box}\underline{\tilde{h}}_{\mu\nu} = 0$. Evaluating the effective stress-energy tensor on-shell with these solutions leads, again, to the Isaacson stress-energy tensor.

A few caveats are in order. As we have stressed before, this result is evaluated at asymptotically-flat, future null infinity, so it does not apply to cosmological spacetimes, e.g. de Sitter spacetime. Not all of the energy that is lost by a system is carried away by GWs to $\mathscr{I}^+$: there is also radiation in the scalar field (which is calculated straightforwardly from $T^{(\vartheta)}_{\mu\nu}$), and both GWs and the scalar field radiation are lost to trapped surfaces. All of these effects must be accounted for in calculating the radiation-reaction of a system. Finally, we did not address modifications to the action of the form $f(\vartheta)R$, which reduce to a classical scalar-tensor theory.

There are several avenues open for future work. Considering classical scalar-tensor modifications is one possible extension. The work should also be extended to the next simplest spacetimes, those that are asymptotically de Sitter. This is appropriate for calculating GWs from inflation, for example. Extending this approach to calculating energy lost to trapped surfaces is another possibility.

The most natural application of this work is in tests of GR with pulsar binaries and with GWs emitted by EMRIs. The former problem requires performing a post-Keplerian expansion of the motion of bodies orbiting each other. The latter requires knowing the BH spacetime (background) solution in the class of modified gravity theories and the geodesic or non-geodesic motion on that spacetime. Both of these programs require knowledge of radiation-reaction in GWs at $\mathscr{I}^+$, which we have here computed for a large class of modified gravity theories.

Chapter 4

Non-Spinning Black Holes in Alternative Theories of Gravity[†]

Abstract

We study two large classes of alternative theories, modifying the action through algebraic, quadratic curvature invariants coupled to scalar fields. We find one class that admits solutions that solve the vacuum Einstein equations and another that does not. In the latter, we find a deformation to the Schwarzschild metric that solves the modified field equations in the small coupling approximation. We calculate the event horizon shift, the innermost stable circular orbit shift, and corrections to gravitational waves, mapping them to the parametrized post-Einsteinian framework.

4.1 Introduction

Although black holes (BHs) are one of the most striking predictions of General Relativity (GR), they remain one of its least tested concepts. Electromagnetic observations have allowed us to infer their existence, but direct evidence of their non-linear gravitational structure remains elusive. In the next decade, data from very long-baseline interferometry [55, 61] and gravitational wave (GW) detectors [58, 161, 16, 83, 2, 12, 137, 134, 179, 178, 9, 136, 100, 176, 138, 149, 54, 102] should allow us to

[†]This chapter originally appeared as Yunes, N., Stein, L. C. (2011), *Nonspinning black holes in alternative theories of gravity*, Phys. Rev. D **83** 104002 [171]. A typographical error which occured in print in Eq. (4.5b) has been corrected here.

image and study BHs in detail. Such observations will test GR in the dynamical, non-linear or strong-field regime, precisely where tests are currently lacking.

Testing strong-field gravity features of GR is of utmost importance to physics and astrophysics as a whole. This is because the particular form of BH solutions, such as the Schwarzschild and Kerr metrics, enter many calculations, including accretion disk structure, gravitational lensing, cosmology and GW theory. The discovery that these metric solutions do not accurately represent real BHs could indicate a strong-field departure from GR with deep implications to fundamental theory.

Such tests require parametrizing deviations from Schwarzschild or Kerr. One such parameterization at the level of the metric is that of *bumpy BHs* [44, 153, 152], while another at the level of the GW observable is the *parameterized post-Einsteinian* (ppE) framework [170, 167]. In both cases, such parameterizations are greatly benefited from knowledge of specific non-GR solutions, but few, 4D, analytic ones are known that represent regular BHs (except perhaps in dynamical Chern-Simons (CS) gravity [169, 6] and Einstein-Dilaton-Gauss-Bonnet (EDGB) gravity [84, 150, 85, 121, 112]).

Most non-GR BH solutions are known through numerical studies. In this approach, one chooses a particular alternative theory, constructs the modified field equations and then postulates a metric ansatz with arbitrary functions. One then derives differential equations for such arbitrary functions that are then solved and studied numerically. Such an approach was used, for example, to study BHs in EDGB gravity [84, 150, 85, 121, 112].

Another approach is to find non-GR BH solutions analytically through approximation methods. In this scheme, one follows the same route as in the numerical approach, except that the differential equations for the arbitrary functions are solved analytically through the aid of approximation methods, for example by expanding in (a dimensionless function of) the coupling constants of the theory. Such a *small-coupling approximation* [37, 46, 169] treats the alternative theory as an *effective and approximate* model that allows for small GR deformations. This approach has been used to find an analytic, slowly-rotating BH solution in dynamical CS modified gravity [169, 6].

But not all BH solutions outside of GR must necessarily be different from standard GR ones. In fact, there exists many modified gravity theories where the Kerr metric remains a solution. This was the topic studied in [129], where it was explicitly shown that the Kerr metric is also a solution of certain $f(R)$ theories, non-dynamical quadratic gravity theories, and certain vector-tensor gravity theories. Based on these fairly generic examples, it was then inferred that the astrophysical observational verification of the Kerr metric could not distinguish between GR and alternative theories of gravity.

Such an inference, however, is not valid, as it was later explicitly shown in [169]. Indeed, there are alternative gravity theories, such as dynamical CS modified gravity, where the Kerr metric is not a solution. This prompted us to study what class of modified gravity theories admit Kerr and which do not. We begin by considering the most general quadratic gravity theory with dynamical couplings, as this is strongly motivated by low-energy effective string actions [38, 27, 73, 72, 34]. When the couplings are static, we recover the results of [129], while when they are dynamic we find that the Kerr metric is not a solution. In the latter case, we find how the Schwarzschild metric must be modified to satisfy the corrected field equations. We explicitly compute the shift in the location of the event horizon and innermost stable circular orbit.

Such modifications to the BH nature of the spacetime induce corrections to the waveforms generated by binary inspirals. We compute such modifications and show that they are of so-called second post-Newtonian (PN) order, i.e. they correct the GR result at $\mathcal{O}(v^4)$ relative to the leading-order Newtonian term, where v is the orbital velocity. We further show that one can map such corrections to the parameterized post-Einsteinian (ppE) framework [178], which proposes a model-independent, waveform family that interpolates between GR and non-GR waveform predictions. This result supports the suggestion that the ppE scheme can handle a large class of modified gravity models.

The remainder of this paper is organized as follows. Sec 4.2 defines the set of theories we will investigate and computes the modified field equations. Sec. 4.3 solves

for BH solutions in this class of theories. Sec. 4.4 discusses properties of the solution and Sec. 4.5 studies the impact that such BH modifications will have on the GW observable. Sec. 4.6 concludes by pointing to future possible research directions. For the remainder of this paper, we use the following conventions: latin letters in index lists stand for spacetime indices; parentheses and brackets in index lists stand for symmetrization and antisymmetrization respectively, i.e. $A_{(ab)} = (A_{ab} + A_{ba})/2$ and $A_{[ab]} = (A_{ab} - A_{ba})/2$; we use geometric units with $G = c = 1$.

4.2 Quadratic Gravity

Consider the wide class of alternative theories of gravity in 4-dimensions defined by modifying the Einstein-Hilbert action through all possible quadratic, algebraic curvature scalars, multiplied by constant or non-constant couplings:

$$S \equiv \int d^4x\sqrt{-g}\left\{\kappa R + \alpha_1 f_1(\vartheta)R^2 + \alpha_2 f_2(\vartheta)R_{ab}R^{ab} + \alpha_3 f_3(\vartheta)R_{abcd}R^{abcd} + \alpha_4 f_4(\vartheta)R_{abcd}{}^*R^{abcd} - \frac{\beta}{2}\left[\nabla_a\vartheta\nabla^a\vartheta + 2V(\vartheta)\right] + \mathcal{L}_{\rm mat}\right\}, \tag{4.1}$$

where g is the determinant of the metric g_{ab}, $(R, R_{ab}, R_{abcd}, {}^*R_{abcd})$ are the Ricci scalar and tensor, the Riemann tensor and its dual [6] respectively, $\mathcal{L}_{\rm mat}$ is the Lagrangian density for other matter, ϑ is a scalar field, (α_i, β) are coupling constants and $\kappa = (16\pi G)^{-1}$. All other quadratic curvature terms are linearly dependent, e.g. the Weyl tensor squared. Theories of this type are motivated from fundamental physics, such as in low-energy expansions of string theory [27, 73, 72, 34].

Let us distinguish between two different types of theories: non-dynamical and dynamical. In the former, all the couplings are constant ($f_i'(\vartheta) = 0$) and there is no scalar field ($\beta = 0$). Varying Eq. (4.1) with respect to the metric and setting $f_i(\vartheta) = 1$, we find the modified field equations

$$G_{ab} + \frac{\alpha_1}{\kappa}\mathcal{H}_{ab} + \frac{\alpha_2}{\kappa}\mathcal{I}_{ab} + \frac{\alpha_3}{\kappa}\mathcal{J}_{ab} = \frac{1}{2\kappa}T^{\rm mat}_{ab}\,, \tag{4.2}$$

where $T^{\rm mat}_{ab}$ is the stress-energy of matter and

$$\mathcal{H}_{ab} \equiv 2R_{ab}R - \frac{1}{2}g_{ab}R^2 - 2\nabla_{ab}R + 2g_{ab}\Box R\,, \tag{4.3a}$$

$$\mathcal{I}_{ab} \equiv \Box R_{ab} + 2R_{acbd}R^{cd} - \frac{1}{2}g_{ab}R_{cd}R^{cd} + \frac{1}{2}g_{ab}\Box R - \nabla_{ab}R\,, \tag{4.3b}$$

$$\mathcal{J}_{ab} \equiv 8R^{cd}R_{acbd} - 2g_{ab}R^{cd}R_{cd} + 4\Box R_{ab} - 2R\,R_{ab} + \frac{1}{2}g_{ab}R^2 - 2\nabla_{ab}R\,, \tag{4.3c}$$

with ∇_a, $\nabla_{ab} = \nabla_a\nabla_b$ and $\Box = \nabla_a\nabla^a$ the first and second covariant derivatives and the d'Alembertian, and using the Weyl identity $4C_a{}^{cde}C_{bcde} = g_{ab}C_{cdef}C^{cdef}$, with C_{abcd} the Weyl tensor.

The dynamical theory is specified through the action in Eq. (4.1) with $f_i(\vartheta)$ some function of the dynamical scalar field ϑ, with potential $V(\vartheta)$. For simplicity, we restrict attention here to functions that admit the Taylor expansion $f_i(\vartheta) = f_i(0) + f_i'(0)\vartheta + \mathcal{O}(\vartheta^2)$ about small ϑ, where $f_i(0)$ and $f_i'(0)$ are constants. The ϑ-independent terms, proportional to $f_i(0)$, lead to the non-dynamical theory, and we thus ignore them henceforth. Let us then concentrate on $f_i(\vartheta) = c_i\vartheta$, where we reabsorb the constants $c_i = f_i'$ into α_i, such that $\alpha_i f_i(\vartheta) \to \alpha_i\vartheta$. The field equations are then

$$G_{ab} + \frac{\alpha_1}{\kappa}\mathcal{H}^{(\vartheta)}_{ab} + \frac{\alpha_2}{\kappa}\mathcal{I}^{(\vartheta)}_{ab} + \frac{\alpha_3}{\kappa}\mathcal{J}^{(\vartheta)}_{ab} + \frac{\alpha_4}{\kappa}\mathcal{K}^{(\vartheta)}_{ab} = \frac{1}{2\kappa}\left(T^{\rm mat}_{ab} + T^{(\vartheta)}_{ab}\right)\,, \tag{4.4}$$

where $T^{(\vartheta)}_{ab} = \frac{\beta}{2}\left[\nabla_a\vartheta\nabla_b\vartheta - \frac{1}{2}g_{ab}\left(\nabla_c\vartheta\nabla^c\vartheta - 2V(\vartheta)\right)\right]$ is the scalar field stress-energy tensor and*

$$\begin{aligned}\mathcal{H}^{(\vartheta)}_{ab} \equiv{}& -4v_{(a}\nabla_{b)}R - 2R\nabla_{(a}v_{b)} + g_{ab}\left(2R\nabla^c v_c + 4v^c\nabla_c R\right)\\ &+ \vartheta\left[2R_{ab}R - 2\nabla_{ab}R - \frac{1}{2}\mathrm{g}_{ab}\left(R^2 - 4\Box R\right)\right]\,,\end{aligned} \tag{4.5a}$$

$$\begin{aligned}\mathcal{I}^{(\vartheta)}_{ab} \equiv{}& -v_{(a}\nabla_{b)}R - 2v^c\left(\nabla_{(a}R_{b)c} - \nabla_c R_{ab}\right) + R_{ab}\nabla_c v^c\\ &- 2R_{c(a}\nabla^c v_{b)} + \mathrm{g}_{ab}\left(v^c\nabla_c R + R^{cd}\nabla_c v_d\right)\\ &+ \vartheta\left[2R^{cd}R_{acbd} - \nabla_{ab}R + \Box R_{ab} + \tfrac{1}{2}\mathrm{g}_{ab}\left(\Box R - R_{cd}R^{cd}\right)\right]\,,\end{aligned} \tag{4.5b}$$

*Equation (4.5b) had an error in print. The error has been corrected here.

$$\mathcal{J}^{(\vartheta)}_{ab} \equiv -8v^c\left(\nabla_{(a}R_{b)c} - \nabla_c R_{ab}\right) + 4R_{acbd}\nabla^c v^d$$
$$- \vartheta\left[2\left(R_{ab}R - 4R^{cd}R_{acbd} + \nabla_{ab}R - 2\Box R_{ab}\right)\right.$$
$$\left. - \tfrac{1}{2}\mathrm{g}_{ab}\left(R^2 - 4R_{cd}R^{cd}\right)\right]\,, \tag{4.5c}$$
$$\mathcal{K}^{(\vartheta)}_{ab} \equiv 4v^c\epsilon_c{}^d{}_{e(a}\nabla^e R_{b)d} + 4\nabla_d v_c{}^* R_{(a}{}^c{}_{b)}{}^d\,, \tag{4.5d}$$

with $v_a \equiv \nabla_a\vartheta$ and ϵ^{abcd} the Levi-Civita tensor. Notice that $\alpha_4\mathcal{K}_{ab} = \alpha_{\rm CS}C_{ab}$, where $\alpha_{\rm CS}$ and C_{ab} are the CS coupling constant and the CS C-tensor [6]. The dynamical quadratic theory includes dynamical CS gravity as a special case. Variation of the action with respect to ϑ yields the scalar field equation of motion

$$\beta\Box\vartheta - \beta\frac{dV}{d\vartheta} = -\alpha_1 R^2 - \alpha_2 R_{ab}R^{ab} - \alpha_3 R_{abcd}R^{abcd} - \alpha_4 R_{abcd}{}^* R^{abcd}\,. \tag{4.6}$$

Both the non-dynamical and dynamical theories arise from a diffeomorphism invariant action, and thus, they lead to field equations that are covariantly conserved, i.e. the covariant divergence of Eq. (4.2) identically vanishes, while that of Eq. (4.4) vanishes upon imposition of Eq. (4.6), unlike in non-dynamical CS gravity [6].

4.3 Non-Spinning Black Hole Solution

4.3.1 Non-dynamical Theories

The modified field equations of the non-dynamical theory have the interesting property that metrics for which the Ricci tensor vanishes are automatically solutions. One can see that if $R_{ab} = 0$, then Eqs. (4.3a)-(4.3c) vanish exactly, thus satisfying the modified field equations in Eq. (4.2). This generalizes the result in [129], as we here considered a more general action.

The reason for this simplification is the Gauss-Bonnet and Pontryagin identities. The integral of the Gauss-Bonnet term $\mathcal{G} \equiv R^2 - 4R_{ab}R^{ab} + R_{abcd}R^{abcd}$ is proportional to the Euler characteristic $\mathcal{E}$, while that of the Pontryagin density $R_{abcd}{}^*R^{abcd}$ is proportional to the Chern number $\mathcal{C}$. Thus, the $R_{abcd}R^{abcd}$ and the $R_{abcd}{}^*R^{abcd}$ terms

can be removed from the action in Eq. (4.1) in favor of $\mathcal{E}$ and $\mathcal{C}$. Since the variation of these constants vanishes identically, the field equations can be rewritten to depend only on the Ricci tensor and its trace.

This feature has a natural generalization for a wider class of alternative theories of gravity. If an action for an alternative theory contains the Riemann tensor or its dual *only* in a form that can be rewritten in terms of topological invariants (with no dynamical couplings), then the field equations will be free of Riemann, and thus, all vacuum GR solutions will also be solutions of such modified theories. Therefore, any action built from powers of the Ricci scalar or products of the Ricci tensor, possibly coupled to dynamical fields, and with Riemann tensors entering only as above, admits all vacuum GR solutions.

These results have important consequences for attempts to test GR in the strong field. Electromagnetic GR tests that aim at probing the Kerr nature of BHs would be insensitive to such modified theories. On the other hand, observations that probe the dynamics of the background, such as GW observations [161, 16, 83, 2, 12, 137, 134, 179, 178, 9, 136, 100, 176, 138, 149, 54, 102], would be able to constrain them.

4.3.2 Dynamical Theories

The modified field equations in the dynamical theory, however, are not as simple, as clearly they are not satisfied when $R_{ab} = 0$. This is because $\mathcal{J}^{(\vartheta)}_{ab}$ depends on $\nabla^c v^d R_{abcd}$ and $\mathcal{K}^{(\vartheta)}_{ab}$ depends on $\nabla_d v_c \, {}^*R_{(a}{}^c{}_{b)}{}^d$. Let us search for small deformations away from the GR Schwarzschild metric that preserve stationarity and spherical symmetry. The only relevant term here then is $\mathcal{J}^{(\vartheta)}_{ab}$, as $\mathcal{K}^{(\vartheta)}_{ab}$ vanishes in spherical symmetry, as already analyzed in [169].

We thus pose the ansatz

$$ds^2 = -f_0\left[1+\epsilon h_0(r)\right]dt^2 + f_0^{-1}\left[1+\epsilon k_0(r)\right]dr^2 + r^2 d\Omega^2\,, \tag{4.7}$$

and $\vartheta = \bar{\vartheta} + \epsilon\tilde{\vartheta}$, where $f_0 \equiv 1 - 2M_0/r$, with M_0 the "bare" or GR BH mass and (t, r, θ, ϕ) are Schwarzschild coordinates, while $d\Omega^2$ is the line element on the

2-sphere. The free functions (h_0, k_0) are small deformations from the Schwarzschild metric, controlled by a function of the coupling constants (α_i, β) that we define below; ϵ is a book-keeping parameter.

Before we solve the field equations, let us discuss the scalar field potential $V(\vartheta)$. There are two distinct choices for this potential: a flat ($V'(\vartheta) = 0$) or non-flat ($V'(\vartheta) \neq 0$) potential. For the non-flat case, the potential must be bounded from below for the theory to be globally stable, and thus it will contain one or more minima. The scalar field would tend towards the minimum of the potential, where the latter could be expanded as a quadratic function about the minimum (assumed here to be at zero): $V \approx \frac{1}{2} m_\vartheta^2 \vartheta^2$. One might treat the flat potential as the limit $m_\vartheta \to 0$ of the above non-flat potential, but this limit is not continuous at the point $m_\vartheta = 0$. The massive case must thus be treated generically and it turns out to be sufficiently complicated that we restrict our attention only to the massless (flat) case[1].

With this ansatz, we can solve the modified field equations and the scalar field's equation of motion order by order in ϵ. Through the small-coupling approximation, we treat $\alpha = \mathcal{O}(\epsilon)$ and $\beta = \mathcal{O}(\epsilon)$. To zeroth-order in ϵ, the field equations are automatically satisfied because the Schwarzschild metric has vanishing Ricci tensor. To this order, the scalar field equation can be solved to find

$$\bar{\vartheta} = \frac{\alpha_3}{\beta} \frac{2}{M_0 r} \left(1 + \frac{M_0}{r} + \frac{4}{3} \frac{M_0^2}{r^2} \right) . \tag{4.8}$$

This is the same solution found in [38] for dilaton hair sourced in EDGB gravity. The scalar field depends only on α_3, since the term proportional to α_4 vanishes identically in a spherically symmetric background.

We can use this scalar field solution to solve the modified field equations to $\mathcal{O}(\epsilon)$. Requiring that the metric be asymptotically flat and regular at $r = 2\,M_0$, we find the unique solution $h_0 \equiv \mathcal{F}(1 + \tilde{h}_0)$ and $k_0 \equiv -\mathcal{F}(1 + \tilde{k}_0)$, where $\mathcal{F} \equiv -(49/40)\ \zeta\ (M_0/r)$

[1]It is worth noting, however, that the potential must respect the symmetries inherited from the fundamental theory that the effective action derives from. A large class of such theories, such as heterotic string theory in the low-energy limit, is shift symmetric, which then forbids the appearance of mass terms.

and

$$\begin{aligned}\tilde{h}_0 &= \frac{2M_0}{r}+\frac{548}{147}\frac{M_0^2}{r^2}+\frac{8}{21}\frac{M_0^3}{r^3}-\frac{416}{147}\frac{M_0^4}{r^4}-\frac{1600}{147}\frac{M_0^5}{r^5}\,, \\ \tilde{k}_0 &= \frac{58}{49}\frac{M_0}{r}+\frac{76}{49}\frac{M_0^2}{r^2}-\frac{232}{21}\frac{M_0^3}{r^3}-\frac{3488}{147}\frac{M_0^4}{r^4}-\frac{7360}{147}\frac{M_0^5}{r^5}\,,\end{aligned} \tag{4.9}$$

and where we have defined the dimensionless coupling function $\zeta \equiv \alpha_3^2/(\beta\kappa M_0^4) = \mathcal{O}(\epsilon)$. This solution is the same as that found in EDGB gravity [98]. Our analysis shows that such a solution is the most general for all dynamical, algebraic, quadratic gravity theories, in spherical symmetry.

The demand that the metric deformation be regular everywhere outside the horizon has led to a term that changes the Schwarzschild BH mass, i.e. there is a correction to g_{tt} and g_{rr} that decays as $1/r$ at spatial infinity. We can then define the physical mass $M \equiv M_0[1+(49/80)\zeta]$, such that the only modified metric components become $g_{tt} = -f(1+h)$ and $g_{rr} = f^{-1}(1+k)$ where $h = \zeta/(3f)(M/r)^3\tilde{h}$ and $k = -(\zeta/f)(M/r)^2\tilde{k}$, and

$$\tilde{h} = 1+\frac{26M}{r}+\frac{66}{5}\frac{M^2}{r^2}+\frac{96}{5}\frac{M^3}{r^3}-\frac{80M^4}{r^4}\,, \tag{4.10}$$

$$\tilde{k} = 1+\frac{M}{r}+\frac{52}{3}\frac{M^2}{r^2}+\frac{2M^3}{r^3}+\frac{16}{5}\frac{M^4}{r^4}-\frac{368}{3}\frac{M^5}{r^5}\,, \tag{4.11}$$

and where $f \equiv 1-2M/r$. Physical observables are related on the renormalized mass, not the bare mass. This renormalization was not performed by [98].

In fact, one need not fix the single constant of integration which appears in finding this solution. Any value of the integration constant, after renormalization, is absorbed into the renormalized mass. Rather than a family of spacetimes, there is a unique spacetime after renormalization.

The sign of the coupling constant can be determined by computing the energy carried by the scalar field in Eq. (4.8). The energy is $E_{(\vartheta)} \equiv \int_\Sigma T^{(\vartheta)}_{ab} t^a t^b \gamma^{1/2} d^3x$, where Σ is a $t =$ const. hypersurface outside of the horizon (so that it is spacelike everywhere), $t^a = (\partial/\partial t)^a$ and γ is the determinant of the metric intrinsic to Σ. We

find that $E_{(\vartheta)} = (9/7)\zeta\kappa\pi M$. For stability reasons, we require that $E_{(\vartheta)} \geq 0$, which then implies $\zeta \geq 0$ and $\alpha_3^2/\beta \geq 0$.

Although we here considered non-spinning BHs, our analysis can be generalized to spinning ones, by separating the theory and its solutions into parity-even and parity-odd sectors. A parity transformation consists of the reflection $x^i \to -x^i$, which for a spinning BH metric implies $a \to -a$, where $|S^i| = M|a|$ is the magnitude of the spin angular momentum. Expanding the spinning BH solution as a power series in a/M, we see that the Kretschmann scalar $R_{abcd}R^{abcd}$ has only even powers of a/M (even parity sector), while the Pontryagin density ${}^*R\,R$ has only odd powers of a/M (odd parity sector). These quantities source the ϑ equation of motion, therefore driving even and odd metric perturbations respectively. The solution found here is of even parity and corresponds to the $\mathcal{O}(a^0)$ part of the metric expansion for a slowly-spinning BH in dynamical quadratic gravity. The next order, $\mathcal{O}(a^1)$, is parity odd and is sourced only by the Pontryagin density, since $R^2, R_{ab}R^{ab}$, and $R_{abcd}R^{abcd}$ are all even under parity. The solution sourced by just the Pontryagin density is identical to that in dynamical Chern-Simons gravity (all $\alpha_i = 0$ except for α_4) and was found in [169]. From the parity arguments presented here, we see that the exact same modification arises at $\mathcal{O}(a^1)$ in the more general dynamical quadratic gravity considered here. Therefore, to $\mathcal{O}(a^1)$, the modification in dynamical quadratic gravity is simply the linear combination of the $\mathcal{O}(a^0)$ solution found here and the $\mathcal{O}(a^1)$ solution found in [169].

4.4 Properties of the Solution

The solution found is spherically symmetric, stationary, asymptotically flat, and regular everywhere except at $r = 0$. It represents a non-spinning BH with a real singularity at the origin, as evidenced by calculating the Kretschmann scalar expanded to $\mathcal{O}(\zeta)$: $K \equiv R_{abcd}R^{abcd} = \bar{K} - 32\zeta M^3/r^7\tilde{K}$, where $\bar{K} = 48M^2/r^6$ and

$$\tilde{K} \;=\; 1 + \frac{M}{2r} + \frac{72M^2}{r^2} + \frac{7M^3}{r^3} + \frac{64}{5}\frac{M^4}{r^4} - \frac{840M^5}{r^5}\,. \tag{4.12}$$

The location of the event horizon, i.e. the surface of infinite redshift, can be computed by solving $g_{tt} = 0$ to find $r_{\rm EH}/M = 2 - (49/40)\zeta$. The metric remains Lorentzian (i.e. $\mathrm{sgn}(g) < 0$) everywhere outside $r_{\rm EH}$ provided ζ is sufficiently small (specifically, $0 < \zeta < (120/361)$).

One can also study point-particle motion in this background. Neglecting internal structure and spins, test-particle motion remains geodesic [71] and the equation of motion reduces to $\dot{r}^2/2 = V_{\rm eff}^{\rm GR} + \delta V_{\rm eff}$, where the overhead dot stands for differentiation with respect to proper time and

$$V_{\rm eff}^{\rm GR} = \frac{E^2}{2} - \frac{L^2}{2r^2}f - \frac{f}{2}\,, \qquad \delta V_{\rm eff} = -\frac{1}{2}E^2 h - \frac{1}{2}V_{\rm eff}^{\rm GR}k\,, \tag{4.13}$$

where (E, L) are the conserved quantities induced by the timelike and azimuthal Killing vectors, i.e. the particle's energy and angular momentum per unit mass.

One can solve for the energy and angular momentum for circular orbits [155] through the conditions $\dot{r} = 0$ and $V'_{\rm eff} = 0$ to find $E = E_{\rm GR} + \delta E$ and $L = L_{\rm GR} + \delta L$, where $E_{\rm GR} = f(1 - 3M/r)^{-1/2}$, $L_{\rm GR} = (Mr)^{1/2}E_{\rm GR}/f$ and

$$\delta E = -\frac{\zeta}{12}\frac{M^3}{r^3}\left(1 - \frac{3M}{r}\right)^{-3/2}\left(1 + \frac{54M}{r} + \frac{198}{5}\frac{M^2}{r^2} + \frac{252}{5}\frac{M^3}{r^3} - \frac{2384}{5}\frac{M^4}{r^4} + \frac{480M^5}{r^5}\right), \tag{4.14}$$

$$\delta L = -\frac{\zeta M}{4}\frac{M^{3/2}}{r^{3/2}}\left(1 - \frac{3M}{r}\right)^{-3/2}\left(1 + \frac{100}{3}\frac{M}{r} - \frac{30M^2}{r^2} + \frac{16}{5}\frac{M^3}{r^3} - \frac{752}{3}\frac{M^4}{r^4} + \frac{320M^5}{r^5}\right). \tag{4.15}$$

From this expression, we can find the modified Kepler law by expanding $\omega \equiv L/r^2$ in the far field limit:

$$\omega^2 = \omega_{\rm GR}^2\left[1 - \frac{\zeta}{2}\left(\frac{M}{r}\right)^2\right] \tag{4.16}$$

where $\omega_{\rm GR}^2 = M/r^3[1 + \mathcal{O}(M/r)]$. If in addition to the above circular orbit conditions one evaluates the marginal stability condition $V''_{\rm eff} = 0$, one finds that the shift in the ISCO location is

$$\frac{r_{\rm ISCO}}{M} = 6 - \frac{16297}{9720}\zeta\,. \tag{4.17}$$

4.5 Impact on Binary Inspiral GWs

As evidenced above, such a modified theory will introduce corrections to the binding energy of binary systems. Consider a binary with component masses $m_{1,2}$ and total mass $m = m_1 + m_2$. The binding energy, to leading $\mathcal{O}(m/r, \zeta)$, can be obtained from $E_{\rm GR}$ and δE in Eq. (4.14) by the transformation $m_1 m_2 \to m^2\eta$ and expanding in $M/r \ll 1$. This trick works to leading order in ζ and in m/r only and it leads to

$$E_b(r) = -\frac{m^2\eta}{2r}\left[1 + \frac{\zeta}{6}\left(\frac{m}{r}\right)^2\right] . \tag{4.18}$$

Using the modified Keplerian relation of the previous Section, this becomes

$$E_b(F) = -\frac{1}{2}\left(2\pi m F\right)^{2/3} - \frac{1}{6} m\eta\zeta\left(2\pi m F\right)^2 , \tag{4.19}$$

to leading $\mathcal{O}(mF, \zeta)$, where F is the orbital frequency and $\eta = m_1 m_2/m^2$ is the symmetric mass ratio. Such a modification to the binding energy will introduce corrections to the binary's orbital phase evolution at leading, Newtonian order.

A calculation of the phase and amplitude waveform correction that accounts only for the leading-order binding energy modification is incomplete. First, higher $\mathcal{O}(m/r)$ terms in E_b are necessary for detailed GW tests. These terms, however, are not necessary to find the leading-order, functional form of the waveform correction; this is all one needs to map these modifications to the ppE scheme.

To be consistent, we must also consider the energy flux carried by the scalar field. This program involves solving for the perturbation on top of the background solution given in Eq. (4.8). The solution can be found using post-Newtonian integration techniques and is in preparation [166].† The modification to radiation reaction due to the scalar field is subdominant (of much higher post-Newtonian order) compared to the modification to the binding energy calculated here, as will be shown in a forthcoming paper [166].†

†The work originally referenced here came to be the following Chapter, Chap. 5.
†Ibid.

Let us now compute the orbital phase correction due to modifications to the binding energy. The orbital phase for a binary in a circular orbit is simply

$$\phi(F) = \int^{F} (E') \, (\dot{E})^{-1} \omega \, d\omega \,, \tag{4.20}$$

where $\omega = 2\pi F$ is the orbital angular frequency, $E' \equiv dE/d\omega$ and $\dot{E} = -(32/5)\eta^2 m^2 r^4 \omega^6$ is the loss of binding energy due to radiation. This expression for $\dot{E}$ is the GR quadrupole form, which was shown [138] to be valid in the small-coupling limit in asymptotically flat spacetimes when the action is of the form we use. Neglecting $\dot{E}^{(\vartheta)}$ and to leading $\mathcal{O}(m\omega, \zeta)$, the orbital phase

$$\phi = \phi_{\rm GR} \left[1 + \frac{25}{3} \zeta \, (2\pi m F)^{4/3} \right] , \tag{4.21}$$

where the GR phase is $\phi_{\rm GR} = -1/(32\eta)(2\pi m F)^{-5/3}$. The leading order correction is of so-called 2PN order, as it scales with $(m\ F)^{4/3}$ (down by $1/c^4$) relative to the leading-order GR result.

Similarly, we can compute the correction to the frequency-domain GW phase in the SPA, by assuming that its rate of change is much more rapid than the GW amplitude's. This phase is (see e.g. [173])

$$\Psi_{\rm GW} = 2\phi(t_0) - 2\pi f t_0 \,, \tag{4.22}$$

where t_0 satisfies the stationary phase condition $F(t_0) = f/2$, with f the GW frequency. Neglecting $\dot{E}^{(\vartheta)}$ and to leading $\mathcal{O}(m\omega, \zeta)$, we find that

$$\Psi_{\rm GW} = \Psi^{\rm GR}_{\rm GW} \left[1 + \frac{50}{3} \zeta \eta^{-4/5} u^{4/3} \right] , \tag{4.23}$$

where $u \equiv \pi \mathcal{M} f$ is the reduced frequency and $\mathcal{M} = \eta^{3/5} m$ is the chirp mass. Similarly, the Fourier-domain amplitude scales as $|\tilde{h}| \propto \dot{F}(t_0)^{-1/2}$, which then leads to

$$|\tilde{h}| = |\tilde{h}|_{\rm GR} \left[1 + \frac{5}{6} \zeta u^{4/3} \eta^{-4/5} \right] , \tag{4.24}$$

where $|\tilde{h}_{\rm GR}|$ is the GW amplitude in GR. In principle, there could be additional corrections to $|h|$ from modifications to the first order equations of motion, but [138] has shown that these vanish in the small coupling approximation.

The modifications introduced to the inspiral waveforms can be mapped to parametrized waveform models that facilitate GR tests. In the ppE framework [170], the simplest parameterization is

$$\tilde{h} = |\tilde{h}|_{\rm GR}(1+\alpha\eta^c u^a)\exp[i\Psi^{\rm GR}_{\rm GW}(1+\beta\eta^d u^b)]\,, \tag{4.25}$$

where $(\alpha, a, \beta, b, c, d)$ are ppE parameters. Our results clearly map to this parameterization with $\alpha = (5/6)\zeta$, $\beta = (50/3)\zeta$, $a = 4/3 = b$ and $c = -4/5 = d$. Since the radiation carried by the scalar field is of higher post-Newtonian order, including it will not change these ppE parameters. Future GW constraint on these parameters could be translated into a bound on the class of alternative theories considered here.

Preliminary studies suggest that GW detectors, such as LIGO, could place interesting constraints on the parameter β. Given a signal-to-noise ratio of 20 for a comparable mass binary inspiral signal, one might be able to constrain $\beta \lesssim 10^{-1}$ when $b = 4/3$ [47]. This bound would translate to a ζ-constraint of $\zeta \lesssim 10^{-2}$, which should be compared to the current double binary pulsar constraint $\zeta \lesssim 10^{7}$ [167]. Since the effect calculated here occurs at 2PN order, systems with strong gravity are required to probe it. 2PN effects are unimportant in describing the spacetime of the solar system and known binary pulsars. GWs sourced in the strong field could place much stronger constraints on non-linear strong field deviations from GR relative to current solar system and binary pulsar bounds.

4.6 Future Work

The study presented here shows that there is a wide class of modified gravity theories where Schwarzschild and Kerr are not solutions, yet their waveform modifications can be mapped to the ppE scheme. This study could be extended by investigating higher-

order in v, PN corrections to the waveform modifications. Such a calculation would require one to solve for the two-body metric in this specific class of theories. Although this can in principle be done within the PN scheme, in practice the calculation will be analytically quite difficult, due to the non-linear terms introduced by the modified theory.

Another possible extension is to investigate the effect of different potential terms to the results presented here. For example, one could postulate a cosine potential and see how this modifies the solutions found. Such cosine potentials arise naturally due to non-linear interactions in effective string actions. The inclusion of such a potential will probably render the problem non-analytic, forcing us to solve the equations of motion for the scalar field numerically.

One other avenue of future research is to find analytic, closed form solutions for BHs rotating arbitrarily fast in dynamical quadratic gravity. The analysis presented here applies only to non-rotating BHs, and we have discussed how it would be modified when considering slowly rotating BHs. Exact, closed form solutions for rapidly rotating BHs, however, remain elusive. One might have to integrate the equations numerically to find such solutions. One possible line of attack is to evolve the field equations in a $3+1$ decomposition, starting with a dense and rotating scalar field configuration. Upon evolution, this scalar field will collapse into a rapidly rotating BH, yielding a numerical representation of the solution one seeks.

Chapter 5

Post-Newtonian, Quasi-Circular Binary Inspirals in Quadratic Modified Gravity[†]

Abstract

We consider a general class of quantum gravity-inspired, modified gravity theories, where the Einstein-Hilbert action is extended through the addition of all terms quadratic in the curvature tensor coupled to scalar fields with standard kinetic energy. This class of theories includes Einstein-Dilaton-Gauss-Bonnet and Chern-Simons modified gravity as special cases. We analytically derive and solve the coupled field equations in the post-Newtonian approximation, assuming a comparable-mass, spinning black hole binary source in a quasi-circular, weak-field/slow-motion orbit. We find that a naive subtraction of divergent piece associated with the point-particle approximation is ill-suited to represent compact objects in these theories. Instead, we model them by appropriate effective sources built so that known strong-field solutions are reproduced in the far-field limit. In doing so, we prove that black holes in Einstein-Dilaton-Gauss-Bonnet and Chern-Simons theory can have hair, while neutron stars have no scalar monopole charge, in diametrical opposition to results in scalar-tensor theories. We then employ techniques similar to the direct integration of the relaxed Einstein equations to obtain analytic expressions for the scalar field, metric perturbation, and the associated gravitational wave luminosity measured at infinity. We find that scalar field emission mainly dominates the energy flux budget, sourcing electric-type (even-parity) dipole scalar radiation and magnetic-type (odd-parity) quadrupole

[†]This chapter originally appeared as Yagi, K., Stein, L. C., Yunes, N., Tanaka, T. (2012), *Post-Newtonian, Quasi-Circular Binary Inspirals in Quadratic Modified Gravity*, Phys. Rev. D **85** 064022 [165].

scalar radiation, correcting the General Relativistic prediction at relative -1PN and 2PN orders. Such modifications lead to corrections in the emitted gravitational waves that can be mapped to the parameterized post-Einsteinian framework. Such modifications could be strongly constrained with gravitational wave observations.

5.1 Introduction

The validity of Einstein's theory in the strong-gravity regime will soon be put to the most stringent tests yet, through the observation of gravitational waves (GWs) from compact object binary inspirals [159, 134, 136]. Such waves carry detailed information about their source and the underlying gravitational theory in play. This information is primarily encoded in the evolution of the GW frequency, which in turn depends directly on the rate of energy transport away from the binary [116]. In general relativity (GR), this transport is performed exclusively by GWs. In modified gravity theories, however, additional (scalar, vectorial or tensorial) degrees of freedom can also carry energy and angular momentum away as they propagate.

Calculating how gravitational waves are corrected in modified gravity theories can be a gargantuan task as the modification can increase the number of propagating degrees of freedom and the non-linearity of the equations that control their propagation. For example, the amount of energy-momentum transported away from a binary system must be computed both from the GWs excited by the corresponding sources, as well as any additional waves associated with extra degrees of freedom [101]. The sources that drive such waves can depend both on derivatives of the metric perturbation and the extra degrees of freedom, which, in turn, are specified by the solution to their own equations of motion. The situation worsens if these are non-linearly coupled, e.g. a scalar field equation of motion that depends on the metric tensor, whose evolution in turn depends on derivatives of the scalar field.

Such calculations, however, are feasible if one treats any GR deviations as *small deformations* [177], which can be formalized through the *small-coupling approximation*, a common technique in perturbation theory to isolate physically relevant solutions in higher-derivative theories [36, 163, 45]. This is a reasonable approximation given that

GR has passed a large number of tests, albeit in the weak-gravity regime. Even in the GW regime, signals will slowly transition from sampling weak fields to moderately strong fields during a full binary inspiral. The strongest GW events will not be able to sample anywhere close to the Plank regime, where one would expect completely new physics. The largest gravitational fields experienced by binaries occur when these merge, and even then, the metric curvature cannot exceed m^{-2}, where m is the total mass of the binary. Earth-based detectors, such as LIGO [89], VIRGO [154] and LCGT [88], and future space-borne detectors, such as LISA [90], will only be able to sample gravitational fields up to this strength.

Of the plethora of modified gravity theories, we choose to focus on a general class that is characterized by the addition of quadratic curvature invariants to the action, coupled to scalar fields with standard kinetic terms (see e.g. Eq. (5.1). Such theories are motivated from loop quantum gravity [13, 131] and heterotic string theory [119], arising generically upon four-dimensional compactification in the low-energy limit. Disjoint sub-classes of quadratic theories reduce to Einstein-Dilaton-Gauss-Bonnet (EDGB) theory [103, 112] and Dynamical Chern-Simons (CS) modified gravity [80, 5].

From a phenomenological standpoint, such quadratic gravity theories are also interesting as straw-men to study small deviations from GR. This is because the new quadratic terms are always small relative to the Einstein-Hilbert term when considering merging binaries. In such systems, the maximum radius of curvature is always much larger than the new scale introduced by the scalar fields. If this were not the case, astrophysical observations would already have constrained quadratic gravity deviations.

Quadratic gravity introduces an equation of motion for the scalar field and modifies the metric field equations. The former is a driven wave equation, whose sources are quadratic curvature invariants. The latter contains new terms that depend on the product of the scalar field and its derivatives with the Riemann tensor, Ricci tensor, Ricci scalar and their derivatives. As such, one might worry that higher derivative terms in the field equations could render the system unstable. One must remember, however, that the action is a truncation (at quadratic order in the present case) of

an *effective theory* derived by integrating out heavy degrees of freedom contained in a more complete theory. Since we truncate the effective action, its validity is limited only to leading-order in the coupling parameters. Accounting for higher-order terms in the coupling would require the inclusion of higher-order terms (cubic, quartic, etc.) in the action [163]. Therefore, the modified field equations should not be considered as an exact system, but rather as an effective one.

Given the above and using the *small-coupling* approximation, the field equations become driven differential equations for the metric deformation and the scalar field. The source of the latter depends only on derivatives of the GR metric perturbation, while the source of the former depends both on the GR metric perturbation and the scalar field. We solve these equations in the post-Newtonian (PN) limit, where in particular we consider comparable-mass, spinning black hole (BH) binaries (electromagnetically uncharged), spiraling in a quasi-circular orbit. This forces the driven differential equations into driven wave equations, which can be studied with PN techniques [50, 142, 143, 22, 20, 23, 21] and then solved via retarded Green function methods.

A complication arises when attempting to solve these equations, as one must choose a prescription to describe BHs and neutron stars (NSs). In standard PN theory and up to a certain high PN order, one can choose a point-particle prescription, essentially because the exterior gravitational field of a compact object is the same as that induced by a point-particle. In modified quadratic gravity, however, both non-spinning [172] and spinning [177], strong-field BH solutions differ from that generated by simple point particles with a mass-monopole and a current-dipole moment; BHs in these theories have additional scalar multipole moments. One can take these effects into account by constructing an *effective* point-particle source that reproduces known, strong-field solutions to leading order in the weak-field region, sufficiently far away from the compact objects. With this effective point-particle prescription, we can then evaluate the source of the driven wave equations and analytically solve them to find the radiative part of the scalar field and metric perturbation.

Executive Summary of Results

Given the length of this paper, let us summarize the main results. We have devised a framework in the small-coupling approximation to solve for compact binary inspirals in modified quadratic gravity theories. One of the key ingredients in this framework is the calculation of effective source terms that allow us to use the point-particle approximation even for theories where such approximation is not valid. We applied this to modified quadratic gravity to find that both NSs and BHs have scalar hair, which leads to dipolar emission. EDGB and CS gravity are exceptions, where although BHs retain scalar monopole and dipole charge, respectively, NSs shed the scalar monopole charge. Therefore, BHs in EDGB generically contains dipolar GW emission, while CS gravity leads to modified quadrupolar emission.

The presence of scalar monopole and dipole hair, and in particular the flux of energy-momentum carried by this hair, leads to a modification in the rate of change of the binary's binding energy. The even-parity sector of the theory leads to scalar hair, which modifies the energy flux at -1PN order relative to the GR quadrupole flux. Of course, such a modification is proportional to the coupling parameter of the theory, which is assumed small. The odd-parity sector leads to dipole hair for spinning BH binaries, which modifies the energy flux at 2PN relative order. If the BH binary components are non-spinning, they have no dipole hair but the binary orbital interaction generates a modification in the energy flux that enters at relative 7PN order. Figure 5-1 shows the energy flux carried by the even-parity scalar field (long dashed line), odd-parity scalar field (dot-dashed for spinning binaries and short dashed line for non-spinning binaries), and the GR quadrupole flux (solid line) as a function of orbital velocity. Observe that when one assumes that BHs are non-spinning, the scalar emission is greatly suppressed.

These energy flux corrections translate into changes to the waveform observables. We explicitly calculate these and map them to the parametrized post-Einsteinian (ppE) framework [178, 48]. Using the results of Cornish et al. [48] we estimate that GW observations could constrain the new length scale introduced in quadratic gravity

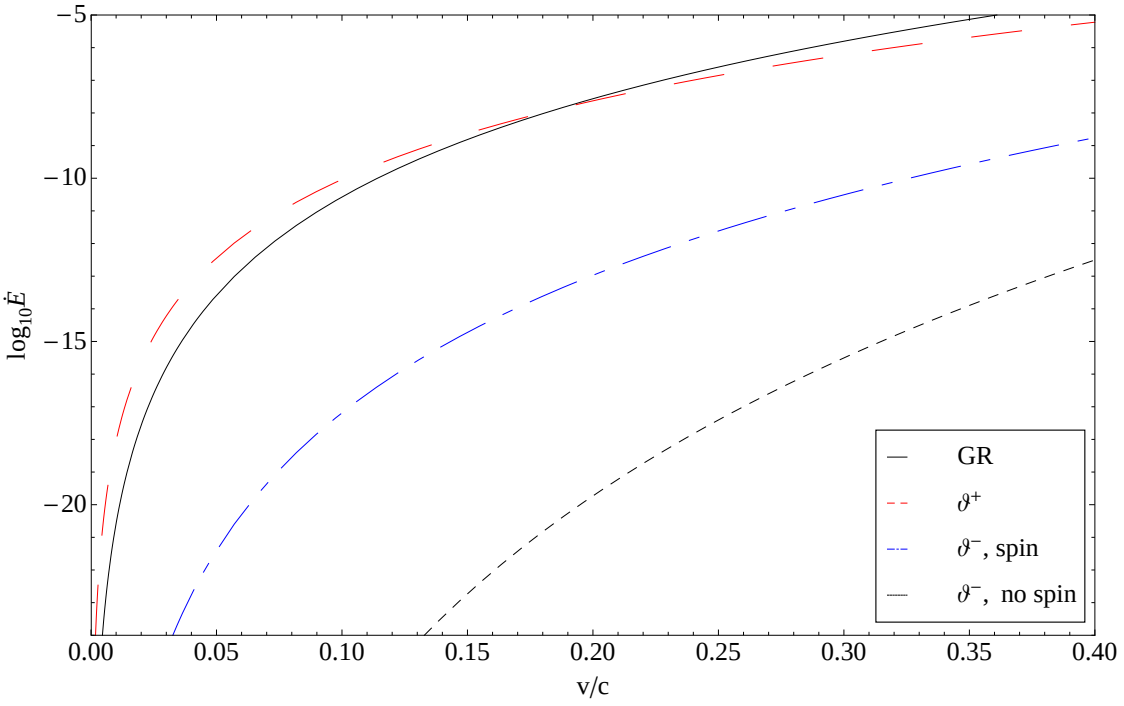

Figure 5-1: Comparison of the energy flux carried by scalar fields of even-parity (dashed red), odd-parity and sourced by spinning BHs (blue dot-dashed) and odd-parity and sourced by non-spinning BHs (short dashed) relative to the GR prediction (solid black) as a function of orbital velocity. We here consider a quasi-circular, BH inspiral with $(m_1, m_2) = (8, 20)M_\odot$, normalized spins $\hat{S}_1^i \equiv |S_1^i|/m_1^2 = -\hat{S}_2^i \equiv -|S_2^i|/m_2^2$ perpendicular to the orbital plane, $|S_A^i| = m_A^2$ and coupling constants $\zeta_3 = 6.25 \times 10^{-3} = \zeta_4$.

(related to the coupling constants of the theory) to roughly the BH horizon scale. With a typical Ad. LIGO stellar-mass BH inspiral observation, one should be able to constrain the even-parity sector to roughly $\mathcal{O}(10)$ km. With a typical LISA extreme-mass ratio inspiral (EMRI) observation, one should be able to constrain the odd-parity sector to roughly $\mathcal{O}(100)$ km. Such projected constraints are much stronger than current Solar System bounds [4, 135, 176, 11].

This paper is organized as follows: Section 5.2 describes the action that will be considered in this paper and reviews the associated modified field equations and the scalar field equation of motion. Section 5.3 expands the field equations in the small-deformation approximation. Sections 5.4 and 5.5 study the scalar field and metric deformation evolution, analytically solving the modified field equations. Section 5.6 computes the energy flux carried by the scalar field and the metric deformation. Section 5.7 considers the impact that such fluxes would have on gravitational waveform phase. Section 5.8 concludes and points to future research.

We have deferred many details of the computational techniques to the appendices. Appendix A shows the NSs in EDGB theory have no scalar monopole charge. Appendix B discusses specific integration techniques. Appendix C estimates the order of the metric correction from the regularized contribution for non-spinning BHs in the odd-parity sector of the modified theory. Appendix D discusses particular integrals that appear when solving the field equations.

Henceforth, we follow mostly the conventions of Misner, Thorne and Wheeler [101]: Greek letters stand for spacetime indices; Latin letters in the middle of the alphabet $i, j, \ldots$, stand for spatial indices only. Parenthesis, square brackets and angled brackets in index lists denote symmetrization, antisymmetrization and the symmetric and trace free (STF) operator, respectively. Capital Latin letters usually refer to a multi-index, such as $x^{\mathcal{Q}} = x^{ijk\cdots}$, where $x^{ijk\cdots} = x^i x^j x^k \ldots$. Partial derivatives are denoted with $\partial_i A = A_{,i} = \partial A/\partial x^i$, while covariant derivatives are denoted with the nabla $\nabla_i A$, for any quantity A. Deformations are labeled with the order-counting parameter ς. Finally, we use geometric units, where $G = c = 1$, except when denot-

ing the order of certain terms in the PN approximation. Throughout, we performed analytic calculations with the xTensor package for Mathematica [95, 30].

5.2 Modified gravity theories

In this Section, we introduce the class of modified gravity theories that we study, by writing down its action and equations of motion. We then proceed to define the small deformation approximation more precisely.

5.2.1 ABC of quadratic gravity

Consider the following 4-dimensional effective action:

$$S \equiv \int d^4x\sqrt{-g}\left\{\kappa R + \alpha_1 f_1(\vartheta)R^2 + \alpha_2 f_2(\vartheta)R_{\mu\nu}R^{\mu\nu} + \alpha_3 f_3(\vartheta)R_{\mu\nu\delta\sigma}R^{\mu\nu\delta\sigma} + \alpha_4 f_4(\vartheta)R_{\mu\nu\delta\sigma}{}^*R^{\mu\nu\delta\sigma} - \frac{\beta}{2}\left[\nabla_\mu\vartheta\nabla^\mu\vartheta + 2V(\vartheta)\right] + \mathcal{L}_{\rm mat}\right\} . \tag{5.1}$$

Here, g stands for the determinant of the metric $g_{\mu\nu}$. R, $R_{\mu\nu}$, $R_{\mu\nu\delta\sigma}$ and ${}^*R_{\mu\nu\delta\sigma}$ are the Ricci scalar and tensor, the Riemann tensor and its dual [6], respectively, with the latter defined as[1] ${}^*R^\mu{}_{\nu\delta\sigma} = (1/2)\varepsilon_{\delta\sigma}{}^{\alpha\beta}R^\mu{}_{\nu\alpha\beta}$ and with $\varepsilon^{\mu\nu\delta\sigma}$ the Levi-Civita tensor. The quantity $\mathcal{L}_{\rm mat}$ is the external matter Lagrangian, ϑ is a field, (α_i, β) are coupling constants and $\kappa = (16\pi)^{-1}$. This action contains all possible quadratic, algebraic curvature scalars with running (i.e. non-constant) couplings, where we assumed that all quadratic terms are coupled to the *same* field. All other quadratic curvature terms are linearly dependent, such as the Weyl tensor squared.

The theory defined by the action above is different from $f(R)$ theories on several counts. First, $f(R)$ theories depend only on the Ricci scalar, while the action above depends on the Ricci tensor, the Riemann tensor and a dynamical field ϑ. Second, $f(R)$ theories are usually treated as exact, while the action presented above is an *effective theory*, truncated to quadratic order in the Riemann tensor. The consequence of this is insisting on the use of order-reduction in the field equations, where we treat

[1] This definition is correct, in agreement with [6], and fixing an inconsequential typo in [137].

all quantities that depend on α_i perturbatively. Such order reduction then leads to the absence of additional polarization modes [137, 138], such as the longitudinal scalar mode that arises in $f(R)$ theories.

The field equations of dynamical quadratic gravity can be obtained by varying the action with respect to all fields. For simplicity, we restrict attention to coupling functions $f_i(\vartheta)$ that admit the Taylor expansion $f_i(\vartheta) = f_i(0) + f_i'(0)\vartheta + \mathcal{O}(\vartheta^2)$ about small ϑ, where $f_i(0)$ and $f_i'(0)$ are constants, and we assume that the asymptotic value of θ at spatial infinity vanishes. Let us further reabsorb $f_i(0)$ into the coupling constants $\alpha_i^{(0)} \equiv \alpha_i f_i(0)$ and $f_i'(0)$ into the constants $\alpha_i^{(1)} \equiv \alpha_i f_i'(0)$. Equation (5.1) then becomes $S = S_{\rm GR} + S_0 + S_1$:

$$S_{\rm GR} \equiv \int d^4x\sqrt{-g}\left\{\kappa R + \mathcal{L}_{\rm mat}\right\}\,, \tag{5.2}$$

$$S_0 \equiv \int d^4x\sqrt{-g}\left\{\alpha_1^{(0)}R^2 + \alpha_2^{(0)}R_{\mu\nu}R^{\mu\nu} + \alpha_3^{(0)}R_{\mu\nu\delta\sigma}R^{\mu\nu\delta\sigma}\right\}\,, \tag{5.3}$$

$$\begin{aligned} S_1 \equiv \int d^4x\sqrt{-g}\Big\{&\alpha_1^{(1)}\vartheta R^2 + \alpha_2^{(1)}\vartheta R_{\mu\nu}R^{\mu\nu} + \alpha_3^{(1)}\vartheta R_{\mu\nu\delta\sigma}R^{\mu\nu\delta\sigma} \\ &+\alpha_4^{(1)}\vartheta R_{\mu\nu\delta\sigma}{}^*R^{\mu\nu\delta\sigma} - \frac{\beta}{2}\left[\nabla_\mu\vartheta\nabla^\mu\vartheta + 2V(\vartheta)\right]\Big\}\,, \end{aligned} \tag{5.4}$$

where clearly $S_{\rm GR}$ is the Einstein-Hilbert plus matter action. Notice that S_0 defines a GR correction that is decoupled from θ. The term proportional to $\alpha_4^{(0)}$ can not affect the classical field equations since it is topological, i.e. the second Chern form, so we have omitted it. Similarly, if $\alpha_i^{(0)}$ are chosen to reconstruct the Gauss-Bonnet invariant, $(\alpha_1^{(0)}, \alpha_2^{(0)}, \alpha_3^{(0)}) = (1, -4, 1)\alpha_{\rm GB}$, then these will not modify the field equations. On the other hand, S_1 defines a modification to GR with a direct (non-minimal) scalar field coupling, such that as the field goes to zero, the modified theory reduces to GR. We here restrict attention to the case $\alpha_i^{(0)} = 0$. From this point forward, we will drop the superscript from $\alpha_i^{(1)}$.

The action above defines a class of modified gravity theories that contains well-known GR extensions. For example, when $\alpha_4 = -\frac{1}{4}\alpha_{\rm CS}$ and all other $\alpha_i = 0$, quadratic gravity reduces to dynamical CS gravity, where $\alpha_{\rm CS}$ is the CS coupling parameter (see e.g. [6]). Alternatively, when $\alpha_4 = 0$, while $(\alpha_1, \alpha_2, \alpha_3) = (1, -4, 1)\alpha_{\rm EDGB}$, quadratic

gravity reduces to Einstein-Dilaton-Gauss-Bonnet theory (see e.g. [112]). Both of these theories are motivated from fundamental physics; they unavoidably arise as low-energy expansions of heterotic string theory [72, 73, 7, 34]. Dynamical CS gravity also arises in loop quantum gravity when the Barbero-Immirzi parameter is promoted to a field in the presence of fermions [144, 97, 67].

Variation of the action with respect to the metric yields the modified field equations:

$$\begin{aligned} G_{\mu\nu} \;+\; & \frac{\alpha_1\vartheta}{\kappa}\mathcal{H}^{(0)}_{\mu\nu} + \frac{\alpha_2\vartheta}{\kappa}\mathcal{I}^{(0)}_{\mu\nu} + \frac{\alpha_3\vartheta}{\kappa}\mathcal{J}^{(0)}_{\mu\nu} \\ & + \frac{\alpha_1}{\kappa}\mathcal{H}^{(1)}_{\mu\nu} + \frac{\alpha_2}{\kappa}\mathcal{I}^{(1)}_{\mu\nu} + \frac{\alpha_3}{\kappa}\mathcal{J}^{(1)}_{\mu\nu} + \frac{\alpha_4}{\kappa}\mathcal{K}^{(1)}_{\mu\nu} \\ = \;& \frac{1}{2\kappa}\left(T^{\rm mat}_{\mu\nu} + T^{(\vartheta)}_{\mu\nu}\right) , \end{aligned} \tag{5.5}$$

where we have defined the short-hands[2‡]

$$\mathcal{H}^{(0)}_{\mu\nu} \equiv 2RR_{\mu\nu} - \frac{1}{2}g_{\mu\nu}R^2 - 2\nabla_{\mu\nu}R + 2g_{\mu\nu}\Box R\,, \tag{5.6a}$$

$$\mathcal{I}^{(0)}_{\mu\nu} \equiv \Box R_{\mu\nu} + 2R_{\mu\delta\nu\sigma}R^{\delta\sigma} - \frac{1}{2}g_{\mu\nu}R^{\delta\sigma}R_{\delta\sigma} + \frac{1}{2}g_{\mu\nu}\Box R - \nabla_{\mu\nu}R\,, \tag{5.6b}$$

$$\mathcal{J}^{(0)}_{\mu\nu} \equiv 8R^{\delta\sigma}R_{\mu\delta\nu\sigma} - 2g_{\mu\nu}R^{\delta\sigma}R_{\delta\sigma} + 4\Box R_{\mu\nu} - 2R\,R_{\mu\nu} + \frac{1}{2}g_{\mu\nu}R^2 - 2\nabla_{\mu\nu}R\,, \tag{5.6c}$$

$$\mathcal{H}^{(1)}_{\mu\nu} \equiv -4(\nabla_{(\mu}\vartheta)\nabla_{\nu)}R - 2R\nabla_{\mu\nu}\vartheta + g_{\mu\nu}\left[2R\Box\vartheta + 4(\nabla^\delta\vartheta)\nabla_\delta R\right] , \tag{5.6d}$$

$$\begin{aligned} \mathcal{I}^{(1)}_{\mu\nu} \equiv & -(\nabla_{(\mu}\vartheta)\nabla_{\nu)}R - 2\nabla^\delta\vartheta\nabla_{(\mu}R_{\nu)\delta} + 2\nabla^\delta\vartheta\nabla_\delta R_{\mu\nu} + R_{\mu\nu}\Box\vartheta \\ & - 2R_{\delta(\mu}\nabla^\delta\nabla_{\nu)}\vartheta + \mathrm{g}_{\mu\nu}\left(\nabla^\delta\vartheta\nabla_\delta R + R^{\delta\sigma}\nabla_{\delta\sigma}\vartheta\right) , \end{aligned} \tag{5.6e}$$

$$\mathcal{J}^{(1)}_{\mu\nu} \equiv -8\left(\nabla^\delta\vartheta\right)\left(\nabla_{(\mu}R_{\nu)\delta} - \nabla_\delta R_{\mu\nu}\right) + 4R_{\mu\delta\nu\sigma}\nabla^{\delta\sigma}\vartheta\,, \tag{5.6f}$$

$$\mathcal{K}^{(1)}_{\mu\nu} \equiv -4\left(\nabla^\delta\vartheta\right)\varepsilon_{\delta\sigma\chi(\mu}\nabla^\chi R_{\nu)}{}^\sigma + 4(\nabla_{\delta\sigma}\vartheta)^*R_{(\mu}{}^\delta{}_{\nu)}{}^\sigma\,, \tag{5.6g}$$

where ∇_μ is the covariant derivative, $\nabla_{\mu\nu} \equiv \nabla_\mu\nabla_\nu$, and $\Box = \nabla_\mu\nabla^\mu$ is the d'Alembertian operator. The ϑ field's stress-energy tensor is

$$T^{(\vartheta)}_{\mu\nu} = \beta\left[(\nabla_\mu\vartheta)(\nabla_\nu\vartheta) - \frac{1}{2}g_{\mu\nu}\left(\nabla_\delta\vartheta\nabla^\delta\vartheta - 2V(\vartheta)\right)\right] . \tag{5.7}$$

[2]This corrects an error in Eq. (5b) of [172].

[‡]The aforementioned error has been corrected in the previous Chapter.

Variation of the action with respect to ϑ yields the ϑ equation of motion:

$$\beta\Box\vartheta - \beta\frac{dV}{d\vartheta} = -\alpha_1 R^2 - \alpha_2 R_{\mu\nu}R^{\mu\nu} - \alpha_3 R_{\mu\nu\delta\sigma}R^{\mu\nu\delta\sigma} - \alpha_4 R_{\mu\nu\delta\sigma}{}^{*}R^{\mu\nu\delta\sigma}\,. \tag{5.8}$$

Notice that when the spacetime is curved by some mass distribution, the right-hand side will be proportional to this mass squared.

The parity of the field ϑ can be inferred from its equation of motion. Since terms of the form R^2 are even-parity, while terms of the form $R_{\mu\nu\delta\sigma}{}^{*}R^{\mu\nu\delta\sigma}$ are odd-parity, the field ϑ is of mixed parity. Note however that the even and odd-parity couplings tend to have different origins from an underlying theory. In this paper we will consider the even and odd-parity cases separately.

The inclusion of dynamics for the ϑ field in the action guarantees that the field equations are covariantly conserved without having to include any additional constraints, i.e. the covariant divergence of Eq. (5.5) identically vanishes, upon imposition of Eq. (5.8). This is a consequence of the action being diffeomorphism invariant. Such invariance is in contrast to the preferred-frame effects present in a non-dynamical theory [80], i.e. in the theory defined by the action in Eq. (5.4) but with $\beta = 0$. In the latter, the field ϑ must be prescribed *a priori*. Moreover, the theory requires the existence of an additional constraint (${}^{*}R\,R = 0$), which is an unphysical consequence of treating ϑ as prior structure [180, 74].

Before proceeding, let us further discuss the scalar field potential $V(\vartheta)$. This potential allows us to introduce additional couplings, such as a mass term, to drive the evolution in Eq. (5.8). However, there are reasons one might restrict such a potential. If the mass is much larger than the inverse length scale of the system that we concern, the effect of such a field on the dynamics of binaries is strongly suppressed. To the contrary, if the mass is much smaller, the presence of mass does not give any significant effects. Therefore we cannot expect to observe the effects of a finite mass without fine tuning. No mass term may appear in a theory with a shift symmetry, which is invariance under $\vartheta \to \vartheta + \text{const}$. Such theories are common in 4D, low-energy, effective string theories [27, 73, 72, 38, 34], such as dynamical CS and

EDGB. For these reasons, and because the assumption makes the resulting equations analytically tractable, we will henceforth assume $V(\vartheta) = 0$.

5.2.2 Small deformations

The "unreasonable" accuracy of GR to explain all experimental data to date suggests that it is an excellent approximation to nature in situations where the gravitational field is very weak and velocities are very small relative to the speed of light. GW detectors will be sensitive to events in situations where the field is stronger than ever previously sampled. This, however, does not imply that GWs will ever sample the Planck/string regime, where one could expect large deviations from GR.

We will here be interested in binary compact object coalescences up until the binary reaches the innermost stable circular orbit (ISCO). Even during merger, the largest curvature that GWs will sample will be limited to the scale determined by the horizon sizes, proportional to m^{-2}. Such scales are far removed from high-energy ones, like the electroweak one, as GW detectors will not be sensitive to mergers of compact objects with masses below a solar mass. Even then, however, GWs can and will probe the *strong field*, which has not been tested before. One is then justified in modeling GWs that may contain deviations from GR as *small deformations*.

The small deformation scheme is also appealing for theoretical reasons. As mentioned earlier, the theories we consider are effective, valid only up to the truncation order. There are higher-order terms that we have here neglected in the action, such as cubic and quartic curvature combinations. Thus, one should not treat these theories as exact nor insist on solving the equations of motion to higher orders in α_i. If this is desired, then higher-order curvature terms should also be included in the action.

One might be worried that such effective theories are unstable, since they lead to field equations with derivatives higher than second order. Such derivatives could lead to instabilities or ghost modes if the Hamiltonian is not bounded from below. Linearization in the coupling parameter, however, has the effect of recasting the field equations in Einstein form with an effective stress-energy tensor that depends on the

GR solution, thus stabilizing the differential equations [36]. Linearization removes modes besides the two that arise in GR [137, 138].

Small deformations can be treated similarly to how one models BH perturbations. That is, we expand the metric as

$$g_{\mu\nu} = g^{\rm GR}_{\mu\nu} + \varsigma\, \mathfrak{h}_{\mu\nu} + O(\varsigma^2)\,, \tag{5.9}$$

where the GR superscript is to remind us that this quantity is a GR solution, while $\mathfrak{h}_{\mu\nu}$ is a metric deformation away from GR. The order-counting parameter ς is kept around only for book-keeping purposes and is to be set to unity in the end.

Applying such an expansion to Eq. (5.8), one finds

$$\beta\Box\vartheta = -\alpha_i\, \mathcal{S}(R^2_{\rm GR}) + \mathcal{O}(\varsigma)\,, \tag{5.10}$$

where $\mathcal{S}(R^2_{\rm GR})$ stands for all source terms evaluated on the GR background $g^{\rm GR}_{\mu\nu}$. The solution to this equation will obviously scale as $\vartheta \propto \alpha_i/\beta$. Applying the decomposition and expansion of Eq. (5.9) to Eq. (5.5) in vacuum, one finds

$$G_{\mu\nu}[\mathfrak{h}_{\mu\nu}] = -\frac{\alpha_i}{\kappa} C_{\mu\nu}[\vartheta, g^{\rm GR}_{\mu\nu}] + \frac{1}{2\kappa} T^{(\vartheta)}_{\mu\nu}[\vartheta]\,, \tag{5.11}$$

where the $\mathcal{O}(\varsigma^0)$ terms automatically vanish, as $g^{\rm GR}_{\mu\nu}$ satisfies the Einstein equations, and we have grouped modifications into the tensor $C_{\mu\nu}$. This tensor and $T^{(\vartheta)}_{\mu\nu}$ are to be evaluated on the GR metric and act as sources for the metric deformation. Notice that, as a differential operator acting on $\mathfrak{h}_{\mu\nu}$, the principal part of these differential equations continues to be strongly hyperbolic, as it is still given by the $G_{\mu\nu}$ differential operator, with the higher derivatives in $C_{\mu\nu}$ and the $T^{(\vartheta)}_{\mu\nu}$ acting as sources. Given this, the metric deformation is proportional to $\xi_i \equiv \alpha_i^2/(\beta\kappa)$, which is our actual perturbation parameter.

Proper perturbation or deformation parameters should be dimensionless, but the ξ_i are dimensional. The dimensions of α and β, of course, depend on the choice of dimensions for the scalar field. We here take the viewpoint that ϑ is dimensionless,

which then forces β to be dimensionless as well as κ, and α to have dimensions of length squared. Then, the deformation parameter ξ has units of length to the fourth power, which is why we define the dimensionless

$$\zeta_i \equiv \xi_i/m^4 = \mathcal{O}(\varsigma)\,, \tag{5.12}$$

as our proper deformation parameter. One could choose different units for the scalar field, but in all cases one arrives at the conclusion that ζ_i is the proper deformation parameter [177].

5.3 Expansion of the field equations

Let us decompose the GR metric tensor into a flat background plus a metric perturbation:

$$g^{\rm GR}_{\mu\nu} = \eta_{\mu\nu} + h_{\mu\nu}\,. \tag{5.13}$$

We emphasize here that throughout this paper, $h_{\mu\nu}$ denotes the metric perturbation in GR while $\mathfrak{h}_{\mu\nu}$ is the metric deformation away from GR.

In expanding the modified field equations, we will also find it useful to define the standard trace-reversed metric perturbation in GR as

$$\bar{h}^{\mu\nu} \equiv \eta^{\mu\nu} - \sqrt{-g_{\rm GR}}g^{\mu\nu}_{\rm GR}\,. \tag{5.14}$$

In particular, notice that when the background is flat $\bar{h}_{\mu\nu} = h_{\mu\nu} - \frac{1}{2}h\eta_{\mu\nu}$ and $h_{\mu\nu} = \bar{h}_{\mu\nu} - \frac{1}{2}\bar{h}\eta_{\mu\nu}$ to linear order in GR. We also define the deformed trace reversed metric perturbation as

$$\bar{\mathfrak{h}}^{\mu\nu} \equiv \left(\eta^{\mu\nu} - \sqrt{-g}g^{\mu\nu}\right) - \bar{h}^{\mu\nu}\,. \tag{5.15}$$

The harmonic gauge condition reduces to $\bar{h}^{\mu\nu}{}_{,\nu} = 0$ and $\bar{\mathfrak{h}}^{\mu\nu}{}_{,\nu} = 0$. Throughout this paper, we only study the GR deformation up to $\mathcal{O}(\alpha_i/\beta)$ for ϑ and $\mathcal{O}(\zeta_i)$ for $\mathfrak{h}_{\mu\nu}$.

5.3.1 Scalar field

The evolution equation for the scalar field at leading order in the metric perturbation becomes

$$\begin{aligned}\Box_\eta \vartheta \;=\; & -\frac{\alpha_1}{\beta}\left(\frac{1}{2\kappa}\right)^2 T_{\rm mat}^2 - \frac{\alpha_2}{\beta}\left(\frac{1}{2\kappa}\right)^2 T^{\mu\nu}_{\rm mat} T^{\rm mat}_{\mu\nu} \\ & -\frac{2\alpha_3}{\beta}(h_{\alpha\beta,\mu\nu}h^{\alpha[\beta,\mu]\nu} + h_{\alpha\beta,\mu\nu}h^{\mu[\nu,\alpha]\beta}) \\ & -\frac{2\alpha_4}{\beta}\epsilon^{\alpha\beta\mu\nu}h_{\alpha\delta,\gamma\beta}h_\nu{}^{[\gamma,\delta]}{}_\mu\,, \end{aligned} \tag{5.16}$$

with relative remainders of $\mathcal{O}(h)$. Here, $\epsilon^{\mu\nu\delta\sigma}$ is the Levi-Civita symbol with convention $\epsilon^{0123} = +1$, and we have used the harmonic gauge condition.

5.3.2 Metric perturbation

Let us now perturb the metric field equations [Eq. (5.5)] about $\varsigma = 0$. The deformed metric wave equation at linear order in $\mathfrak{h}_{\mu\nu}$ becomes

$$\begin{aligned}\frac{\kappa}{2}\Box_\eta \mathfrak{h}_{\mu\nu} =& \,\alpha_1\vartheta\tilde{\mathcal{H}}^{(0)}_{\mu\nu} + \alpha_2\vartheta\tilde{\mathcal{I}}^{(0)}_{\mu\nu} + \alpha_3\vartheta\tilde{\mathcal{J}}^{(0)}_{\mu\nu} \\ & + \alpha_1\tilde{\mathcal{H}}^{(1)}_{\mu\nu} + \alpha_2\tilde{\mathcal{I}}^{(1)}_{\mu\nu} + \alpha_3\tilde{\mathcal{J}}^{(1)}_{\mu\nu} + \alpha_4\tilde{\mathcal{K}}^{(1)}_{\mu\nu} \\ & - \frac{1}{2}\delta T^{\rm mat}_{\mu\nu} - \frac{1}{2}T^{(\vartheta)}_{\mu\nu}\,, \end{aligned} \tag{5.17}$$

where the tensors on the right-hand side are given by

$$\tilde{\mathcal{H}}^{(0)}_{\mu\nu} = -4\left(h_\rho{}^{[\sigma,\rho]}{}_{\sigma\mu\nu} - \eta_{\mu\nu}\Box_\eta h_\rho{}^{[\sigma,\rho]}{}_\sigma\right)\,, \tag{5.18}$$

$$\tilde{\mathcal{I}}^{(0)}_{\mu\nu} = \Box_\eta h_{\nu[\rho,\mu]}{}^\rho - \Box_\eta h^\rho{}_{[\rho,\mu]\nu} - 2h_\rho{}^{[\sigma,\rho]}{}_{\sigma\mu\nu} + \eta_{\mu\nu}\Box_\eta h_\rho{}^{[\sigma,\rho]}{}_\sigma\,, \tag{5.19}$$

$$\tilde{\mathcal{J}}^{(0)}_{\mu\nu} = 4\left(-\Box_\eta h_{\nu[\mu,\rho]}{}^\rho - \Box_\eta h^\rho{}_{[\rho,\mu]\nu} - h_\rho{}^{[\sigma,\rho]}{}_{\sigma\mu\nu}\right)\,, \tag{5.20}$$

$$\tilde{\mathcal{H}}^{(1)}_{\mu\nu} = -8h_\rho{}^{[\sigma,\rho]}{}_{\sigma(\mu}\vartheta_{,\nu)} - 4h_\rho{}^{[\sigma,\rho]}{}_\sigma\vartheta_{,\mu\nu} + 4\eta_{\mu\nu}\left(2h_\rho{}^{[\sigma,\rho]}{}_{\sigma\delta}\vartheta^{,\delta} + h_\rho{}^{[\sigma,\rho]}{}_\sigma\Box_\eta\vartheta\right)\,, \tag{5.21}$$

$$\begin{aligned}\tilde{\mathcal{I}}^{(1)}_{\mu\nu} =& -2h_\rho{}^{[\sigma,\rho]}{}_{\sigma(\mu}\vartheta_{,\nu)} - 2\left(h^\delta{}_{[\rho,(\nu]\mu)}{}^\rho - h^\rho{}_{[\rho,(\nu]\mu)}{}^\delta\right)\vartheta_{,\delta} - 2\left(h_{(\nu[\mu),\rho]}{}^\delta{}^\rho + h^\rho{}_{[\rho,(\mu]\nu)\delta}\right)\vartheta^{,\delta} \\ & - 2\left(h^\delta{}_{[\rho,(\mu]}{}^\rho\vartheta_{,\nu)\delta} - h^\rho{}_{[\rho,(\mu]}{}^\delta\vartheta_{,\nu)\delta}\right) + \eta_{\mu\nu}\left\{2h_\rho{}^{[\sigma,\rho]}{}_{\sigma\delta}\vartheta^{,\delta} + \left(h^{\sigma[\rho,\delta]}{}_\rho - h_\rho{}^{[\rho,\delta]\sigma}\right)\vartheta_{,\sigma\delta}\right\} \\ & + \Box_\eta\vartheta\left(h_{(\mu}{}^\delta{}_{,\nu)\delta} - \frac{1}{2}\Box_\eta h_{\mu\nu} - \frac{1}{2}h_{,\mu\nu}\right)\,, \end{aligned} \tag{5.22}$$

$$\tilde{\mathcal{J}}^{(1)}_{\mu\nu} = -8\left(h^{\delta}{}_{[\rho,(\nu]\mu)}{}^{\rho} + h^{\rho}{}_{[\rho,(\nu]\mu)}{}^{\delta} - \frac{1}{2}h_{,\mu\nu}{}^{\delta} + \frac{1}{2}\Box_{\eta}h_{\mu\nu}{}^{,\delta}\right)\vartheta_{,\delta} + 4\left(h_{\sigma[\mu,\delta]\nu} - h_{\nu[\mu,\delta]\sigma}\right)\vartheta^{,\sigma\delta}\,, \tag{5.23}$$

$$\tilde{\mathcal{K}}^{(1)}_{\mu\nu} = \vartheta^{,\delta}{}_{,\sigma}\eta_{\nu\alpha}\bar{\varepsilon}^{\alpha\sigma\beta\gamma}\left(h_{\mu[\gamma,\beta]\delta} + h_{\delta[\beta,\gamma]\mu}\right) - 2\vartheta^{,\delta}\epsilon_{\delta\sigma\chi\mu}h^{\sigma}{}_{[\alpha}{}^{,\alpha\chi}{}_{\nu]} + (\mu \leftrightarrow \nu)\,, \tag{5.24}$$

where $\Box_\eta$ is the d'Alembertian of flat spacetime, $h = h_\mu{}^\mu$, and $T^{(\vartheta)}_{\mu\nu}$ is given as

$$T^{(\vartheta)}_{\mu\nu} = \beta\left(\vartheta_{,\mu}\vartheta_{,\nu} - \frac{1}{2}\eta_{\mu\nu}\vartheta_{,\delta}\vartheta^{,\delta}\right)\,. \tag{5.25}$$

The quantity $\delta T^{\rm mat}_{\mu\nu}$ stands for the perturbation to the energy-momentum tensor for matter. Even when dealing with BHs, $\delta T^{\rm mat}_{\mu\nu} \neq 0$ because we treat BHs as distributional point particles and their trajectories are generically modified at $\mathcal{O}(\varsigma)$. However, in this paper we concentrate on the dissipative sector of the theory only, and not on modifications to the shape of the orbits (conservative dynamics). The latter does modify the GW phase evolution [172, 177], as we discuss in Sec. 5.8.

The evolution equation for the metric perturbation takes on the same form (a sourced wave equation) as that for the scalar field. The source terms in both of these equations depend on the GR metric perturbation, which we here assume to be that of a compact binary quasi-circular inspiral in the PN approximation, i.e. moving at small velocities relative to the speed of light and producing weak gravitational fields. We provide explicit expressions for the GR metric perturbation in the subsequent subsection.

5.3.3 Post-Newtonian metric and trajectories

In this subsection, we provide explicit expressions for the linear metric perturbation in GR that we use to evaluate all source terms. We are here interested in a binary system, composed of two compact objects with masses m_1 and m_2 and initially separated by

a distance $r_{12} \equiv b$. The objects' trajectories can be parameterized via

$$\mathbf{x}_1 \equiv x_1^i = +\frac{m_2}{m} b \left[\cos\omega t, \sin\omega t, 0\right] , \tag{5.26}$$

$$\mathbf{x}_2 \equiv x_2^i = -\frac{m_1}{m} b \left[\cos\omega t, \sin\omega t, 0\right] , \tag{5.27}$$

where $m \equiv m_1 + m_2$ is the total mass and where we have assumed they are located on the x–y plane. Throughout this paper, vectors are sometimes denoted with a boldface. We also define

$$\mathbf{x}_{12} \equiv x_{12}^i = x_1^i - x_2^i, \tag{5.28}$$

$$\mathbf{n}_{12} \equiv n_{12}^i = (x_1^i - x_2^i)/b, \tag{5.29}$$

$$\mathbf{n}_A \equiv n_A^i = (x^i - x_A^i)/r_A, \tag{5.30}$$

where we follow the conventions of [21], with

$$r_A \equiv |x^i - x_A^i|. \tag{5.31}$$

We further assume these objects are on a quasi-circular orbit with leading-order angular velocity $\omega = (1/b)(m/b)^{1/2}$ and orbital velocity $v = (m/b)^{1/2}$. The orbital separation b is assumed constant, as its time-evolution is driven by GW emission at high-order in v/c.

The GR spacetime metric for such a binary is expanded as in Eq. (5.13). In the near zone, the metric perturbation is given by

$$h_{00} = 2U_1 + (1 \leftrightarrow 2) + \mathcal{O}(v^4) , \tag{5.32}$$

$$h_{0i} = -4V_{1i} + (1 \leftrightarrow 2) + \mathcal{O}(v^5) , \tag{5.33}$$

$$h_{ij} = 2U_1\delta_{ij} + (1 \leftrightarrow 2) + \mathcal{O}(v^4) , \tag{5.34}$$

where $\mathcal{O}(v^A)$ stands for an $(A/2)$PN remainder, i.e. a term of $\mathcal{O}((v/c)^A)$, and the notation $+(1 \leftrightarrow 2)$ means that one should add the same terms with the labels 1 and

2 interchanged. The potentials U_A and V_{Ai} with $A = (1, 2)$ are defined as

$$U_A = \int \frac{\rho'_A}{|\boldsymbol{x} - \boldsymbol{x}'|} d^3x' \,, \qquad V_{Ai} = \int \frac{\rho'_A v'_{Ai}}{|\boldsymbol{x} - \boldsymbol{x}'|} d^3x' \,, \tag{5.35}$$

where ρ_A and $v^i_A \equiv \dot{x}^i_A$ are the density and the center of mass velocities of the respective objects, with the overhead dot standing for time differentiation. Field variables associated with a prime, e.g. ρ'_A, are to be evaluated at $\boldsymbol{x}'$. In the point-particle limit, the metric becomes

$$h_{00} = \frac{2m_1}{r_1} + (1 \leftrightarrow 2) \,, \tag{5.36}$$

$$h_{0i} = -\frac{4m_1}{r_1} v^i_1 + (1 \leftrightarrow 2) \,, \tag{5.37}$$

$$h_{ij} = \frac{2m_1}{r_1} \delta_{ij} + (1 \leftrightarrow 2) \,, \tag{5.38}$$

with remainders of relative $\mathcal{O}(v^2)$. We have kept the PN leading terms in the metric that are proportional to m_A only, but higher-order terms can be found in [25], while terms proportional to the spin of each BH can be found in [141].

5.4 Scalar field evolution

In this section, we solve the evolution equation for the scalar field both for field points in the far and near-zones, as defined in Sec. 5.4.1. The former will allow us to evaluate the energy flux carried by the scalar field at infinity, while the latter will be essential to find effective source terms that reproduce the known strong field solutions and to solve the evolution equations for the metric deformation.

5.4.1 Zones

As shown in Fig. 5-2, let us decompose the geometry into three regions: an inner zone (IZ), a near zone (NZ) and a far zone (FZ); see e.g. [10, 183, 82] for further details. The IZs are centered at each object with radii $\mathcal{R}_{\rm IZ}$. These radii are defined as the boundary inside which either $T^{\rm mat}_{\mu\nu} \neq 0$ or the usual PN approximation breaks down

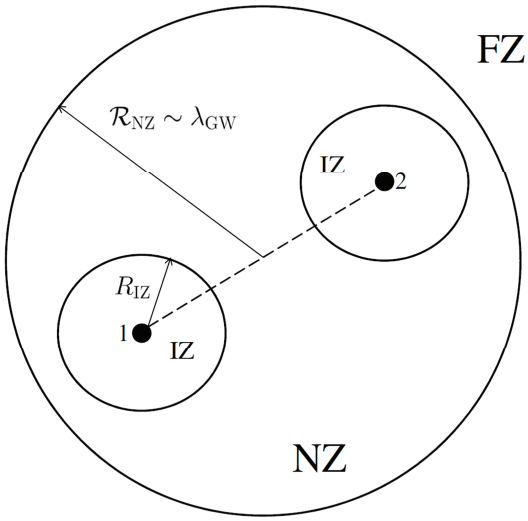

Figure 5-2: We consider three zones, inner zone (IZ), near zone (NZ) and far zone (FZ). The IZs are centered at each object and their radii $\mathcal{R}_{\rm IZ}$ satisfy $\mathcal{R}_{\rm IZ} \ll b$. The NZ is centered at the center of mass of the two bodies and the radius $\mathcal{R}_{\rm NZ}$ satisfies $\mathcal{R}_{\rm NZ} \sim \lambda_{\rm GW}$, where $\lambda_{\rm GW}$ is the GW wavelength.

due to strong-gravity effects. We here take them to be sufficiently larger than m_A and much less than b. The NZ is centered at the binary's center of mass with radius $\mathcal{R}_{\rm NZ}$ and excluding the IZs. This radius is defined as the boundary outside which time-derivatives cannot be assumed to be small compared with spatial derivatives due to the wave-like nature of the metric perturbation. We here take this boundary to be roughly equal to $\lambda_{\rm GW}$, where $\lambda_{\rm GW}$ denotes the GW wavelength. The FZ is also centered at the binary's center of mass, but it extends outside $\mathcal{R}_{\rm NZ}$.

One can only apply the PN formalism when the gravitational field is weak and velocities are small. When we deal with strong field sources like BHs and NSs, therefore, one can use the PN scheme in the NZ and FZ only. In the IZs, one may not be able to use PN theory, since the gravitational field may be too strong. In this case, we have to asymptotically match our PN solution in the NZ with the strong field solutions valid in the IZs, inside some buffer regions that overlap both NZ and each IZ (see Refs. [53, 148, 50] for a description of how to carry this out in GR). The strong field solution for BHs was found in Refs. [172] and [177] in the class of theories considered here.

5.4.2 Near zone solutions

Since the NZ is in the weak field regime, we can apply the PN formalism to compact binary systems. Let us consider the even and odd-parity sectors separately.

Even-parity sector

The evolution equation for the even-parity sector is

$$\Box_\eta \vartheta = -64\pi^2 \frac{\alpha_1}{\beta}\rho^2 - 64\pi^2 \frac{\alpha_2}{\beta}\rho^2 - \frac{2\alpha_3}{\beta}\left(h_{\alpha\beta,\mu\nu}h^{\alpha[\beta,\mu]\nu} + h_{\alpha\beta,\mu\nu}h^{\mu[\nu,\alpha]\beta}\right) , \tag{5.39}$$

with $\rho \equiv \rho_1 + \rho_2$ and remainders of $\mathcal{O}(h^3)$.

First, let us consider weakly-gravitating objects, i.e. not BHs or NSs, in which case the PN expansion is valid also in the IZ. By substituting the GR PN metric of Eqs. (5.32)-(5.34), the NZ solution to the above wave equation at leading PN order becomes

$$\begin{aligned} \vartheta &= 16\pi \frac{\alpha_1}{\beta}\int_{\mathcal{M}} \rho'^2 \frac{d^3x'}{|\boldsymbol{x}-\boldsymbol{x}'|} + 16\pi \frac{\alpha_2}{\beta}\int_{\mathcal{M}} \rho'^2 \frac{d^3x'}{|\boldsymbol{x}-\boldsymbol{x}'|} \\ &\quad + \frac{1}{\pi}\frac{\alpha_3}{\beta}\int_{\mathcal{M}} \left(2U'_{,ij}U'_{,ij} + \Box_\eta U' \Box_\eta U'\right) \frac{d^3x'}{|\boldsymbol{x}-\boldsymbol{x}'|} , \end{aligned} \tag{5.40}$$

again with remainders of $\mathcal{O}(h^3)$, with $U \equiv U_1 + U_2$ and $\mathcal{M}$ denoting the constant-time, NZ+IZ hypersurface. We can safely neglect the contribution from the FZ, since the fall-off of the source term is sufficiently fast.

The solution in Eq. (5.40) can be simplified by integrating by parts several times and using that $\Box U = -4\pi\rho$ and $\Box|\boldsymbol{x}-\boldsymbol{x}'|^{-1} = -4\pi\delta^{(3)}(\boldsymbol{x}-\boldsymbol{x}')$ to obtain

$$\begin{aligned} \vartheta &= 16\pi \frac{\alpha_1}{\beta}\int_{\mathcal{M}} \rho'^2 \frac{d^3x'}{|\boldsymbol{x}-\boldsymbol{x}'|} + 16\pi \frac{\alpha_2}{\beta}\int_{\mathcal{M}} \rho'^2 \frac{d^3x'}{|\boldsymbol{x}-\boldsymbol{x}'|} \\ &\quad + 48\pi \frac{\alpha_3}{\beta}\int_{\mathcal{M}} \rho'^2 \frac{d^3x'}{|\boldsymbol{x}-\boldsymbol{x}'|} \\ &\quad - 8\frac{\alpha_3}{\beta}\int_{\mathcal{M}} \rho' U'_{,i}\left(\frac{1}{|\boldsymbol{x}-\boldsymbol{x}'|}\right)_{,i} d^3x' \\ &\quad - 4\frac{\alpha_3}{\beta}\int_{\mathcal{M}} U'_{,i}U'_{,i}\delta^{(3)}(\boldsymbol{x}-\boldsymbol{x}')d^3x' . \end{aligned} \tag{5.41}$$

Expanding this solution in terms of particles 1 and 2, we arrive at

$$\vartheta = \vartheta_{\rm self} + \vartheta_{\rm cross}\,, \tag{5.42}$$

with

$$\begin{aligned}\vartheta_{\rm self} \;=\; & \frac{16\pi}{\beta}\left(\alpha_1+\alpha_2+3\alpha_3\right)\int_{\mathcal{M}} {\rho'}_1^2 \frac{d^3x'}{|\boldsymbol{x}-\boldsymbol{x}'|} \\ & -8\frac{\alpha_3}{\beta}\int_{\mathcal{M}} \rho'_1 U'_{1,i}\left(\frac{1}{|\boldsymbol{x}-\boldsymbol{x}'|}\right)_{,i} d^3x' \\ & -4\frac{\alpha_3}{\beta}U_{1,i}U_{1,i} + (1\leftrightarrow 2)\,,\end{aligned} \tag{5.43}$$

and

$$\vartheta_{\rm cross} = -8\frac{\alpha_3}{\beta}\left[\int_{\mathcal{M}}\left(\rho'_1 U'_{2,i}+\rho'_2 U'_{1,i}\right)\left(\frac{1}{|\boldsymbol{x}-\boldsymbol{x}'|}\right)_{,i} d^3x' + U_{1,i}U_{2,i}\right]. \tag{5.44}$$

$\vartheta_{\rm self}$ is the part of ϑ that can be evaluated by considering a single object only, while $\vartheta_{\rm cross}$ is the part that depends on the fields of both bodies.

The integrals that define both $\vartheta_{\rm self}$ and $\vartheta_{\rm cross}$ have support in the IZs only, and thus, the NZ integral operator is homogeneous (source-free). When we discuss the NZ behavior of fields associated with compact objects, such as BHs or NSs, we cannot directly evaluate such IZ integrals. These are derived under the assumption that the PN expansion is valid everywhere, which fails for compact objects in the IZs. Instead, we need to determine these homogeneous solutions through asymptotic matching. Before doing so, it is helpful to study the meaning of each term for weakly-gravitating objects.

Neglecting the size of the weakly-gravitating objects, the first term in Eq. (5.43) in the NZ is evaluated as

$$\int_{\mathcal{M}} {\rho'}_1^2 \frac{d^3x'}{|\boldsymbol{x}-\boldsymbol{x}'|} \approx \frac{1}{r_1}\int_{\mathcal{M}} {\rho'}_1^2 d^3x'\,, \tag{5.45}$$

with remainders of relative $\mathcal{O}(m/r)$, while the second term becomes

$$\begin{aligned}\int_{\mathcal{M}} \rho_1' \;\; U_{1,i}' \left(\frac{1}{|\boldsymbol{x}-\boldsymbol{x}'|}\right)_{,i} d^3x' &\approx \frac{n_1^i}{r_1^2}\int_{\mathcal{M}} \rho_1' U_{1,i}' d^3x' \\ &= -\frac{n_1^i}{r_1^2}\int_{\mathcal{M}} \rho_1(\boldsymbol{x}')\left(\int_{\mathcal{M}} \rho_1(\boldsymbol{y})\frac{x'^i - y^i}{|\boldsymbol{x}'-\boldsymbol{y}|^2} d^3y\right) d^3x' \\ &= 0\,. \end{aligned} \tag{5.46}$$

The last equality can be shown by exchanging the integration variables[3]. Thus, one can approximate $\vartheta_{\rm self}$ as

$$\vartheta_{\rm self} = \frac{q_1}{r_1} - 4\frac{\alpha_3 m_1^2}{\beta r_1^4} + (1 \leftrightarrow 2)\,, \tag{5.47}$$

with the scalar monopole charge defined by

$$q_A \equiv \frac{16\pi}{\beta}\left(\alpha_1 + \alpha_2 + 3\alpha_3\right)\int_{\rm IZ} \rho_A'^2 d^3x'\,, \tag{5.48}$$

with $A = (1, 2)$. Here we put "IZ" to the integral to emphasize that the integration can be restricted to both IZs because the integrand is localized.

The first term in Eq. (5.47) represents the monopole field around object 1. These monopole fields give the leading PN contribution in the NZ unless both monopole charges q_1 and q_2 vanish. This is indeed the case in EDGB theory, where $(\alpha_1, \alpha_2, \alpha_3) = (1, -4, 1)\alpha_{\rm EDGB}$. We will later show that this cancellation does really survive even if we consider NSs. If this cancellation occurs, the higher order terms of $\mathcal{O}(m^2/r^2)$ in the expansion of Eq. (5.45) become the dominant contribution to ϑ. The second term in Eq. (5.47) is much higher PN order compared with the first term and hence sub-dominant in the NZ.

Let us now consider $\vartheta_{\rm self}$ for compact objects, where the IZ integrals must be treated carefully. Since the PN expansion is no longer valid in the IZ, one cannot use the simple extrapolation of the above result. In Sec. 5.4.3, we match the NZ solution

[3]In fact, this integral vanishes to all orders in x. This is because $(\rho_1 U_{1,i})_{,i}$ is spherically symmetric, and thus, when it acts as a source to a wave equation, the solution should either scale as $1/r$ or it should vanish identically. We have here shown that there is no $1/r$ part.

to the one obtained for isolated BHs in the strong-field [172, 177]. We will not discuss the matching for NSs in this paper, but the order of magnitude estimate

$$q_A = \sum_{i=1}^{3} q_{i,A} = \sum_{i=1}^{3} \frac{\alpha_i}{\beta} \mathcal{O}\left(\frac{m_A^2}{R_A^3}\right) \tag{5.49}$$

should still be valid, where R_A is the radius of the Ath NS. When $\alpha_1 + \alpha_2 + 3\alpha_3 = 0$, the cancellation observed in the weakly gravitating objects may still persist even for NSs. However, the cancellation will not in general be exact, except for the EDGB subcase. In EDGB theory, the NS scalar monopole charge vanishes independently of the equation of state. Mathematically speaking, this is because the monopole charge is given by the integral of the Gauss-Bonnet invariant $R_{\rm GB} \equiv R^2 - 4R_{\mu\nu}R^{\mu\nu} + R_{\mu\nu\rho\sigma}R^{\mu\nu\rho\sigma}$, which vanishes for any simply-connected, asymptotically flat geometry. A more explicit proof is given in Appendix A.

Let us now return to the $\vartheta_{\rm cross}$ contribution and consider first weakly-gravitating objects. To evaluate Eq. (5.44), one can use point-particle expansions of the potentials and the density, i.e. $\rho_A = m_A \delta^{(3)}(\boldsymbol{x} - \boldsymbol{x}_A)$ and $U_A = m_A/r_A$. Simple substitution leads to

$$\vartheta_{\rm cross} \approx 8\frac{\alpha_3 m_1 m_2}{\beta m^4}\left[m^4\left(\frac{n_1^j}{r_1^2}\frac{n_2^j}{r_2^2} + \frac{n_{12}^j}{b^2}\frac{n_2^j}{r_2^2} - \frac{n_{12}^j}{b^2}\frac{n_1^j}{r_1^2}\right) + \mathcal{O}\left(\frac{m^5}{r^5}\right)\right] . \tag{5.50}$$

The first term in parentheses comes from the term $U_{1,i}U_{2,i}$ in Eq. (5.44). The remaining two terms come from the integral in Eq. (5.44). The second and third terms in parentheses look like scalar dipole moments for bodies 2 and 1 respectively. However, a Taylor expansion about the center of mass of each body, shows that the $1/r_A^2$ piece of $\vartheta_{\rm cross}$ cancels, which implies that there is no scalar dipole.

Let us now consider $\vartheta_{\rm cross}$ for compact objects. As discussed in the previous paragraph, one might expect a scalar dipole charge induced by the acceleration of object 1 due to the gravitational field of object 2 ($\propto U_{2,i}(\boldsymbol{x}_1)$). In GR, however, acceleration is understood as geodesic motion in a perturbed geometry. The deviation of the local geometry from the unperturbed isolated geometry originates due to tides, and

this is a relative 4PN effect. This is much smaller than the scalar monopole charge contribution from $\vartheta_{\rm self}$.

To summarize, the dominant contribution to ϑ comes from the monopole charge associated with each object, which depends on its internal structure.

Odd-parity sector

In the odd-parity case, the scalar field evolution equation is

$$\Box_\eta \vartheta = -\frac{2\alpha_4}{\beta}\epsilon^{\alpha\beta\mu\nu} h_{\alpha\delta,\gamma\beta} h_\nu{}^{[\gamma,\delta]}{}_\mu \,, \tag{5.51}$$

plus terms of $\mathcal{O}(h^3)$. Again, we first consider weakly gravitating objects. At leading PN order, the above equation becomes

$$\begin{aligned} \Box_\eta \vartheta &= \frac{2\alpha_4}{\beta}\epsilon_{ijk}(h_{00,mi}h_{k0,jm} + h_{0l,jm}h_{kl,im}) \\ &= -32\frac{\alpha_4}{\beta}\epsilon_{ijk}U_{,im}V_{k,jm} \,, \end{aligned} \tag{5.52}$$

with remainders of relative $\mathcal{O}(v^2)$. As in the even-parity case, we write the solution to this wave equation as

$$\vartheta = \vartheta_{\rm self} + \vartheta_{\rm cross} \,, \tag{5.53}$$

where

$$\vartheta_{\rm self} = \frac{8}{\pi}\frac{\alpha_4}{\beta}\epsilon_{ijk}\int_{\mathcal{M}} U'_{1,im}V'_{1k,jm}\frac{d^3x'}{|\boldsymbol{x}-\boldsymbol{x}'|} + (1 \leftrightarrow 2) \,, \tag{5.54}$$

and

$$\vartheta_{\rm cross} = \frac{8}{\pi}\frac{\alpha_4}{\beta}\epsilon_{ijk}\int_{\mathcal{M}} U'_{1,im}V'_{2k,jm}\frac{d^3x'}{|\boldsymbol{x}-\boldsymbol{x}'|} + (1 \leftrightarrow 2) \,. \tag{5.55}$$

Let us first consider self-interaction terms $\vartheta_{\rm self}$. Integrating by parts several times, we find

$$\begin{aligned}\vartheta_{\rm self} &= -16\frac{\alpha_4}{\beta}\epsilon_{ijk}\Bigg[\int_{\mathcal{M}}\rho_1' V_{1k,j}'\left(\frac{1}{|\boldsymbol{x}-\boldsymbol{x}'|}\right)_{,i} d^3x' \\ &\quad + \int_{\mathcal{M}} U_{1,i}'\rho_1' v_{1k}'\left(\frac{1}{|\boldsymbol{x}-\boldsymbol{x}'|}\right)_{,j} d^3x' \\ &\quad + \int_{\mathcal{M}} U_{1,i}' V_{1k,j}'\delta^{(3)}(\boldsymbol{x}-\boldsymbol{x}')d^3x' + (1\leftrightarrow 2)\Bigg], \end{aligned} \tag{5.56}$$

where we have used the relations $\Box U_1 = -4\pi\rho_1$, $\Box V_1^k = -4\pi\rho_1 v_1^k$ and $\Box|\boldsymbol{x}-\boldsymbol{x}'|^{-1} = -4\pi\delta^{(3)}(\boldsymbol{x}-\boldsymbol{x}')$. The third term vanishes when we take the point-particle limit[4], i.e. $\rho_A = m_A\delta^{(3)}(\boldsymbol{x}-\boldsymbol{x}_A)$, $U_A = m_A/r_A$ and $V_{Ai} = m_A v_{Ai}/r_A$.

Let us evaluate the first and the second terms in the NZ. Keeping only the leading PN term in the NZ, we find

$$\begin{aligned}\vartheta_{\rm self} &= 16\frac{\alpha_4}{\beta}\epsilon_{ijk}\frac{n_{1,i}}{r_1^2}\int_{\mathcal{M}}\rho_1'(V_{1k,j}' - U_{1,j}'v_{1k}')d^3x' + (1\leftrightarrow 2) \\ &= \frac{n_{1,i}}{r_1^2}\mu_i^{(1)} + (1\leftrightarrow 2)\,, \end{aligned} \tag{5.57}$$

where we have defined

$$\mu_i^{(A)} \equiv 32\frac{\alpha_4}{\beta}\epsilon_{ijk}\int_{\rm IZ}\rho_A' V_{Ak,j}' d^3x'\,. \tag{5.58}$$

This leading-order PN term in $\vartheta_{\rm self}$ represents a magnetic-type dipole.

As in the even-parity case, to extend this result to compact objects we have to determine the value of $\mu_i^{(A)}$ by matching the NZ solution in Eq. (5.57) to a strong field solution. This will be carried out in Sec. 5.4.3 for the BH case. For NSs, we just present an order of magnitude estimate based on a simple extrapolation of weakly-

[4] The vanishing of this term is a general consequence of the symmetry of the system. The source term contains an ϵ^{ijk} symbol, which must be contracted with other vectors to produce a scalar. We here have only two possible vectors to contract with, i.e. the velocity v_1^i and the unit vector n_1^i from object 1. Hence, any contraction with the Levi-Civita symbol should vanish.

gravitating results:

$$\mu^i_{(A)} = \frac{\alpha_4}{\beta}\mathcal{O}\left(\frac{m_A S^i_A}{R^3_A}\right) , \tag{5.59}$$

where S^i_A is the spin angular momentum of the object. Following the procedure in Appendix A, we can show that NSs cannot have scalar monopole charge in the dynamical CS case.

Next, we consider the cross term $\vartheta_{\rm cross}$ in the weakly-gravitating case. Integrating by parts several times, we find

$$\begin{aligned}\vartheta_{\rm cross} \;=\; & -16\frac{\alpha_4}{\beta}\epsilon_{ijk}\Bigg[\int_{\mathcal{M}}\rho'_1 V'_{2k,j}\left(\frac{1}{|\boldsymbol{x}-\boldsymbol{x}'|}\right)_{,i} d^3x' \\ & + \int_{\mathcal{M}} U'_{1,i}\rho'_2 v'_{2k}\left(\frac{1}{|\boldsymbol{x}-\boldsymbol{x}'|}\right)_{,j} d^3x' \\ & + \int_{\mathcal{M}} U'_{1,i}V'_{2k,j}\delta^{(3)}(\boldsymbol{x}-\boldsymbol{x}')d^3x' + (1\leftrightarrow 2)\Bigg] .\end{aligned} \tag{5.60}$$

One can take the point-particle limit of this expression without any trouble to obtain

$$\vartheta_{\rm cross} = -16\frac{\alpha_4 m_1 m_2}{\beta m^4}\,\epsilon_{ijk}v_{12k}\left[m^4\left(\frac{n^i_{12}n^j_1}{r^2_1 b^2}+\frac{n^i_{12}n^j_2}{r^2_2 b^2}+\frac{n^i_1 n^j_2}{r^2_1 r^2_2}\right)+\mathcal{O}\left(\frac{m^5}{r^5}\right)\right] . \tag{5.61}$$

These terms are of relative $\mathcal{O}(v^5)$ compared to the leading-order term of $\vartheta_{\rm self}$.

As for compact objects, the results found in the even-parity case also apply here. Terms proportional to $1/r^2_A$ in the above expression suggest that each object has a dipole component induced by the companion. When we expand this expression around $r_A \ll b$, however, the terms proportional to $1/(r^2_A b^2)$ cancel each other, as in the even-parity case, leading to no induced dipole moment. Even if this were not the case, however, the corrections to the dipole moment would be higher order than the contributions from $\vartheta_{\rm self}$.

To conclude, the dominant contribution to ϑ is clearly that of $\vartheta_{\rm self}$ given in Eq. (5.61), which again depends on the structure of the source and thus violates the effacement principle.

5.4.3 Matching near zone and strong-field solutions and finding the effective source terms

In alternative theories of gravity, the point-particle limit is not always valid and the multipole moments of compact objects may depend on the internal structure of the source. In the previous subsections, we found that the dominant contributions to the scalar field come from self-interaction terms, which in turn depend on certain structure constants. In this subsection, we determine these constants by matching the ϑ solution to that of an isolated BH.

Even-parity sector

In the even-parity case, the monopole charges q_1 and q_2 in Eq. (5.47) must be determined by matching to a BH solution. An isolated BH sources a scalar field [172], whose leading PN behavior is

$$\vartheta_{\rm YS} = \frac{2\alpha_3}{\beta m_A^2}\frac{m_A}{r_A}\,. \tag{5.62}$$

Matching this solution to the NZ solution of Eq. (5.47) we obtain

$$q_A = \frac{2\alpha_3}{\beta m_A}\,. \tag{5.63}$$

Notice that this monopole charge does not depend on (α_1, α_2), as for pure BH spacetimes, these coupling constants appear in combination with the Ricci scalar and tensor, which vanishes. This is to be contrasted with the NS case, in which q_A depends on α_1 and α_2 as well as α_3 and vanishes in EDGB theory. Interestingly, BHs do not have scalar hair in more traditional (Brans-Dicke type) scalar-tensor theories, while NSs do possess them. This situation is reversed in EDGB theory.

The matching carried out above dealt with the monopole part of ϑ. That is, we have ignored any tidal deformation of either BH induced by its binary companion. In BH perturbation theory, one can calculate the deformation of the isolated BH metric to find that it depends on the sum of electric and magnetic tidal tensors, leading to a

metric deformation that scales as $(r_1/b)^2(m_2/b)$ for $r_1 \ll b$ [10, 183, 93, 117, 182, 82]. Thus, in the IZ of object 1, tidal deformations lead to corrections of $\mathcal{O}(m^3/b^3)$, which are much smaller than the effects considered here. Therefore, it suffices in this section to consider an isolated BH when matching the scalar fields.

With this at hand, we can now treat BHs in even-parity, quadratic modified gravity as delta function sources of matter energy density, and with effective scalar density

$$\rho_\vartheta = q_A \delta^{(3)}(\boldsymbol{x} - \boldsymbol{x}_A). \tag{5.64}$$

In the PN expansion such sources reproduce the BH solution found by Yunes and Stein [172] at leading order.

Let us make a few observations about the effective source term approach. First, notice that the scalar field diverges as $m_A \to 0$, which violates the small-coupling approximation. This is related to the fact that as one shrinks a BH, the radius of curvature at the horizon also goes to zero, probing increasingly shorter length scales. When the small-coupling approximation is violated, one can no longer neglect the scalar field's stress-energy tensor and the $(\mathcal{H}_{\mu\nu}, \mathcal{I}_{\mu\nu}, \mathcal{J}_{\mu\nu}, \mathcal{K}_{\mu\nu})$ tensors that would dominate over the Einstein tensor. Of course, one cannot take this limit seriously, as we are considering here a low-energy effective theory, which is missing higher-curvature terms that would need to be included. Notice also that this is different from the behavior of scalar fields in traditional scalar-tensor theories, where the scalar field vanishes in the $m_A \to 0$ limit.

Odd-parity sector

In the odd-parity case, the dipole charges of the respective objects in Eq. (5.57) are to be determined by matching against the appropriate BH solutions. An isolated non-spinning BH in the odd-parity case does not support a scalar field. By contrast, a spinning BH does, and in the slow-rotation limit, neglecting higher order PN

corrections, it is given by [177]

$$\vartheta_{\rm YP} = -\frac{5}{2}\frac{\alpha_4}{\beta r_A^2} n_A^i \chi_A^i \,, \tag{5.65}$$

where $\chi_A \equiv S_A^i/m_A^2$ is the normalized spin angular momentum vector of the Ath BH. Matching this solution to the NZ $\vartheta_{\rm self}$ in Eq. (5.57), we obtain

$$\mu_A^i = \frac{5}{2}\frac{\alpha_4}{\beta}\chi_A^i \,. \tag{5.66}$$

With this at hand, we can now treat BHs in odd-parity, quadratic modified gravity as distributional sources of matter energy density and effective scalar density

$$\rho_\vartheta = -\mu_A^i \delta^{(3)}(\boldsymbol{x} - \boldsymbol{x}_A)_{,i} \,.$$

In the PN expansion, such sources reproduce the BH solution found by Yunes and Pretorius [177] at leading order.

Let us make a few observations about this solution. First, notice that the pseudo-scalar dipole charge is well behaved in the limit $m_A \to 0$, because there is a maximum BH spin $|\chi_A^i| < 1$. Second, notice that in the $|\chi_A^i| \to 0$ limit, this dipole charge vanishes, which is a consequence of Birkhoff's theorem holding in CS gravity [180, 74, 6]. Namely, non-spinning BHs in CS theory are the same as BHs in GR (i.e. Schwarzschild BHs). Therefore, in this case the point-particle limit is well-justified and the metric deformation or the scalar field does not depend on the internal structures of non-spinning sources.

5.4.4 Far-zone field point solutions

Let us assume that we have the wave equation

$$\Box_\eta \vartheta = \tau(t, x) \,, \tag{5.67}$$

where τ denotes the source term. The far-zone field point solution to this wave equation is given as [160, 114]

$$\vartheta^{\rm FZ} = -\frac{1}{4\pi}\sum_{m=0}^{\infty}\frac{(-1)^m}{m!}\partial_M\left[\frac{1}{r}\int_{\mathcal{M}}\tau(u,x'^i)x'^M\right], \tag{5.68}$$

with $u \equiv t-r$. By using $u_{,i} = -n_i$ and by keeping only terms proportional to $1/r$, the above solution reduces to

$$\vartheta^{\rm FZ} = -\frac{1}{4\pi}\frac{1}{r}\sum_{m=0}^{\infty}\frac{1}{m!}\frac{\partial^m}{\partial t^m}\int_{\mathcal{M}}\tau(u,x'^i)\left(n_j x'^j\right)^m d^3x'\,. \tag{5.69}$$

Here, the region $\mathcal{M}$ denotes the hypersurface of $t-r=$ const. In the following, we apply these formulas to the even and odd parity cases separately.

Even-parity sector

Following the discussion in Sec. 5.4.2, the evolution equation for the scalar field is dominantly

$$\Box_\eta\vartheta = -4\pi q_1\delta^{(3)}(\boldsymbol{x}-\boldsymbol{x}_1) + (1\leftrightarrow 2)\,. \tag{5.70}$$

From Eq. (5.69), this wave equation can be solved as

$$\begin{aligned}\vartheta^{\rm FZ} =& \frac{1}{r}\sum_m\frac{1}{m!}\frac{\partial^m}{\partial t^m}\int_{\mathcal{M}}q_1\delta^{(3)}(\boldsymbol{x}'-\boldsymbol{x}_1)(n_j\,x'^j)^m d^3x' \\ &+ (1\leftrightarrow 2)\,.\end{aligned} \tag{5.71}$$

The $m=0$ term gives

$$\vartheta^{\rm FZ} = \frac{q}{r}\,, \tag{5.72}$$

where we have defined the total scalar monopole charge $q \equiv q_1+q_2$. Recall that this monopole charge q refers to the scalar field, and not to an electromagnetic one. For a BH binary or a NS binary in a quasi circular orbit, q only changes during merger, as mass is carried away in radiation. Thus, monopole radiation is inefficient and suppressed.

For the $m = 1$ case, we find

$$\vartheta^{\rm FZ} = \frac{\dot{D}_i n^i}{r}\,, \tag{5.73}$$

where we have defined the total scalar dipole moment as

$$D^i \equiv q_1 x_1^i + q_2 x_2^i\,. \tag{5.74}$$

When we evaluate this for circular orbits, we find

$$\vartheta^{\rm FZ} = \frac{1}{r}\left(q_1\frac{m_2}{m} - q_2\frac{m_1}{m}\right) v_{12i} n^i\,, \tag{5.75}$$

where we have defined the relative velocity $v_{12}^k \equiv v_1^k - v_2^k$.

The $m = 1$ term clearly leads to dipole radiation in the FZ, which is less relativistic than GR quadrupole radiation, becoming stronger at smaller velocities. Of course, this term is proportional to the coupling constants of the theory, which are assumed much smaller than one. . Reference [172] failed to recognize such dipolar emission because they considered the motion of test particles that had no scalar charge. We cannot think of any mechanism that would suppress such dipolar radiation.

Odd-parity sector: spinning bodies

As in the previous Section, the evolution equation for the scalar field is dominantly

$$\Box_\eta \vartheta = 4\pi \mu_1^i \delta^{(3)}(\boldsymbol{x} - \boldsymbol{x}_1)_{,i} + (1 \leftrightarrow 2)\,. \tag{5.76}$$

By using Eq. (5.68), the far-zone field point solution is obtained as

$$\vartheta^{\rm FZ} = -\sum_{m=0}^{\infty} \frac{(-1)^m}{m!}\partial_M \left[\frac{1}{r}\int_{\mathcal{M}} \mu_1^i \delta^{(3)}(\boldsymbol{x}' - \boldsymbol{x}_1)_{,i} x'^M d^3x' + (1 \leftrightarrow 2)\right]. \tag{5.77}$$

When $m = 0$ there is obviously no contribution to the scalar field. When $m = 1$,

$$\int_{\mathcal{M}} \delta^{(3)}(\boldsymbol{x} - \boldsymbol{x}_1)_{,i} x^j d^3x = -\delta_{ij}\,, \tag{5.78}$$

and thus

$$\vartheta^{\rm FZ} = \frac{\mu_i n^i}{r^2} + \frac{\dot{\mu}_i n^i}{r}\,, \tag{5.79}$$

with $\mu_i \equiv \mu_{1i} + \mu_{2i}$. Notice that we recover the solution of Yunes and Pretorius [177] for the first term of the above equation with μ^i_A given as in Eq. (5.66). These terms will not strongly radiate because $\dot{\mu}_i$ is non-vanishing only for spin-precessing systems. Even then, such radiation would be suppressed by the ratio of the orbital timescale to the precession timescale.

The $m = 2$ contribution, by contrast, depends on the much shorter orbital timescale. We look for terms of $\mathcal{O}(r^{-1})$ since they are the only ones that contribute to the energy flux at infinity. Keeping in mind that the function being differentiated depends on retarded time, we can rewrite Eq. (5.77) as

$$\begin{aligned}\vartheta^{\rm FZ} = &-\frac{1}{r}\sum_m \frac{1}{m!}\frac{\partial^m}{\partial t^m}\int_{\mathcal{M}} \mu^i_1 \delta^{(3)}(\boldsymbol{x}' - \boldsymbol{x}_1)_{,i}(n_k\, x'^k)^m d^3x' \\ &+ (1 \leftrightarrow 2)\,.\end{aligned} \tag{5.80}$$

When $m = 2$, we have that

$$\mu^i_1 \int_{\mathcal{M}} \delta^{(3)}(\boldsymbol{x} - \boldsymbol{x}_1)_{,i} x^p x^q d^3x + (1 \leftrightarrow 2) = -2\mu^{pq}\,, \tag{5.81}$$

where the pseudo-tensor quadrupole moment (not to be confused with $\mu^i\mu^j$) is defined as

$$\mu^{ij} \equiv x_1^{(i}\mu_1^{j)} + x_2^{(i}\mu_2^{j)}\,. \tag{5.82}$$

The $m = 2$ contribution becomes

$$\vartheta^{\rm FZ} = \frac{1}{r}\ddot{\mu}_{ij} n^{ij} = -\frac{1}{r}\omega^2 \mu_{ij} n^{ij}\,, \tag{5.83}$$

where the final equality is evaluated on a circular orbit. Notice that such a scalar field will strongly radiate because μ^{ij} depends on the orbital timescale.

Odd-parity sector: non-spinning bodies

When both objects are non-spinning, the self-interaction terms produced by the effective source identically vanish. One is then left with the source term constructed from the product of the gravitational fields of objects 1 and 2. These terms will be proportional to $m_1 m_2$. As we will see, there are many contributions that turn out to vanish upon NZ integration. For pedagogical reasons, we will show here explicitly how this happens and eventually arrive at contributions that do not vanish.

The evolution equation for the scalar field to leading PN order is

$$\Box_\eta \vartheta_{\rm FZ} = -32\frac{\alpha_4}{\beta}\epsilon_{ijk} m_1 m_2 v_{12k} \left(\frac{1}{r_1}\right)_{,im} \left(\frac{1}{r_2}\right)_{,jm} , \tag{5.84}$$

where we substituted the NZ metric components in the point-particle approximation. The leading order term of the solution to this differential equation, i.e. the $m = 0$ term in the sum of Eq. (5.69), is evaluated as

$$\begin{aligned} \vartheta_{\rm FZ} &= \frac{8}{\pi}\frac{\alpha_4}{\beta} m_1 m_2 \epsilon_{ijk} \frac{v_{12}^k}{r} \int_{\mathcal{M}} \left(\frac{1}{r_1}\right)_{,im} \left(\frac{1}{r_2}\right)_{,jm} d^3x \\ &= -16\frac{\alpha_4}{\beta} m_1 m_2 \epsilon_{ijk} \frac{v_{12}^k}{r} \partial_i^{(1)} \partial_j^{(2)} \partial_m^{(1)} \partial_m^{(2)} Y = 0 \,. \end{aligned} \tag{5.85}$$

Here we integrated over the NZ+IZ hypersurface $\mathcal{M}$ without taking any care of the strong gravity region in the IZs. One can easily show that the contribution from the IZs is not large in the present case. In the second line, we replaced partial derivatives with respect to x^i acting on $1/r_A$ with (minus the) particle derivatives with respect to x_A^i:

$$\frac{\partial}{\partial x^i} \to -\frac{\partial}{\partial x_A^i} \equiv -\partial_i^{(A)}, \tag{5.86}$$

with $A = (1, 2)$. We commuted these particle derivatives with the integral, and finally obtained a typical NZ integral, discussed in Appendix B. From Eq. (B.4), we know that $Y = b$, and by taking all particle derivatives, the last equality is established.

We could have inferred that the $m = 0$ term in the sum does not contribute for non-spinning BHs without any explicit calculations. The argument here is similar to

that in footnote 4. Possible vectors to contract with the Levi-Civita symbol include the velocities v_A^i and the unit vectors n_A^i, but not spin vectors S_A^i, as we here consider non-spinning BHs. In particular, for the $m = 0$ case, there cannot be any FZ vectors n^i present. Thus, all vectors that can be contracted onto the Levi-Civita symbol must lie in the same orbital plane and this obviously vanishes. This argument should be true at all PN orders[5].

Let us then consider the next-order term. This will arise from the leading-order source term [right-hand side of Eq. (5.84)] with $m = 1$ in the NZ sum:

$$\begin{aligned}\vartheta_{\rm FZ} &= \frac{8}{\pi}\frac{\alpha_4}{\beta}\frac{m_1 m_2}{r} n^p \epsilon_{ijk} v_{12}^k \frac{\partial}{\partial t}\int_{\mathcal{M}} \left(\frac{1}{r_1}\right)_{,im}\left(\frac{1}{r_2}\right)_{,jm} x^p d^3x \\ &= -16\frac{\alpha_4}{\beta}\frac{m_1 m_2}{r} n^p \epsilon_{ijk} v_{12}^k \frac{\partial}{\partial t}\partial_i^{(1)}\partial_j^{(2)}\partial_m^{(1)}\partial_m^{(2)} Y_p \,, \end{aligned} \tag{5.87}$$

where we have used Eq. (B.3), which defines Y_p. By direct evaluation, one can show that this term also identically vanishes. The first non-vanishing contribution coming from an $m = 1$ term must then be $\mathcal{O}(v^3)$ smaller than the ordering of the $m = 0$ term.

Finally, let us consider the (next)^2-order term. This can arise only from the leading-order source term with $m = 2$ in the NZ sum:

$$\begin{aligned}\vartheta_{\rm FZ} &= \frac{4}{\pi}\frac{\alpha_4}{\beta}\frac{m_1 m_2}{r} n^{pq} \epsilon_{ijk} \frac{\partial^2}{\partial t^2} v_{12}^k \int_{\mathcal{M}} \left(\frac{1}{r_1}\right)_{,im}\left(\frac{1}{r_2}\right)_{,jm} x^p x^q d^3x \\ &= -8\frac{\alpha_4}{\beta}\frac{m_1 m_2}{r} n^{pq} \epsilon_{ijk} \frac{\partial^2}{\partial t^2} v_{12}^k \partial_i^{(1)}\partial_j^{(2)}\partial_m^{(1)}\partial_m^{(2)} \left(Y_{\langle pq\rangle} + \frac{1}{3}\delta_{pq} S\right) \,, \end{aligned} \tag{5.88}$$

which simplifies to

$$\vartheta_{\rm FZ} = 16\frac{\alpha_4}{\beta}\frac{1}{r}\frac{\eta m \delta m}{b} \epsilon_{ijk} n_{ip} \omega^2 v_{12}^k n_{12}^{jp} \,, \tag{5.89}$$

where we have defined the mass difference $\delta m \equiv m_1 - m_2$ and the symmetric mass ratio $\eta \equiv m_1 m_2/m^2$. We have here used Kepler's law and expanded the STF tensors. This

[5]One may think that one can construct a vector that does not lie in the orbital plane by taking the cross product of two vectors that lie on this plane, e.g. $\boldsymbol{n}_{12} \times \boldsymbol{v}_{12}$. However, since GR is parity even, such a vector cannot be present in the PN metric.

is the dominant FZ behavior of the scalar field, which as we see is much suppressed relative to the odd-parity solution we found for spinning BHs.

5.4.5 Summary of this section

Let us summarize the results found so far for later use. In the even-parity case, generically at least one of the binary component objects will have a scalar monopole charge. Since the scalar field excitation due to the induced monopole is dominant, we neglect all the other less important contributions. Weakly gravitating objects need not have a scalar monopole charge if $\alpha_1 + \alpha_2 + 3\alpha_3 = 0$, and BHs have no scalar monopole charge if $\alpha_3 = 0$. In EDGB theory, NSs have no scalar monopole charge. In the odd-parity case, the dominant contribution is the magnetic-type scalar dipole moment induced by spins. Generically, astrophysical objects will possess spin, but we will continue to include non-spinning results to compare with previous work.

In the NZ, we can parametrize the leading PN terms of the scalar field as

$$\vartheta_{\rm NZ} = \frac{A}{r_1^a b^b} + \frac{B}{r_1^c r_2^d} + (1 \leftrightarrow 2)\,, \tag{5.90}$$

where (A, B, a, b, c, d) are given in Table 5.1 and for compactness of the Table we define

$$\sigma^{pq}_{\rm NZ} \equiv -16\frac{\alpha_4}{\beta}\eta m^2 \epsilon_{pqs} v_{12}^s\,. \tag{5.91}$$

In the FZ, we can parametrize the scalar field as

$$\vartheta_{\rm FZ} = \frac{C}{r}\,, \tag{5.92}$$

where C is also given in Table 5.1 and we define

$$\sigma^{pq}_{\rm FZ} \equiv 16\frac{\alpha_4}{\beta}\eta\, m\, \delta m \frac{\omega^2}{b}\epsilon_{qjk} v_{12}^k n_{12}^{jp}\,, \tag{5.93}$$

	A	B	C	a	b	c	d
Even-P	q_1	0	$\dot{D}_i n^i$	1	0	–	–
Odd-P, Spins	$\mu_1^i n_1^i$	0	$\ddot{\mu}_i n^{ij}$	2	0	–	–
Odd-P, No Spins	$\sigma_{\rm NZ}^{pq} n_{12}^p n_1^q$	$\frac{1}{2}\sigma_{\rm NZ}^{pq} n_1^p n_2^q$	$\sigma_{\rm FZ}^{pq} n^{pq}$	2	2	2	2

Table 5.1: Scalar field parameters, as defined in Eqs. (5.90) and (5.92). The quantities q_1 and μ_1^i are defined in Eqs. (5.63) and (5.66), while $\sigma_{\rm NZ}^{pq}$ is defined in Eq. (5.91). The quantities D_i and μ_i are defined in Eqs. (5.74) and (5.77), while $\sigma_{\rm FZ}^{pq}$ is given in Eq. (5.93).

5.5 Metric evolution

In this section, we solve the evolution equations for the metric deformation in the FZ, so that we can calculate the gravitational energy flux at infinity. Note that throughout, we use the Newtonian relationship $v^2 = m/b$ (and similarly for the acceleration). This relationship must be corrected at higher PN order or at $\mathcal{O}(\varsigma)$. As we mentioned earlier, here we do not take into account the corrections to the orbital motion due to the conservative force at $\mathcal{O}(\varsigma)$. These conservative effects do not interfere at $\mathcal{O}(\varsigma)$ with the radiative effects that we are concerned with in this paper. Therefore the corrections to the GW waveform become a simple summation of these two different types of effects.

For the FZ field points, the solution to the metric deformation equation of motion [Eq. (5.17)] can be read from Eq. (5.69):

$$\mathfrak{h}_{ij} = -\frac{8}{r}\sum_{m=0}^{\infty}\frac{1}{m!}\frac{\partial^m}{\partial t^m}\int_{\mathcal{M}}\tilde{\mathcal{C}}_{ij}\,(n^k x'^k)^m d^3x' + O\left(r^{-2}\right)\,, \tag{5.94}$$

where we have defined the source term as

$$\begin{aligned}\tilde{\mathcal{C}}_{ij} =& \alpha_1\left(\vartheta\tilde{\mathcal{H}}_{ij}^{(0)} + \tilde{\mathcal{H}}_{ij}^{(1)}\right) + \alpha_2\left(\vartheta\tilde{\mathcal{I}}_{ij}^{(0)} + \tilde{\mathcal{I}}_{ij}^{(1)}\right)\\ &+ \alpha_3\left(\vartheta\tilde{\mathcal{J}}_{ij}^{(0)} + \tilde{\mathcal{J}}_{ij}^{(1)}\right) + \alpha_4\tilde{\mathcal{K}}_{ij}^{(1)} - \frac{1}{2}T_{ij}^{(\vartheta)}\,.\end{aligned} \tag{5.95}$$

Notice that this corresponds to an IZ+NZ integration for FZ field points, where we have neglected the FZ integration because it is subdominant.

The integrals presented above have to be carried out also in the IZ, where the PN expansion is not valid anymore. In GR, however, such divergences can be ignored, using a regularization scheme. Since both the true solution and an appropriately regularized solution satisfy the field equations in the NZ, their difference due to the IZ contribution is only through a homogeneous solution. Such homogeneous solutions are regular in the NZ and FZ, but can be divergent in the IZ. They are characterized by the multipole moments of the respective objects, which can be determined by studying tidal perturbations around a strongly gravitating object. One can then perform matching of the metric solution, as for the scalar solution, but the metric matching is beyond the scope of this paper. In what follows, we only consider the regularized contribution, following Hadamard *partie finie* (FP) regularization [24]. We comment more on the divergent contribution at the end of this Section.

5.5.1 Even-parity sector

Let us focus on the metric perturbation in the even-parity sector first. The leading order term both in the PN and $1/r$ expansion at infinity is formally given by

$$\mathfrak{h}_{ij} = \mathfrak{h}^T_{ij} + \mathfrak{h}^{\mathcal{J}}_{ij}\,, \tag{5.96}$$

$$\mathfrak{h}^T_{ij} \equiv \frac{4}{r}\int_{\mathcal{M}} T^{(\vartheta)}_{ij} d^3x\,, \tag{5.97}$$

$$\mathfrak{h}^{\mathcal{J}}_{ij} \equiv -\frac{8\alpha_3}{r}\int_{\mathcal{M}} \tilde{\mathcal{J}}_{ij} d^3x\,, \tag{5.98}$$

where we have defined $\tilde{\mathcal{J}}_{ij} \equiv \vartheta\tilde{\mathcal{J}}^{(0)}_{ij} + \tilde{\mathcal{J}}^{(1)}_{ij}$. The source terms $\tilde{\mathcal{H}}_{\mu\nu}$ and $\tilde{\mathcal{I}}_{\mu\nu}$ do not contribute to this expression since they identically vanish in the NZ where $R_{\mu\nu} = 0$.

We can estimate the order of magnitude of both $\mathfrak{h}^{\mathcal{J}}_{ij}$ and $\mathfrak{h}^T_{ij}$ as follows:

$$\mathfrak{h}^T_{ij} \sim \mathcal{O}\left(\beta\frac{m}{r}v^{-2}\vartheta^2\right) = \zeta_3\frac{m}{r}v^2 \times \mathcal{O}\left(1\right)\,, \tag{5.99}$$

$$\mathfrak{h}^{\mathcal{J}}_{ij} \sim \mathcal{O}\left(\frac{\alpha_3}{m^2}\frac{m}{r}v^4\vartheta\right) = \zeta_3\frac{m}{r}v^2 \times \mathcal{O}\left(v^4\right)\,. \tag{5.100}$$

Here we factored out v^2 in the final expressions, since the GR leading quadrupolar field is also proportional to v^2. Clearly, the dominant contribution comes from Eq. (5.99).

Let us now make this computation more precise. The stress-energy tensor will contain self-interactions of the form $\vartheta_{A,i}\vartheta_{A,j}$ and cross terms of the form $\vartheta_{1,i}\vartheta_{2,j}$. The former case leads to divergent integrals, which must be determined by strong-field matching, so we do not consider them here. Let us concentrate on the latter, which take the form

$$T^{(\vartheta)}_{ij} = \beta\left(\vartheta_{,i}\vartheta_{,j} - \frac{1}{2}\delta_{ij}\vartheta_{,\mu}\vartheta^{,\mu}\right) \tag{5.101}$$

$$\approx \beta q_1 q_2\left[2\left(\frac{1}{r_1}\right)_{,(i}\left(\frac{1}{r_2}\right)_{,j)} - \delta_{ij}\left(\frac{1}{r_1}\right)_{,k}\left(\frac{1}{r_2}\right)_{,k}\right], \tag{5.102}$$

which sources the metric perturbation

$$\begin{aligned}
\mathfrak{h}_{ij} &= \frac{4}{r}\int_{\mathcal{M}} T^{(\vartheta)}_{ij} d^3x\,, \\
&= -\frac{4\pi}{r}\beta q_1 q_2\left(2\partial^{(1)}_i\partial^{(2)}_j b - \delta_{ij}\partial^{(1)}_k\partial^{(2)}_k b\right) + (1\leftrightarrow 2)\,, \\
&= -\frac{16\pi}{r}\beta\frac{q_1 q_2}{b}n^{ij}_{12}\,,
\end{aligned} \tag{5.103}$$

where we used an integration formula for the triangle potential given in Appendix B. We can see that this correction is 0PN relative to the radiative metric perturbation in GR, just as we predicted in Eq. (5.99). However, this correction turns out to be still smaller in the energy flux than the dipole scalar radiation, which gives a -1PN correction.

5.5.2 Odd-parity sector

We now focus on the odd-parity sector, for which the solution is given by the term proportional to α_4 in Eq. (5.94), namely

$$\mathfrak{h}_{ij} = \mathfrak{h}^T_{ij} + \mathfrak{h}^{\mathcal{K}}_{ij}\,, \tag{5.104}$$

$$\mathfrak{h}^{\mathcal{K}}_{ij} \equiv -\frac{8\alpha_4}{r}\int_{\mathcal{M}}\tilde{\mathcal{K}}^{(1)}_{ij} d^3x\,. \tag{5.105}$$

The stress-energy contribution $\mathfrak{h}^T_{ij}$ is the same as in Eq. (5.101).

The $\mathcal{K}$ contribution to Eq. (5.104) is more involved. The leading-order behavior of the $\mathcal{K}$ tensor is

$$\begin{aligned}\tilde{\mathcal{K}}^{(1)}_{ij} \;=\; & \dot{\vartheta}_{,k}\epsilon_{jkl}h_{00,il} + \dot{\vartheta}_{,k}\epsilon_{jlm}(h_{im,lk} + h_{lk,im}) \\ & + \vartheta_{,kl}\epsilon_{jlm}(h_{i0,mk} + h_{mk,i0} - h_{k0,im} - h_{im,k0}) \\ & - \vartheta_{,k}\epsilon_{ikl}(2h_{0[m,j]lm} - 2\dot{h}_{l[j,m]m} - \dot{h}_{00,jl}) \\ & - 2\dot{\vartheta}\epsilon_{ikl}h_{k[j,m]lm} + (i \leftrightarrow j)\,. \end{aligned} \tag{5.106}$$

Other terms are of higher PN order. By applying the Lorenz or harmonic gauge condition $h^{\mu\nu}{}_{,\nu} = 0$, substituting $h_{ij} = h_{00}\delta_{ij}$ into Eq. (5.106), and using $\epsilon_{jkl}h^{\mu\nu,kl} = \epsilon_{jkl}\vartheta_{,kl} = 0$, we get

$$\begin{aligned}\tilde{\mathcal{K}}^{(1)}_{ij} =& 2\dot{\vartheta}_{,k}\epsilon_{jkl}h_{00,il} - 2\vartheta_{,km}\epsilon_{jkl}h_{0[m,i]l} \\ & - 2\vartheta_{,k}\epsilon_{jkl}h_{0[m,i]lm} + 2\vartheta_{,k}\epsilon_{jkl}\dot{h}_{00,il} + (i \leftrightarrow j)\,. \end{aligned} \tag{5.107}$$

The $\tilde{\mathcal{K}}_{ij}$ term in Eq. (5.104) is then a sum of four terms, namely

$$\mathfrak{h}^{\mathcal{K}}_{ij} = \sum_{n=1}^{4} \mathfrak{h}^{(n)}_{ij}\,, \tag{5.108}$$

where we have defined

$$\mathfrak{h}^{(1)}_{ij} = -\frac{16\alpha_4}{r}\int_{\mathcal{M}} \dot{\vartheta}_{,k}\epsilon_{jkl}h_{00,il}d^3x + (i \leftrightarrow j)\,, \tag{5.109}$$

$$\mathfrak{h}^{(2)}_{ij} = +\frac{16\alpha_4}{r}\int_{\mathcal{M}} \vartheta_{,km}\epsilon_{jkl}h_{0[m,i]l}d^3x + (i \leftrightarrow j)\,, \tag{5.110}$$

$$\mathfrak{h}^{(3)}_{ij} = +\frac{16\alpha_4}{r}\int_{\mathcal{M}} \vartheta_{,k}\epsilon_{jkl}h_{0[m,i]lm}d^3x + (i \leftrightarrow j)\,, \tag{5.111}$$

$$\mathfrak{h}^{(4)}_{ij} = -\frac{16\alpha_4}{r}\int_{\mathcal{M}} \vartheta_{,k}\epsilon_{jkl}\dot{h}_{00,il}d^3x + (i \leftrightarrow j)\,. \tag{5.112}$$

When we substitute the PN metric into the above terms, the right-hand sides depend on the velocity vectors v_A^i (which depend on time only). The field ϑ is given in Eq. (5.90) and its derivative can be computed simply from that equation. Since this field is a NZ one, it depends on time through the positions of the objects, which implies that its time derivative can be converted into a spatial derivative via $\partial_t f(r_1) = -v_1^i \partial_i f(r_1)$.

Let us begin by making a simple order of magnitude estimate of how large the regularized contribution is. For this, it suffices to look at Eqs. (5.99) and (5.109):

$$\mathfrak{h}_{ij}^T \sim \mathcal{O}\left(\beta \frac{m}{r} v^{-2} \vartheta^2\right) , \tag{5.113}$$

$$\mathfrak{h}_{ij}^{\mathcal{K}} \sim \mathcal{O}\left(\frac{\alpha_4}{m^2} \frac{m}{r} v^5 \vartheta\right) . \tag{5.114}$$

The ϑ field here is that of the NZ, and hence

$$\mathfrak{h}_{ij}^T \sim \zeta_4 \frac{m}{r} v^2 \times \mathcal{O}\left(\chi^2 v^4 + \eta \chi v^9 + \eta^2 v^{14}\right) , \tag{5.115}$$

$$\mathfrak{h}_{ij}^{\mathcal{K}} \sim \zeta_4 \frac{m}{r} v^2 \times \mathcal{O}\left(\chi v^7 + \eta v^{12}\right) , \tag{5.116}$$

where χ stands for the magnitude of χ_1^i and χ_2^i. From this analysis, $\mathfrak{h}_{ij}^T$ is clearly larger for rapidly spinning objects, leading to a 2PN effect.

For the non-spinning case, one might expect the $\mathcal{K}$ contribution to lead to a 6PN effect, but as we explain in Appendix C, these leading-order effects actually vanish. This cancellation can also rather easily be seen by integrating by parts in Eqs. (5.109)-(5.112). After discarding boundary terms (taking into account the boundary term is equivalent to adding homogeneous solutions, corresponding to deformed multipole moments of compact objects), we obtain expressions of the form $\epsilon_{jkl}\, \vartheta\, h_{00,kl\ldots}$, which obviously vanishes by the antisymmetry of the Levi-Civita tensor. We carry out a more careful analysis in Appendix C, where we explicitly show that the leading and first sub-leading order terms vanish.[6] The first non-vanishing term is then of $\mathcal{O}(v^2)$

[6] In Appendix C, we only show this for non-spinning BHs, but a similar calculation can be performed for spinning BHs to $\mathcal{O}(\chi)$.

smaller than the order of magnitude estimates in Eqs. (5.115) and (5.116), leading to 7PN and 4.5PN contributions at $\mathcal{O}(\chi^0)$ and $\mathcal{O}(\chi^1)$, respectively.

Since the largest contribution seems to arise for spinning BHs from the $\mathfrak{h}^T_{ij}$ term, let us consider this in more detail. Two possible contributions are generated here: one that depends only on self-interaction terms, and one that depends on the cross-interaction. The former leads to divergent integrals, which need to be matched from strong-field solutions, and we do not consider these here. The latter leads to the metric deformation

$$\begin{aligned}
\mathfrak{h}^T_{ij} &= -\frac{4\pi}{r}\beta\mu_1^k\mu_2^l\left(2\partial^{(1)}_{ik}\partial^{(2)}_{jl}Y - \delta_{ij}\partial^{(1)}_{pk}\partial^{(2)}_{pl}Y\right) + (1\leftrightarrow 2) \\
&= \frac{8\pi\beta}{rb^3}\Big\{2\mu_1^{(i}\mu_2^{j)} - 12n_{12}^{(i}\mu_1^{j)}\left(n_{12}^k\mu_{2k}\right) \\
&\quad + 3n_{12}^{ij}\left[5\left(n_{12}^k\mu_{1k}\right)\left(n_{12}^l\mu_{2l}\right) - \mu_{1k}\mu_2^k\right]\Big\} + (1\leftrightarrow 2)\,, \qquad (5.117)
\end{aligned}$$

which is clearly of the order predicted in Eq. (5.115), i.e. 2PN order relative to GR. This is of the same order as the energy flux correction carried by the pseudo-scalar radiation.

5.5.3 Multipole moments

In this Subsection, we discuss the additional contribution from the IZs, which enter as additional homogeneous solutions in the NZ and FZ, These contributions are homogeneous in the sense that they arise from sources that have support only in the IZs, and thus they vanish in the NZ and FZ (see e.g. the discussion prior to Eq. (5.45)). The homogeneous solutions are characterized by the mass and current multipole moments of the strong-field bodies, which must be determined by matching to strong gravity solutions in the IZ. When we solve the non-linear equations of motion iteratively, the source terms in general can be classified into two pieces: a self-interaction part and a cross-interaction part, as in the case of ϑ in Sec. 5.4. The cross-interaction part is sourced by the companion, while the self-interaction part is not.

The self-interaction part is rather easy to handle because matching involves only a single isolated object. As described in Sec. 5.4.2, these self-interaction terms can be thought of as homogeneous solutions that have support only in the IZ. As such, in the small-coupling approximation, they satisfy homogenous field equations that take Einstein form. If the spin of the object is neglected, the only possible linear perturbation to such a homogeneous solution that is compatible with asymptotic flatness is a shift of the body's mass (in the $1/r$ piece of the (t,t) and diagonal parts of the metric). In essence, this is a consequence of Birkhoff's theorem, which holds for homogeneous solutions. Such a shift is consistent with the strong-field, non-spinning BH solution in EDGB theory found in [172]. In that case, the mass shift is simply $m_A \to (49/80)\zeta_3 m_A$.

For spinning objects, one expects there to be higher multipole moments in the strong-field solution. However, one should be able to absorb current dipole moment modifications by a redefinition of the spin parameter, while the mass dipole moment will be absorbed by the redefinition of the position of the center of mass. Therefore, the leading-order corrections that survive are the mass quadrupole moment, which produces a metric perturbation in the NZ proportional to $1/r^3$. As we will see, when we consider FZ solution, there is an additional factor of v^2 that enters.

Therefore, contributions to the energy flux from the quadrupole or higher multipole moments are at least 3PN order relative to that from the GR quadrupole formula. We will later find that corrections to the energy flux due to scalar radiation appear at -1PN and 2PN relative order for the even and odd-parity cases, respectively. Hence, the contributions from the multipole moments that we discussed here are definitely smaller than those introduced by scalar radiation in the even-parity case, and at most, the same order in the odd-parity case.

Let us take a look at spinning BHs in the odd-parity sector in more detail. At $\mathcal{O}(\chi)$ there is freedom in adding a homogeneous solution proportional to $1/r^2$ in the h_{0i} component. This corresponds to a freedom in shifting the Kerr parameter measured at infinity. Reference [177] set this homogeneous solution to zero so that there is no shift in the Kerr parameter. At $\mathcal{O}(\chi^2)$, there should be corrections proportional to

$1/r^3$ in h_{ij} which shifts the quadrupole moment. Since there is no parameter in the Kerr geometry that can absorb this correction in the quadrupole moment, this $1/r^3$ correction cannot be eliminated.

The effective source term that reproduces this correction should look like

$$\Box \mathfrak{h}_{ij} = -4\pi Q_1 u_i u_j (\delta_{kl} - 3\hat{S}_{1,k}\hat{S}_{1,l})\delta^{(3)}(\boldsymbol{x} - \boldsymbol{x}_1)_{,kl} + (1 \leftrightarrow 2)\,, \tag{5.118}$$

where $Q_A = \mathcal{O}(\zeta_4 m_A a_A^2)$ and $\hat{S}_{A,k} \equiv S_A^i/m_A^2$ is a unit spin angular momentum vector. The solution of this wave equation at $\mathcal{O}(1/r)$ is given by

$$\mathfrak{h}_{ij} = \frac{1}{r}\sum_{m=0}^{\infty}\frac{1}{m!}\frac{\partial^m}{\partial t^m} u_i u_j (\delta_{kl} - 3\hat{S}_{1,k}\hat{S}_{1,l}) Q_1 \int_{\mathcal{M}} \delta^{(3)}(\boldsymbol{x} - \boldsymbol{x}_1)_{,kl} (\boldsymbol{n}\cdot\boldsymbol{x})^m d^3x + (1 \leftrightarrow 2)\,. \tag{5.119}$$

The leading-order contributions at $m = 0$ (2PN) and $m = 1$ (2.5PN) vanish, leading to the first non-zero contribution at $m = 2$

$$\mathfrak{h}_{ij} = \mathcal{O}\left(\frac{1}{r} Q\omega^2 v^2\right) = \zeta_4 \frac{m}{r} v^2 \times \mathcal{O}\left(\chi^2 v^6\right)\,, \tag{5.120}$$

which is 3PN relative to GR. Therefore, the self-interacting correction in the metric at $\mathcal{O}(\chi^2)$ is smaller compared to the corrections in the energy flux carried by the scalar field and the metric field with regularized modification.

The cross-interaction part is more complicated. In this case, we have to consider the induced multipole moments due to the presence of the secondary object. Thus, even if we consider non-spinning objects, higher multipole moments might be induced. Another important difference is that neither the mass monopole nor the spin dipole can be simply absorbed by a redefinition of the mass and spin of each object. This is because the shifts of these multipole moments depend on the orbital parameters, such as separation b. Notice, however, that the effects of the secondary object propagate only through the scalar field or the gravitational tidal force.

The order of magnitude of the former scalar field effect is more complicated to estimate and it depends on the situation. In the even-parity case, ϑ sourced by the

secondary body at the position of the primary body is proportional to $1/b$. In EDGB theory, since ϑ has shift symmetry within the context of the classical theory, the effects are suppressed by the gradient of the field, i.e. they are proportional to $1/b^2$. In the odd-parity case, there is again shift symmetry and the monopole scalar charge is absent. Because of these two reasons, the suppression is proportional to $1/b^3$ in CS theory. These suppressions will be sufficient to conclude that the effects are relatively at least 1PN and 3PN in the even and odd-parity cases respectively, which is smaller than the effects induced by scalar radiation.

In the odd-parity non-spinning case, the latter gravitational tidal force dominates over the scalar propagation effect. To calculate this tidal force properly requires asymptotic matching between the IZ solution and a strong-field, perturbed Schwarzschild solution in CS gravity. Perturbations of the Schwarzschild spacetime can be decomposed as a sum over electric and magnetic tidal tensors (see e.g. [117]). The former scale as $1/b^3(1 + v + v^2 + \ldots)$, while the latter scales as $v/b^3(1 + v + v^2 + \ldots)$ [82]. Such tidal deformations will induce gravitational waves that will scale as the second-time derivatives of the electric and magnetic quadrupole deformations, i.e. they will scale as $\omega^2/b^3(1+v+v^2+\ldots)$ and $\omega^2 v/b^3(1+v+v^2+\ldots)$. In GR, the leading order effect is induced by the electric quadrupole moment and it scales as ω^2/b^3, a 5PN order effect. In CS, we expect the magnetic quadrupole moment to provide the leading-order deformation, and the results of Pani, et al. [113] suggest that this scales as a 6PN order effect.

5.6 Energy flux

The inspiral of a compact binary system is controlled by the system's change in binding energy and angular momentum. The binding energy changes according to the dissipation of energy carried by all dynamical fields, which here includes the metric perturbation and the scalar field. The stress-energy tensor (SET) associated with each field quantifies the density and flux of energy and momentum. The energy loss is calculated as the integral of the energy flux through a 2-sphere of radius r in

the limit $r \to \infty$ and in the direction of the sphere's outward unit normal n^i. That is, for some field φ (be it h_{ij}, $\mathfrak{h}_{ij}$, or ϑ) with SET $T^{(\varphi)}_{\mu\nu}$,

$$\dot{E}^{(\varphi)} = \lim_{r\to\infty} \int_{S^2_r} \left\langle T^{(\varphi)}_{ti} n^i \right\rangle_\omega r^2 d\Omega \,, \tag{5.121}$$

where the angle brackets with subscript ω stand for orbit averaging.

The total energy flux can be ordered in powers of ς as

$$\dot{E} = \dot{E}_{\rm GR} + \varsigma\, \delta\dot{E} + \mathcal{O}(\varsigma^2) \,. \tag{5.122}$$

The GR energy flux $\dot{E}^{\rm GR}$ is given by the GR metric perturbation only, without any contributions from the scalar field at $\mathcal{O}(\varsigma^0)$, as there is no scalar field in GR. For circular orbits, this is

$$\dot{E}_{\rm GR} = -\frac{32}{5}\eta^2 v^{10} \,. \tag{5.123}$$

The $\mathcal{O}(\varsigma)$ correction, $\delta\dot{E}$, can be decomposed into

$$\delta\dot{E} = \delta\dot{E}^{(\vartheta)} + \delta\dot{E}^{(\mathfrak{h})} \,, \tag{5.124}$$

where the first term is the scalar field contribution and the second term is the contribution of the deformed metric perturbation.

The scalar field contribution is calculated with the SET given by Eq. (5.7):

$$\delta\dot{E}^{(\vartheta)} = \beta \lim_{r\to\infty} \int_{S^2_r} \left\langle \dot{\vartheta}\; n^i\; \partial_i\vartheta \right\rangle_\omega r^2 d\Omega \,. \tag{5.125}$$

Since we are taking the $r \to \infty$ limit, ϑ must be that valid in the FZ.

The metric deformation contribution to the energy flux is slightly more subtle. This modification to the GR flux can have three distinct sources: (i) the effective SET in terms of h_{ij} and $\mathfrak{h}_{ij}$ may be functionally different, but as shown in [138], this is not so for the class of theories we consider here[7]; (ii) The orbital equations of

[7]Reference [138] showed that the TT gauge exists in quadratic gravity as $r \to \infty$. Any non-TT propagating mode that is sourced in the NZ vanishes in the FZ at all orders. This is in contrast to scalar-tensor theories in the Jordan frame, where the scalar "breathing" mode is present in the

motion, and the associated relations $m/b = v^2$ and $\omega = v^3/m$, might be modified at $\mathcal{O}(\varsigma)$, as was partially calculated in [172]; (iii) The generation mechanism of the FZ metric perturbation is modified, i.e. the radiative part of the metric perturbation is deformed. We consider here only the dissipative modifications introduced by (iii), as (ii) would require an analysis of the equations of motion, which is beyond the scope of this paper[8].

Letting $H_{\alpha\beta} = h_{\alpha\beta} + \varsigma \mathfrak{h}_{\alpha\beta} + \mathcal{O}(\varsigma^2)$, the effective SET of GWs is given by [138]

$$T^{(H)}_{\mu\nu} = \frac{1}{32\pi} \left\langle H^{\rm TT}_{\alpha\beta,(\mu} H^{\alpha\beta}_{{\rm TT},\nu)} \right\rangle_\lambda \,, \tag{5.126}$$

where the angle brackets with a subscript λ stand for a quasi-local average over several wavelengths and TT stands for the transverse-traceless projection

$$H^{\rm TT}_{ij} = \Lambda_{ij,kl} H_{kl} \,, \qquad \Lambda_{ij,kl} = P_{ik}P_{jl} - \frac{1}{2} P_{ij}P_{kl} \,, \tag{5.127}$$

with $P_{ij} = \delta_{ij} - n_{ij}$ the projector onto the plane perpendicular to the line from the source to a FZ field point. Expanding this SET in orders of ς, the $\mathcal{O}(\varsigma^0)$ part leads to $\dot{E}_{\rm GR}$, while the $\mathcal{O}(\varsigma)$ part is

$$T^{(\mathfrak{h})}_{\mu\nu} = \frac{1}{16\pi} \left\langle h^{\rm TT}_{\alpha\beta,(\mu} \mathfrak{h}^{\alpha\beta}_{{\rm TT},\nu)} \right\rangle_\lambda \,, \tag{5.128}$$

which leads to

$$\delta\dot{E}^{(\mathfrak{h})} = \frac{1}{16\pi} \lim_{r\to\infty} \int_{S^2_r} \left\langle \left\langle h^{\rm TT}_{\alpha\beta,(t} \mathfrak{h}^{\alpha\beta}_{{\rm TT},i)} \right\rangle_\lambda \, n^i \right\rangle_\omega r^2 d\Omega \,. \tag{5.129}$$

metric. This difference comes from the way the metric deformation and the scalar field couple in the field equations. In the quadratic gravity case, ϑ does not multiply $G_{\mu\nu}$ in the field equations (the Einstein-Hilbert sector of the action is unmodified), while the opposite is true in scalar-tensor theories in the Jordan frame. Therefore, in the former $\mathfrak{h}_{\mu\nu}$ and ϑ decouple in the $r \to \infty$ limit and there is no breathing mode. In contrast, in the latter the coupling between $\mathfrak{h}_{\mu\nu}$ and ϑ remains in the limit $r \to \infty$, leading to a non-vanishing breathing mode and a modification to the effective SET.

[8]The distinction between (ii) and (iii) can be ambiguous at higher PN order, because how the orbital parameters are modified depends on the gauge choice. However, as long as we impose the harmonic gauge condition on both GR and the deformed metric perturbations, we do not have to worry about this gauge issue at least up to next-to-leading PN order.

As before, the $h_{\alpha\beta}$ and $\mathfrak{h}_{\alpha\beta}$ are those valid in the FZ.

5.6.1 Scalar field correction to the energy flux

Even-parity sector

In the even-parity case, $\vartheta^{\rm FZ}$ is dominated by the dipole component [Eq. (5.73)], which we repeat here for convenience: $\vartheta^{\rm FZ} = \dot{D}_i n^i/r$, where D_i is the NZ dipole given in Eq. (5.74). This is inserted into the energy loss formula, Eq. (5.125). Since the FZ scalar field depends on retarded time, both time and spatial derivatives can be written as time derivatives of the NZ moments. This gives

$$\delta\dot{E}^{(\vartheta)} = -\beta \int_{S^2_\infty} \left\langle \ddot{D}_i \ddot{D}_j n^{ij} \right\rangle_\omega d\Omega = -\frac{4\pi}{3}\beta \left\langle \ddot{D}^i \ddot{D}_i \right\rangle_\omega , \tag{5.130}$$

which for circular orbits gives

$$\delta\dot{E}^{(\vartheta)} = -\frac{4\pi}{3}\beta\omega^4 |D|^2 = -\frac{4\pi}{3}\frac{\beta}{m^4}(m_2 q_1 - m_1 q_2)^2 v^8 . \tag{5.131}$$

Note that here, as before, the $m \to 0$ limit diverges, because the effective theory breaks down on short length scales and $\varsigma \ll 1$ is violated.

When the compact bodies are BHs, their scalar monopole charges are given by Eq. (5.63), $q_A = 2\alpha_3/(\beta m_A)$, which then leads to

$$\delta\dot{E}^{(\vartheta)} = -\frac{1}{3}\zeta_3 \frac{1}{\eta^2}\frac{\delta m^2}{m^2} v^8 . \tag{5.132}$$

Comparing this with the GR energy flux, we find

$$\frac{\delta\dot{E}^{(\vartheta)}}{\dot{E}^{\rm GR}} = \frac{5}{96}\zeta_3 \frac{1}{\eta^4}\frac{\delta m^2}{m^2} v^{-2} , \tag{5.133}$$

a relative -1PN effect. That is, the energy lost to the scalar field due to dipole radiation would enter as a lower-order in v effect than the energy loss in GR. If one takes the limit $m_2 \to \infty$ while keeping (m_1, v) fixed, then the above ratio scales as m_1^{-4}; i.e. the energy flux ratio is sensitive to the smallest horizon scale of the system.

The effect is of a similar size for comparable stellar-mass binary and EMRI system. A SMBH-SMBH binary experiences the smallest effect.

Odd-parity sector: spinning bodies

The scalar field $\vartheta^{\rm FZ}$ is here dominated by the quadrupole component [Eq. (5.83)], which we repeat here for convenience $\vartheta^{\rm FZ} = \ddot{\mu}_{ij} n^{ij}/r = -\omega^2 \mu_{ij} n^{ij}/r$, where the quadrupole tensor μ_{ij} is defined in Eq. (5.82). Inserting this into the energy loss formula [Eq. (5.125)] gives

$$\begin{aligned} \delta\dot{E}^{(\vartheta)} &= -\beta \int_{S^2_\infty} \left\langle \dddot{\mu}_{ij} \dddot{\mu}_{kl} n^{ijkl} \right\rangle_\omega d\Omega \,, \\ &= -\frac{4\pi}{15}\beta \left\langle \left[2\dddot{\mu}_{ij}\dddot{\mu}^{ij} + \left(\dddot{\mu}^{i}{}_{i}\right)^2 \right] \right\rangle_\omega \,. \end{aligned} \tag{5.134}$$

Let us evaluate this for quasi-circular orbits with non-precessing spins. The third time derivative of the quadrupole tensor μ_{ij} becomes

$$\dddot{\mu}^{ij} = b^{-3} \left(m_1 v_{12}^{(i} \mu_2^{j)} - m_2 v_{12}^{(i} \mu_1^{j)} \right) \,, \tag{5.135}$$

and the total energy flux is

$$\delta\dot{E}^{(\vartheta)} = -\frac{5}{48}\zeta_4 \left[\bar{\Delta}^2 + 2 \left\langle (\bar{\Delta}\cdot\hat{v}_{12})^2 \right\rangle_\omega \right] v^{14} \,, \tag{5.136}$$

where $\hat{v}_{12}$ is the unit vector in the direction of the relative velocity and the dimensionless quantity $\bar{\Delta}$ is defined as

$$\bar{\Delta}^i \equiv \frac{m_2}{m}\chi_1 \hat{S}_1^i - \frac{m_1}{m}\chi_2 \hat{S}_2^i \,. \tag{5.137}$$

Notice that $\delta\dot{E}^{(\vartheta)}$ in Eq. (5.136) is finite in the EMRI limit. Note also that when both spins are perpendicular to the orbital plane, $\bar{\Delta}$ is as well, and the second term of $\delta\dot{E}^{(\vartheta)}$ vanishes. Comparing Eq. (5.136) with GR,

$$\frac{\delta\dot{E}^{(\vartheta)}}{\dot{E}^{\rm GR}} = \frac{25}{1536}\zeta_4 \frac{1}{\eta^2} \left[\bar{\Delta}^2 + 2 \left\langle (\bar{\Delta}\cdot\hat{v}_{12})^2 \right\rangle_\omega \right] v^4 \,, \tag{5.138}$$

hence scalar radiation in the odd-parity sector is clearly a relative 2PN effect. This effect was not included in the work of Pani et al. [113], who found a 7PN correction, since their simulations did not include spins. If one takes the limit $m_2 \to \infty$ while keeping (m_1, v) fixed, then the above ratio scales as $m_1^{-2} m_2^{-2}$; i.e. the energy flux ratio is sensitive to the geometric mean of the two horizon scales in the system. This implies that the effect is greatest for comparable stellar-mass binaries.

Odd-parity sector: non-spinning bodies

The odd-parity $\vartheta_{\rm FZ}$ in Eq. (5.89) can be used to evaluate the energy loss in Eq. (5.125):

$$\begin{aligned}
\delta\dot{E}^{(\vartheta)} =& -256\kappa\zeta_4\delta m^2\eta^2\left(\frac{m}{b}\right)^8\int_{S^2_\infty} d\Omega\left[\partial_t\left(\epsilon^{ijk}n^{ip}v^k_{12}n^{jp}_{12}\right)\right]^2 \\
=& -256\kappa\zeta_4\eta^2\frac{\delta m^2}{m^2}\left(\frac{m}{b}\right)^{10}\int_{S^2_\infty} d\Omega\left(\epsilon^{ijk}n^{ip}v^{kp}_{12}n^j_{12}\right)^2 \\
=& -\frac{64}{15}\zeta_4\eta^2\frac{\delta m^2}{m^2}\left(\frac{m}{b}\right)^{12}\,. \qquad (5.139)
\end{aligned}$$

Compared to the GW radiation in GR [Eq. (5.123)], this scalar radiation becomes

$$\frac{\delta\dot{E}^{(\vartheta)}}{\dot{E}^{\rm GR}} = \frac{2}{3}\frac{\delta m^2}{m^2}\zeta_4\, v^{14}\,, \qquad (5.140)$$

which shows that this is a relative 7PN effect. In contrast with the cases of even-parity and odd-parity with spins, this effect is dominantly controlled by the total mass, rather than the mass ratio. The effect is greatest for a system of stellar-mass BHs.

The above result can be compared to numerical calculations recently performed by Pani et al. [113]. They estimated the effect of scalar radiation in dynamical CS gravity [6] for non-spinning, circular EMRIs. They numerically solved the master perturbation equations on a Schwarzschild background to obtain the time evolution of the scalar field and the metric perturbation, caused by a non-spinning point particle. Figure 5-3 compares their results to ours, found in Eq. (5.140). Observe that the numerical results of Pani et al. are in excellent agreement with our post-Newtonian

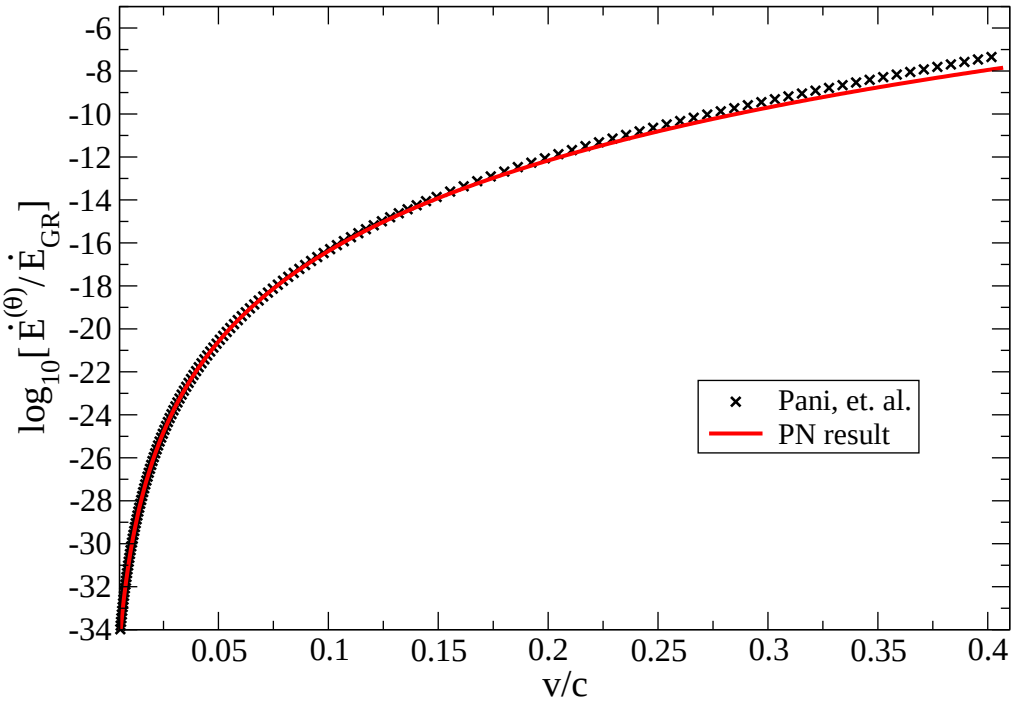

Figure 5-3: Comparison of Eq. (5.140) to the numerical results of Pani et al. [113]. The latter can be mapped to the generic quadratic gravity action of Eq. (5.4) by letting $\alpha_4 = -\alpha_{\rm CS}/4$, which then implies that $\zeta_4 = -\zeta_{\rm CS}/16$. We here used $\zeta_4 = 6.25 \times 10^{-3}$, which is equivalent to their parameter $\zeta_{\rm CS} = 0.01$. Observe that at low velocities, in the regime where the PN approximation is valid, the two curves agree.

calculation, which extends it to comparable mass-ratios (notice the factor of $\delta m/m$).

5.6.2 Metric deformation correction to the energy flux

For the even-parity case, the correction to the energy flux that arises from the deformation to the gravitational metric perturbation is at least of 0PN order relative to GR. This is higher PN order compared to the scalar dipole radiation found in Sec. 5.6.1, and thus, we will not consider it further.

For the odd-parity case with spinning BHs, one of the leading contribution comes from the metric correction sourced by $T^{(\vartheta)}_{ij}$, which is given in Eq. (5.117). Inserting this metric perturbation into Eq. (5.129), the energy flux correction relative to GR

becomes

$$\frac{\delta \dot{E}^{(h)}}{\dot{E}^{\rm GR}} = \frac{75}{16}\frac{\zeta_4}{\eta}\chi_1\chi_2 \left\langle \hat{S}_1^i \hat{S}_2^j \left(2\hat{v}_{ij}^{12} - 3n_{<ij>}^{12}\right)\right\rangle_\omega v^4 \,, \tag{5.141}$$

which is of relative 2PN order, just as the contribution due to scalar radiation in Eq. (5.138). Notice that both the metric deformation and scalar field corrections to the energy flux are of $\mathcal{O}(\chi^2)$, but the latter is larger by a factor of $\mathcal{O}(\eta^{-1})$.

We expect $\mathcal{O}(\chi)$ corrections to the energy flux due to the metric deformation to be higher PN order. For very slowly spinning binaries, however, they may give larger corrections compared to the $\mathcal{O}(\chi^2)$ 2PN ones presented here.

In the odd-parity sector with non-spinning objects, the regularized contributions to the metric deformation can only provide energy flux corrections of at least 7PN order. However, as explained in Sec. 5.5.3, we expect that matching strong-field solutions to the non-regular NZ ones may generate 6PN corrections in the energy flux, similar to those found by Pani et al. [113].

5.7 Impact on gravitational wave phase

How do all these modifications to the energy flux affect the GW observable? To answer this question, we compute the Fourier transform of the phase of the GW response function in the stationary phase approximation (SPA), where we assume the GW phase changes much more rapidly than the GW amplitude [57].

We begin by parameterizing all the corrections to the energy flux that we have studied so far via the following power law:

$$\dot{E} = \dot{E}_{\rm GR}(1 + Av^a) \,, \tag{5.142}$$

where (A, a) are summarized in Table 5.2 for the four different sectors considered.

With the generic energy flux parameterization, the orbital phase for a quasi-circular inspiral becomes

$$\begin{aligned}\phi(F) &= \int^F \frac{dE}{d\omega}\left(\frac{dE}{dt}\right)^{-1}\omega d\omega \\ &= \phi_{\rm GR}(F)\left[1+\frac{5}{a-5}A(2\pi mF)^{a/3}\right], \end{aligned} \tag{5.143}$$

where F and $\omega = 2\pi F$ are the linear and angular orbital frequency, $\phi_{\rm GR} = -1/(32\eta)(2\pi mF)^{-5/3}$ is the GR orbital phase and $E(\omega) = -(\mu/2)(m\omega)^{2/3}$ is the binary's binding energy to Newtonian order. Recall here that $m = m_1 + m_2$ is the total mass of the binary, while $\mu = m_1 m_2/m$ is the reduced mass and $\eta = \mu/m$ is the symmetric mass ratio. Equation (5.143) is not valid when $a = 5$ (a 2.5PN correction), as then the integrand becomes proportional to ω^{-1}, which leads to a log term.

Before we compute the Fourier phase, we must first define t_0, the time at which the stationary phase condition is satisfied $F(t_0) = f/2$, where f is the GW frequency. This condition can be solved to yield

$$t_0 = t_{0,\rm GR}\left(1-\frac{8}{8-a}A(\pi mf)^{a/3}\right), \tag{5.144}$$

where $t_{0,\rm GR}$ is the GR t_0. Again, this expression is not valid at $a = 8$, because once more the correction to $t_0(f)$ would be a log term.

With this at hand, we can now compute the Fourier phase in the SPA:

$$\begin{aligned}\Psi_{\rm GW} &= 2\phi(t_0) - 2\pi f t_0 \\ &= \Psi_{\rm GR}\left[1-\frac{40}{(a-5)(a-8)}A\eta^{-a/5}(\pi\mathcal{M}f)^{a/3}\right], \end{aligned} \tag{5.145}$$

where $\Psi_{\rm GR} \equiv (3/128)(\pi\mathcal{M}f)^{-5/3}$, and where $\mathcal{M} = \eta^{3/5}m$ is the chirp mass. Again, these expressions are not valid when $a = 5$ or $a = 8$, for the reasons described above.

The corrections to the GW phase found here map directly to the parameterized post-Einsteinian (ppE) framework [178]. In that framework, one postulates that modified gravity theories affect the Fourier phase of the GW response function in the

Sector	A	a
Even-Parity	$\frac{5}{96}\zeta_3\frac{1}{\eta^4}\frac{\delta m^2}{m^2}$	-2
Odd-P, Spins (ϑ)	$\frac{25}{1536}\zeta_4\frac{1}{\eta^2}\left[\bar{\Delta}^2+2\left\langle(\bar{\Delta}\cdot\hat{v}_{12})^2\right\rangle_\omega\right]$	$+4$
Odd-P, Spins (h)	$\frac{75}{16}\zeta_4\frac{1}{\eta}\langle S_1^i S_2^j\left(2\hat{v}_{ij}^{12}-3n_{<ij>}^{12}\right)\rangle_\omega$	$+4$
Odd-P, No Spin	$\frac{2}{3}\zeta_4\frac{\delta m^2}{m^2}$	$+14$

Table 5.2: Coefficients of the relative energy flux.

SPA via

$$\Psi_{\rm GW}^{\rm ppE}=\Psi_{\rm GR}+\beta_{\rm ppE}\left(\pi\mathcal{M}f\right)^{b_{\rm ppE}}\,, \tag{5.146}$$

where $(\beta_{\rm ppE},b_{\rm ppE})$ are ppE parameters. We see that this is identical to the corrections introduced by a change in the energy flux, with the mapping

$$\beta_{\rm ppE}=-\frac{15}{16}\frac{A}{(a-5)(a-8)}\eta^{-a/5}\,,\qquad b_{\rm ppE}=\frac{a-5}{3}\,. \tag{5.147}$$

This is not surprising, as the ppE framework was in part motivated by studying power-law (in velocity) modifications to the energy flux and the binding energy [178].

We have then found that a large number of energy flux corrections associated with extra gravitational and scalar field emissions can be mapped to the ppE framework. In the even parity case, the leading-order frequency exponent $b_{\rm ppE}=-7/3$, while in the odd-parity case $b_{\rm ppE}=-1/3$, unless the binary is non-spinning in which case $b_{\rm ppE}=+3$.

The results found in this paper could help in the generalization of the ppE framework to more generic quasi-circular inspirals. The original framework considered only non-spinning, equal mass inspirals, while recently Cornish et al. [48] generalized it to non-spinning, unequal mass systems through $A\to A\eta^c$. In this paper we have found that A does not only depend on a simple power law of η, but also on the mass difference $\delta m/m=\sqrt{1-4\eta}$ and on combinations of the spins. For single detections, however, such a generalization is not needed as one only measures a single number, $\beta_{\rm ppE}$, and one cannot extract the dependencies on η, $\delta m/m$, and the spins.

Although we currently lack any GW detections, we can still estimate the projected constraints that such detections would place on quadratic gravity. According to Table 5.2, the even-parity sector leads to the strongest deviations from GR, since a is the most negative. Therefore, we consider EDGB theory, $(\alpha_1, \alpha_2, \alpha_3, \beta) = (1, -4, 1, \alpha_{\rm EDGB}^{-1})\alpha_{\rm EDGB}$, as a simple sub-case of the even-parity sector. Let us first imagine that we have detected a GW with Ad. LIGO and signal-to-noise ratio (SNR) of 20 that is consistent with GR and that originates from a non-spinning BH binary with masses $(m_1, m_2) = (6, 12)M_\odot$. Given such a detection, Cornish *et al.* [48] estimated the projected bound $|\beta_{\rm ppE}| \lesssim 5 \times 10^{-4}$ for $b_{\rm ppE} = -\frac{7}{3}$, which implies $|\alpha_{\rm EDGB}|^{1/2} \lesssim 4 \times 10^5$ cm. Let us now assume that we have detected a GW with LISA classic with and SNR of 879 and still consistent with GR, but that originates from a non-spinning BH binary with masses $(m_1, m_2) = (10^6, 3 \times 10^6)M_\odot$ at $z = 1$. Given such a detection, Cornish *et al.* [48] estimated a bound on $|\beta_{\rm ppE}| \lesssim 10^{-6}$ for the same value of $b_{\rm ppE}$ as before, which leads to $\alpha_{\rm EDGB}^{1/2} \lesssim 10^{10}$ cm. In both cases, notice that these projected bounds are consistent with the small-coupling requirement $\zeta_i \ll 1$; i.e. saturating the projected Ad. LIGO and LISA constraints we have $\zeta_{\text{Ad. LIGO}} \sim 3 \times 10^{-2}$ and $\zeta_{\rm LISA} \sim 10^{-5}$ for those particular binary systems, which is clearly much less than unity.

Comparing these results with the current constraint obtained by the Cassini satellite, $|\alpha_{\rm EDGB}|^{1/2} < 1.3 \times 10^{12}$cm [11], we see that Ad. LIGO and LISA could constrain $\alpha_{\rm EDGB}$ much more strongly. Unfortunately, it seems difficult to put constraints on EDGB with binary pulsar observations, since NSs have no scalar monopole charge in this theory. We emphasize again that this is opposite to the expectation from scalar-tensor theories, in which NSs have scalar monopole charges while BHs do not. Finally, one cannot estimate the bounds one could place on dynamical CS gravity, since one would have to properly account for modifications to the conservative equations of motion, which we have not calculated here.

5.8 Conclusions and discussions

We have studied the binary inspiral problem in a wide class of quadratic gravity theories in the slow-motion, weak-gravity regime. The structure of a compact object in such theories affects the exterior scalar field sourced by the object. Despite this, we can model a compact object by an effective scalar field source characterized by its scalar monopole and dipole moments. The scalar monopole charge is enhanced inversely proportional to the mass of the object, while the dipole charge is independent of the mass for a fixed dimensionless spin parameter. With this effective source, we then derived and solved the modified field equations for the scalar field and metric deformation.

We find that the scalar field generically emits dipole radiation in the even-parity sector, and quadrupole radiation in the odd-parity sector. Such radiation affects the rate of change of the binary energy at relative -1PN order in the even-parity case and relative 2PN order in the odd-parity case. The quadrupole contribution depends quadratically on the BH spins, and thus it is suppressed for non-spinning binaries. In that case, the odd-parity contribution becomes of relative 7PN order, as found numerically in [113]. We have found excellent agreement between their numerical results and our analytical calculations.

We have also calculated the metric perturbation in the FZ and its associated energy flux. In the even-parity sector, the dominant metric contribution leads to a 0PN relative correction in the energy flux, which is smaller than the -1PN correction induced by scalar dipolar radiation. In the odd-parity sector and for spinning BHs, the metric perturbation leads to a 2PN modification to the energy flux, which is of the same order as that induced by quadrupolar scalar radiation. In the odd-parity sector and for non-spinning BHs, we expect the energy flux correction due to the metric deformation is suppressed to at least of 6PN order, as found by Pani *et al.* [113].

Whether these corrections can be measured or constrained depends on whether they are degenerate with GR terms in the physical observable, i.e. the waveform. A -1PN effect cannot be degenerate, as there are no such terms predicted in GR. A 2PN

effect, however, could be degenerate with a spin-spin interaction for quasi-circular inspirals with aligned or counter-aligned spin components. That is, a renormalization of the spin magnitudes of both bodies can eliminate this 2PN effect, assuming one truncates the waveform at that order. If higher-order PN waveforms are used, or if the orbit is more generic (i.e. if there is precession or eccentricity), then this degeneracy can be broken.

We also calculated the effects of such energy flux modifications on the gravitational waveform. The waveform phase depends sensitively on the rate of change of the orbital frequency, which in turn is governed by the rate of change of energy. We calculated the corrections that would be induced in the waveform and mapped them to the ppE framework. We then used a recent ppE study [48] to estimate the constraints that Ad. LIGO and LISA could potentially place on quadratic gravity theories. Given a GW detection, we found that the magnitude of the new length scale introduced by quadratic gravity theories (associated with a ratio of their coupling constants) could constrain at a level controlled by the smallest length-scale probed in the inspirals, i.e. the size of the smallest compact object's event horizon or surface. The best projected bounds achievable with Ad. LIGO will thus come from stellar-mass BH or NS inspirals, while LISA will benefit the most from EMRIs. Since NSs have no scalar monopole charge in EDGB theory, this theory cannot be constrained from binary pulsar observations. This property is diametrically opposite to scalar-tensor theories where BHs have no hair.

There are several possible avenues for future work. Since we here mainly considered corrections due to the dissipative sector of the theory, one possibility is to calculate the non-dissipative corrections that would modify the binding energy and the equations of motion. There are two effects that should be accounted for: new scalar-scalar forces and metric deformations. Let us consider the former first. In the even parity case, compact objects have an associated scalar monopole charge, and thus, there is an additional scalar force with a $1/r$ potential that should lead to a relative 0PN correction in the equations of motion. Similarly, in the odd-parity case, a spinning compact body possesses a current dipole charge, and hence, dipole-dipole

interactions should arise. Since the dipole potential is proportional to $1/r^2$, while the dipole charge couples to the first derivative of the potential, the equations of motion should be corrected at relative 2PN order.

Another non-dissipative modification is induced by deformations of the background metric tensor. In the even-parity sector, such corrections enter at relative 0PN order, as found by Yunes and Stein [172]. In the odd-parity sector, there is no metric deformation for isolated non-spinning BHs, but for spinning ones there is a correction proportional to r^{-4} to the (t, i) components [177], which then leads to a 4.5PN correction in the equations of motion when we consider boosted BHs. This then implies the following: (i) in the even-parity case, the conservative corrections to the equations of motion do not affect the leading-order modification to the waveforms, since this is dominated by the -1PN scalar radiation effect; (ii) in the odd-parity case, the conservative corrections from the metric deformation can be neglected, but those due to the scalar-scalar force will contribute at the same order as the effect calculated here. A complete analysis of the waveform observable would thus require the calculation of such a scalar-scalar, conservative effect.

Another possibility could be to study modified quadratic gravity in the context of BH perturbation theory. This would be a tremendous effort that would have to be split into separate parts. First, one would have to find an analytic, strong-field solution for arbitrarily-fast rotating BHs in quadratic gravity. This has only been found in the slow-rotation limit both in the even-parity [172] and odd-parity sectors [177]. Once this is accomplished, one would have to study the evolution of metric perturbations away from this solution. Such evolution equations would have to be decoupled in terms of some master function to derive Teukolsky-like master equations. Finally, with these equations at hand, one would have to solve them numerically, when the perturbations are sourced by a small object in a tight orbit. Such an analysis would be interesting because one would be able to derive not only the corrections to the energy flux carried out to infinity, but also that which is absorbed by the BH horizons and which we ignored in this paper.

A final follow-up would be to study how NS solutions are modified in quadratic gravity [111] and how the energy flux from NS binaries is modified. This could then lead to direct constraints on quadratic gravity theories from double binary pulsar observations. Such constraints could be stronger , relative to current Solar System constraints, as they could potentially provide constraints of roughly the order of magnitude of the NS radius. Of course, in the case of EDGB theory or dynamical CS gravity, these constraints might not be stronger as NSs have no scalar monopole charge in such theories.

Chapter 6

Outlook

Let us recall where we started and see how far we've come. The overarching goal was to investigate and develop tests and probes of strong gravity. Whereas the rest of physics has been developed from a closed loop between experiment and theory, there has not been any feedback in the realm of gravity. We simply haven't had the opportunity to probe the regime where the predictions of GR may break down, or haven't been lucky enough for nature to present these systems to us. To close the loop, we must know *how* to probe strong gravity.

These probes can be broken down into two types: discovery/serendipity/null tests, and targeted tests. Null tests are constructed to look for any deviations from observables in GR; targeted tests are designed to find, for some particular class of BGR theory, which systems show the greatest potential deviation from a GR observable.

Chapter 2 worked towards null tests: it focused on improving our ability to make predictions from EMRIs in GR. To use EMRIs as a probe of strong gravity will require not only understanding all of the relevant physics, but also numerical methods which are sufficiently precise that they are faithful to the continuum limit. The simulation must not contaminate the observable signature through noise or an unfaithful dispersion relationship. The exponential convergence and phase relationship convergence are good steps in this direction. But much more work remains, most importantly, inclusion of the source term, which will require domain decomposition.

Chapters 3, 4, and 5 worked towards targeted tests in a large class of BGR theories. To perform gravitational wave tests of BGR theories, one needs to know the properties of gravitational waves, the corrections to compact object structure, the corrections to the motions of objects, and the radiation which they generate.

Chap. 3 studied the properties of GWs near asymptotically flat space in BGR theories: the available polarizations, their propagation, and their energy content. The conclusions are surprisingly simple for the class of theories studied: that gravitational waves look much the same as they do in GR. However, there are BGR theories which do not fall into the category of theories considered here, and the real universe is not asymptotically flat. Both of these points are potential future refinements of this work.

Chap. 4 found the strong-field correction to Schwarzschild in a class of BGR theories. However, for the foreseeable future, pulsar tests will be more powerful than black holes, using radio timing. One potential future avenue of study is the correction to the strong-field structure of neutron stars, making it possible to constrain BGR theories through radio pulsar timing.

Chap. 5 built on the previous two pieces of work and, using the post-Newtonian formalism, calculated the correction to the gravitational observables of the comparable mass-ratio inspiral in a class of BGR theories. This is a very large problem and also paves the way for future work. Most importantly, this work only considered circular orbits, but eccentric orbits are observed in radio pulsar timing. Calculating the same observables for eccentric orbits is very important for constraining these theories. The dominant contribution will be very straightforward, but surprisingly, currently nobody knows how to calculate the angular momentum carried by gravitational waves out at spatial infinity in any theories except for GR. This is not only an important calculation for constraining BGR theories, but also of fundamental importance to our understanding of the structure of theories of gravity.

Can we yet ask nature how gravity acts? Maybe, if we learn to speak her language. So far we are just children, learning basic building blocks. Our vocabulary may be sufficient to ask for simple things, the bare necessities: how compact objects orbit in the post-Newtonian expansion; approximate EMRI trajectories. But we are learning

at an astounding rate and will soon be able to form full sentences: enough to use pulsar timing to constrain BGR theories; hopefully, in the near future, we can generate self-consistent EMRI waveforms. These ideas are so close at hand that we are compelled to continue to study nature's language, in the hopes of understanding her. If nature is kind, and we continue our studies, we will understand her very soon.

Appendix A

The Balding of Neutron Stars in EDGB Gravity

In this appendix, we consider the scalar field equation in EDGB gravity for isolated NSs. Integrating the evolution equation, we find

$$\int \sqrt{-g}\Box\vartheta d^4x \propto \int \sqrt{-g}\mathcal{R}^2_{\rm GB} d^4x\,, \tag{A.1}$$

where we have defined the Gauss-Bonnet invariant $\mathcal{R}^2_{\rm GB} \equiv R^2 - 4R_{\mu\nu}R^{\mu\nu} + R_{\mu\nu\delta\sigma}R^{\mu\nu\delta\sigma}$. Since the Gauss-Bonnet combination is a topological invariant, the right-hand side identically vanishes for any simply-connected, asymptotically flat spacetime. Moreover, since we are considering isolated NSs, these must be stationary, and so the time integration can be removed.

With all of this and using Stokes' theorem, Eq. (A.1) becomes

$$\int \sqrt{-g}(\partial_i\vartheta)n^i dS = \int \sqrt{-g}(\partial_r\vartheta)dS = 0\,, \tag{A.2}$$

where n^i is the radial unit vector and the integral is performed over the 2-sphere at spatial infinity. Notice that $\sqrt{-g} \sim r^2$, while the scalar field must decay at infinity for it to have a finite energy.

Equation (A.2) does not vanish at spatial infinity for all scalar field solutions, i.e. if we model $\vartheta = \vartheta_n/r$ with ϑ_n a constant, then Eq. (A.2) leads to the unique solution $\vartheta_n = 0$. This is a physicists's proof that the EDGB scalar field cannot have scalar monopole charge for a spherically symmetric NS. Similarly, one can show that NSs cannot have scalar monopole charge in dynamical CS gravity; the proof laid out above carries through with the replacement $\mathcal{R}^2_{\rm GB} \to {}^*R\,R$, since ${}^*R\,R$ is also a topological invariant.

Appendix B

Integration techniques

In this appendix, we provide some useful integration techniques. When computing near-zone integrals, we are faced many times with integrals of the form

$$\int d^3x \frac{x_{\langle L\rangle}}{r_1 r_2}\,. \tag{B.1}$$

When the point-particle approximation is valid, such near-zone integrals can be Hadamard regularized by keeping only the finite part. Let us then define [19]

$$Y_{\langle L\rangle}(\boldsymbol{x}_1,\boldsymbol{x}_2) = -\frac{1}{2\pi}\underset{B=0}{\mathrm{FP}}\int d^3x |\tilde{\boldsymbol{x}}|^B \frac{x_{\langle L\rangle}}{r_1 r_2}\,, \tag{B.2}$$

to be evaluated in the near-zone and where $\mathrm{FP}_{B=0}$ stands for the finite part operator (in the limit $B\to 0$) and $|\tilde{\boldsymbol{x}}|$ is an analytic continuation factor [19]. The solution to this integral is

$$Y_{\langle L\rangle} = \frac{b}{l+1}\sum_{q=0}^{l} x_1^{\langle L-Q} x_2^{Q\rangle}\,. \tag{B.3}$$

The first few $Y_{\langle L\rangle}$ are simply

$$Y_0 = Y = b\,, \qquad Y_i = \frac{b}{2}\left(x_1^i + x_2^i\right)\,, \tag{B.4}$$

$$Y_{\langle ij\rangle} = \frac{b}{3}\left(x_1^{\langle ij\rangle} + x_1^{\langle i} x_2^{j\rangle} + x_2^{\langle ij\rangle}\right)\,, \tag{B.5}$$

$$Y_{\langle ijk\rangle} = \frac{b}{4}\left(x_1^{\langle ijk\rangle} + x_1^{\langle ij} x_2^{k\rangle} + x_1^{\langle i} x_2^{jk\rangle} + x_2^{\langle ijk\rangle}\right)\,. \tag{B.6}$$

The solution to the $Y_{\langle L\rangle}$ integral can also be derived by using certain Poisson integral identities [114]:

$$P\left(f_{,i}g_{,i}\right) = -\frac{1}{2}\left[fg + P\left(fg_{,ii}\right) + P\left(gf_{,ii}\right) - \mathcal{B}_p(fg)\right] , \tag{B.7}$$

where we have defined

$$P(f) \equiv \frac{1}{4\pi}\int_{\mathcal{M}} \frac{f(t,x')}{|\boldsymbol{x}-\boldsymbol{x}'|} d^3x' , \tag{B.8}$$

and the boundary term is

$$\mathcal{B}_p(g) \equiv \frac{1}{4\pi}\oint_{\partial\mathcal{R}} \left[\frac{g(t,x')}{|\boldsymbol{x}-\boldsymbol{x}'|}\partial'_r \ln\left[g(t,x')|\boldsymbol{x}-\boldsymbol{x}'|\right]\right]_{r'=\mathcal{R}} \mathcal{R}^2 d\Omega' . \tag{B.9}$$

As usual, we retain only those terms that are independent of the boundary $\mathcal{R}$.

Finally, there is yet another type of integral that commonly appears in near-zone integration:

$$\int_{\mathcal{M}} \frac{d^3x'}{|\boldsymbol{x}'-\boldsymbol{x}_1||\boldsymbol{x}'-\boldsymbol{x}_2||\boldsymbol{x}'-\boldsymbol{x}|} . \tag{B.10}$$

Let us then define the so-called *triangle* potential [115]

$$\mathcal{G}(\boldsymbol{x}_1,\boldsymbol{x}_2,\boldsymbol{x}_3) \equiv \frac{1}{4\pi}\int_{\mathcal{M}} \frac{d^3x'}{|\boldsymbol{x}'-\boldsymbol{x}_1||\boldsymbol{x}'-\boldsymbol{x}_2||\boldsymbol{x}'-\boldsymbol{x}_3|} . \tag{B.11}$$

It is a bit of a miracle that the above integral has the closed-form solution $\mathcal{G}(\boldsymbol{x}_A,\boldsymbol{x}_B,\boldsymbol{x}_C) = 1 - \ln\Delta(ABC)$, with $\Delta(ABC) \equiv |\boldsymbol{x}_A-\boldsymbol{x}_B| + |\boldsymbol{x}_B-\boldsymbol{x}_C| + |\boldsymbol{x}_C-\boldsymbol{x}_A|$.

One can show that the triangle potential satisfies a set of relations, including [115]

$$\begin{aligned}
\partial_i^{(1)}\partial_i^{(2)}\mathcal{G}(\boldsymbol{x}_1,\boldsymbol{x}_2,\boldsymbol{x}) &= \frac{1}{2}\left[\frac{1}{b}\left(\frac{1}{r_1}+\frac{1}{r_2}\right) - \frac{1}{r_1 r_2}\right] , \\
\partial_{il}^{(1)}\partial_{jl}^{(2)}\mathcal{G}(\boldsymbol{x}_1,\boldsymbol{x}_2,\boldsymbol{x}) &= -\frac{1}{2}\left[\frac{n_1^i n_2^j}{r_1^2 r_2^2} + \frac{n_{12}^i n_2^j}{b^2 r_2^2} - \frac{n_{12}^j n_1^i}{b^2 r_1^2}\right. \\
&\qquad \left. + 3\frac{n_{12}^{\langle ij\rangle}}{b^3}\left(\frac{1}{r_1}+\frac{1}{r_2}\right)\right] ,
\end{aligned} \tag{B.12}$$

and more generally

$$\partial_i^{(B)}\partial_j^{(C)}\mathcal{G}(ABC) = \frac{1}{\Delta(ABC)^2}(n^i_{AB} - n^i_{BC})(n^j_{AC} + n^j_{BC}) + \frac{1}{r_{BC}\Delta(ABC)}(\delta_{ij} - n^i_{BC}n^j_{BC})\,, \tag{B.13}$$

where $\mathcal{G}(ABC) \equiv \mathcal{G}(\boldsymbol{x}_A, \boldsymbol{x}_B, \boldsymbol{x}_C)$.

Appendix C

Odd-Parity, Non-Spinning, Regularized Contribution in the Metric Correction

We consider here the odd-parity sector for non-spinning binaries, where, for the scalar field, the magnetic-type dipole moment vanishes, $\mu_A^i = 0$, since $\chi_A = 0$. For the regularized contribution, we only need to consider the cross-interaction terms since the isolated non-spinning BH solution in the odd-parity case is simply the Schwarzschild metric. The $\tilde{K}_{ij}^{(1)}$ source term gives the largest contribution and one is then left only with the pseudo-scalar generated by interaction terms, as given in Eq. (5.61).

The metric deformation is given by Eq. (5.94), the $m = 0$ piece of which can be split as in Eqs. (5.109)-(5.112). Before tackling each of these terms separately, let us point out that many of them identically vanish. For example, one of the contribution

in Eq. (5.109) is proportional to

$$
\begin{aligned}
I_{ijqn} \equiv & m_1 \epsilon_{jkl} \int_{\mathcal{M}} \partial^{(1)}_{qnk} \left(\frac{1}{r_1}\right) \partial^{(1)}_{il} \left(\frac{1}{r_1}\right) d^3x \\
& + m_2 \epsilon_{jkl} \int_{\mathcal{M}} \partial^{(1)}_{qnk} \left(\frac{1}{r_1}\right) \partial^{(2)}_{il} \left(\frac{1}{r_2}\right) d^3x \\
= & -2\pi m_1 \epsilon_{jkl} \lim_{2\to 1} \partial^{(1)}_{qnk} \partial^{(2)}_{il} Y(\boldsymbol{x}_1, \boldsymbol{x}_2) \\
& - 2\pi m_2 \epsilon_{jkl} \partial^{(1)}_{qnk} \partial^{(2)}_{il} Y(\boldsymbol{x}_1, \boldsymbol{x}_2) = 0 \,. \qquad \text{(C.1)}
\end{aligned}
$$

It is critical in this calculation and in the calculations that follow to replace the x^i derivatives by particles derivatives, i.e. derivatives with respect to x^i_1 and x^i_2.

Let us then tackle the first contribution to the dissipative metric deformation. Equations (5.109)-(5.112) can then be rewritten as

$$
\begin{aligned}
\mathfrak{h}^{(1)}_{ij} = & 2048\pi \frac{\alpha_4^2}{\beta} \frac{m_1^2 m_2}{r} \Big[b\omega^2 \left(I_{1ij} + I_{2ij}\right) \\
& - v_{1n}(I_{3ijn} + I_{4ijn}) - v_{2n}(I_{5ijn} + I_{6ijn}) \\
& + (i \leftrightarrow j) \Big] + (1 \leftrightarrow 2) \,, \qquad \text{(C.2)} \\
\mathfrak{h}^{(2)}_{ij} = & -4096\pi \frac{\alpha_4^2}{\beta} \frac{m_1^2 m_2}{r} v_{1[n} \Big[I_{3i]jn} + I_{4i]jn} \\
& + I_{5i]jn} + I_{6i]jn} + (i \leftrightarrow j) \Big] + (1 \leftrightarrow 2) \,, \qquad \text{(C.3)} \\
\mathfrak{h}^{(3)}_{ij} = & 4096\pi \frac{\alpha_4^2}{\beta} \frac{m_1^2 m_2}{r} v_{1[n} \\
& \times \Big[I_{7i]jn} + I_{8i]jn} + (i \leftrightarrow j) \Big] + (1 \leftrightarrow 2) \,, \qquad \text{(C.4)} \\
\mathfrak{h}^{(4)}_{ij} = & -2048\pi \frac{\alpha_4^2}{\beta} \frac{m_1^2 m_2}{r} v_{1n} \\
& \times \Big[I_{7ijn} + I_{8ijn} + (i \leftrightarrow j) \Big] + (1 \leftrightarrow 2) \,, \qquad \text{(C.5)}
\end{aligned}
$$

where we have defined

$$
\begin{aligned}
I_{1ij} &\equiv \epsilon_{jkl}\epsilon_{pqs} n_{12s} J^{(1)}_{pk,q,il}\,, \\
I_{2ij} &\equiv \epsilon_{jkl}\epsilon_{pqs} n_{12s} J^{(1)}_{p,qk,il}\,, \\
I_{3ijn} &\equiv \epsilon_{jkl}\epsilon_{pqs} v_{12s} J^{(1)}_{pkn,q,il}\,, \\
I_{4ijn} &\equiv \epsilon_{jkl}\epsilon_{pqs} v_{12s} J^{(1)}_{pn,qk,il}\,, \\
I_{5ijn} &\equiv \epsilon_{jkl}\epsilon_{pqs} v_{12s} J^{(1)}_{pk,qn,il}\,, \\
I_{6ijn} &\equiv \epsilon_{jkl}\epsilon_{pqs} v_{12s} J^{(1)}_{p,qkn,il}\,, \\
I_{7ijn} &\equiv \epsilon_{jkl}\epsilon_{pqs} v_{12s} J^{(1)}_{pk,q,iln}\,, \\
I_{8ijn} &\equiv \epsilon_{jkl}\epsilon_{pqs} v_{12s} J^{(1)}_{p,qk,iln}\,,
\end{aligned}
\tag{C.6}
$$

and

$$
J^{(p)}_{A,B,C} = \lim_{3\to p} \partial^{(1)}_A \partial^{(2)}_B \partial^{(3)}_C \mathcal{G}(ABC)\,, \tag{C.7}
$$

with A, B, C denoting the multi-index lists. We provide a more detailed discussion of J tensors in Appendix D. One can then show through explicit computation that the two terms combine to give $I_{1ij} + I_{2ij} = 0$, $I_{3ijn} + I_{4ijn} = 0$, $I_{5ijn} + I_{6ijn} = 0$, and $I_{7ijn} + I_{8ijn} = 0$. Therefore $\mathfrak{h}^{(1\cdots4)}_{ij} = 0$ at leading order.

Let us now look at contributions that are smaller by $\mathcal{O}(v)$. Such a correction can arise from two different terms: (i) the $\mathcal{O}(v)$ correction to the source term with $m = 0$ in the sum of Eq. (5.94), or (ii) the $\mathcal{O}(v^0)$ correction to the source term with $m = 1$ in the sum of Eq. (5.94). For case (i), the next-order terms consist of two time derivatives and one factor of h_{0i} (or three time derivatives and one factor of h_{ij}), which when combined are $\mathcal{O}(v^2)$ smaller than the $\mathcal{O}(v^0)$ contribution shown to vanish previously. Also, the next-order terms in the PN metric appears at $\mathcal{O}(v^2)$ higher relative to the leading-order terms. Finally, $\vartheta^{\rm NZ}$ in Eq. (5.55) expanded as in Eq. (2.27) of [160] with $m = 1$ in the sum, gives an $\mathcal{O}(v)$ relative contribution to $\partial_k \vartheta$,

but explicit calculation shows that

$$\begin{aligned}\vartheta^{\rm NZ} &= \frac{8}{\pi}\frac{\alpha}{\beta}m_1 m_2 \epsilon_{ijk}\frac{\partial}{\partial t}\left[v_{12k}\int_{\mathcal{M}}\left(\frac{1}{r_1}\right)_{,il}\left(\frac{1}{r_2}\right)_{,jl}d^3x\right]\\ &= \frac{8}{\pi}\frac{\alpha}{\beta}m_1 m_2 \epsilon_{ijk}\frac{\partial}{\partial t}\left[v_{12k}\partial^{(1)}_{il}\partial^{(2)}_{jl}\int_{\mathcal{M}}\frac{1}{r_1}\frac{1}{r_2}d^3x\right]\\ &= 16\frac{\alpha}{\beta}m_1 m_2 \epsilon_{ijk}\frac{\partial}{\partial t}\left[v_{12k}\partial^{(1)}_{l}\partial^{(2)}_{ijl}b\right] = 0\,. \end{aligned} \tag{C.8}$$

For case (ii), the resulting $\dot{\mathfrak{h}}_{ij}$ contains one n^i vector. The correction to the energy flux consists of $\dot{\mathfrak{h}}_{ij}$ multiplied by $h^{\rm TT}_{ij}$ and averaged over a 2-sphere. However, since the leading contribution in $h^{\rm TT}_{ij}$ contains even numbers of n^i vectors, the correction only contains angular integrals of odd numbers of n^i's which vanish exactly upon integration.

Since there is no $\mathcal{O}(G^3, v)$ relative contribution to $\partial_t \mathfrak{h}_{ij}$, the first, non-vanishing contribution must be at least $\mathcal{O}(v^2)$ smaller than what we computed in Eqs. (C.2)-(C.5), which amounts to a 7PN correction to the energy flux carried by the metric deformation, in the odd-parity, non-spinning case.

Appendix D

Evaluating J tensors

Recall that the definition of the J tensors is

$$J^{(p)}_{A,B,C} = \lim_{3\to p} \partial^{(1)}_A \partial^{(2)}_B \partial^{(3)}_C \mathcal{G}(ABC)\,. \tag{D.1}$$

The limit $3 \to p$ which appears must be taken with care. There may be terms proportional to

$$\lim_{3\to p} \frac{1}{r_{p3}}\,, \tag{D.2}$$

which have no finite part. In the evaluation of the J tensors, only the finite part of the limit is kept. That is, a function can be expanded as a Laurent series about these points, and the finite part scales as $(r_{p3})^0$ in the limit as $3 \to p$.

Another type of problematic limit is

$$\lim_{3\to p} n^i_{p3} \quad \text{or} \quad \lim_{3\to p} n^{ij}_{p3}\,, \tag{D.3}$$

which does not formally exist, since it depends on the path taken as we describe below. Parameterize the path that particle 3 takes to the location of particle p by the continuously differentiable path $\gamma(\lambda)$, with λ a parameter of path length and $\lambda = 0$ the location of particle p. There are an infinite number of paths one could choose, and each can be parameterized in two senses. Taking the limit along this path "from

below" (i.e. from smaller values of λ to larger values) yields

$$\lim_{3\to p,\ \gamma^-} n^i_{p3} \to -\hat{v}^i_\gamma(0)\,, \tag{D.4}$$

where $\hat{v}_\gamma$ is the tangent vector to the curve γ. Taking the limit from above, we find

$$\lim_{3\to p,\ \gamma^+} n^i_{p3} \to +\hat{v}^i_\gamma(0)\,. \tag{D.5}$$

The limit depends on the path's tangent at the point of particle p, and the direction in which the limit is taken. Clearly, the final answer must be unique, which implies the limit must vanish.

A unique prescription to this problem is formalized as Hadamard regularization [18]. This can be summarized as follows. All possible paths are considered, with tangent vectors $\hat{v}_\gamma$. The average is then taken by integrating, e.g.

$$\lim_{3\to p} \cdots n^{ij}_{p3} \cdots = \int \frac{d\Omega(\hat{v}_\gamma)}{4\pi} \cdots \hat{v}^{ij}_\gamma \cdots\,. \tag{D.6}$$

The first few such limits, for example, are

$$\lim_{3\to p} n^i_{p3} = 0\,, \tag{D.7}$$

$$\lim_{3\to p} n^{ij}_{p3} = \frac{1}{3}\delta^{ij}\,. \tag{D.8}$$

Bibliography

[1] Alex Abramovici et al. Ligo: The laser interferometer gravitational wave observatory. *Science*, 256:325–333, 1992.

[2] Stephon Alexander, Lee Samuel Finn, and Nicolas Yunes. A gravitational-wave probe of effective quantum gravity. *Phys. Rev.*, D78:066005, 2008.

[3] Stephon Alexander and Jerome Martin. Birefringent gravitational waves and the consistency check of inflation. *Phys. Rev.*, D71:063526, 2005.

[4] Stephon Alexander and Nicolas Yunes. Parametrized post-newtonian expansion of chern-simons gravity. *Phys. Rev.*, D75:124022, 2007.

[5] Stephon Alexander and Nicolas Yunes. Chern-Simons Modified Gravity as a Torsion Theory and its Interaction with Fermions. *Phys. Rev.*, D77:124040, 2008.

[6] Stephon Alexander and Nicolas Yunes. Chern-Simons Modified General Relativity. *Phys. Rept.*, 480:1–55, 2009.

[7] Stephon H. S. Alexander and Jr. Gates, S. James. Can the string scale be related to the cosmic baryon asymmetry? *JCAP*, 0606:018, 2006.

[8] Stephon H. S. Alexander, Michael E. Peskin, and M. M. Sheikh-Jabbari. Leptogenesis from gravity waves in models of inflation. *Phys. Rev. Lett.*, 96:081301, 2006.

[9] M. E. S. Alves, O. D. Miranda, and J. C. N. de Araujo. Probing the f(R) formalism through gravitational wave polarizations. *Physics Letters B*, 679:401–406, August 2009.

[10] Kashif Alvi. An approximate binary-black-hole metric. *Phys. Rev.*, D61:124013, 2000.

[11] Luca Amendola, Christos Charmousis, and Stephen C. Davis. Solar System Constraints on Gauss-Bonnet Mediated Dark Energy. *JCAP*, 0710:004, 2007.

[12] K G Arun and Clifford M Will. Bounding the mass of the graviton with gravitational waves: Effect of higher harmonics in gravitational waveform templates. 2009.

[13] Abhay Ashtekar and Jerzy Lewandowski. Background independent quantum gravity: A status report. *Class. Quant. Grav.*, 21:R53, 2004.

[14] Leor Barack. Gravitational self force in extreme mass-ratio inspirals. *Class. Quant. Grav.*, 26:213001, 2009.

[15] Leor Barack, Amos Ori, and Norichika Sago. Frequency-domain calculation of the self-force: The high-frequency problem and its resolution. *Phys. Rev. D*, 78:084021, Oct 2008.

[16] Emanuele Berti, Alessandra Buonanno, and Clifford M. Will. Estimating spinning binary parameters and testing alternative theories of gravity with LISA. *Phys. Rev.*, D71:084025, 2005.

[17] Emanuele Berti, Vitor Cardoso, and Clifford Will. Gravitational-wave spectroscopy of massive black holes with the space interferometer LISA. *Phys. Rev. D*, 73(6), March 2006.

[18] L. Blanchet and B. R. Iyer. Hadamard regularization of the third post-Newtonian gravitational wave generation of two point masses. *Phys. Rev. D*, 71(2):024004–+, January 2005.

[19] L. Blanchet, B. R. Iyer, and B. Joguet. Gravitational waves from inspiraling compact binaries: Energy flux to third post-Newtonian order. *Phys. Rev. D*, 65(6):064005–+, March 2002.

[20] Luc Blanchet. Second postNewtonian generation of gravitational radiation. *Phys. Rev.*, D51:2559–2583, 1995.

[21] Luc Blanchet. Gravitational radiation from post-newtonian sources and inspiralling compact binaries. *Living Rev. Relativity*, 9:4, 2006.

[22] Luc Blanchet and Thibault Damour. Hereditary effects in gravitational radiation. *Phys.Rev.*, D46:4304–4319, 1992.

[23] Luc Blanchet, Thibault Damour, and Bala R. Iyer. Gravitational waves from inspiralling compact binaries: Energy loss and wave form to second postNewtonian order. *Phys.Rev.*, D51:5360, 1995.

[24] Luc Blanchet and Guillaume Faye. Hadamard regularization. *J. Math. Phys.*, 41:7675–7714, 2000.

[25] Luc Blanchet, Guillaume Faye, and Benedicte Ponsot. Gravitational field and equations of motion of compact binaries to 5/2 post-newtonian order. *Phys. Rev.*, D58:124002, 1998.

[26] Luc Blanchet, Moh'd S. S. Qusailah, and Clifford M. Will. Gravitational recoil of inspiralling black-hole binaries to second post-newtonian order. *Astrophys. J.*, 635:508, 2005.

[27] David G. Boulware and Stanley Deser. String Generated Gravity Models. *Phys.Rev.Lett.*, 55:2656, 1985.

[28] J.P. Boyd. *Chebyshev and Fourier Spectral Methods*. Dover books on mathematics. Dover Publications, 2001.

[29] D. R. Brill and J. B. Hartle. Method of the Self-Consistent Field in General Relativity and its Application to the Gravitational Geon. *Physical Review*, 135:271–278, July 1964.

[30] D. Brizuela, J. M. Martín-García, and G. A. Mena Marugán. xPert: computer algebra for metric perturbation theory. *General Relativity and Gravitation*, 41:2415–2431, October 2009.

[31] R Broucke. Algorithm: ten subroutines for the manipulation of Chebyshev series. *Commun. ACM*, 16(4):254–256, April 1973.

[32] A. Buonanno and T. Damour. Effective one-body approach to general relativistic two-body dynamics. *Phys. Rev. D*, 59:084006, Mar 1999.

[33] Marta Burgay et al. An increased estimate of the merger rate of double neutron stars from observations of a highly relativistic system. *Nature.*, 426:531–533, 2003.

[34] Cliff P. Burgess. Quantum gravity in everyday life: General relativity as an effective field theory. *Living Reviews in Relativity*, 7(5), 2004.

[35] M. Cambiaso and L. F. Urrutia. Extended solution space for Chern-Simons gravity: The slowly rotating Kerr black hole. *Phys. Rev. D*, 82(10):101502, November 2010.

[36] M. Campanelli, C. O. Lousto, and J. Audretsch. Perturbative method to solve fourth-order gravity field equations. *Phys. Rev. D*, 49:5188–5193, May 1994.

[37] Manuela Campanelli, C. O. Lousto, and J. Audretsch. A Perturbative method to solve fourth order gravity field equations. *Phys. Rev.*, D49:5188–5193, 1994.

[38] B. A. Campbell, N. Kaloper, and K. A. Olive. Classical hair for Kerr-Newman black holes in string gravity. *Physics Letters B*, 285:199–205, July 1992.

[39] W B Campbell and T Morgan. Debye potentials for the gravitational field: ERRATUM. *Physica*, 53:264, January 1971.

[40] Priscilla Canizares, Carlos F Sopuerta, and José Luis Jaramillo. Pseudospectral collocation methods for the computation of the self-force on a charged particle: Generic orbits around a Schwarzschild black hole. *Phys. Rev. D*, 82(4):44023, August 2010.

[41] S. M. Carroll. *Spacetime and geometry. An introduction to general relativity.* San Francisco, CA, USA: Addison Wesley, 2004.

[42] LIGO Scientific Collaboration. LIGO: The Laser Interferometer Gravitational-Wave Observatory. 2007.

[43] N. A. Collins and S. A. Hughes. Towards a formalism for mapping the spacetimes of massive compact objects: Bumpy black holes and their orbits. *Phys. Rev. D*, 69(12):124022, June 2004.

[44] Nathan A. Collins and Scott A. Hughes. Towards a formalism for mapping the spacetimes of massive compact objects: Bumpy black holes and their orbits. *Phys. Rev.*, D69:124022, 2004.

[45] A. Cooney, S. Dedeo, and D. Psaltis. Neutron stars in f(R) gravity with perturbative constraints. *Phys. Rev. D*, 82(6):064033–+, September 2010.

[46] Alan Cooney, Simon DeDeo, and Dimitrios Psaltis. Gravity with Perturbative Constraints: Dark Energy Without New Degrees of Freedom. *Phys. Rev.*, D79:044033, 2009.

[47] N. Cornish, L. Sampson, N. Yunes, and F. Pretorius, 2011. in preparation.

[48] Neil Cornish, Laura Sampson, Nico Yunes, and Frans Pretorius. Gravitational Wave Tests of General Relativity with the Parameterized Post-Einsteinian Framework. 2011. Accepted to Phys. Rev. D.

[49] Mihalis Dafermos and Igor Rodnianski. Decay for solutions of the wave equation on Kerr exterior spacetimes I-II: The cases $|a| \ll M$ or axisymmetry. 2010.

[50] T. Damour. Gravitational radiation and the motion of compact bodies. In N. Deruelle & T. Piran, editor, *Gravitational Radiation*, pages 58–+, 1983.

[51] K. Danzmann. LISA - An ESA cornerstone mission for the detection and observation of gravitational waves. *Advances in Space Research*, 32:1233–1242, October 2003.

[52] K. Danzmann and A. Rudiger. LISA technology - concept, status, prospects. *Class. Quant. Grav.*, 20:S1–S9, 2003.

[53] Peter D. D'Eath. Dynamics of a small black hole in a background universe. *Phys. Rev.*, D11:1387–1403, 1975.

[54] Walter Del Pozzo, John Veitch, and Alberto Vecchio. Testing General Relativity using Bayesian model selection: Applications to observations of gravitational waves from compact binary systems. 2011.

[55] S. S. Doeleman, V. L. Fish, A. E. Broderick, A. Loeb, and A. E. E. Rogers. Detecting Flaring Structures in Sagittarius A* with High-Frequency VLBI. *Astrophys. J.*, 695:59–74, April 2009.

[56] S. Drasco and S. A. Hughes. Gravitational wave snapshots of generic extreme mass ratio inspirals. *Phys. Rev. D*, 73(2):024027, January 2006.

[57] Serge Droz, Daniel J. Knapp, Eric Poisson, and Benjamin J. Owen. Gravitational waves from inspiraling compact binaries: Validity of the stationary phase approximation to the Fourier transform. *Phys.Rev.*, D59:124016, 1999.

[58] Douglas M. Eardley, David L. Lee, Alan P. Lightman, Robert V. Wagoner, and Clifford M. Will. Gravitational-wave observations as a tool for testing relativistic gravity. *Phys. Rev. Lett.*, 30(18):884–886, Apr 1973.

[59] Eigen. `http://eigen.tuxfamily.org/`.

[60] FFTW. `http://www.fftw.org/`.

[61] Vincent L. Fish, Sheperd S. Doeleman, Avery E. Broderick, Abraham Loeb, and Alan E.E. Rogers. Detecting Changing Polarization Structures in Sagittarius A* with High Frequency VLBI. *Astrophys.J.*, 706:1353–1363, 2009.

[62] E. E. Flanagan and T. Hinderer. Transient resonances in the inspirals of point particles into black holes. *ArXiv e-prints*, September 2010.

[63] É. É. Flanagan and S. A. Hughes. The basics of gravitational wave theory. *New Journal of Physics*, 7:204–+, September 2005.

[64] E. E. Flanagan, S. A. Hughes, and U. Ruangsri. Resonantly enhanced and diminished strong-field gravitational-wave fluxes. 2012. Forthcoming.

[65] É. É. Flanagan and R. M. Wald. Does back reaction enforce the averaged null energy condition in semiclassical gravity? *Phys. Rev. D*, 54:6233–6283, November 1996.

[66] Matteo Frigo and Steven G. Johnson. The design and implementation of FFTW3. *Proceedings of the IEEE*, 93(2):216–231, 2005. Special issue on "Program Generation, Optimization, and Platform Adaptation".

[67] Jr. Gates, S.James, Sergei V. Ketov, and Nicolas Yunes. Seeking the Loop Quantum Gravity Barbero-Immirzi Parameter and Field in 4D, N = 1 Supergravity. *Phys.Rev.*, D80:065003, 2009.

[68] S. J. Gates, Jr., S. V. Ketov, and N. Yunes. Seeking the loop quantum gravity Barbero-Immirzi parameter and field in 4D, N=1 supergravity. *Phys. Rev. D*, 80(6):065003–+, September 2009.

[69] J N Goldberg. Spin-s Spherical Harmonics and $\eth$. *J. Math. Phys.*, 8(11):2155, 1967.

[70] Samuel E. Gralla. Motion of Small Bodies in Classical Field Theory. *Phys. Rev.*, D81:084060, 2010.

[71] Samuel E. Gralla and Robert M. Wald. A Rigorous Derivation of Gravitational Self-force. *Class. Quant. Grav.*, 25:205009, 2008.

[72] Michael B. Green, J. H. Schwarz, and Edward Witten. Superstring Theory. Vol. 1: Introduction. Cambridge, Uk: Univ. Pr. (1987) 469 P. (Cambridge Monographs On Mathematical Physics).

[73] Michael B. Green, J. H. Schwarz, and Edward Witten. *Superstring Theory. Vol. 2: Loop Amplitides, Anomalies and Phenomenology.* Cambridge University Press, Cambridge, UK, 1987.

[74] Daniel Grumiller and Nicolas Yunes. How do Black Holes Spin in Chern-Simons Modified Gravity? *Phys. Rev.*, D77:044015, 2008.

[75] GSL. `http://www.gnu.org/software/gsl/`.

[76] David Guarrera and A. J. Hariton. Papapetrou energy-momentum tensor for chern-simons modified gravity. 2007.

[77] Seth Hopper and Charles R. Evans. Gravitational perturbations and metric reconstruction: Method of extended homogeneous solutions applied to eccentric orbits on a schwarzschild black hole. *Phys. Rev. D*, 82:084010, Oct 2010.

[78] R. A. Isaacson. Gravitational Radiation in the Limit of High Frequency. I. The Linear Approximation and Geometrical Optics. *Phys. Rev.*, 166:1263–1271, February 1968.

[79] R. A. Isaacson. Gravitational Radiation in the Limit of High Frequency. II. Nonlinear Terms and the Effective Stress Tensor. *Phys. Rev.*, 166:1272–1279, February 1968.

[80] R. Jackiw and S. Y. Pi. Chern-simons modification of general relativity. *Phys. Rev.*, D68:104012, 2003.

[81] T. Jacobson. Thermodynamics of Spacetime: The Einstein Equation of State. *Physical Review Letters*, 75:1260–1263, August 1995.

[82] Nathan K. Johnson-McDaniel, Nicolas Yunes, Wolfgang Tichy, and Benjamin J. Owen. Conformally curved binary black hole initial data including tidal deformations and outgoing radiation. *Phys.Rev.*, D80:124039, 2009.

[83] D. I. Jones. Bounding the Mass of the Graviton Using Eccentric Binaries. *Ap. J. Letters*, 618:L115–L118, January 2005.

[84] P. Kanti, N. E. Mavromatos, J. Rizos, K. Tamvakis, and E. Winstanley. Dilatonic Black Holes in Higher Curvature String Gravity. *Phys. Rev.*, D54:5049–5058, 1996.

[85] P. Kanti, N. E. Mavromatos, J. Rizos, K. Tamvakis, and E. Winstanley. Dilatonic black holes in higher-curvature string gravity. II: Linear stability. *Phys. Rev.*, D57:6255–6264, 1998.

[86] M. Kramer et al. Tests of general relativity from timing the double pulsar. *Science*, 314:97–102, 2006.

[87] William Krivan, Pablo Laguna, Philippos Papadopoulos, and Nils Andersson. Dynamics of perturbations of rotating black holes. *Physical Review D (Particles*, 56:3395, September 1997.

[88] LCGT. `http://gw.icrr.u-tokyo.ac.jp/lcgt/`.

[89] LIGO. `http://www.ligo.caltech.edu`.

[90] LISA. `http://www.esa.int/science/lisa`, `http://lisa.jpl.nasa.gov`.

[91] A. G. Lyne et al. A Double-Pulsar System - A Rare Laboratory for Relativistic Gravity and Plasma Physics. *Science*, 303:1153–1157, 2004.

[92] M. A. H. MacCallum and A. H. Taub. The averaged Lagrangian and high-frequency gravitational waves. *Communications in Mathematical Physics*, 30:153–169, June 1973.

[93] Karl Martel and Eric Poisson. Gravitational perturbations of the schwarzschild spacetime: A practical covariant and gauge-invariant formalism. *Phys. Rev.*, D71:104003, 2005.

[94] J. Martín-García, R. Portugal, and L. Manssur. The Invar tensor package. *Computer Physics Communications*, 177:640–648, October 2007.

[95] J. M. Martín-García. xPerm: fast index canonicalization for tensor computer algebra. *Computer Physics Communications*, 179:597–603, October 2008.

[96] J. M. Martín-García, D. Yllanes, and R. Portugal. The Invar tensor package: Differential invariants of Riemann. *Computer Physics Communications*, 179:586–590, October 2008.

[97] Simone Mercuri and Victor Taveras. Interaction of the Barbero–Immirzi Field with Matter and Pseudo-Scalar Perturbations. 2009.

[98] S. Mignemi and N. R. Stewart. Dilaton axion hair for slowly rotating Kerr black holes. *Phys. Lett.*, B298:299–304, 1993.

[99] Y. Mino, M. Sasaki, M. Shibata, H. Tagoshi, and T. Tanaka. Chapter 1. Black Hole Perturbation. *Progress of Theoretical Physics Supplement*, 128:1–121, 1997.

[100] Chandra Kant Mishra, K.G. Arun, Bala R. Iyer, and B.S. Sathyaprakash. Parametrized tests of post-Newtonian theory using Advanced LIGO and Einstein Telescope. *Phys.Rev.*, D82:064010, 2010.

[101] C. W. Misner, K.S. Thorne, and J. A. Wheeler. *Gravitation*. W. H. Freeman & Co., San Francisco, 1973.

[102] C. Molina, Paolo Pani, Vitor Cardoso, and Leonardo Gualtieri. Gravitational signature of Schwarzschild black holes in dynamical Chern-Simons gravity. *Phys. Rev.*, D81:124021, 2010.

[103] Filipe Moura and Ricardo Schiappa. Higher-derivative corrected black holes: Perturbative stability and absorption cross-section in heterotic string theory. *Class.Quant.Grav.*, 24:361–386, 2007.

[104] K. Nakamura. Second-Order Gauge Invariant Perturbation Theory — Perturbative Curvatures in the Two-Parameter Case. *Progress of Theoretical Physics*, 113:481–511, March 2005.

[105] K. Nakamura. "Gauge" in General Relativity: Second-order general relativistic gauge-invariant perturbation theory. *ArXiv e-prints*, November 2007.

[106] William Nelson, Joseph Ochoa, and Mairi Sakellariadou. Constraining the Noncommutative Spectral Action via Astrophysical Observations. *Phys. Rev. Lett.*, 105:101602, 2010.

[107] William Nelson, Joseph Ochoa, and Mairi Sakellariadou. Gravitational Waves in the Spectral Action of Noncommutative Geometry. *Phys. Rev.*, D82:085021, 2010.

[108] Ezra Newman and Roger Penrose. An Approach to Gravitational Radiation by a Method of Spin Coefficients. *Journal of Mathematical Physics*, 3:566, May 1962.

[109] odeint. `http://headmyshoulder.github.com/odeint-v2/`.

[110] Y. Pan, A. Buonanno, L. T. Buchman, T. Chu, L. E. Kidder, H. P. Pfeiffer, and M. A. Scheel. Effective-one-body waveforms calibrated to numerical relativity simulations: Coalescence of nonprecessing, spinning, equal-mass black holes. *Phys. Rev. D*, 81(8):084041, April 2010.

[111] P. Pani, E. Berti, V. Cardoso, and J. Read. Compact stars in alternative theories of gravity: Einstein-Dilaton-Gauss-Bonnet gravity. *prd*, 84(10):104035, November 2011.

[112] Paolo Pani and Vitor Cardoso. Are black holes in alternative theories serious astrophysical candidates? The case for Einstein-Dilaton- Gauss-Bonnet black holes. *Phys. Rev.*, D79:084031, 2009.

[113] Paolo Pani, Vitor Cardoso, and Leonardo Gualtieri. Gravitational waves from extreme mass-ratio inspirals in Dynamical Chern-Simons gravity. *Phys. Rev.*, D83:104048, 2011.

[114] M. E. Pati and C. M. Will. Post-Newtonian gravitational radiation and equations of motion via direct integration of the relaxed Einstein equations: Foundations. *Phys. Rev. D*, 62(12):124015–+, December 2000.

[115] Michael E. Pati and Clifford M. Will. PostNewtonian gravitational radiation and equations of motion via direct integration of the relaxed Einstein equations. 2. Two-body equations of motion to second postNewtonian order, and radiation reaction to 3.5 postNewtonia order. *Phys.Rev.*, D65:104008, 2002.

[116] Andrzej Królak Piotr Jaranowski. Gravitational-wave data analysis. formalism and sample applications: The gaussian case. *Living Reviews in Relativity*, 8(3), 2005.

[117] Eric Poisson. Metric of a tidally distorted, nonrotating black hole. *Phys.Rev.Lett.*, 94:161103, 2005.

[118] Eric Poisson, Adam Pound, and Ian Vega. The motion of point particles in curved spacetime. *Living Reviews in Relativity*, 14(7), 2011.

[119] J. Polchinski. *String Theory*. October 1998.

[120] J. Polchinski. *String theory. Vol. 2: Superstring theory and beyond*. Cambridge University Press, Cambridge, UK, 1998.

[121] M. Pomazanov, V. Kolubasova, and S. Alexeyev. The problem of singularities of higher order curvature corrections in four dimensional string gravity. 2003.

[122] Adam Pound. Motion of small bodies in general relativity: foundations and implementations of the self-force. 2010.

[123] Adam Pound. Self-consistent gravitational self-force. *Phys. Rev.*, D81:024023, 2010.

[124] Adam Pound. Singular perturbation techniques in the gravitational self-force problem. *Phys. Rev.*, D81:124009, 2010.

[125] Adam Pound and Eric Poisson. Osculating orbits in Schwarzschild spacetime, with an application to extreme mass-ratio inspirals. *Phys. Rev.*, D77:044013, 2008.

[126] W. H. Press, S. A. Teukolsky, W. T. Vetterling, and B. P. Flannery. *Numerical Recipes: The Art of Scientific Computing*. Cambridge University Press, 2007.

[127] William H Press and Saul A Teukolsky. Perturbations of a Rotating Black Hole. II. Dynamical Stability of the Kerr Metric. *Astrophysical Journal*, 185:649, October 1973.

[128] T. Prince. LISA: The Laser Interferometer Space Antenna. *American Astronomical Society Meeting*, 202:3701, May 2003.

[129] D. Psaltis, D. Perrodin, K. R. Dienes, and I. Mocioiu. Kerr Black Holes Are Not Unique to General Relativity. *Physical Review Letters*, 100(9):091101–+, March 2008.

[130] C. Rovelli. Notes for a brief history of quantum gravity. *ArXiv General Relativity and Quantum Cosmology e-prints*, June 2000.

[131] Carlo Rovelli. Quantum gravity. 2004. Published in Cambridge Monographs on Mathematical Physics, pages 1-480, year 2004.

[132] J. J. Sakurai. *Modern quantum mechanics*. 1985.

[133] W Schmidt. Celestial mechanics in Kerr spacetime. *Class. Quantum Grav.*, 19:2743, May 2002.

[134] Bernard F. Schutz, Joan Centrella, Curt Cutler, and Scott A. Hughes. Will Einstein Have the Last Word on Gravity? 2009.

[135] Tristan L. Smith, Adrienne L. Erickcek, Robert R. Caldwell, and Marc Kamionkowski. The effects of Chern-Simons gravity on bodies orbiting the Earth. *Phys. Rev.*, D77:024015, 2008.

[136] C. F. Sopuerta. A Roadmap to Fundamental Physics from LISA EMRI Observations. *GW Notes, Vol. 4, p. 3-47*, 4:3–47, September 2010.

[137] Carlos F. Sopuerta and Nicolas Yunes. Extreme- and Intermediate-Mass Ratio Inspirals in Dynamical Chern-Simons Modified Gravity. *Phys. Rev.*, D80:064006, 2009.

[138] L. C. Stein and N. Yunes. Effective gravitational wave stress-energy tensor in alternative theories of gravity. *Phys. Rev. D*, 83(6):064038–+, March 2011.

[139] H. Stephani, D. Kramer, M. MacCallum, C. Hoenselaers, and E. Herlt. *Exact solutions of Einstein's field equations*. 2003.

[140] Pranesh A Sundararajan, Gaurav Khanna, and Scott A Hughes. Towards adiabatic waveforms for inspiral into Kerr black holes: A new model of the source for the time domain perturbation equation. *Phys. Rev. D*, 76:104005, November 2007.

[141] Hideyuki Tagoshi, Akira Ohashi, and Benjamin J. Owen. Gravitational field and equations of motion of spinning compact binaries to 2.5 postNewtonian order. *Phys.Rev.*, D63:044006, 2001.

[142] Hideyuki Tagoshi and Misao Sasaki. PostNewtonian expansion of gravitational waves from a particle in circular orbit around a Schwarzschild black hole. *Prog.Theor.Phys.*, 92:745–772, 1994.

[143] Takahiro Tanaka, Hideyuki Tagoshi, and Misao Sasaki. Gravitational waves by a particle in circular orbits around a Schwarzschild black hole: 5.5 post-Newtonian formula. *Prog. Theor. Phys.*, 96:1087–1101, 1996.

[144] Victor Taveras and Nicolas Yunes. The Barbero-Immirzi Parameter as a Scalar Field: K- Inflation from Loop Quantum Gravity? *Phys. Rev.*, D78:064070, 2008.

[145] Saul A Teukolsky. Rotating Black Holes: Separable Wave Equations for Gravitational and Electromagnetic Perturbations. *Physical Review Letters*, 29:1114, October 1972.

[146] Saul A Teukolsky. Perturbations of a Rotating Black Hole. I. Fundamental Equations for Gravitational, Electromagnetic, and Neutrino-Field Perturbations. *Astrophysical Journal*, 185:635, October 1973.

[147] K. S. Thorne. Multipole expansions of gravitational radiation. *Rev. Mod. Phys.*, 52:299–339, 1980.

[148] Kip S. Thorne and James B. Hartle. Laws of motion and precession for black holes and other bodies. *Phys. Rev.*, D31:1815–1837, 1984.

[149] M. Tinto and M. E. D. S. Alves. LISA sensitivities to gravitational waves from relativistic metric theories of gravity. *Phys. Rev. D*, 82(12):122003–+, December 2010.

[150] Takashi Torii, Hiroki Yajima, and Kei-ichi Maeda. Dilatonic black holes with Gauss-Bonnet term. *Phys. Rev.*, D55:739–753, 1997.

[151] S. J. Vigeland and S. A. Hughes. Spacetime and orbits of bumpy black holes. *Phys. Rev. D*, 81(2):024030, January 2010.

[152] Sarah J. Vigeland. Multipole moments of bumpy black holes. *Phys. Rev.*, D82:104041, 2010.

[153] Sarah J. Vigeland and Scott A. Hughes. Spacetime and orbits of bumpy black holes. *Phys. Rev.*, D81:024030, 2010.

[154] VIRGO. `http://www.virgo.infn.it`.

[155] R.M. Wald. *General Relativity*. The University of Chicago Press, Chicago, 1984.

[156] B F Whiting. Mode stability of the Kerr black hole. *J. Math. Phys.*, 30:1301, June 1989.

[157] Bernard F Whiting and Larry R Price. Metric reconstruction from weyl scalars. *Classical and Quantum Gravity*, 22(15):S589, 2005.

[158] C. M. Will. *Theory and Experiment in Gravitational Physics*. March 1993.

[159] Clifford M. Will. The confrontation between general relativity and experiment. *Living Reviews in Relativity*, 9(3), 2006.

[160] Clifford M. Will and Alan G. Wiseman. Gravitational radiation from compact binary systems: gravitational waveforms and energy loss to second post-Newtonian order. *Phys. Rev.*, D54:4813–4848, 1996.

[161] Clifford M. Will and Nicolas Yunes. Testing alternative theories of gravity using LISA. *Class. Quant. Grav.*, 21:4367, 2004.

[162] R. Woodard. Avoiding Dark Energy with 1/R Modifications of Gravity. In L. Papantonopoulos, editor, *The Invisible Universe: Dark Matter and Dark Energy*, volume 720 of *Lecture Notes in Physics, Berlin Springer Verlag*, pages 403–+, 2007.

[163] Richard P. Woodard. Avoiding dark energy with 1/R modifications of gravity. *Lect. Notes Phys.*, 720:403–433, 2007.

[164] xAct. `http://www.xact.es/`.

[165] K. Yagi, L. C. Stein, N. Yunes, and T. Tanaka. Post-Newtonian, quasicircular binary inspirals in quadratic modified gravity. *Phys. Rev. D*, 85(6):064022, March 2012.

[166] Kent Yagi and N. Yunes, 2011. in preparation.

[167] N. Yunes and S. A. Hughes. Binary pulsar constraints on the parametrized post-Einsteinian framework. *Phys. Rev. D*, 82(8):082002–+, October 2010.

[168] N. Yunes, R. O'Shaughnessy, B. J. Owen, and S. Alexander. Testing gravitational parity violation with coincident gravitational waves and short gamma-ray bursts. *Phys. Rev. D*, 82(6):064017–+, September 2010.

[169] N. Yunes and F. Pretorius. Dynamical Chern-Simons modified gravity: Spinning black holes in the slow-rotation approximation. *Phys. Rev. D*, 79(8):084043–+, April 2009.

[170] N. Yunes and F. Pretorius. Fundamental theoretical bias in gravitational wave astrophysics and the parametrized post-Einsteinian framework. *Phys. Rev. D*, 80(12):122003–+, December 2009.

[171] N. Yunes and L. C. Stein. Nonspinning black holes in alternative theories of gravity. *Phys. Rev. D*, 83(10):104002, May 2011.

[172] N. Yunes and L. C. Stein. Nonspinning black holes in alternative theories of gravity. *Phys. Rev. D*, 83(10):104002–+, May 2011.

[173] Nicolas Yunes, K. G. Arun, Emanuele Berti, and Clifford M. Will. Post-Circular Expansion of Eccentric Binary Inspirals: Fourier-Domain Waveforms in the Stationary Phase Approximation. *Phys. Rev.*, D80:084001, 2009.

[174] Nicolas Yunes, Alessandra Buonanno, Scott A. Hughes, M. Coleman Miller, and Yi Pan. Modeling Extreme Mass Ratio Inspirals within the Effective-One-Body Approach. *Phys. Rev. Lett.*, 104:091102, 2010.

[175] Nicolas Yunes et al. Extreme Mass-Ratio Inspirals in the Effective-One-Body Approach: Quasi-Circular, Equatorial Orbits around a Spinning Black Hole. 2010.

[176] Nicolas Yunes, Richard O'Shaughnessy, Benjamin J. Owen, and Stephon Alexander. Testing gravitational parity violation with coincident gravitational waves and short gamma-ray bursts. *Phys. Rev.*, D82:064017, 2010.

[177] Nicolas Yunes and Frans Pretorius. Dynamical Chern-Simons Modified Gravity I: Spinning Black Holes in the Slow-Rotation Approximation. *Phys. Rev.*, D79:084043, 2009.

[178] Nicolas Yunes and Frans Pretorius. Fundamental Theoretical Bias in Gravitational Wave Astrophysics and the Parameterized Post-Einsteinian Framework. *Phys. Rev.*, D80:122003, 2009.

[179] Nicolas Yunes, Frans Pretorius, and David Spergel. Constraining the evolutionary history of Newton's constant with gravitational wave observations. *Phys.Rev.*, D81:064018, 2010.

[180] Nicolas Yunes and Carlos F. Sopuerta. Perturbations of Schwarzschild Black Holes in Chern-Simons Modified Gravity. *Phys. Rev.*, D77:064007, 2008.

[181] Nicolas Yunes and David N. Spergel. Double Binary Pulsar Test of Dynamical Chern-Simons Modified Gravity. *Phys. Rev.*, D80:042004, 2009.

[182] Nicolas Yunes and Wolfgang Tichy. Improved initial data for black hole binaries by asymptotic matching of post-Newtonian and perturbed black hole solutions. *Phys. Rev.*, D74:064013, 2006.

[183] Nicolas Yunes, Wolfgang Tichy, Benjamin J. Owen, and Bernd Bruegmann. Binary black hole initial data from matched asymptotic expansions. 2005.

[184] R. Zalaletdinov. Space-time Averages of Classical Physical Fields. *ArXiv General Relativity and Quantum Cosmology e-prints*, October 2004.

[185] R. M. Zalaletdinov. Averaging out the Einstein equations. *General Relativity and Gravitation*, 24:1015–1031, October 1992.

[186] R. M. Zalaletdinov. Averaged Lagrangians and MacCallum–Taub's Limit in Macroscopic Gravity. *General Relativity and Gravitation*, 28:953–979, August 1996.

[187] Anıl Zenginoğlu. A geometric framework for black hole perturbations. *Phys. Rev. D*, 83(1):127502, June 2011.

[188] Anıl Zenginoğlu and Gaurav Khanna. Null infinity waveforms from extreme-mass-ratio inspirals in kerr spacetime. *Phys. Rev. X*, 1:021017, Dec 2011.